H 24/3175

MONASH UNIVERSITY
THESIS ACCEPTED IN SATISFACTION OF THE
REQUIREMENTS FOR THE DEGREE OF
DOCTOR OF PHILOSOPHY
ON..... 3 May 2002 .....
.....[redacted].....
for Sec. Research Graduate School Committee

Mutational analysis of the proteinase and helicase regions of the Dengue virus type 2 NS3 protein.

Thesis submitted for the degree of
Doctor of Philosophy at Monash University

by

Anita Esther Matusan B.Sc. (Hons).

November 2001

Department of Microbiology
Monash University
Victoria, 3800, Australia.

This thesis is dedicated to my husband Cameron and my family.
Without their love and support this work would not have been possible.

TABLE OF CONTENTS

SUMMARY VII

STATEMENT IX

ACKNOWLEDGEMENTS X

PUBLICATIONS XI

ABBREVIATIONS XII

CHAPTER ONE

INTRODUCTION 1

1.1 The family *Flaviviridae* 1

1.2 Medical aspects of dengue 2

1.3 The flavivirus virion 5

1.4 The flavivirus genome 5

1.5 Viral entry and translation 6

1.6 Proteolytic processing: an overview 7

1.7 Flavivirus proteins 9

1.7.1 The C protein 9

1.7.2 The prM and M proteins 10

1.7.3 The E protein 11

1.7.4 The NS1 protein 12

1.7.5 The NS2A and NS2B proteins 14

1.7.6 The NS3 protein 16

1.7.7 The NS4A and NS4B proteins 17

1.7.8 The NS5 protein 19

1.8 The viral proteinase 20

1.8.1 Constitution of the viral proteinase 20

1.8.2 Proteinase X-ray crystal structure 21

1.9 The viral helicase 23

1.9.1 Classification of NS3 helicase 24

1.9.2 The NS3 helicase 25

1.9.3 Basal and nucleic acid stimulated NTPase activity 25

1.9.4 RNA binding activity 26

1.9.5 RNA helicase activity 26

1.9.6 Function of the conserved motifs in NS3 helicase 28

1.9.6(a) Helicase motif I 28

1.9.6(b) Helicase motif II 29

1.9.6(c) Helicase motif III 30

1.9.6(d) Helicase motif VI 30

1.9.7 Helicase X-ray crystal structure 32

1.9.8 Structure directed mutagenesis of hepatitis C virus helicase motif VI 34

1.9.9 Models of unwinding 35

1.10 Replication of viral RNA 36

1.11 Vaccine development and use of genomic length cDNA of flaviviruses 37

1.12 Clustered charged-to-alanine mutagenesis 41

1.13 Aims and experimental approaches 42

CHAPTER TWO

MATERIALS AND METHODS 44

2.1 Cell lines and cell culture media ____ 44

2.2 Growth and plaque assay of virus stocks ____ 44

2.3 Polyethylene glycol precipitation of viruses ____ 45

2.4 Growth of parental and mutant viruses in BHK-21 cells at 33°C and 37°C ____ 46

2.5 Cloning of cDNA ____ 46

2.5.1 Generation of blunt ends ____ 46

2.5.2 Alkaline phosphatase treatment of vectors for cloning ____ 47

2.5.3 DNA electrophoresis and purification ____ 47

2.5.4 Ligation of vector and insert DNA ____ 47

2.5.5 Transformation of ligation reactions into competent *E. coli* ____ 48

2.5.6 Small scale preparations of plasmid DNA ____ 48

2.5.7 Large scale preparation of plasmid DNA ____ 49

2.6 Automated sequencing of DNA ____ 49

2.7 Plasmids used in this study ____ 49

2.8 Mutagenesis by overlap extension PCR ____ 50

2.9 Transcription of RNA from plasmids containing genomic length DEN-2 ____ 51

2.10 Electroporation of genomic length RNA into BHK-21 cells ____ 52

2.11 Indirect immunofluorescence ____ 53

2.12 RT-PCR of viral RNA ____ 54

CHAPTER THREE

MUTATIONAL ANALYSIS OF THE PROTEINASE REGION OF THE DEN-2 VIRUS NS3 PROTEIN ____ 56

3.1 Introduction ____ 56

3.2 Materials and methods ____ 58

3.2.1 Construction of the proteinase mutant pDVWS501NS3$_{32-36}$ ____ 58

3.2.2 Construction of the charged-to-alanine mutants pDVWS501NS3$_{63-66}$, pDVWS501NS3$_{91-94}$, pDVWS501NS3$_{169-173}$ and pDVWS501NS3$_{179-181}$ ____ 59

3.2.2(a) Construction of the plasmid pDVSO8298 ____ 60

3.2.2(b) Construction of the clustered charged-to-alanine mutants pDVWS501NS3$_{63-66}$, and pDVWS501NS3$_{179-181}$ ____ 60

3.2.2(c) Construction of the clustered charged-to-alanine mutants pDVWS501NS3$_{91-94}$, and pDVWS501NS3$_{169-173}$ ____ 60

3.2.3 RT-PCR of viral RNA ____ 61

3.2.4 Growth curves of parental and mutant DEN-2 viruses ____ 61

3.2.5 Serial passage of V_{32-36} and V_{91-94} in C6/36 cells ____ 62

3.2.6 Coordinates and calculations ____ 62

3.3 Results ____ 63

3.3.1 Analysis of virus replication ____ 63

3.3.2 Growth of viruses V2, V_{63-66}, $V_{169-173}$, and $V_{179-181}$ in C6/36 and BHK-21 cells ____ 65

3.3.3 Serial passage of V_{32-36} and V_{91-94} in C6/36 cells ____ 66

3.4 Discussion ____ 67

3.4.1 Virus production ____ 68

3.4.2 Virus stability on passaging ____ 69

3.4.3 Structural interpretation ____ 71

3.5 Concluding remarks ____ 74

CHAPTER FOUR

MUTATIONAL ANALYSIS OF THE HELICASE REGION OF THE DEN-2 VIRUS NS3 PROTEIN 76

4.1 Introduction 76

4.2 Materials and methods 79

4.2.1 The pGEX-3X expression vector 79

4.2.2 Construction of the parental plasmid pGX74%NS3 79

4.2.3 Mutagenesis of the parental plasmid pGX74%NS3 80

4.2.3(a) Construction of the charged-to-alanine mutants pGX74%$NS3_{169\text{-}173}$, pGX74%$NS3_{179\text{-}181}$ and pGX74%$NS3_{184\text{-}186}$ 80

4.2.3(b) Consrtuction of the motif I and II mutants pGX74%$NS3_{G198A}$, pGX74%$NS3_{K199A}$ and pGX74%$NS3_{M283F}$ 81

4.2.3(c) Construction of the motif VI mutant pGX74%$NS3_{R457A,R458A}$ 81

4.2.3(d) Construction of the charged-to-alanine mutants pGX74%$NS3_{334\text{-}336}$, pGX74%$NS3_{376\text{-}380}$ and pGX74%$NS3_{436\text{-}439}$ 81

4.2.4 Synthesis and purification of NS3 proteins 82

4.2.5 Polyacrylamide gel electrophoresis (SDS-PAGE) of recombinanat proteins 82

4.2.6 Immunoblots 83

4.2.7 ATPase assay 84

4.2.8 Helicase assay 84

4.2.9 Construction of the charged-to-alanine mutants pDVWS501$NS3_{169\text{-}173}$, pDVWS501$NS3_{179\text{-}181}$ and pDVWS501$NS3_{184\text{-}186}$ 86

4.2.10 Construction of the motif I, II and VI mutants pDVWS501$NS3_{K199A}$, pDVWS501$NS3_{M283F}$ and pDVWS501$NS3_{R457A,R458A}$ 87

4.2.11 Construction of the charged-to-alanine mutants pDVWS501NS3$_{334-336}$, pDVWS501NS3$_{376-380}$ and pDVWS501NS3$_{436-439}$ 87

4.2.12 RT-PCR of viral RNA 87

4.2.13 Temperature shift experiments 88

4.2.13(a) Dot blot hybridizations 88

4.2.13(b) Radiolabelling of infected cells and radioimmunoprecipitation 89

4.2.13(c) SDS-PAGE of radiolabelled proteins 91

4.2.14 Serial passage of $V_{334-336}$ in C6/36 cells 91

4.3 Results 92

4.3.1 Mutagenesis of the helicase region of NS3 92

4.3.2 Synthesis of truncated parental and mutant NS3 in *E. coli* 93

4.3.3 NS3-mediated ATPase activity 94

4.3.4 RNA helicase activity of NS3 mutants 95

4.3.5 Analysis of virus replication 96

4.3.6 Growth of viruses V2, $V_{169-173}$, $V_{179-181}$ and V_{M283F} in BHK-21 cells 98

4.3.7 Temperature shift experiments with virus V_{M283F} 99

4.3.8 Serial passage of $V_{334-336}$ in C6/36 cells 100

4.4 Discussion 101

4.4.1 NS3-mediated ATPase and RNA helicase activity 102

4.4.2 Virus production 105

4.5 Concluding remarks 108

CHAPTER FIVE

GENERAL DISCUSSION AND CONCLUSIONS 110

BIBLIOGRAPHY 115

SUMMARY

The protein NS3 of *Dengue virus type 2* is the second largest nonstructural protein specified by the virus and is known to possess multiple enzymatic activities, including a serine proteinase located in the amino terminal one third, and a NTPase and helicase in the remaining carboxy terminal two thirds of the protein. One aim of this work was to identify changes in the DEN-2 NS3 gene that restrict virus replication. This involved the incorporation of mutations into a genomic length DEN-2 cDNA clone from which (infectious) RNA could be transcribed. Thirteen sites distributed throughout NS3 were mutagenized in this study.

The effects of four clustered charged-to-alanine mutations ($K_{63}RIE_{66}$, $E_{91}GEE_{94}$, $E_{169}KSIE_{173}$ and $E_{179}DD_{181}$) and the mutation of a highly conserved hydrophobic region ($G_{32}YSQI_{36}$) in the NS3 proteinase on viral replication in cell culture were analyzed. Infectious virus was recovered for all five mutants albeit with a reduced plaque size. Two of the five mutant viruses showed significantly reduced plaque titres. The substitutions to alanine in the conserved hydrophobic region were more disruptive to virus production than changes at hydrophilic sites by charged-to-alanine mutagenesis.

Another aim was to investigate the importance of residues in the DEN-2 NS3 helicase region for enzymatic activity and viral replication. DEN-2 NS3 lacking the proteinase region was synthesized as a fusion protein with glutathione *S*-transferase in *E. coli*. The effect of ten mutations on ATPase and RNA helicase activity were examined. Residues at four sites within helicase motifs I, II and VI were substituted, and six sites outside motifs were altered by clustered charged-to-alanine mutagenesis.

The mutations were also tested for their effects on virus replication by incorporation into genomic length cDNA.

Two mutations, both in motif I (G198A and K199A) abolished both ATPase and helicase activity. Two further mutations, one in motif VI (R457A,R458A) and the other a clustered charged-to-alanine substitution at $R_{376}KNGK_{380}$, abolished helicase activity only. No virus was detected for any mutation which prevented helicase activity, demonstrating the requirement of this enzyme for virus replication. The remaining six mutations resulted in varying levels of enzyme activities and four permitted virus replication. For the two non-replicating viruses, encoding clustered changes at $R_{184}KR_{186}$ and $D_{436}GEE_{439}$, these residues may be surface-located and therefore the viruses may be defective through altered interaction of NS3 with other components of the viral replication complex. Two of the replicating viruses displayed a temperature sensitive phenotype. One contained a clustered mutation at $D_{334}EE_{336}$ and grew too poorly for further characterization. However, virus with a M283F substitution in motif II was examined in a temperature shift experiment (33°C to 37°C) and showed reduced RNA synthesis at the higher temperature. This study demonstrated that mutagenesis in the viral NS3 proteinase and helicase can be used to produce growth-restricted flaviviruses that may be useful in the production of attenuated vaccine strains.

STATEMENT

I declare that this thesis contains no material which has been accepted for the award of any other degree or diploma at any university and that, to the best of my knowledge and belief, this thesis contains no material previously published or written by another person, except when due reference is made in the text of the thesis.

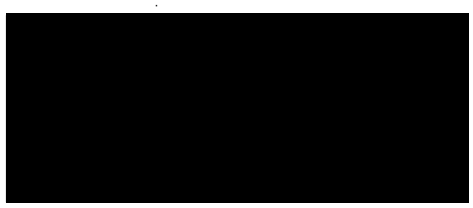

Anita E. Matusan

ACKNOWLEDGEMENTS

My sincere thanks go to Associate Professor Peter J. Wright for his supervision and advice throughout my project and during the preparation of this thesis. I would like to thank Dr. Andrew Davidson for his useful advice and patience while I have been working and writing this thesis. Thank you also to the Chairman (past and present) of the Monash Microbiology Department for making available the Department's facilities and equipment.

Special thanks go to Dr. Melinda Pryor and Dr. Rosa Gualano for their guidance and advice during the early stages of this project. Many thanks also go to Vivien Vasic for her help with tissue culture and automated sequencing, along with Mark Cauchi, Heidi Dryburgh and Elise Webber. Thanks to Khim Ho for synthesis of oligonucleotides, Dr. John Menting for helpful discussions about protein purification and Leslie Gladman who always ensured radiolabel arrived promptly. I would also like to acknowledge my colleagues from the virology laboratories for their advice and friendship, especially Sally Symes for reading this thesis.

To my parents Josip and Tereza, parents-in-law David and Shirley, sister Marianne and great friends Dale Smith, Paula Lawrenz, Wayne Dollery and Tomasovic families, who have supported and encouraged me for many years, thank you for listening, understanding and challenging me throughout my Ph. D.

Finally, I would like to thank my husband, Cameron Wallace for his love, support and encouragement. I'm looking forward to our weekends!

PUBLICATIONS

Some of the major findings presented in Chapters Three and Four are described in the following publications:

Matusan, A. E., Kelley, P. G., Pryor, M. J., Whisstock, J. C., Davidson, A. D. & Wright, P. J. (2001). Mutagenesis of the dengue virus type 2 NS3 proteinase and the production of growth-restricted virus. *Journal of General Virology* **82**, 1647-1656.

Matusan, A. E., Pryor, M. J., Davidson, A. D. & Wright, P. J. (2001). Mutagenesis of the dengue virus type 2 NS3 protein within and outside helicase motifs: effects on enzyme activity and virus replication. *Journal of Virology* **75**, 9633-9643.

ABBREVIATIONS

ATP	adenosine 5′-triphosphate
BME	Eagle's basal medium
bp	base pairs
BSA	bovine serum albumin
BVDV	bovine viral diarrhoea virus
cDNA	complementary DNA
CPE	cytopathic effects
cpm	counts per minute
DEN	dengue virus
DHF	dengue haemorrhagic fever
DMEM	Dulbecco's modified Eagle's medium
dNTPs	deoxynucleotide triphosphates
DNA	deoxyribonucleic acid
DSS	dengue shock syndrome
ER	endoplasmic reticulum
FCS	foetal calf serum
GST	glutathione *S*-transferase
HBSS	Hanks buffered salts solution
HCV	Hepatitis C virus
hr	hour
IF	immunofluorescence

IPTG	isopropyl-β-D-thiogalacto-pyranoside
JEV	Japanese encephalitis virus
kDa	kilodalton
KUN	kunjin virus
min	minute
MOI	multiplicity of infection
NGC	New Guinea C (strain of DEN-2)
NS	nonstructural
nt	nucleotides
NTPase	nucleoside triphosphatase
OE-PCR	overlap extension-polymerase chain reaction
PAGE	polyacrylamide gel electrophoresis
PBS	phosphate buffered saline
PCR	polymerase chain reaction
PDK	primary dog kidney (cells)
p.e.	post electroporation
PEG	polyethylene glycol
pfu	plaque forming units
p.i.	post infection
RIP	radioimmunoprecipitation
RNA	ribonucleic acid
rNTPs	ribonucleoside triphosphates
RT-PCR	reverse transcription-polymerase chain reaction
sec	seconds

SDS	sodium dodecyl sulfate
SDS-PAGE	sodium dodecyl sulphate-polyacrylamide gel electrophoresis
TBE	tick-borne encephalitis virus
UTR	untranslated region
WNV	West Nile virus
YFV	yellow fever virus

CHAPTER ONE: INTRODUCTION

1.1 The family *Flaviviridae*

The family *Flaviviridae* consists of the *Flavivirus, Pestivirus* and *Hepacivirus* genera (reviewed in van Regenmortel, 2000). There are about 80 members of the genus *Flavivirus*, which can be further sub-divided based on serological relatedness and sequence comparisons of flaviviral genomes (Blok *et al.*, 1989; Calisher *et al.*, 1989; Kuno *et al.*, 1998; Zanotto *et al.*, 1996). Most flaviviruses are arthropod borne, being transmitted by mosquitoes or ticks. Other flaviviruses are transmitted between bats or rodents without known insect vectors, and for some, the mode of transmission is not known (reviewed in Monath & Heinz, 1996).

Calisher *et al.* (1989) performed cross-neutralization tests on 66 flaviviruses, and grouped serologically related viruses into one of eight antigenic complexes. The four serotypes of *Dengue virus* (DEN-1 to 4) were grouped into a single antigenic complex. Similar groupings to the serological classifications have been produced following sequence analysis of flaviviral genomes (Blok *et al.*, 1989; Kuno *et al.*, 1998; Monath & Heinz, 1996; Zanotto *et al.*, 1996). The four dengue viruses are more closely related to each other than to the other flaviviruses, with dengue strains of the same serotype varying by ≤ 10% at the nucleotide (nt) level and ≤ 4% at the amino acid (aa) level (Blok *et al.*, 1992; Monath, 1994). A recent study by Worobey *et al.* (1999), which compared 71 published dengue sequences, predicted that recombination occurs in natural populations of dengue virus. A second study by Tolou *et al.* (2001) presented evidence, based on the analysis of DEN-1 genome sequences, for

recombination in natural populations of one Asian and two African DEN-1 strains. Therefore, it is likely that flaviviruses have evolved by recombination and divergent mutational change (Blok *et al.*, 1992; Zanotto *et al.*, 1996).

Throughout this thesis the term flavivirus is used exclusively to refer to members of the genus *Flavivirus*, and not to members of other genera within the family *Flaviviridae*.

1.2 Medical aspects of dengue

The first epidemic of a dengue-like disease was recorded in Philadelphia in 1780 (Rush, 1789). Since then, the principal vector of dengue, the *Aedes aegypti* mosquito, has spread the virus to most of the tropical and sub-tropical regions of the world, exposing more than half the world's human population to the disease (Halstead, 1988). Dengue fever (DF) and the more severe forms of secondary disease, dengue haemorrhagic fever (DHF) and dengue shock syndrome (DSS) are currently the most important human diseases caused by arboviruses (Monath, 1994). It is estimated that up to 100 million cases of DF and 250,000 cases of DHF occur annually on a worldwide basis (Monath, 1994).

The symptoms of DF appear two to seven days after the bite of an infected mosquito. The self-limited infection is often subclinical in children, but most adult infections result in disease (Sinniah & Igarashi, 1995). Symptoms may include fever, headache, muscle and joint pains, anorexia, severe fatigue and variable skin rashes (Monath, 1994; Sinniah & Igarashi, 1995). Dengue infections can also cause encephalitis (Lum *et al.*, 1996; Miagostovich *et al.*, 1997). Although DF can be

debilitating, it is seldom fatal, with improvement usually seen by the second week. However, convalescence can be protracted (Monath, 1994).

The more severe form of dengue virus infection, DHF/DSS was first observed in the Philippines in the 1950s (Hammon *et al.*, 1960). DHF is characterized by high continuous fever, blood-clotting abnormalities, increased vascular permeability and abnormal haemostasis. Progression to DSS is associated with multi-organ failure, haemorrhagic diathesis, hepatomegaly and circulatory disturbances leading to shock (Nimmannitya, 1987). The fatality rate of untreated DHF/DSS was initially as high as 20-50%, but the introduction of intravenous fluid replacement therapy has reduced the fatality rate to between 0.5-4% (Sinniah & Igarashi, 1995).

All four dengue virus serotypes cause DHF/DSS. However, the reasons for the variability in the morbidity and mortality experienced with dengue virus infections is not well understood. There are several factors that may influence the severity of a dengue infection. These include antibody dependent enhancement (ADE) of viral infection and the virulence of the dengue strain.

Dengue infection induces long term immunity to the infecting serotype, but only short term immunity to the others (Halstead, 1988). ADE of viral infection is characterized by enhanced infection of cells bearing Fc receptors. Mononuclear phagocytic cells are target cells of dengue virus, and virus complexed with non-neutralizing antibodies gains additional entry into these cells via Fc receptors (Halstead & O'Rourke, 1977*a*; Halstead & O'Rourke, 1977*b*; Halstead *et al.*, 1977). Subsequent activation of infected monocytes and other immune cells directed against dengue antigens may lead to the release of host immune factors such as cytokines and other chemical modulators, that in turn may result in haemorrhage and increased vascular permeability (Kurane *et al.*, 1994).

Recently Leitmeyer *et al.* (1999) sought to identify differences between viruses associated with DF (the American genotype) and those with the potential to cause DHF/DSS (the Southeast Asian genotype) by sequence analysis of 11 dengue viruses. This study found 55 amino acid changes consistently detected between the two DEN-2 genotypes that had been associated with distinct clinical presentations in humans. However, only 11 of these resulted in a charge or side chain polarity difference. Furthermore, sequence differences (which may affect initiation of translation) were observed within the 5′ untranslated region (UTR), and changes were also present in the 3′ UTR. The latter were predicted to change RNA secondary structures and possibly affect RNA replication. A study by Shurtleff *et al.* (2001) compared the 3′ UTR sequences of 50 DEN-2 strains from a range of geographical regions, including Southeast Asia and the Americas. Their data showed no correlation between variation in the 3′ UTR and disease severity.

Recently Pryor *et al.* (2001) demonstrated that a DEN-2 strain from the Americas, which had not been associated with severe disease, replicated less well in monocyte-derived macrophages (MDMs) than Asian strains. This study also demonstrated that amino acid 390 in the E glycoprotein is important for virus replication in MDMs. Viruses with Asp 390 (present in American strains) showed reduced replication in MDMs when compared with viruses with Asn 390 (found in Thai strains). Identification of amino acid residues associated with disease severity may aid vaccine design.

1.3 The flavivirus virion

Flavivirus virions are approximately 50 nm in diameter, with 5-10 nm surface projections. The nucleocapsid, composed of the structural capsid (C) protein and genomic RNA, is about 30 nm in diameter and is surrounded by a host cell derived lipid bilayer (Murphy, 1980). The other viral structural proteins, membrane (M) and envelope (E), are embedded in the bilayer by carboxy terminal hydrophobic anchors (Rice, 1996). More details on the structural proteins are described later in this chapter.

1.4 The flavivirus genome

Yellow fever virus (YFV) is the prototype flavivirus, and the genome of the 17D vaccine strain of YFV was the first flavivirus genome to be sequenced (Rice *et al.*, 1985). Since then, the nucleotide sequences of many other flaviviruses, including all four serotypes of dengue virus, have been determined and all have a common genomic structure (reviewed by Chambers *et al.*, 1990*a*; Rice, 1996).

The flavivirus genome is an infectious single-stranded (ss) RNA of approximately 11 kb (Stollar *et al.*, 1967). The 5′ end of the genome has a type I methyl cap (m7GpppAmp) followed by the conserved dinucleotide AG. Mosquito and tick borne flaviviruses lack a 3′ terminal poly(A) tail and terminate with the dinucleotide CU. Some isolates of *Tick borne encephalitis virus* (TBE) contain an internal poly(A) tract within the 3′ UTR (Mandl *et al.*, 1991; Wallner *et al.*, 1995).

The flavivirus genome RNA contains a single long open reading frame (ORF) flanked by 5′ and 3′ UTRs with the potential to form specific secondary structures

possibly required for translation, replication and packaging of the genome (Brinton *et al.*, 1986; Mandl *et al.*, 1998).

The 5′ UTRs of flaviviruses are 95-132 nt in length with significant conservation among flaviviruses of the same serocomplex but with little sequence conservation between serocomplexes (Brinton & Dispoto, 1988). Despite this, predicted secondary structures are similar, suggesting an important function for the 5′ UTR. The 3′ UTRs of flaviviruses are 114-750 nt in length, with the 3′ terminal 90 nt forming a stable secondary structure (Brinton *et al.*, 1986; Hahn *et al.*, 1987*b*). This 90 nt region of the genomic RNA of *Japanese encephalitis virus* (JEV) was sufficient to bind the RNA polymerase protein NS5 (Chen *et al.*, 1997*a*).

1.5 Viral entry and translation

Flaviviruses are able to infect and replicate in a range of hosts and cultured cells. The flavivirus E protein mediates the binding of virus to cells (Anderson *et al.*, 1992; Chen *et al.*, 1996). It is known that DEN-4 binds to glycoproteins of M_r 40,000 and 45,000 on the surface of *Aedes albopictus* C6/36 mosquito cells (Salas-Benito & del Angel, 1997), and DEN-2 binds to a highly sulfated form of heparan sulfate on Vero cells (Chen *et al.*, 1997*b*). In addition, a complex of flavivirus and subneutralizing concentrations of antibody may bind to Fc receptors, facilitating virus uptake in cells with such receptors (Porterfield, 1985). This entry mechanism is termed ADE, and may have a role in the development of DHF/DSS.

Following attachment, virus particles accumulate in coated pits on the plasma membrane, which pinch off to form prelysosomal vesicles. The low pH within these vesicles activates membrane fusion via E, and release of the nucleocapsid into the

cytoplasm (reviewed by Greber *et al.*, 1994). The E protein of TBE virus is irreversibly rearranged from a homodimeric to homotrimeric form at acidic pH; this process appears to be required for fusion (Allison *et al.*, 1995).

Direct fusion of DEN-2 virions with the cell membranes of baby hamster kidney (BHK), *Aedes albopictus* C6/36 mosquito and monkey kidney (LLC-MK2) cells and human peripheral blood monocytes has been observed (Hase *et al.*, 1989; Lim & Ng, 1999; Se-Theo *et al.*, 2000).

Following the uncoating of nucleocapsids and the release of viral RNA into the cell, translation begins. Translation of genomic RNA is associated with the rough endoplasmic reticulum, and usually occurs at the first AUG in the ORF, but potentially could also occur at a second AUG located immediately downstream in those flavivirus species where it is present (Castle *et al.*, 1985; Osatomi & Sumiyoshi, 1990).

1.6 Proteolytic processing: an overview

The polyprotein is cleaved co- and post- translationally by host and viral proteinases to produce the virion and replicase components (Chambers *et al.*, 1990*a*; Crawford & Wright, 1987; Rice *et al.*, 1985). The three structural proteins C, M (which is derived from the precursor prM) and E are encoded in the 5' end of the genome, and the seven nonstructural genes, NS1, NS2A, NS2B, NS3, NS4A, NS4B and NS5 are located after the structural genes (Rice, 1996) (Fig. 1.1).

Four proteinases are involved in flavivirus polyprotein processing: the host enzymes signalase and furin, an additional host proteinase with a similar specificity to signalase, and the viral NS2B/3 proteinase. The cleavage mechanisms of each of these

proteinases to generate the individual viral proteins will be discussed in detail in section 1.7.

Briefly, the host signal peptidase or signalase, associated with the endoplasmic reticulum (ER), is responsible for cleavage at the C/prM, prM/E, E/NS1 and NS4A/NS4B junctions (Lin *et al.*, 1993*b*; Markoff, 1989; Nowak *et al.*, 1989). Maturation of prM to M is mediated by the cellular endoproteinase furin, in the acidic post-Golgi vesicles, at a late stage of virus assembly (Murray *et al.*, 1993; Randolph *et al.*, 1990; Ruiz *et al.*, 1989; Stadler *et al.*, 1997). Cleavage at the NS1/NS2A junction is effected by a host membrane-bound ER proteinase, possibly a signalase or another unknown proteinase (Falgout & Markoff, 1995).

The remaining primary cleavages at the NS2A/NS2B, NS2B/NS3, NS3/NS4A and NS4B/NS5 junctions occur in the cytosol and are mediated by the virus-encoded chymotrypsin-like serine proteinase NS2B/3 (Cahour *et al.*, 1992; Falgout *et al.*, 1991; Preugschat *et al.*, 1990; Rice & Strauss, 1990). The consensus sequence at the junction of these proteins consist of a pair of basic amino acids preceeding the cleavage site (Arg-Arg↓, Arg-Lys↓, Lys-Arg↓) or Gln-Arg↓ at the NS2B/NS3 junction in dengue viruses, and followed by either a Gly, Ser or Ala (Biedrzycka *et al.*, 1987; Mackow *et al.*, 1987; Rice *et al.*, 1985; Speight *et al.*, 1988). The viral proteinase also cleaves at additional sites within C and the nonstructural proteins NS2A, NS4A and NS3, in the latter case producing NS3′ and NS3″ (Arias *et al.*, 1993; Lin *et al.*, 1993*a*; Nestorowicz *et al.*, 1994; Nowak *et al.*, 1989; Pugachev *et al.*, 1992; Teo & Wright, 1997; Yamshchikov & Compans, 1994).

1.7 Flavivirus proteins

1.7.1 The C protein

The virion C proteins are small (9-14 kDa) and are highly positively charged, being enriched with Arg and Lys residues, presumably for interaction with the negatively charged viral RNA to form the flavivirus nucleocapsid (Chang, 1997, Rice *et al.*, 1985). Sequence identity of the C proteins is low among flaviviruses, however, the hydrophilicity profile is conserved (Mandl *et al.*, 1988). The carboxy terminus of full length C has a hydrophobic sequence that serves as a membrane anchor, and also functions as a signal sequence for prM (Ruiz *et al.*, 1989).

Processing of the full length C protein may involve three separate cleavages. Firstly, cellular methionine aminopeptidase removes the initial Met from the amino terminus for some flaviviruses (e.g. YFV and JEV) (Rice *et al.*, 1985), although the initial Met of others (e.g. DEN-3) is not cleaved (Osatomi & Sumiyoshi, 1990).

There are two possibilities for the order of the two cleavages that generate and remove the carboxy terminus of full length C to produce virion C. Nowak *et al.* (1989) proposed that following translocation of prM into the ER lumen via the carboxy terminal hydrophobic domain of the full length C, co-translational cleavage at the amino terminus of prM by host signalase generates an membrane-anchored form of full length C. This protein then undergoes secondary cleavage at a conserved cluster of basic residues by the NS2B/3 viral proteinase (14 aa upstream of the C/prM signalase site for DEN-2) to form the carboxy terminus of mature virion C. Others support this order of processing, and suggest upregulation of signal peptidase cleavage by interaction with the nonstructural proteins, particularly NS2B, and that

the NS2B/3 proteinase cleavage depends on, or is facilitated by, interaction of C with viral RNA (Yamshchikov & Compans, 1993l; Yamshchikov & Compans, 1995; Yamshchikov *et al.*, 1997).

An alternative model is that of coordinated cleavages in which the viral proteinase NS2B/3 cleaves at the conserved cluster of basic residues upstream of the carboxy terminus of the full length C protein, followed by a secondary cleavage mediated by the host signal peptidase to generate the amino terminus of prM. This model is supported by data which shows that signal peptidase cleavage cannot occur efficiently at the C/prM junction in the absence of an active viral proteinase (Amberg *et al.*, 1994; Amberg & Rice, 1999; Lobigs, 1993; Stocks & Lobigs, 1995; Stocks & Lobigs, 1998). In addition, Lee *et al.* (2000) demonstrated that substitutions in the prM signal sequence which disrupt coordinated cleavages at the C/prM junction, when incorporated into a genomic length cDNA clone, had a negative effect on mutant virus replication. All recovered viruses had reversions and second site mutations in the prM translocation signal sequence.

1.7.2 The prM and M proteins

The prM protein (21-26 kDa) is the glycosylated precursor to the structural protein M (7-9 kDa) (Rice, 1996). The prM protein is translocated into the ER lumen using the carboxy terminal hydrophobic signal sequence of C. Here glycosylation of prM occurs. The carboxy terminus of prM has two hydrophobic domains separated by a charged residue, providing a stop transfer sequence for prM, and a signal sequence for translocation of the E protein into the ER lumen (Gruenberg & Wright, 1992; Mandl *et al.*, 1989*a*; Markoff, 1989; Ruiz *et al.*, 1989). It is in the ER lumen that the

prM/E junction is cleaved by host signal peptidase (Chambers *et al.*, 1990*a*). The host proteinase furin is involved in the secondary cleavage of prM to the mature form M (Stadler *et al.*, 1997) after the conserved cleavage sequence Arg-X-Arg/Lys-Arg, where X is variable (Coia *et al.*, 1988; Rice *et al.*, 1985). The amino terminal pr is hydrophilic and contains one to three glycosylation sites and six conserved Cys residues (Chambers *et al.*, 1990*a*; Murray *et al.*, 1993; Nowak & Wengler, 1987).

The prM protein is important in preserving the conformation of the E protein at acidic pH (Heinz *et al.*, 1994) with prM and E association (Wengler & Wengler, 1989) preventing immature virions exhibiting fusion activity before leaving the cell (Guirakhoo *et al.*, 1991). Antibodies directed against prM and M proteins may be important in flavivirus infections, since Takegami *et al.* (1982) showed that polyclonal antibodies against the M protein of JEV had neutralising activity, while Kaufman *et al.* (1989) demonstrated that prM-specific monoclonal antibodies protected mice against dengue infection.

1.7.3 The E protein

The E protein (55-60 kDa) is the major protein of the virion and is glycosylated in most but not all flaviviruses (Castle *et al.*, 1985; Coia *et al.*, 1988). The protein is the most conserved structural protein and is important for virion assembly, receptor binding (Anderson *et al.*, 1992; Chen *et al.*, 1997*b*; Summers *et al.*, 1989), membrane fusion (Guirakhoo *et al.*, 1989; Kimura & Ohyama, 1988), haemagglutination (Shapiro *et al.*, 1971), and is the main target for neutralizing antibody in the protective immune response (reviewed in Gould *et al.*, 1990).

Rey *et al.* (1995) determined the X-ray crystal structure of a soluble fragment of E (amino acids 1-395) of TBE. The protein has three domains. Domain I includes the only glycan of TBE and several surface exposed regions. Domain II is believed to be involved in E protein dimerization and viral and endosomal membrane fusion. Domain III is likely to be involved in cellular attachment (Chen *et al.*, 1997*b*; Rey *et al.*, 1995).

The carboxy terminus of prM contains hydrophobic domains for translocation of the E protein across the ER (Markoff, 1989; Nowak *et al.*, 1989; Ruiz *et al.*, 1989). The E protein is then processed at its amino and carboxy termini by a host signal peptidase (Chambers *et al.*, 1990*a*). The E protein contains two adjacent hydrophobic regions at the carboxy terminus for stop transfer and membrane anchoring of E, and signal sequences for NS1 translocation (Falgout *et al.*, 1989; Markoff, 1989; Nowak *et al.*, 1989; Ruiz *et al.*, 1989; Wright *et al.*, 1989).

1.7.4 The NS1 protein

The NS1 protein (42-51 kDa) is the first nonstructural protein in the flavivirus polyprotein. It follows the E protein, which contains a hydrophobic signal sequence for the translocation of NS1 into the ER (Biedrzycka *et al.*, 1987; Cauchi *et al.*, 1991).

After translocation into the lumen of the ER, the E/NS1 junction is cleaved by a host signalase, and NS1 undergoes core glycosylation at up to three N-linked glycosylation sites (Chambers *et al.*, 1990*a*; Falgout *et al.*, 1989; Nowak *et al.*, 1989; Wright *et al.*, 1989). The NS1/NS2A junction is cleaved by an unidentified proteinase which requires a minimum length of eight amino acids at the carboxy terminus of NS1 as well as downstream NS2A sequences (at least the amino terminal 145 aa)

(Falgout *et al.*, 1989; Falgout & Markoff, 1995; Hori & Lai, 1990; Pethel *et al.*, 1992).

A study by Jacobs *et al.* (2000) showed, that in the presence of the first 26 aa of NS2A, the DEN-2 NS1 glycoprotein can be processed to a glycosyl-phosphatidylinositol (GPI)-linked form that can be expressed on the surface of DEN-2 infected cells. The authors suggest that subsequent antibody-induced signal transduction by GPI-linked NS1 may contribute to the pathogenesis of dengue viruses.

Newly synthesised NS1 is a monomer and rapidly dimerizes, becoming membrane bound and more hydrophobic (Winkler *et al.*, 1988; Winkler *et al.*, 1989). Dimerization and secretion of the protein is dependent on the carboxy terminal portion of the protein which contains several strictly conserved Cys residues (Coia *et al.*, 1988; Pryor & Wright, 1993).

Muylaert *et al.* (1997) demonstrated, by mutagenesis of the first glycosylation site of YFV NS1, that translocation and modification of YFV NS1 is important for efficient viral RNA replication. Studies using immunofluorescence and immunoelectron microscopy provide evidence that NS1 may be involved in RNA replication (Mackenzie *et al.*, 1996; Westaway *et al.*, 1997*b*). The role of NS1 in replication may include direct interaction with other viral proteins (particularly NS4A) during assembly of the replication complex (RC) and directing the RC to membranes (Lindenbach & Rice, 1997; Lindenbach & Rice, 1999).

1.7.5 The NS2A and NS2B proteins

The flavivirus NS2A (23-25 kDa) and NS2B (13-15 kDa) proteins are small hydrophobic proteins with low overall sequence conservation but with similar hydrophobicity profiles amongst flaviviruses, suggesting membrane association (Coia *et al.*, 1988; Hahn *et al.*, 1988; Mandl *et al.*, 1989*b*). A role for NS2A in replication has been proposed as it appears to be associated with double stranded (ds) RNA and the RC (Chu & Westaway, 1992; Mackenzie *et al.*, 1998; Westaway *et al.*, 1997*b*). For DEN-2, the amino terminal 26 aa of NS2A can act as a GPI-anchor addition signal sequence for NS1 (Jacobs *et al.*, 2000).

NS2A is also required for correct cleavage of NS1 at its carboxy terminus (see above) (Falgout *et al.*, 1989), although the proteinase responsible for cleavage of NS1/NS2A, as stated earlier, is unknown (Falgout & Markoff, 1995). Processing at the NS2A/NS2B and NS2B/NS3 junctions occurs in the cytosol and is mediated by the viral NS2B/3 proteinase which can cleave in *cis* and in *trans* with varying efficiencies (Chambers *et al.*, 1991; Falgout *et al.*, 1991; Lobigs, 1992; Preugschat *et al.*, 1990). An additional cleavage within NS2A by the viral proteinase NS2B/3 has been reported for YFV and JEV (Chambers *et al.*, 1990*a*; Jan *et al.*, 1995; Nestorowicz *et al.*, 1994). Nestorowicz *et al.* (1994) identified a cleavage site, Gln-Lys↓Thr (designated NS2A$^{\alpha}$) at residues 132-134 of YFV NS2A (length 167 aa) that generates the smaller 20 kDa form of NS2A. Mutations which abolished this or the normal NS2A/NS2B cleavage were introduced into genomic length YFV cDNA and virus was not recovered indicating the importance of the different forms of NS2A in virus replication (Nestorowicz *et al.*, 1994). There seems to be no obligate order for processing of YFV NS2A, as processing at the NS2A/NS2B junction occurred in

polyproteins containing mutations that abolished the NS2A$^{\alpha}$ site, and vice versa (Nestorowicz *et al.*, 1994).

The NS2B protein is required as a cofactor to enhance or modulate the NS3 proteinase activity, possibly by enabling NS3 to form a stable conformation for activity (Chambers *et al.*, 1993; Falgout *et al.*, 1993; Falgout *et al.*, 1991; Preugschat *et al.*, 1990). The sequences in NS2B required for interaction with NS3 have been studied (Chambers *et al.*, 1993; Droll *et al.*, 2000; Falgout *et al.*, 1993). Falgout *et al.* (1993) identified a sequence of 40 aa (overall hydrophilic) in DEN-4 NS2B (Leu_{53}-Thr_{92}) which contains some residues highly conserved among flaviviruses, and which is required for both proteinase activity and association of NS2B with the NS3 proteinase (Chambers *et al.*, 1993) (Fig. 1.2). For the hepacivirus *Hepatitis C virus* (HCV) NS3/4A proteinase, which is activated by the downstream NS4A protein, the cofactor activity resides in a hydrophobic 12 aa central region of NS4A (Bartenschlager *et al.*, 1995; Butkiewicz *et al.*, 1996; Failla *et al.*, 1994; Koch *et al.*, 1996; Lin *et al.*, 1995). By comparisons of sequence alignments, Brinkworth *et al.* (1999) identified the central hydrophobic region of 12 aa (within the previously identified 40 aa segment) of DEN-2 NS2B (Gly_{69}-Glu_{80}) analogous to the NS4A cofactor sequence of HCV proteinase (Fig. 1.2). The NS2B/3 viral proteinase is described in more detail later in this chapter.

In addition to activating proteolytic activity, NS2B may promote membrane association of the NS3/NS2B complex by way of hydrophobic regions (Brinkworth *et al.*, 1999; Clum *et al.*, 1997; Droll *et al.*, 2000). Immunocytochemical analysis of cells infected with *Kunjin virus* (KUN) has shown that NS2B and NS3 are present within specific virus-induced cytoplasmic convoluted and paracrystalline membrane structures where polyprotein processing is proposed to occur, releasing nonstructural

proteins for assembly of the RC (Mackenzie *et al.*, 1999; Mackenzie *et al.*, 1998; Westaway *et al.*, 1999; Westaway *et al.*, 1997*b*). This complex probably consists of the viral proteins NS1, NS2A, NS3, NS4A and NS5 (Khromykh *et al.*, 1999*b*).

Evidence for a function of NS2B in addition to proteolysis has been obtained for YFV. Deletion mutagenesis of hydrophobic regions of YFV NS2B resulted in unchanged levels of proteolytic activity in a cell-free translation system, but no virus replication when introduced into genomic length YFV cDNA (Chambers *et al.*, 1993). It is possible that these mutations disrupt the assembly or function of the replication complex. Chu and Westaway (1992) have also shown that NS2B can be isolated in fractions containing the NS5 protein, the RNA dependent RNA polymerase (RdRp).

1.7.6 The NS3 protein

NS3 is the second largest (68.5-69.5 kDa) nonstructural protein and is highly conserved among flaviviruses (Coia *et al.*, 1988; Deubel *et al.*, 1988; Mandl *et al.*, 1989*b*; Rice *et al.*, 1986). NS3 is a multifunctional protein with enzymatic motifs for proteinase, helicase, nucleoside triphosphatase (NTPase) and RNA triphosphatase activities (Fig. 1.3) (Bazan & Fletterick, 1989; Koonin & Dolja, 1993; Wengler & Wengler, 1993).

Site directed mutagenesis, deletion analysis, and the recently reported X-ray crystal structure of the NS3 proteinase of DEN-2 indicate that the proteinase region is contained within the amino terminal 181 amino acids of NS3 (Chambers *et al.*, 1990*b*; Li *et al.*, 1999; Murthy *et al.*, 1999; Preugschat *et al.*, 1990). The carboxy terminal two-thirds of NS3 has seven motifs characteristic of RNA helicases of the DExH subfamily. Several forms of recombinant proteins containing the carboxy terminal

helicase region of flavivirus NS3 have been shown to possess RNA stimulated NTPase activity (Borowski *et al.*, 2001; Kuo *et al.*, 1996; Li *et al.*, 1999; Takegami *et al.*, 1994; Warrener *et al.*, 1993; Wengler & Wengler, 1991) and RNA helicase activity (Borowski *et al.*, 2001; Li *et al.*, 1999; Utama *et al.*, 2000*b*). The RNA helicase activity of NS3 will be discussed further in section 1.9.

Both termini of the NS3 protein are generated by the viral NS2B/3 proteinase (Chambers *et al.*, 1995). The NS2B/3 proteinase cleaves after a Gln-Arg doublet at the carboxy terminus of NS2B in dengue viruses, whereas cleavage usually occurs after a pair of basic amino acids (Arg-Arg , Lys-Arg, Arg-Lys) (Biedrzycka *et al.*, 1987; Mackow *et al.*, 1987; Speight *et al.*, 1988).

A truncated form of NS3, the 50 kDa NS3′ protein can be detected in lysates of flavivirus infected cells (Arias *et al.*, 1993; Pugachev *et al.*, 1992; Zhang & Padmanabhan, 1993). For DEN-2, NS3′ contains the amino terminal approximately 450 aa of NS3 and is produced by cleavage within helicase motif VI, after two conserved Arg residues at NS3 positions 457-458 (Arias *et al.*, 1993; Teo & Wright, 1997). The remainder of NS3 (NS3″) was detected as a 19 kDa protein (161 aa) and prior cleavage at the NS2B/NS3 site was not required for formation of NS3′ and NS3″ (Teo & Wright, 1997).

1.7.7 The NS4A and NS4B proteins

The flavivirus NS4A (16-16.4 kDa) and NS4B (26.5-28 kDa) proteins are small hydrophobic proteins which show little sequence conservation amongst flaviviruses, although their hydrophobicity plots amongst flaviviruses are remarkably similar (Chambers *et al.*, 1990*a*; Coia *et al.*, 1988; Mandl *et al.*, 1989*b*).

Cleavage at the NS3/NS4A junction is mediated by the viral proteinase (Cahour *et al.*, 1992; Falgout *et al.*, 1991; Lin *et al.*, 1993*a*; Preugschat & Strauss, 1991). Cleavage at the NS4A/NS4B junction has been studied for YFV and DEN-4 (Cahour *et al.*, 1992; Falgout *et al.*, 1991; Lin *et al.*, 1993*b*; Preugschat & Strauss, 1991). Lin *et al.* (1993*b*) demonstrated that the amino terminus of YFV NS4B is generated by a signalase cleavage. However, it appears that this cleavage requires prior cleavage by the NS2B/3 viral proteinase at a conserved site called 4A/2K, located 23 residues upstream of the signalase cleavage site (Preugschat & Strauss, 1991). In contrast, the results obtained with DEN-4 showed that signalase cleavage at the NS4A/NS4B junction could occur in the absence of the NS2B/3 viral proteinase (Cahour *et al.*, 1992; Falgout *et al.*, 1991). The NS4B/NS5 cleavage is effected by the viral proteinase, and may occur when the proteinase is present in *trans* (Cahour *et al.*, 1992; Chambers *et al.*, 1991).

NS4A is predicted to be membrane spanning and was shown by cryoimmunoelectron microscopy to be associated with vesicle packets, (within which the KUN RC is located) and enriched in convoluted membranes and paracrystalline structures (Mackenzie *et al.*, 1998; Westaway *et al.*, 1997*b*). It has been proposed that NS4A may play a targeting or membrane anchoring role within the RC (Khromykh *et al.*, 1999*a*; Khromykh *et al.*, 1999*b*; Lindenbach & Rice, 1999; Mackenzie *et al.*, 1998). NS4A binding to other proteins of the RC, particularly NS3, NS5, NS2A, and possibly NS1 and also strongly to itself, has been demonstrated (Mackenzie *et al.*, 1998). The colocalization of NS4A in vesicle packets is consistent with evidence obtained by Lindenbach and Rice (1999), using the YFV infectious clone, which demonstrated that an NS1-NS4A interaction is important for viral RNA replication.

The NS4B protein is the largest of the four small hydrophobic proteins of flaviviruses. NS4B is membrane associated in the cytoplasm, and has been shown to migrate to the nucleus and spread throughout the nucleoplasm (Khromykh *et al.*, 2000; Westaway *et al.*, 1997*a*). A role for NS4B in viral replication has not yet been shown, and NS4B is not present in the proposed KUN RC (Khromykh *et al.*, 2000; Mackenzie *et al.*, 1998; Westaway *et al.*, 1997*a*; Westaway *et al.*, 1997*b*).

1.7.8 The NS5 protein

The NS5 protein (103-105 kDa) is the largest and most conserved flavivirus protein (Coia *et al.*, 1988; Hahn *et al.*, 1988). The carboxy terminal half of NS5 has eight conserved RdRp motifs (Koonin, 1991; O'Reilly & Kao, 1998). These motifs are presumed to be involved in RNA binding, catalytic activity and the formation of correct secondary structures of RdRps (Koonin, 1991; O'Reilly & Kao, 1998). Recombinant NS5 of DEN-1 and KUN has been shown to possess RdRp activity *in vitro* (Guyatt, 1999; Tan *et al.*, 1996).

The amino terminal half of the flavivirus NS5 protein contains two conserved regions characteristic of methyltransferases that use *S*-adenosylmethionine (SAM) as the methyl group donor (Koonin & Dolja, 1993). Deletion of the SAM binding site in the NS5 gene of the KUN genomic length clone abolished viral replication (Khromykh *et al.*, 1998).

Forwood *et al.* (1999) identified a bipartite nuclear localization sequence spanning 37 aa (residues 369-405 of DEN-2) within the linker region between the SAM binding site and RdRp region. Studies have shown that the NS5 protein can be detected in the nucleus of infected cells (Buckley *et al.*, 1992; Kapoor *et al.*, 1995).

This nuclear localization sequence may play a role in targeting NS5 to the nucleus in a regulated manner during the virus infectious cycle (Forwood *et al.*, 1999; Kapoor *et al.*, 1995).

There is also evidence that NS5 interacts with both NS3 and stem loop structures in the 3′ UTR, possibly playing a role in the initiation of negative strand RNA synthesis (Chen *et al.*, 1997*a*; Kapoor *et al.*, 1995). The involvement of NS5 in viral replication is further discussed in section 1.10.

1.8 The viral proteinase

1.8.1 Constitution of the viral proteinase

The flavivirus-encoded proteinase has been shown to consist of two of the nonstructural proteins, NS2B and NS3. Site directed mutagenesis and deletion analysis have established that the proteinase region is contained within approximately the amino terminal 181 aa of NS3 (Chambers *et al.*, 1990*b*; Preugschat *et al.*, 1990). For DEN-2, the minimal NS3 proteinase region required for cleavage of the NS2B/NS3 site is 167 residues (Li *et al.*, 1999). Four regions were identified within the amino terminal 181 aa of flaviviruses which shared homology with chymotrypsin-like serine proteinases (Bazan & Fletterick, 1989; Gorbalenya & Koonin, 1989). Three of these regions contain one amino acid of the catalytic triad (His_{51}, Arg_{75}, Ser_{135} in DEN-2), while the fourth is proposed to be part of the substrate binding region (Fig. 1.3) (Preugschat & Strauss, 1991; Valle & Falgout, 1998). The X-ray crystal structure for this part of DEN-2 NS3 was described recently by Murthy *et al.* (1999), and will be discussed in section 1.8.2.

The NS3 protein alone exhibits little proteinase activity and the cofactor NS2B protein is needed to enhance or modulate proteinase activity (Chambers *et al.*, 1991; Falgout *et al.*, 1991; Preugschat *et al.*, 1990). The NS2B and NS3 proteins of DEN-2 form a stable complex, suggesting that the enzymatically active proteinase is a heterodimer (Arias *et al.*, 1993).

1.8.2 Proteinase X-ray crystal structure

Murthy *et al.* (1999) reported the X-ray crystal structure at 2.1Å resolution of residues 1-185 of the NS3 proteinase domain from the New Guinea C (NGC) strain of DEN-2. Brinkworth *et al.* (1999) constructed a homology model of the DEN-2 NS2B/3 proteinase based on the structure of the HCV complex of NS3 and NS4A (Yan *et al.*, 1998). These structures confirmed earlier predictions that the NS3 proteinase adopts a chymotrypsin-like fold and showed the enzyme active site and the cofactor binding site.

The NS3 proteinase folds into two structural domains which are separated by a substrate binding cleft which contains the active site with the catalytic triad (Murthy *et al.*, 1999). In the homology model of DEN-2 NS2B/3, the cofactor is located within a hydrophobic core formed by the amino terminal region of the NS3 proteinase (Brinkworth *et al.*, 1999). Although there are structural similarities between the DEN-2 and HCV NS3 proteinases, there are also notable differences. The HCV NS3 proteinase structure has a zinc binding site and a long hydrophobic amino terminal loop which are absent in the DEN-2 proteinase structure (Kim *et al.*, 1996; Love *et al.*, 1996; Murthy *et al.*, 1999; Yan *et al.*, 1998). These differences may be characteristic of significant differences in the mode of catalysis by HCV and DEN-2

proteinases. Substrate specificities, particularly at the P1 position are different i.e. HCV prefers a Cys at P1 for some cleavages, whereas DEN-2 prefers a basic residue (Lys or Arg) for all cleavages (Bartenschlager *et al.*, 1993; Chambers *et al.*, 1990*a*; Eckart *et al.*, 1993). In addition, a 40 aa segment of NS2B that was overall hydrophilic is required for DEN-4 NS3 proteinase activation, whereas the HCV NS4A activation peptide is 12 largely hydrophobic amino acids (Butkiewicz *et al.*, 1996; Falgout *et al.*, 1993; Lin *et al.*, 1995; Tomei *et al.*, 1996). Brinkworth *et al.* (1999) identified a largely hydrophobic 12 aa region corresponding to the shorter hydrophobic cofactor of HCV NS4 within the previously described 40 aa hydophilic segment of DEN-2 NS2B. Recently, the hydrophobic 12 aa sequence, located within the conserved 40 aa NS2B sequence of YFV was mutated by charged-to-alanine mutagenesis. Three residues were changed individually and did not significantly reduce proteinase activity in a cell-free system, indicating this region is not critical for cofactor-proteinase interaction or enzyme activity *in vitro*; however the effects of the mutations on virus replication was not analyzed (Droll *et al.*, 2000).

Previously, deletion mutagenesis of the entire NS2B protein (both within and external to the overall hydrophilic 40 aa segment) was used to analyze the regions within NS2B important for proteinase activity. Deletions of as few as three amino acids had a deleterious effect on protein conformation and therefore may impair NS2B-NS3 association (Chambers *et al.*, 1993; Falgout *et al.*, 1993). Thus the precise region of NS2B required for NS2B-NS3 association and hence for optimal NS3 proteinase activity is still unknown.

1.9 The viral helicase

RNA viruses evolve rapidly, leading to sequence divergence even among related viruses within a family (Koonin & Dolja, 1993). Thus, only critical functional motifs are conserved between virus groups, primarily the motifs within proteins involved in various aspects of viral replication, transcription and translation, such as RNA helicases (Gorbalenya & Koonin, 1989; Koonin & Dolja, 1993).

RNA helicases catalyze the unidirectional unwinding of duplex RNAs *in vitro* (containing a ssRNA region of at least 3 nt) in the presence of a divalent cation and require the hydrolysis of the β-γ bond of a suitable NTP or deoxy-NTP (usually ATP) as an energy source (Lain *et al.*, 1990; Paolini *et al.*, 2000*a*). Assays of the NTPase and RNA binding activity of putative viral RNA helicases have also been extensively studied, and are discussed in later sections.

Although definitive experiments for a flavivirus have not been reported, RNA helicase activity is thought to be essential for virus growth. This was shown for the pestivirus *Bovine viral diarrhea virus* (BVDV) by Gu *et al.* (2000), who demonstrated that mutagenesis of two invariant residues in motifs I and II, and deletion of motif VI, abolished virus replication and more specifically minus strand synthesis.

Replication of the flavivirus positive-sense RNA genome initially requires the translation of virion RNA to produce the viral proteins, especially those needed for replication. The incoming RNA also serves as a template for the synthesis of a complementary negative-sense RNA strand. Negative-sense RNA strands are, in turn, used as templates to synthesize positive strands. RNA synthesis occurs asymmetrically in a semiconservative fashion. This semiconservative replication involves two RNA species: the replicative form (RF), defined as a duplex RNA

molecule, which serves as a recycling template, and the replicative intermediate (RI) which is partially double-stranded, with nascent single-stranded tails (for a review see Westaway, 1987). These RNA species are detected both in infected cells and in *in vitro* assays (Brinton, 1986; Chambers *et al.*, 1990*a*). As the negative and positive RNA strands are complementary, NS3 RNA helicase is thought to be required for strand separation. NS3 RNA helicase may also be involved in translation by removing positive strand RNA secondary structures and allowing progression of the ribosomes on template RNA.

1.9.1 Classification of NS3 helicase

DNA and RNA helicases of prokaryotic, eukaryotic, and viral origin have unique arrays of conserved amino acid sequence motifs enabling their classification into three distinct superfamilies (Gorbalenya & Koonin, 1989; Koonin & Dolja, 1993; Lain *et al.*, 1989). Classification is mainly based on sequence motifs that are shared among proteins in each superfamily, but not across superfamilies. Superfamilies 1 and 2 possess seven conserved motifs, with members of superfamily 3 possessing only three such motifs (Fig 1.4) (Koonin & Dolja, 1993). Although the number of motifs may not be conserved across the superfamilies, some specific motifs are (motifs I and II) (Fig. 1.4), and are presumably required for replication (Eagles *et al.*, 1994; Fuller-Pace, 1994). DEN-2 NS3 helicase and related NS3-like proteins in the family *Flaviviridae* are classified in helicase superfamily 2 (Gorbalenya & Koonin, 1989).

1.9.2 The NS3 helicase

For flaviviruses, RNA helicase activity has been demonstrated for DEN-2, JEV and *West Nile virus* (WNV) (Borowski *et al.*, 2001; Li *et al.*, 1999; Utama *et al.*, 2000*b*). Details of the helicases of the virus family *Flaviviridae* will be presented later in this section.

The flavivirus serine proteinase and RNA helicase domains of NS3 can be synthesized independently and are catalytically active (Chambers *et al.*, 1993; Chambers *et al.*, 1990*b*; Droll *et al.*, 2000; Falgout *et al.*, 1993; Falgout *et al.*, 1991; Kuo *et al.*, 1996; Li *et al.*, 1999; Preugschat *et al.*, 1990; Utama *et al.*, 2000*b*; Warrener *et al.*, 1993; Wengler & Wengler, 1991). The NS2B and the amino terminal proteinase domain of NS3 are not required for the *in vitro* enzyme activity of the NS3 helicase domain.

1.9.3 Basal and nucleic acid stimulated NTPase activity

RNA stimulated NTPase activity has been demonstrated for the putative RNA helicase proteins of flaviviruses (Borowski *et al.*, 2001; Kuo *et al.*, 1996; Li *et al.*, 1999; Takegami *et al.*, 1994; Utama *et al.*, 2000*b*; Warrener *et al.*, 1993; Wengler & Wengler, 1991), pestiviruses (Tamura *et al.*, 1993; Warrener *et al.*, 1995), HCV (Gallinari *et al.*, 1998; Gwack *et al.*, 1999; Hong *et al.*, 1996; Jin & Peterson, 1995; Kim *et al.*, 1995; Kim *et al.*, 1997*a*; Lin & Kim, 1999; Preugschat *et al.*, 1996; Suzich *et al.*, 1993; Wardell *et al.*, 1999), and *Hepatitis G virus* (Laxton *et al.*, 1998).

For the flavivirus NS3 proteins synthesized and assayed for NTPase activity to date, the majority were truncated and demonstrated a dependence on the addition of 2-

3 mM Mg^{2+} or Mn^{2+}. Activity could be stimulated for JEV, WNV, YFV, and DEN-2 NS3 proteins by the addition of single stranded polynucleotides (Borowski *et al.*, 2001; Kuo *et al.*, 1996; Li *et al.*, 1999; Warrener *et al.*, 1993; Wengler & Wengler, 1991). The exception was the full length NS3 protein of DEN-1 which was not stimulated by the addition of poly(A) or poly(U), but was shown to be specifically stimulated by the DEN-1 NS5 protein (Cui *et al.*, 1998). A summary of flavivirus ATPases is shown in Table 1.1.

1.9.4 RNA binding activity

The DEN-1 full length NS3 is the only flavivirus protein assayed for RNA binding activity to date. This protein was shown to bind specifically to the 3′ UTR of DEN-1 in RNA band shift assays (Cui *et al.*, 1998). Furthermore, it bound preferentially to a 94 nt RNA transcript from the 3′ UTR of DEN-1 in the presence of various unlabelled competitor RNAs (Cui *et al.*, 1998).

1.9.5 RNA helicase activity

Li *et al.* (1999) first demonstrated NS3 helicase activity for a flavivirus using a His-tagged polyprotein corresponding to the carboxy terminal 458 (amino acids 161-618) residues of DEN-2 NS3, synthesized in *E. coli*. Recently, helicase activity was demonstrated for the flaviviruses JEV and WNV. The JEV helicase assayed was also a truncated (amino acids 163-619) form of the NS3 protein with a His-tag, synthesized in *E. coli* (Utama *et al.*, 2000*a*; Utama *et al.*, 2000*b*). The WNV helicase was purified from virus infected Vero cells (Borowski *et al.*, 2001).

Mutational analyses of JEV, *Vaccinia virus* and HCV helicases have shown that viral RNA helicase activity requires the energy released during NTP hydrolysis, but NTPase activity does not require helicase activity (Gross & Shuman, 1995; Heilek & Peterson, 1997; Preugschat *et al.*, 1996; Utama *et al.*, 2000*a*). In contrast, recently Borowski *et al.* (2001) showed that by using compounds that are potent modulators of enzyme activity, the WNV NTPase/helicase activities could be inhibited or activated independently of each other, implying that NTPase activity is not directly coupled to helicase activity. In common with other helicases, the flavivirus NS3 helicase requires the Mg^{2+} or Mn^{2+} dependent hydrolysis of NTPs to provide the energy for unwinding (Borowski *et al.*, 2001; Li *et al.*, 1999; Utama *et al.*, 2000*a*; Utama *et al.*, 2000*b*).

Previous work on *Vaccinia virus* NTP phosphorylase II (NPH-II), BVDV and HCV NS3 helicases have shown a requirement of a minimum 3 nt single stranded region (3′ extension) in order to unwind double stranded RNA, in a 3′ to 5′ direction (defined by the strand with the extension) (Gross & Shuman, 1996*b*; Hong *et al.*, 1996; Paolini *et al.*, 2000*a*; Warrener & Collett, 1995). In addition to double stranded RNA unwinding, these enzymes demonstrate RNA-DNA heteroduplex unwinding, with the HCV and BVDV NS3 helicase proteins also unwinding double stranded DNA (Gross & Shuman, 1996*b*; Gwack *et al.*, 1996; Gwack *et al.*, 1997; Heilek & Peterson, 1997; Tai *et al.*, 1996). Double stranded RNA and DNA substrates have been used as templates to demonstrate unwinding by flavivirus NS3 helicases (Borowski *et al.*, 2001; Li *et al.*, 1999; Utama *et al.*, 2000*a*; Utama *et al.*, 2000*b*). To date, assays of helicases *in vitro* have not shown any sequence specificity in their nucleic acid substrate requirement.

1.9.6 Function of the conserved motifs in NS3 helicase

Mutational and structural analyses of the conserved helicase proteins of viruses of the *Flaviviridae* have begun to elucidate roles for the various motifs in NTPase/helicase enzymatic activities. Motifs I and II (also known as Walker motifs A and B respectively) (Fig. 1.4), are common to members of all three helicase superfamilies (Koonin & Dolja, 1993; Walker *et al.*, 1982). Motifs Ia, IV and V have not, as yet, been ascribed a function. Motif VI, although present in both superfamilies 1 and 2, is quite different between superfamilies (Koonin & Dolja, 1993). The roles of motifs I, II, III and VI in enzyme activity will be discussed in later sections.

1.9.6(a) Helicase motif I

Motif I is characterized by an amino acid sequence of 2-5 hydrophobic residues followed by G/AxxGxGKS/T (x represents any amino acid) (Fuller-Pace, 1994; Gorbalenya & Koonin, 1989). This motif forms an NTP binding pocket and is a common motif in NTP binding proteins (Saraste *et al.*, 1990). Mutational and crystallographic studies show motif I forms a phosphate binding loop or P loop (Fig. 1.5), and that the invariant Lys residue in the purine binding consensus sequence GxGKT contributes to the binding of purine nucleotides by interaction with the β and γ phosphoryl group(s) of the nucleotide (Clertant & Cuzin, 1982; Gross & Shuman, 1995; Kim *et al.*, 1998; Subramanya *et al.*, 1996). Substitution of the corresponding Lys residue of helicase motif I in HCV and BVDV inhibited or abolished basal and nucleic acid stimulated NTPase and RNA helicase activities (Gu *et al.*, 2000; Heilek & Peterson, 1997; Kim *et al.*, 1997*b*; Min *et al.*, 1999; Wardell *et al.*, 1999) and also

stopped virus replication when incorporated into a BVDV genomic length cDNA (Gu *et al.*, 2000).

1.9.6(b) Helicase motif II

Helicases can be further classified into DEAD, DExH, and DExx subfamilies based on the sequence of motif II (Luking *et al.*, 1998; Schmid & Linder, 1992). DEN-2, along with other flaviviruses, belong to the DExH (DEAH) subfamily. Three X-ray crystal structures of the related HCV NS3 helicase show that motif II is positioned close to motif I (Cho *et al.*, 1998; Kim *et al.*, 1998; Yao *et al.*, 1997). For several kinases, the first conserved Asp has been shown to bind a Mg^{2+}-NTP complex for NTP hydrolysis (Black & Hruby, 1992; Pai *et al.*, 1990; Yan & Tsai, 1991). Mutational studies of motif II DExH helicases of HCV and JEV have shown this motif is important for helicase activity (Gross & Shuman, 1995; Heilek & Peterson, 1997; Kim *et al.*, 1997*b*; Min *et al.*, 1999; Utama *et al.*, 2000*a*; Utama *et al.*, 2000*b*; Wardell *et al.*, 1999). Interestingly, Ala substitution of the conserved His residue in motif II of HCV and JEV NS3, and *Vaccinia virus* NPH-II, had little effect on NTPase, but abolished helicase activity, uncoupling the two activities (Gross & Shuman, 1995; Gu *et al.*, 2000; Heilek & Peterson, 1997; Utama *et al.*, 2000*a*). In contrast, in a separate study, Kim *et al.* (1997*b*) showed mutation of the same HCV NS3 His residue to Ala did not abolish helicase activity, but only reduced it to 60% of parental activity. The authors speculate that the reason for the disparity may be due to variation in the methods of expression (types of fusions and truncations), the purification procedures, assay conditions and/or any additional mutation within the mutant HCV NS3 protein which was not fully sequenced.

1.9.6(c) Helicase motif III

Motif III contains a conserved TATPP sequence which is unique to helicase superfamily 2 (Fig. 1.4) (Koonin & Dolja, 1993). Analysis of the HCV NS3 X-ray crystal structure indicates this motif functions as a switch or hinge region to couple conformational changes accompanying NTP hydrolysis (Yao *et al.*, 1997). To date, this motif has not been targeted for mutagenesis in any flavivirus NS3 protein, but Kim *et al.* (1997*b*) mutated the first Thr in the related HCV NS3 protein to Ala. This mutant possessed parental levels of basal ATPase activity. Unlike the parental protein, the ATPase activity of the mutant protein was not stimulated by the addition of poly(U). The mutant protein retained RNA binding activity, but had RNA helicase activity only 50% of the parental protein.

1.9.6(d) Helicase motif VI

The role of the final motif VI, QRxGRxGR, in flavivirus NS3 helicase is unresolved. Mutational studies of motif VI in other helicases have resulted in conflicting data. Initial mutagenesis studies of motif VI of eIF-4A resulted in a loss of RNA binding and reduced ATPase activity (Pause *et al.*, 1993). It was suggested this region is necessary and sufficient for RNA binding. However, the RNA binding activity of *Vaccinia virus* NPH-II protein was largely unaffected following mutagenesis of motif VI, while ATPase and RNA helicase activity were abolished (Gross & Shuman, 1996*a*).

Mutagenesis of this motif in HCV NS3 helicase also generated conflicting results. Table 1.2 shows a summary of mutagenesis studies performed on the HCV

RNA helicases. A variety of assays and truncated versions of NS3 have been used. Wardell *et al.* (1999) demonstrated that Arg_{467} is required for both ATPase and helicase activities, whilst replacement of Gln_{460} significantly reduced ATPase activity and abolished helicase activity (subscript numbers are amino acid positions in HCV NS3). The researchers did not investigate RNA binding activity of these mutants.

Kim *et al.* (1997*b*) extensively mutated motif VI, changing all six residues between, and including, Gln_{460} and Arg_{467}. Gln_{460} was required for the helicase and ATPase enzymatic activity, but not for RNA binding. This was consistent with the helicase but not the ATPase assay results obtained by Wardell *et al.* (1999), using full-length NS3. Kim *et al.* (1997*b*) demonstrated that mutagenesis of Arg_{461} residue had little effect on enzymatic activity. However, Arg_{462} was shown to be important for RNA binding by both Kim *et al.* (1997*b*), and Chang *et al.* (2000). Gly_{463} and Trp_{465} appeared to be less important for helicase activity (Kim *et al.*, 1997*b*). Arg_{464} was shown to be critical for enzyme activity following substitution with Ala (Kim *et al.*, 1997*b*; Min *et al.*, 1999). Chang *et al.* (2000) and Min *et al.* (1999) both demonstrated significant reduction in RNA binding by the substitution of Arg_{464} with Ala. However, Kim *et al.* (1997*b*) reported parental levels of RNA binding for this mutation. In general, these studies indicate a role of motif VI in RNA binding probably involving Arg_{462} and/or Arg_{464}.

In two separate studies (not shown in Table 1.2), researchers constructed truncated forms of the HCV NS3 protein (both retaining and lacking all or parts of motif VI) and showed that the truncated proteins bound to RNA (Kanai *et al.*, 1995; Kim *et al.*, 1997*a*). These authors then hypothesized that other regions outside motif VI may also be involved in RNA binding, and that the HCV NS3 protein can bind to RNA regardless of its NTPase and RNA helicase activity.

1.9.7 Helicase X-ray crystal structure

To date, no X-ray crystal structure or homology model of a flavivirus NS3 helicase has been reported, but three X-ray crystal structures of the related HCV NS3 helicase domain have been solved (Cho *et al.*, 1998; Kim *et al.*, 1998; Yao *et al.*, 1997). In addition, one of these studies solved the structure of the HCV NS3 helicase domain complexed with a single stranded DNA oligonucleotide $(dU)_8$ (Fig. 1.5) (Kim *et al.*, 1998). The X-ray crystallographic structures of four other non-viral helicases have also been reported: the DNA helicases PcrA, Rep, UvrB and eIF-4A (Caruthers *et al.*, 2000; Korolev *et al.*, 1997; Machius *et al.*, 1999; Subramanya *et al.*, 1996; Theis *et al.*, 1999). The structures of RNA and DNA helicases have similar folding topologies and tertiary structures, and conserved motifs superimposed at the same spatial positions within the structures, even though there is limited amino acid sequence homology (Caruthers *et al.*, 2000; Korolev *et al.*, 1998).

The HCV helicase consists of three structural domains with residues conserved among superfamily 2 helicases lining an interdomain cleft between the first two domains. These first two domains have an adenylate kinase-like fold, and a phosphate-binding loop in the first domain. The structure reported by Kim *et al.* (1998) showed the bound $(dU)_8$ oligonucleotide lying in a groove between the first two domains and the third, contacting relatively few conserved residues with no strong sequence specific interactions. Most of the interactions between the enzyme and bound $(dU)_8$ oligonucleotide involved hydrogen bonds with the phosphate backbone but not the bases of the oligonucleotide. However, a significant enzyme-base interaction involves a hydrophobic stacking interaction between Trp_{501} of the HCV helicase and the $(dU)_8$ base at the 3′ end of the bound oligonucleotide, and

Val_{432} interacts with the $(dU)_4$ base (Kim *et al.*, 1998). Additionally, the helicase protein contacts the phosphate backbone via structurally equivalent and symmetrical residues in domains 1 and 2. That is, Ser_{370} and Thr_{411} in domain 2 interact with $(dU)_3$ and $(dU)_5$ respectively, and these interactions are nearly identical to those between Ser_{231} and Thr_{269} with $(dU)_7$ and $(dU)_8$ of domain 1. All of these helicase residues are conserved in all HCV NS3 helicases (Kwong *et al.*, 2000) which show an overall variation in amino acid sequence of up to approximately 10%.

Motifs I and II are positioned in domain 1 which is connected to domain 2 by a flexible linker region which corresponds to motif III (Cho *et al.*, 1998; Kim *et al.*, 1998; Yao *et al.*, 1997). Motif II is proximal to the motif I phosphate binding loop and both motifs are thought to be involved in binding of the Mg^{2+}-ATP substrate. The side chains of the conserved Asp_{290} and Glu_{291} of motif II point towards an open area thought to be occupied by this substrate. Also, the motif II His_{293} residue is located at the bottom of the interdomain cleft and has been shown by mutational analysis to be important for the coupling of enzymatic activities. Kim *et al.* (1998) showed that residues in motif V line the interface between domains 1 and 2, and also contact the $(dU)_8$ oligonucleotide, particularly Thr_{411} which makes a hydrogen bond to the phosphate of $(dU)_3$.

The conserved Gln_{460} in motif VI (QRxGRxGR) is positioned at the bottom of the cleft between domains 1 and 2, and is predicted to interact with the His_{293} of the DExH motif located on the inner cleft face of domain I (Kim *et al.*, 1998). The conserved Arg residues of motif VI lie on the inner face of domain 2, facing motifs I and II on the inner face of domain 1 (Kim *et al.*, 1998).

1.9.8 Structure directed mutagenesis of hepatitis C virus helicase motif VI

As previously mentioned, Kim *et al.* (1998) identified several interactions between the conserved residues Ser_{231}, Thr_{269}, Ser_{370}, Thr_{411} and Trp_{501} of the helicase and a $(dU)_8$ oligonucleotide. Lin and Kim (1999) studied the roles of these residues in enzymatic activity and RNA binding using a truncated NS3 protein. The results showed that mutation of the Ser residues to Ala had no effect on protein function, with enzymatic activity and RNA binding being indistinguishable from parental HCV helicase. In contrast, mutagenesis of the Thr and Trp residues to Ala resulted in reduced RNA binding and abolished RNA helicase and poly(U) stimulated ATPase activity, although basal ATPase activity remained intact. Paolini *et al.* (2000*b*) also mutated the Trp_{501} residue to Ala in a full length NS3 protein, and their results confirmed the essential role of Trp_{501} in stabilizing the enzyme-ssRNA complex. However, the reduction in helicase activity of this full length NS3 mutant protein was less than that seen for the truncated mutant protein reported by Lin and Kim (1999), possibly due to stabilization of the helicase mediated by the presence of the amino terminal region of NS3.

In addition to Ala substitution, Lin and Kim (1999) also substituted Trp_{501} with Leu and Phe to test protein-ssRNA interaction. The substitution with Leu resulted in a protein with enzymatic and RNA binding activities similar to that of the Ala mutant described above, whereas, substitution with Phe resulted in a protein preparation with parental levels of enzymatic and RNA binding activities. These findings suggest that the phenyl ring is critical for stacking interactions with the uridine ring. Paolini *et al.* (2000*b*), also substituted Val_{432} with Gly and found that interaction with RNA and poly(U) stimulated ATPase activity only slightly.

Therefore, Val_{432} appeared to form less extensive interactions with the $(dU)_8$ oligonucleotide than the aromatic ring of Trp_{501}. These mutational analyses are consistent with the mechanistic model of RNA unwinding proposed by Kim *et al.* (1998) described below.

1.9.9 Models of unwinding

To date, three models for the mechanism of HCV NS3 helicase have been proposed, one for each of the published crystal structures (Cho *et al.*, 1998; Kim *et al.*, 1998; Yao *et al.*, 1997). However, the Yao *et al.* (1997) and Cho *et al.* (1998) models were based on X-ray crystal structures of HCV helicase without oligonucleotide. Therefore, only the model proposed by Kim *et al.* (1998) based on the HCV NS3 helicase domain complexed with a single stranded DNA oligonucleotide $(dU)_8$ will be presented here.

In a recent review by Kwong *et al.* (2000), this model was discussed using the additional results obtained following mutagenesis studies of both motif VI (Kim *et al.*, 1997*b*) and the RNA binding channel (Lin & Kim, 1999) (Fig. 1.6).

In this model, a 3′ single stranded tail of a duplex nucleic acid substrate binds to the groove which separates domain 3 from domains 1 and 2. In the absence of ATP, the HCV helicase adopts an open form, in which the interdomain cleft between domains 1 and 2 are apart. Upon binding of the β phosphate group of ATP to the phosphate binding loop (motif I), Asp_{290} of motif II binds to Mg^{2+} and orientates the ATP-Mg^{2+} complex for hydrolysis. Arg_{464} and Arg_{467} of motif VI in domain 2 interact with the γ and α phosphate groups of the bound ATP thereby closing the cleft between domains 1 and 2. Formation of the closed conformation results in the

movement of domains 1 and 3 as a rigid unit along the bound polynucleotide strand in a 3′ to 5′ direction. The Val_{432} and Trp_{501} serve to lock the polynucleotide in place while the hydrolysis of ATP facilitates opening of the cleft releasing ADP and resetting domain 2, which remains flexible relative to the other two domains. This restores the open form of the helicase and results in the unidirectional movement of the helicase in a 3′ to 5′ direction.

Dimerization or oligomerization of NS3 helicase has been suggested to be important for optimal helicase activity (Levin & Patel, 1999). A dimer model for the HCV NS3 helicase has been proposed based on an X-ray crystal structure reported by Cho *et al.* (1998), and dimerization was recently supported by a mutational study by Khu *et al.* (2001), who demonstrated strong NS3-NS3 interactions using a yeast two-hybrid assay. Mutants which disrupted the interaction between two helicase molecules correlated with a loss of helicase activity (Khu *et al.*, 2001).

However, other structural (Kim *et al.*, 1998; Yao *et al.*, 1997), mutational (Lin & Kim, 1999) and sedimentation centrifugation experiments (Porter *et al.*, 1998), indicated that the HCV helicase appears to act as a monomer and dimerization is not required for activity. Khu *et al.* (2001) suggest that the discrepancy may reflect a difference in unwinding efficiencies of higher oligomers, being more efficient than monomers at unwinding duplex nucleic acids.

1.10 Replication of viral RNA

Flaviviral RNA synthesis begins with the translation of virion RNA, followed by production of negative strands which serve as templates for positive strand synthesis. A model for the formation of the flavivirus replication complex and

initiation of RNA negative strand synthesis was recently proposed (Khromykh *et al.*, 1999*b*) (Fig. 1.7). Following translation of the viral positive sense RNA on the rough endoplasmic reticulum, the polyprotein is cleaved by signal peptidases in the ER lumen or by the viral proteinase NS2B/3 in the induced convoluted membranes and paracrystalline arrays (Westaway *et al.*, 1997*b*). Individual nonstructural proteins either migrate to the nucleus (NS4B) or are transported to vesicle packets (NS1, NS3, NS5, NS2A and NS4A). NS3 probably binds NS5 and may also bind NS2A forming a complex which possibly attaches to stem loop structures within the 3′ UTR via NS2A (Chen *et al.*, 1997*a*; Cui *et al.*, 1998; Kapoor *et al.*, 1995; Khromykh *et al.*, 1999*b*; Mackenzie *et al.*, 1998). This RNA-protein complex is transported to the membrane site of replication by affinity of the hydrophobic regions of NS2A interacting with those of homodimeric NS4A. NS4A, in turn, is bound by hydrophilic extensions in the lumen of the ER between transmembrane domains to dimeric NS1 in the ER lumen (Khromykh *et al.*, 1999*b*; Lindenbach & Rice, 1999; Mackenzie *et al.*, 1996; Mackenzie *et al.*, 1998). The assembled replication complex enables the NS5 RdRp to bind to the template positive strand and negative strand synthesis commences. This is then followed, late in replication, by the synthesis of progeny infectious positive strands on the nascent template negative strand (Rice, 1996).

1.11 Vaccine development and use of genomic length cDNA of flaviviruses

An effective vaccine against DEN virus is currently not available, and the ideal DEN vaccine would protect against all four serotypes (Halstead, 1988; Sinniah & Igarashi, 1995). A live attenuated virus is used as a safe, effective and cost efficient vaccine against YFV but no other live flavivirus vaccines have been licensed.

Approved inactivated virus vaccines are available for TBE and JEV (Rice, 1996). Several strategies have been used toward the development of a DEN vaccine, including recombinant subunit protein vaccines, DNA plasmid vaccines, whole virus inactivated vaccines and live attenuated virus vaccines. Here, only the live attenuated virus vaccines and the related use of flavivirus genomic length cDNAs and chimeric viruses will be briefly discussed.

Early attempts to develop DEN virus vaccines focussed on attenuation of the virus by serial passage in mouse brain. However, this produced monovalent candidate vaccines of limited usefulness (Trent *et al.*, 1997).

The U.S. Army sought to produce live, attenuated DEN vaccines by serial passage in primary dog kidney (PDK) cells. The candidate vaccines had several biological markers usually associated with attenuation in the high passage viral strains. These include temperature sensitivity, reduced plaque size, loss of neurovirulence for suckling mice and decreased viremia in monkeys. However, all were found to be either over-attenuated and poorly immunogenic, or to cause varying degrees of dengue-like illness when tested in humans (Eckels *et al.*, 1984; Edelman *et al.*, 1994; Rice, 1996). This suggested that the biological markers were not completely predictive of attenuation in humans.

The molecular basis of viral virulence has been studied by sequencing the genomes of these modified viruses and the parental virulent viruses from which they were derived, and comparing nucleotide and amino acid differences following passage. For example, Puri *et al.* (1997) demonstrated that there were 25 nt and 11 aa changes between a virulent DEN-1 strain and a candidate vaccine strain obtained following 27 passages in PDK cells. DEN-1 viruses passaged 10 and 20 times in PDK cells were also tested in humans (Edelman *et al.*, 1994), and sequencing of cDNA

from all viruses located multiple mutations that were probable markers of attenuation (Puri *et al.*, 1997). However, when multiple changes are present, defining which combinations of mutations are important for attenuation requires the construction of a series of viruses containing single point mutations or combinations of mutations by site directed mutagenesis of genomic length cDNAs (Gritsun *et al.*, 2001; Gualano *et al.*, 1998; Kapoor *et al.*, 1995; Lai *et al.*, 1991).

Live attenuated vaccine candidates have been developed for all four serotypes of DEN by serial passage of wild-type viruses in PDK cells or other cell types at Mahidol University, Bangkok, Thailand (Bhamarapravati *et al.*, 1987; Yoksan *et al.*, 1986). The Mahidol candidate DEN-2 vaccine virus (PDK-53) was derived from the virulent parental strain 16681 following 53 passages in PDK cells. The PDK-53 virus vaccine was successfully tested in humans, being safe, immunogenic and inducing a T-cell memory response (Bhamarapravati *et al.*, 1987; Dharakul *et al.*, 1994; Vaughn *et al.*, 1996). Kinney *et al.* (1997) showed there are nine nucleotide and five amino acid differences between the two viruses. A recent study by Butrapet *et al.* (2000) used an infectious DEN-2 genomic length cDNA clone to construct 18 recombinant viruses to analyse four mutations within the 5′ UTR, prM, NS1 and NS3. It was concluded that the attenuation markers are in the 5′ UTR, NS1 and NS3.

Several studies have shown that there are no universal markers of flavivirus attenuation (Barrett *et al.*, 1990; Butrapet *et al.*, 2000; Hahn *et al.*, 1987*a*; Kinney *et al.*, 1997; McMinn *et al.*, 1995; Ni *et al.*, 1994; Puri *et al.*, 1997). It is likely that an overall attenuated phenotype is due to the combined effects of several mutations.

Another approach has sought to generate live, attenuated genetically engineered vaccines using infectious cDNAs encompassing the whole viral genome. This technique enables the identification of specific mutations that modify viral

functions and may have potential in producing attenuated viruses (Bonaldo *et al.*, 2000).

Another approach has been the construction of chimeric flaviviruses, using infectious cDNAs derived from viruses of known attenuation. Huang *et al.* (2000) constructed a chimeric virus containing the structural genes of DEN-1 16007 virus or its vaccine candidate PDK-13, combined with the nonstructural genes of DEN-2 16681 virus or its vaccine candidate PDK-53. The chimeric virus containing the parental DEN-1 16007 virus structural genes with the DEN-2 PDK-53 virus nonstructural genes induced higher mouse neutralizing antibodies against DEN-1 virus than did the DEN-1 PDK-13 vaccine virus or chimeric viruses which had DEN-1 PDK-13 structural genes, while retaining attenuation markers. Therefore, assuming attenuating markers of DEN-2 PDK-53 are retained in other chimeric viruses containing the DEN-2 PDK-53 nonstructural genes, infectious clones derived from DEN-2 PDK-53 are promising vectors for the development of chimeric vaccines containing the structural genes of all dengue serotypes (Huang *et al.*, 2000).

The DEN-2 (strain PUO-218) prM and E genes have been inserted into the infectious cDNA clone of the YFV vaccine strain YF 17D, generating the chimeric virus ChimeriVax-D2. The chimeric virus was shown to replicate efficiently and to be attenuated in mice (exhibiting less encephalitis) and producing less viraemia in monkeys (Guirakhoo *et al.*, 2000). It was genetically stable, immunogenic and initial challenge experiments showed good protection. However, human trials are still being evaluated. The researchers have recently described the construction of three additional YF 17D/DEN chimeras using the prM and E genes of DEN-1, DEN-3 and DEN-4 clinical isolates (Guirakhoo *et al.*, 2001). These viruses were tested as monovalent or tetravalent formulations in non-human primates, with almost all animals producing

neutralizing antibodies against all four DEN serotypes, demonstrating effective simultaneous immunization.

1.12 Clustered charged-to-alanine mutagenesis

Cunningham and Wells (1989) originally described the method of alanine-scanning mutagenesis in which single Ala mutations were introduced into the human growth hormone protein at sites that had been implicated in receptor recognition. Ala was chosen as it eliminates the side chain beyond the β carbon without altering the main-chain configuration and does not cause extreme electrostatic or steric effects. Clustered charged-to-alanine scanning mutagenesis is a variant of this method (Bass *et al.*, 1991; Gibbs & Zoller, 1991). It involves scanning the sequence of a protein for clusters of two or more charged residues within a stretch of five residues. Each charged residue within a cluster is then substituted with Ala. Substitutions of charged residues with Ala have generally been shown to exert little effect on protein conformation (Gibbs & Zoller, 1991) as most charged residues, particularly those found in clusters, are expected to reside on the solvent-exposed surfaces of folded proteins contributing little to the overall protein stability (Diamond & Kirkegaard, 1994). Therefore disruption of such clusters of surface charges might not disrupt the overall protein stability, but instead interfere with electrostatic or hydrogen-bonding interactions with other molecules, or with the solvent, making these interactions more thermosensitive (Alber, 1989; Wertman *et al.*, 1992).

Diamond and Kirkegaard (1994) used clustered charged-to-alanine mutagenesis of the 3D protein of poliovirus (which has polymerase activity and forms part of the replication complex) to generate several temperature sensitive (*ts*) mutants

with defects in viral RNA synthesis. This allowed identification of regions required for RNA replication and for interaction between the polymerase and other components of the replication complex.

Droll *et al.* (2000) recently completed charged-to-alanine mutagenesis of YFV NS2B and the proteinase region of NS3 in order to define regions of the proteins important for the formation of the proteinase complex and enzymatic activity. This study did not, however, test any of the mutants for their effect on virus replication. The only reported *ts* mutant of a flavivirus was obtained following charged-to-alanine mutagenesis of the YFV NS1 protein (Muylaert *et al.*, 1997).

1.13 Aims and experimental approaches

Dengue is the most important arthropod borne viral disease in tropical and subtropical regions of the world, and a safe and effective vaccine is not yet available. Mutagenesis of genomic length cDNA has the potential to produce genetically defined attenuated dengue viruses. The highly conserved and multifunctional NS3 protein, described in the preceding literature survey, is a possible target for the production of attenuated viruses. It is also a target for the design of antiviral drugs, thus providing an incentive for investigating the DEN-2 NS3 protein in detail.

A major goal of this project was to generate growth-restricted and potentially attenuated mutant DEN-2 viruses. Mutations that restrict, but do not prevent, viral replication are candidates for incorporation into live virus vaccine strains including DEN-2 and other flaviviruses (Chambers *et al.*, 1997). The main aim of the experiments described in chapter three was therefore to produce such mutations in the NS3 proteinase. Since previous studies on several flaviviruses have targeted the four

conserved proteinase motifs and the cleavage sites (Chambers *et al.*, 1990*b*; Valle & Falgout, 1998), in this work, locations outside these regions of NS3 were chosen. In particular, by avoiding motifs, it was reasoned that proteinase activity may be retained and that mutations may not be lethal.

To this end, five sites distributed through the amino terminal proteinase region of DEN-2 NS3 were mutagenized. The effects of four clustered charged-to-alanine mutations and the mutation of a highly conserved hydrophobic region in the NS3 proteinase on viral replication in cell culture were analyzed. The results were interpreted with reference to the location of the mutations mapped on the X-ray crystal structure of the DEN-2 NS3 proteinase (Murthy *et al.*, 1999) and a model of the NS2B/3 complex (Brinkworth *et al.*, 1999). Chapter three describes the production of these growth-restricted mutant viruses and evaluation of their replicative properties.

Another aim was to investigate the importance of selected residues in the DEN-2 NS3 helicase region for ATPase and RNA helicase activity *in vitro*, and viral replication, with the goal of generating growth-restricted DEN-2 viruses containing mutations within the NS3 helicase. Two types of mutations were analyzed: (i) point mutations within helicase motifs I, II and VI; and (ii) clustered charged-to-alanine mutations external to helicase motifs. Mutant proteins were synthesized as amino terminal truncated fusion proteins in *E. coli*, purified and assayed for ATPase and RNA helicase activities. Mutations were also incorporated into genomic-length DEN-2 cDNA to investigate their effects on viral replication. Chapter four describes the production of mutant proteins and contains the results of enzymatic assays. It also describes the production of the viruses containing helicase mutations and the evaluation of their replicative properties.

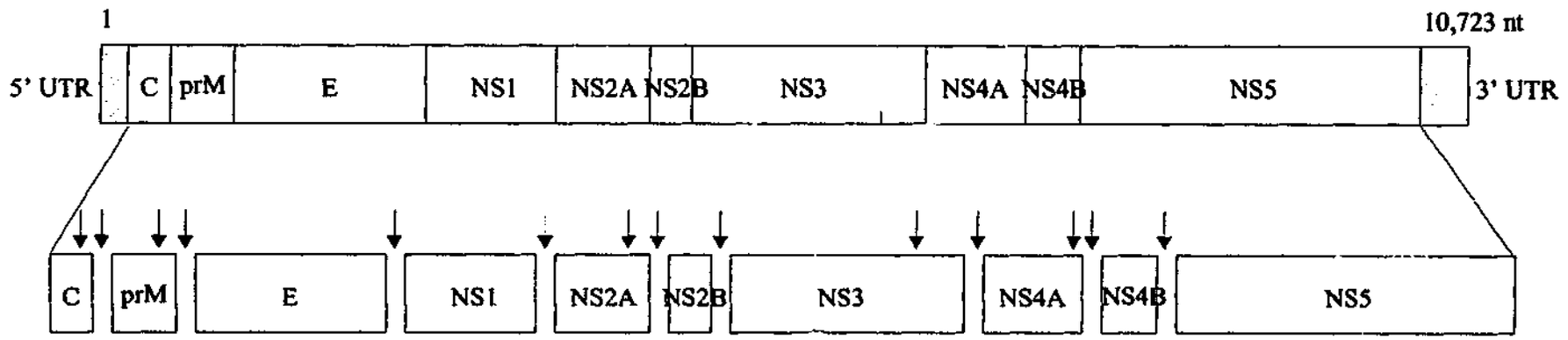

Fig. 1.1 Schematic of the flavivirus genome structure and polyprotein processing.

The top depicts the viral genome with the 5′ and 3′ untranslated regions (UTRs). Boxes below the genome indicate mature proteins generated by polyprotein processing. Proteolytic cleavage sites and the viral and host proteases responsible are shown. The internal cleavage sites within C, prM, NS3, NS2A and NS4A are shown.

```
                1         11        21        31        41        51
consensus       SWP NE   AVGLV  L   L   D     GP   GGLL   YV  G S DL LE AA V
DEN-1           ...L..GIM...I.SI.LSS.LKN.VP-LA..LIA..M.IAC..IS.S.A..S..K..E.
DEN-2           ...L..AIM...M.SI.ASS.LKN.IP-MT..LVA....TVC..LT.R.A..E..R..D.
DEN-3           ...L..GVM.....SI.ASS.LRN.VP-MA..LVA....IAC..IT.T.A..TV.K..D.
DEN-4           ...L..GIM.....SL.GSA.LKN.VP-LA..MVA....LAA..MS.S.A..S..K..N.
JEV             G..AT.FLS....MFAIVGG.AEL.IESMSI.FMLA..MAVS..VS.KAT.MW.DR..DI
WNV             G..AT.VMT....MFAIVGG.AEL.IDSMAI.MTIA..MFAAF.IS.K.T.MWI.RT.DI
YFV             .I.V..ALA.A...GV.AG-.AFQEMENFL..IAV..I.MMLVSVA.RVDG.E.KKLGE.
TBE             --SFS.PLTV..VMLT.AGGMMRHTSQEALCALAVASF.LLML.LGTRKMQ.VA.WSGC.
HCV (NS4A)      ----------------------------------------------------STWV.VGGVLA
                                                                    1         11

                61        71        81        91        101       111
consensus        WE EAEI GSS    V  D DG F     E       L     L  S   P  I-P
DEN-1           S..E...HS.A.HNIL.EVQD..TMKIKDE.RDDTLTI.LKATL.AV.GVY.MS...ATL
DEN-2           K..DQ...S...PILSITISE..SMSIKNE.EEQTLTI.IRTGL.VI.GLF.VS...ITA
DEN-3           T..E...QT.V.HNLMITV.D..TMRIKDD.TENILTV.LKTAL.IV.GIF.CS...ATL
DEN-4           Q.DEM.D.T...PIIE.KQ.E..S.SIRDV.ETNMITL.VKLALITV.GLY.LA...VTM
JEV             S..M..A.T...RRLD.KL.D..D.HLIDDPGVPWKVW.LRMSCIGLAALT.WA.V.AAF
WNV             S..SD...T...ERVD.RL.D..N.QLMNDPGAPWKIWMLRMVC.AI.AYT.WA.L.SVV
YFV             A..E....S...ARYD.ALSEQ.E.KLLSE.KVPWDQVVMTSLA.VGAAIH.FAL.LLVL
TBE             E.HP.LVNE.GEVSLR.RQ.SM.N.HLTEL.KEERVMAFWLLAG.AA.AFHWSG..LGVM
HCV (NS4A)      ALAAYCLTT..VVIVGRIILSGRPAVIPDR.VLYQEFDEMEEC
                          21        31        41        51

                121       131
consensus         W      --  R
DEN-1           FV.YFWQKK..KQ.
DEN-2           AA.YLWEVK..KQ.
DEN-3           LV.HTWQKQ..TQ.
DEN-4           TL.YMWQVK..TQ.
JEV             GY.LTLKT-..TK.
WNV             GF.ITLQY-..TK.
YFV             AG.LFHVRG..AR-
TBE             GL.TLSEMMRSAR.
```

Fig. 1.2 Alignment of several flavivirus NS2B amino acid sequences and HCV NS4A.

Dots stand for identical amino acid residues while dashes represent gaps introduced to allow maximal homology. The hydrophilic 40 amino acid cofactor domain of NS2B is shown in red; in green is the central hydrophobic region, which was identified in DEN-2 by Brinkworth *et al.* (1999) as the probable homologue to the HCV NS4A peptide in the HCV NS3/4A proteinase (Yan *et al.*, 1998). The position of amino acids in the consensus NS2B sequence are listed above the sequence, while the position of amino acids within HCV NS4A are listed below the sequence. Amino acid sequences derived from the following viruses are aligned (GenBank accession numbers are shown in brackets): DEN-1 (AF180817); DEN-2 (AF038403); DEN-3 (AF317645); DEN-4 (AF326573); JEV (AF045551); WNV (AF196835); YFV (YFU21055); TBE (L40361) and HCV (D17763).

Fig. 1.3 Alignment of several flavivirus NS3 amino acid sequences and hepacivirus HCV NS3. Dots stand for identical amino acid residues while dashes represent gaps introduced to allow maximal homology. The four serine proteinase boxes are shown in blue boxes, with the catalytic triad indicated with asteriscks above each residue. The seven helicase motifs are shown as pink boxes. The conserved sequence element proposed to be involved in 5′ terminal RNA triphosphatase activity is shown for the flaviviruses in an orange box. The position of amino acids in the NS3 consensus sequence are listed above the sequence. The same virus GenBank accession numbers were used for this NS3 sequence alignment as was for the NS2B alignment (Fig. 1.2).

```
                1          11         21         31         41         51
consensus        GVLWD PSP     K ---     GVYRI  RGLL----------------G  QVG----
DEN-1           S.....T...PEVERA...VLDD.I...LQ.....................RS.......
DEN-2           A.....V...PPVG.A...ELED.A...KQK.I..................YS.I.....
DEN-3           S.....V...PETQ.A...ELEE.....KQQ.IF.................KT.......
DEN-4           S.A...V...AATK.A...ALSE.....MQ...F.................KT.......
JEV             G..F..T...KPCL.G...DTTT.....MA..I..................TY.A.....
WNV             G.....T...KEYK.G...DTTT.....MT.....................SY.A.....
TBE             SDLVFSGQGGRERGDKP.FEVRD.....FSP...W.................QR.......
HCV             GREVLLG.ADDYREMGWRLLAPITA.AQQT....GTIVTSLTGRDKNVVT.EV..LSTAT

                61         71         81         91        101        111
                                      *                    *
consensus       ---VGV                          RL P WA                L   W   E
DEN-1           ......FQ                        K..E.S..S              RFQGS.NTG.E
DEN-2           ...A..YK                        K.IE.S..D              K.EGE.KEG.E
DEN-3           ......QK                        K..E.N..S              R.SAQ.QKG.E
DEN-4           .....IHM                        G..E.S..D              R.GDK.DKE.D
JEV             ......MY                        GK.T.Y.GS              RFDRK.NGTDD
WNV             ...A..MV                        G..D.Y.GS              K.QHK.NGQDE
TBE             .....YGF                        AVAG.Y..D              S.EEK.KG-.T
HCV             QTFL.TTV                        HPALQMYTN              -GAKSL.P

                121        131        141        151        161        171
                                                                *
consensus       VQV A EFGKN     QT PG -F T  GE- GAV                    G
DEN-1           ...I.V.....PKNV..T..T..F..E...V..I                     .
DEN-2           ...L.L.. ..PRAV..K..L..K.NA.T.I...                     .
DEN-3           ...I.V.....PKNF..M..I..Q.TT...I..I                     .
DEN-4           ...L.I.....PKHV..K..L..K.LT...I...                     .
JEV             ...IVV....EAVNI..K..I..PPPF...V...                     .
WNV             ..MIVV.....VENV..K...V..K.PE...I...                    .
TBE             ...H.FP..RAHEVH.CQ..E.LLLDT.RRM...                     .
HCV             CACGSSDLYLVTRDADVI.ARRRGDSTASLLSPR                     .

                181        191        201        211        221        231
consensus       V T ---- G YVSAI Q     E  ---          K   T  DLHPGSGKT R L
DEN-1           .T....S.T.....A.AKASQ.GP...LPEIEDEVFR.RNLSIM  .  .  .  R.Y
DEN-2           .R....S.A.....A.TEKSI.D-...NPEIEDDIFR.RKLTIM  .  A  .  K.Y
DEN-3           .K....N.G...G.A.TNAEPDGP...TPELEEEMFK.RNLTIM  .  .  .  RKY
DEN-4           .K....S.D.....T.AERIG.P-...DYEVDEDIFR.KRLTIM  .  A  .  K.L
JEV             LG....D.S.....V.GDRQE.PV...PDAYTPSMLK.KQMVLL  P  .  .  TRKI
WNV             MP....N.S.I...V.GERMD.PI...PAGFEPEMLR.KQLVLL  .  A  .  TRTI
TBE             .-....NET...S.A.GEVEKSRPNLPQAVVGMGWTA.GQLVLM  .  .  .  FHTV
HCV             .RGVAKSLQFIPVETLSTQARSPS.FSDNSTPPAVPQSYQVGYLHAPT..  .  STK-V

                241        251        261        271        281        291
consensus       P IVREAI RRTRTLILAPTRVVAAEM EAL GLP-IRYQT AV  EHTG EIVD MCHA
DEN-1           A......K.K.  .  .  .  .  S.A...K.V.......T..KS....K....L....
DEN-2           A......K.G.  .  .  .  .  E...R.........P.IRA....R....L....
DEN-3           A......K...  .  .  .  .  E...K.........T.TKS....R....L....
DEN-4           S.....LK...  .  .  .  .  E...R.........P..KS....R....L....
JEV             Q.IKD..QQ..  .  AV .  .  A...R....V....S..QR..Q.N....V....
WNV             Q.IK...N...  .  AV .  .  A...R.........S..PR..N.N....V....
TBE             ELI.QC.D...  .  V  .  LK..ER..N.KR.V.FHSP..SDQQM.GA...V....
HCV             AY.AQGYNVLVLNPSV.A.TGEGSF.SR.YGID.N..TGNRT.T---..AKLT-YSTYG

                301        311        321        331        341        351
consensus       TFT RLLSP RVPNYNLIIMDEAHFTDPASIAARGYIST VE- GEAAAIFMTATPPG
DEN-1           ...M.....V......M.  .  .  .  .  .  .  .  .R.G.M....  .  .  .SV
DEN-2           ...M.....V......A.  .  .  .  .  .  .  .  .R...M....G  .  .  .SR
DEN-3           ...M.....V......A.  .  .  .  .  .  .  .  .R.G.M....  .  .  .TA
DEN-4           ...T....ST......V.  .  .  .  .  .  .S.V........R...M.  .  .  .AT
JEV             .L.H..M..N......FV  .  .  .  .  .  .  .  .A.K...L..  .  .  .TT
WNV             .L.H..M..H......FV  .  .  .  .  .  .  .  .K...L....  .  .  .TS
TBE             .YVN.R.L.QGRQ.WEVA  .  .  .  .  W...H......HLY.LAK.ENKC.LVL.  .  .KS
HCV             K.LADGGCSGG--A.DV.C.C.AQ.AT..LGI.TVLDQA.TA.VRLTVLA.  .  .SI
```

```
                361       371       381       391       401       411
consensus       DPFP SN PI D E EIPER W SG  WITD  GKTVEVPSIKGN IA CLR  GKKV
DEN-1           EA..Q..AI.Q.E.RD....S.N..YD....FP...T..A...S..D..N...KN..R.
DEN-2           ....Q..A..M.E.R.....S.S..HE.V..FK...S..A...A..D..A...KN....
DEN-3           .A..Q..A..Q.E.RD....S.N..NE....FV...S..A...A..D..N...KN....
DEN-4           ....Q..S..E.I.R.....S.NT.FD....YQ...S..A...A..D..N...KS....
JEV             ....D..A..H.LQD...D.A.S..YE....YA...S..A.V.A..E..M..QRA....
WNV             ....E..S..S.LQT...D.A.N..YE...EYT...S..A...V..E..L..QRA....
TBE             E...E..GA.TSE.KQ...GE.RD.FD...EYE.R.A..S..A.K.GV..RT..QK..S.
HCV             T-V.H..IEEVALGS.GEIPFYGKAIPIALLKG.RHTLCHTKKKCDE..SK..GM.LNA

                421       431       441       451       461       471
consensus       IQL RKTFDTEY KTK  DWDFVVTTDISEMGANFKADRVID R   KP I-L  G  RV
DEN-1           ...S........Q...NN..T..V..A.....R.D...P.RCL..V...KD.PE..
DEN-2           ...S.....S..V..RTN..T..V..A.....V.K.P...P.RCM..V...TD.EE..
DEN-3           ...S........Q...LN..T..V..A.....K.D...P.RCL..V...TD.PE..
DEN-4           ...S........P...LT..T..V..A.....R.G...P.RCL..V...TD.PE..
JEV             ...N..SY....P.C.NG..T..V..A.....G.S...C.KSV..T...EE.EG..
WNV             V..N..SYE...P.C.ND..T..V..A.....K.S...S.KSV..T..ITE.EG..
TBE             .C.NS...EKD.TRVRDEKP..T..V..A.....QDVS...G.TNI..--.-EEVDG..
HCV             VAYY.G-L.VSVIP.-TG.-VV.GA..ALMT.ETGDFDS...CNVAVEQYVDFSLDPTFS

                481       491       501       511       521       531
consensus       IL GP PVTTASAAQRRGRIGRNP    D Y Y G ----------    D   AHWTE
DEN-1           ..A..M..V.....T...QNKEG.Q.I.M.Q..........PLNN.EDH.....
DEN-2           ..A..M..HS....A...T...KNEN.Q.I.M.E..........PLEN.EDC...K.
DEN-3           ..A..M..V.....V...QKEN.Q.IFM.Q..........PLNK.EDH.....
DEN-4           ..A..I..P.....T...AQED.Q.VFS.D..........PLKN.EDH.....
JEV             F.GN.S.I.S.....V...NQVG.E.H.G.A..........TSED.SNL.....
WNV             ..GE.SA..A.....I...SQVG.E.C.G.H..........TNED.SNF.....
TBE             E.T.TRR..T.....V..HEGR-T.E.I.S.Q..........CDDD.SGLVQ.K.
HCV             .ETRTA.QDAV.RS....T..GRLG-TYR.VAS.ERPSGMFDSVVLCECY.AGCS-.YD

                541       551       561       571       581       591
consensus       AK LLDNI TP G I     PEREK    DGEYRLRGE RK F EL R  --DLPVWLAY
DEN-1           ..M.....N..E.I.PALYE.....SAAI.........A..T.V..M.RG........S.
DEN-2           ..M.....N..E.I.PSMFE.....VDAI.........A..T.VD.M.RG..........
DEN-3           ..M.....N..E.I.PALFE.....SAAI......K..S..T.V..M.RG.........H
DEN-4           ..M.....Y..E.I.PTLFG.....TQAI...F.....Q..T.V..M.RG........S.
JEV             ..IM....HM.N.LVVQLYG.....AFTM.........EK.N.L..L.TA..........
WNV             .RIM....NM.N.L.AQFYQ.....VYTM.........E..N.L..L.TA..........
TBE             .QI.....T.LR.PVATFYG..QD.MPEVA.HF..TE.K..H.RH.LTHC...FTP...W
HCV             LQPAETTVRLRAYLSTPGLPVCQDHLDFWESVFTGLTHIDAH.LSQTKQQGLNFSYLT..

                601       611       621       631       641       651
consensus       KVA  G-  Y DR WCFDG R N ILE N  -VEI T  GE K LRPRWLDAR Y D  A
DEN-1           ...SE..FQ.S..R.....E.N.QV..E.MD....W.KE..R.K.........T.S.PL.
DEN-2           R..AE..IN.A..R.....IKN.Q...E.VE....W.KE..R.K.K.......I.S.PLT
DEN-3           ...SE..IK.T..K.....E.N.Q...E.MD....W.KE..K.K.........T.S.PL.
DEN-4           ...SA..IS.K..E...T.E.N.Q...E.ME....W.RE..K.K.........V.A.PM.
JEV             ...SN..IQ.T..K.....P.T.A...D.TE....V.RM..R.I.K.......V.A.HQ.
WNV             ...AA..VS.H..R.....P.T.T...D.NE...VI.KL..R.I.....I...V.S.HQ.
TBE             H..ANV.SSVTS.N.TWE.PEE.AVD.A.GDL.TFRSPN.AERT...V.R...MFREGRD
HCV             QATVCARAQAPPPS.DEMWKCLVRLKPTLHGPTPLLYRL.--PVQNETC.THPITKYLM.

                661       671
consensus       LK FK FA GR
DEN-1           .RE..E..A..R
DEN-2           ..E..E..A..K
DEN-3           ..E..D..A..K
DEN-4           ..D..E..S..K
JEV             ..W..D..A.KR
WNV             ..A..D..S.KR
TBE             IRE.VAY.S..R
HCV             CMSADLEVTT--
```

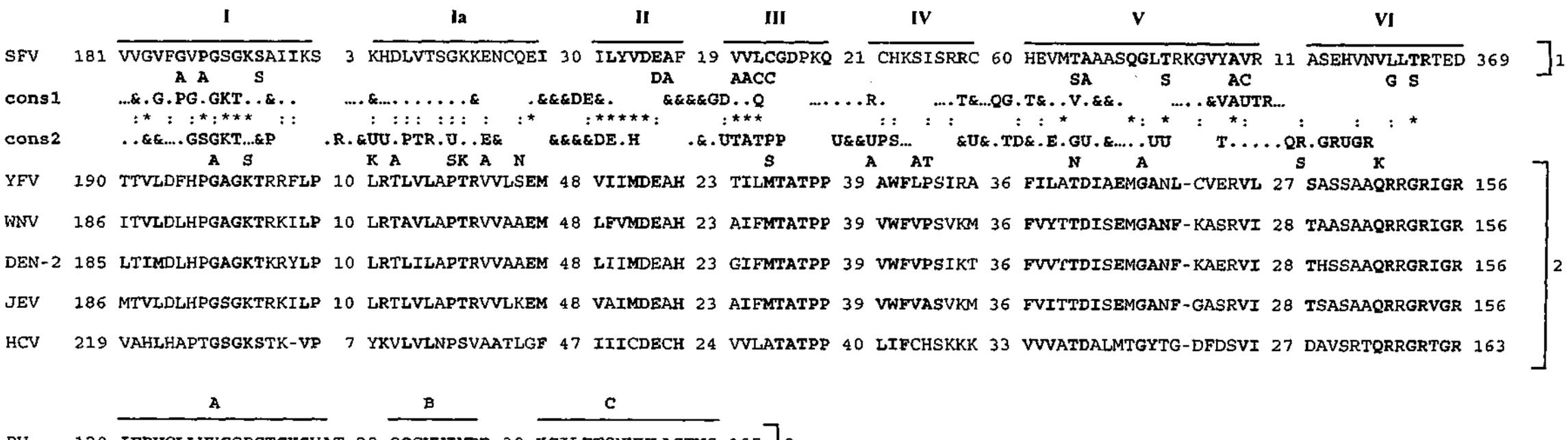

Fig. 1.4 Conserved sequence motifs in the distantly related positive strand RNA virus helicases of superfamilies 1, 2 and 3. The consensus patterns are shown separately for the three superfamilies (cons1, 2 and 3). Residues present in all three patterns (upper case), U designates a bulky aliphatic residue (I,L,V,M), @ designates an aromatic residue (F,Y,W), & designates a bulky hydrophobic residue (either aliphatic or aromatic), and (.) dot designates any residue. Asterisks indicate positions where the consensus residues are identical or similar, and colons indicate where the consensus residue(s) of one of the families is not present in the other families but is still found in a significant proportion of its members. The residues conforming to the consensus are highlighted by bold typing. The motifs are designated as in (Gorbalenya *et al.*, 1989; Gorbalenya *et al.*, 1990). The number of amino acid residues between the motifs and the distances from the protein termini are shown. Adapted from (Koonin & Dolja, 1993).

Fig. 1.5 Fold of HCV NS3 helicase domain complexed with ssDNA. Ribbon diagram illustrating the overall fold of the NS3 helicase with bound $(dU)_8$. Domain 1 is coloured blue, domain 2 red and domain 3 green. The DNA oligonucleotide is coloured yellow. This figure was adapted from that of Kim *et al.* (1998).

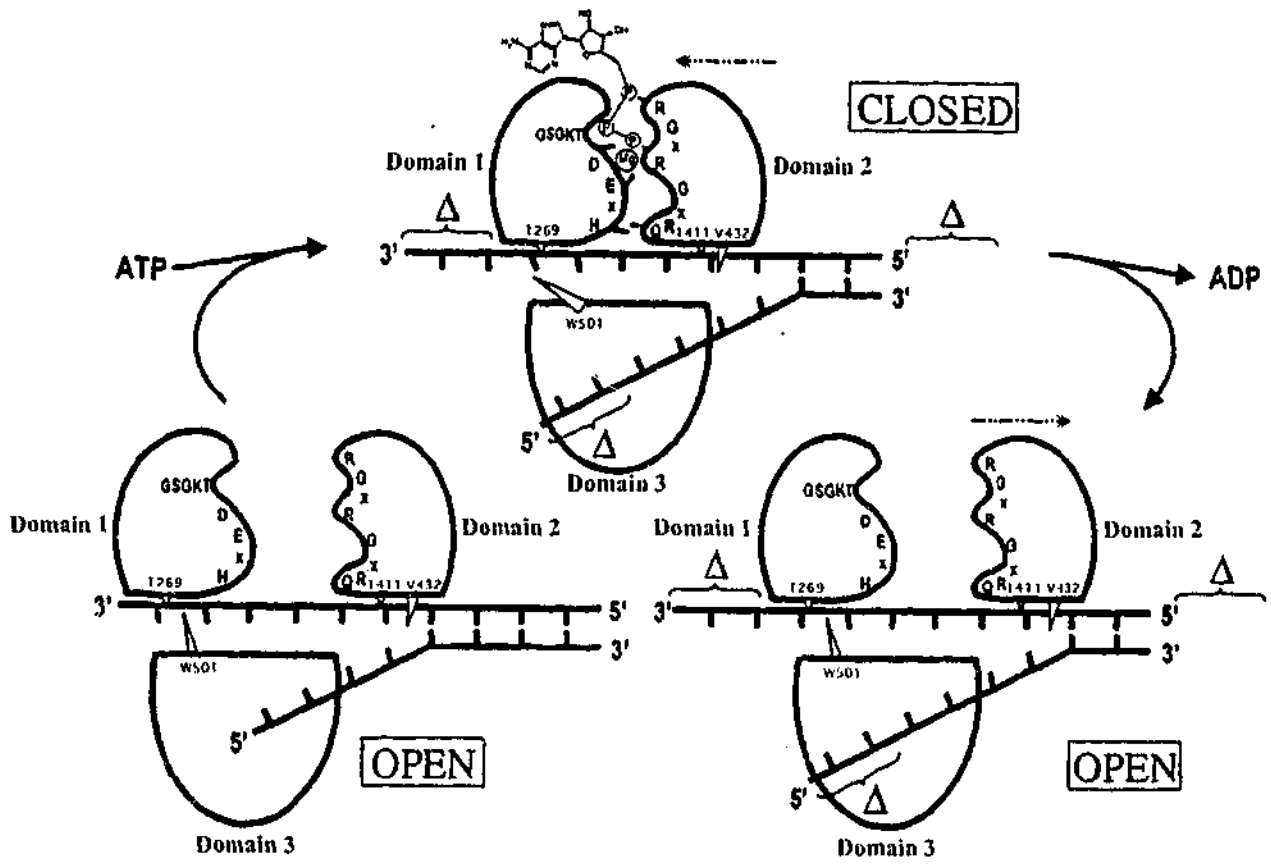

Fig. 1.6 Diagram of the unwinding model proposed by Kwong *et al.* (2000). See text for a detailed explanation of this proposed model of unwinding. The three HCV helicase domains are shown in the same orientation as for Fig. 1.5. Motifs I, II and VI, the conserved residues T269, T411, V432 and W501 and the location of the duplex nucleic acid are shown. The binding of the polynucleotide by NS3 helicase (probably mediated by T269 and T411) in the absence of ATP leaves a large cleft (open form, bottom left) between domains 1 and 2. Following ATP binding (top) the flexible domain 2 closes onto domains 1 and 3, reducing the interdomain cleft, mainly because of interactions between ATP-Mg^{2+} and the conserved residues of motifs I, II and VI. Closure of the ATP binding cleft probably leads to the translocation of domains 1 and 3 in a 3′ to 5′ direction along the bound polynucleotide strand. Hydrolysis of ATP enables opening of the cleft and release of ADP (bottom right). The role of V432 and W501 in the RNA binding channel is to lock the polynucleotide in place while domain 2 resets. This figure was adapted from that of Kim & Lin (1999).

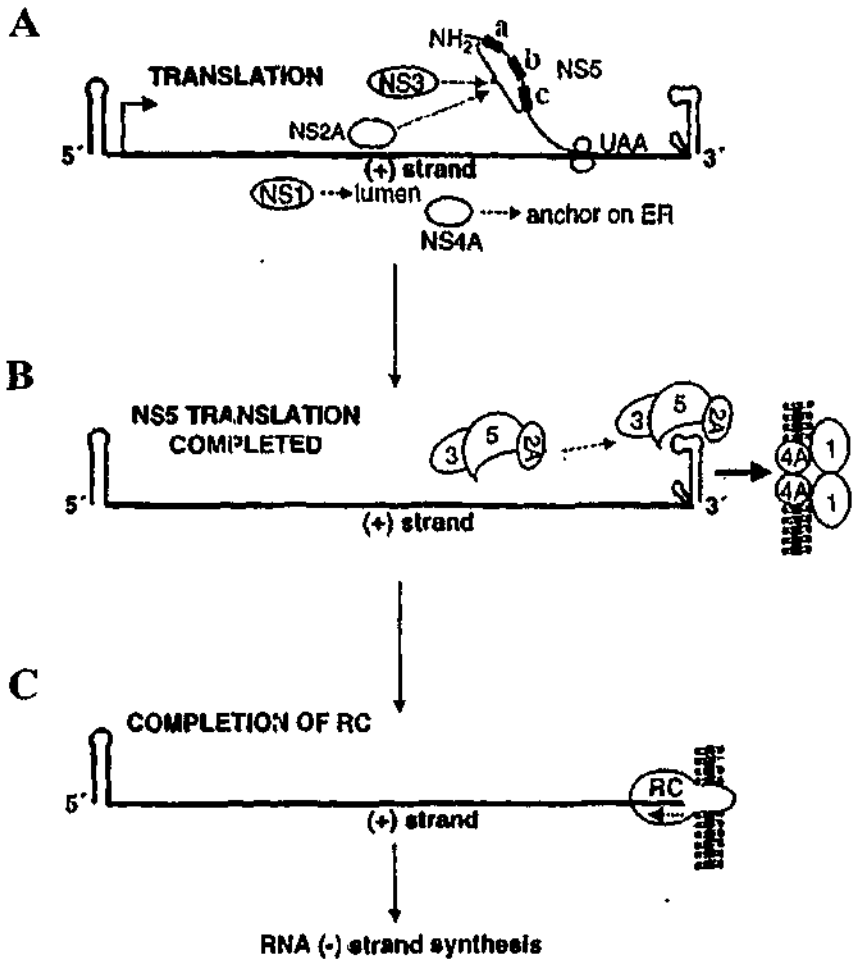

Fig. 1.7 Diagram of the formation of the flavivirus RC and initiation of negative (-) strand synthesis proposed by Khromykh *et al.* (1999*b*). Diagram is taken and modified from Khromykh *et al.* (1999*b*); see text for a more detailed explanation of this model. (A) NS3 is proposed to bind NS5 at one or more of the conserved regions designated a, b, or c, possibly associated also with NS2A. (B) Following translation, the complex probably attaches to the 3′ terminal stem-loop of the 3′ UTR via NS2A and possibly NS3 and NS5. The complex attached to the RNA positive (+) strand is transported to the membrane site of replication by affinity of the hydrophobic regions of NS2A interacting with those of dimeric NS4A, which in turn is bound by hydrophilic extensions in the ER lumen between transmembrane domains to dimeric NS1 in the lumen. (C) The RC is now complete and may undergo rearrangement as the RdRp motifs of NS5 bind the template (+) strand, allowing replication to proceed. The dashed arrow indicates the 5′ to 3′ direction of synthesis of the nascent RNA (-) strand.

Table 1.1: Comparison of various flavivirus helicase proteins reported in the literature.

Virus	NS3 residues	NS3 source	NTPase activity	Reference
WNV	Sequencing experiments revealed two amino termini 63-619 and 66-619	Purified from virus infected Vero cells.	Modest stimulation at high ATP concentrations by poly(dA), no stimulation and even inhibition with other polynucleotides.	(Borowski *et al.*, 2001)
WNV	168-619	Purified from virus infected BHK cells.	Stimulation by poly(A).	(Wengler & Wengler, 1991)
YFV	1-623 164-623	Synthesized in *E. coli* with amino terminal Cre fusion.	Stimulation by poly(A), poly(U), poly(C) and poly(ACU), no stimulation by poly(dA), poly(dC) and poly(dG).	(Warrener *et al.*, 1993)
JEV	1-619 149-619 324-619	Synthesized in *E. coli* with amino terminal His fusion.	324-619 truncated fusion protein had no NTPase activity. Nucleoside triphosphate preference GTP>ATP>UTP>CTP. Polynucleotide stimulation preference poly(U)>poly(C)>poly(A).	(Kuo *et al.*, 1996)
JEV	1-619	Synthesized in *E. coli* with amino terminal maltose binding protein fusion.	Protein possessed basal ATPase activity, however polynucleotide stimulation was not tested.	(Takegami *et al.*, 1994)
JEV	163-619	Synthesized in *E. coli* with carboxy terminal His fusion.	Stimulation by poly(U).	(Utama *et al.*, 2000*b*)
JEV	163-619	Synthesized in *E. coli* with carboxy terminal His fusion.	Preference for GTP, stimulation by poly(U).	(Utama *et al.*, 2000*a*)
DEN-2	1-618 161-618 181-618	Synthesized in *E. coli* with carboxy terminal His fusion, analysis performed using 161-618 truncated fusion protein.	Nucleoside triphosphate preference ATP>GTP>UTP>CTP. Polynucleotide stimulation preference poly(A)>poly(U)>poly(C). Inhibition by poly(G).	(Li *et al.*, 1999)
DEN-1	1-619	Synthesized in *E. coli* with amino terminal GST fusion, GST removed by thrombin cleavage.	Nucleoside triphosphate preference ATP>GTP>UTP>CTP. No polynucleotide stimulation by poly(A) or poly(U), stimulation by NS5.	(Cui *et al.*, 1998)

Table 1.2: Mutational analysis of the functional significance of motif VI of the HCV NS3 protein.

HCV residues	Motif VI								Basal ATPase[1]	RNA stimulated ATPase[1]	RNA binding[1]	RNA helicase[1]	Reference
	Q_{460}	R_{461}	R_{462}	G_{463}	R_{464}	Y_{465}	G_{466}	R_{467}					
1-631	H								↓↓	nt[2]	nt	–	(Wardell *et al.*, 1999)
								K	–	nt	nt	–	
166-631	H								–	–	↑	–	(Kim *et al.*, 1997)
		A							↑	↓	wt	wt	
			L[3]						↓	↓↓	↓	↓↓	
				A					↓↓	↓↓	wt	wt	
					A				↓↓	–	wt	–	
				A					↓↓	–	wt	–	
						N			↓↓	↓↓	wt	wt	
							A		↓↓	↓↓	↑	↓	
								K	–	–	wt	–	
166-631				A					–	–	–	–	(Min *et al.*, 1999)
16-608		A							nt	nt	↓↓	nt	(Chang *et al.*, 2000)
			D	T					↓	nt	↓↓	–	
				A					nt	nt	↓↓	nt	

[1] Activity observed represented by (-) no detectable activity, (wt) parental activity, (↑) activity increased compared with parental activity, (↓) activity reduced compared with parental activity, (↓↓) activity greatly reduced compared with parental activity.

[2] nt, not tested.

[3] Changes associated with decreased RNA binding are shown in red.

CHAPTER TWO: MATERIALS AND METHODS

This chapter details the materials and methods that are general to all studies described in this thesis. Specific procedural details for each study are presented in individual methods sections accompanying each results chapter.

2.1 Cell lines and cell culture media

Baby hamster kidney (BHK-21) and *Aedes albopictus* C6/36 cells were grown in Eagle's basal medium (BME) containing Earle's salts, and supplemented with 7.5-10% foetal calf serum (FCS), 2 millimolar (mM) glutamine and 100 units per millilitre (U/ml) of both penicillin and streptomycin. The medium was adjusted to pH 7.2 with $NaHCO_3$. BHK-21 cells were grown at 37°C in an atmosphere of 5% CO_2 while C6/36 cells were grown at 28°C in 2.5% CO_2.

2.2 Growth and plaque assay of virus stocks

The NGC strain of DEN-2 was first described by Sabin & Schlesinger (1945). Stocks of DEN-2 were grown and titrated by plaque assay in C6/36 cells. Infected C6/36 and BHK-21 cells were maintained in BME with 2% FCS. The method for plaque assays was described by Gualano *et al.* (1998). Plaque assays were performed using one day old 70% confluent cells in six well trays (Greiner). Serial ten fold dilutions of virus were prepared in Hanks buffered salts solution (HBSS). The cells were washed in phosphate buffered saline (PBS) and 150 microlitres (µl) of diluted

virus was added to each well. The trays were incubated at 28°C for 1 hour (hr) with rocking every 10 minutes (min) to redistribute the inoculum. The inocula were removed and the cells overlaid with 5 ml/well of an equal mix of double strength maintenance medium (preheated to 42°C) and 2% SeaPlaque agarose (FMC BioProducts) (preheated to 55°C). Five days post infection (p.i.) the cells were overlaid with 2.5 ml of the overlay mix, containing 0.018% neutral red. Plaques were counted seven days p.i..

2.3 Polyethylene glycol precipitation of viruses

To produce high titre stocks of DEN-2 viruses, a method of polyethylene glycol (PEG) precipitation described by Della & Westaway (1972) was used. Subconfluent C6/36 cells in 175 cm^2 flasks were infected with virus and incubated at 28°C. When approximately 10-20% of the cells showed cytopathic effects (CPE), the culture medium was collected and stored at 4°C. Fresh maintenance medium (BME with 2% FCS) was added to the flask, which was returned to the incubator. Usually within a further 24 hr, 70% of the cells exhibited CPE and the culture medium was pooled with the first collection.

Cell debris was removed by centrifugation at 12000 g at 4°C. A one fifth volume of 40% PEG in 1X HBSS was added to the clarified medium and held on ice for 1 hr with occasional mixing. The medium was again centrifuged at 12000 g at 4°C and the concentrated virus pellet was resuspended in 2 ml of Tris buffered saline (12 mM Tris-HCl pH 7.5, 120 mM NaCl) with 0.1% bovine serum albumin (BSA). The

50 fold virus concentrate was kept overnight at 4°C and then dispensed into aliquots and stored at –70°C.

2.4 Growth of parental and mutant viruses in BHK-21 cells at 33°C and 37°C

BHK-21 cells were seeded into 30 mm^2 petri dishes and grown to 70-80% confluency. Cells were infected with parental and mutant viruses at a multiplicity of infection (MOI) of 1.0 at either 33°C or 37°C. After a 1 hr incubation, the inoculum was removed and the cell monolayer was washed twice with PBS. To each petri dish, 3 ml of maintenance media was added, and cells were further incubated at 33°C or 37°C. At 3 days p.i. inoculum from a petri dish for each virus was harvested, and titred by plaque assay in C6/36 cells at 28°C (see section 2.2).

2.5 Cloning of cDNA

2.5.1 Generation of blunt ends

To generate DNA fragments with blunt ends, the 3' recessed ends were filled in using the Klenow fragment of DNA polymerase I (New England Biolabs). Following a restriction enzyme digest, 15 µM deoxynucleotriphosphates (dNTPs) and 5 units of DNA polymerase I were added to the digest mixture and incubated at 25°C for 30 min. The reaction was stopped by heating at 75°C for 10 min. DNA was purified by gel electrophoresis (see section 2.5.3).

2.5.2 Alkaline phosphatase treatment of vectors for cloning

Vectors were digested with the appropriate restriction enzyme(s) and vectors were dephosphorylated using calf intestinal phosphatase (CIP) in dephosphorylation buffer (Boehringer Mannheim), as described by Sambrook *et al.* (1989). The DNA was then purified by electrophoresis (see section 2.5.3).

2.5.3 DNA electrophoresis and purification

Most DNA fragments were separated by electrophoresis in 0.8% agarose gels (FMC BioProducts) prepared and run in 1X TAE buffer (40 mM Tris acetate pH 7.5, 2 mM EDTA). DNA was purified from agarose gels using the QIAEX II Gel Extraction Kit (QIAGEN), as specified by the manufacturer.

Very small PCR products were separated by electrophoresis in 7.5% polyacrylamide gels using the mini-Protean II vertical electrophoresis cell (Bio-Rad). Electrophoresis was carried out in 1X TBE buffer (90 mM Tris borate pH 7.5, 2 mM EDTA) at 200 volts (V) for 25 min. DNA was purified from polyacrylamide gels using the QIAEX II Gel Extraction Kit (QIAGEN), as specified by the manufacturer.

2.5.4 Ligation of vector and insert DNA

Ligation mixes contained vector and insert DNA at a molar ratio of 1:3. DNA was ligated in a 15 µl volume using 1 unit of T4 DNA ligase in T4 DNA ligase buffer (Boehringer Mannheim). Ligation reactions were incubated overnight at 15°C.

2.5.5 Transformation of ligation reactions into competent *E. coli*

Competent *E. coli* DH5α cells were prepared using the method of Hanahan (1985). For transformations, 50 µl of thawed competent cells were added to the ligation mixture, and kept on ice for 40 min. The samples were heat shocked at 42°C for 90 seconds (sec) and returned to ice for a further 2 min. Cells were then incubated on a shaker at 37°C for 1 hr in 150 µl of SOC (2% tryptone, 0.5% yeast extract, 8 mM NaCl, 2.5 mM KCl, 10 mM $MgCl_2$, 20 mM glucose). The total volume of transformed cells was then plated onto Luria-Bertani (LB) agar plates (1% tryptone, 0.5% yeast extract, 15 g/ml agar, 0.17M NaCl) containg 100 µg/ml ampicillin (Amp) and incubated at 37°C overnight.

2.5.6 Small scale preparation of plasmid DNA

Small scale preparations of plasmid DNA for screening of plasmids with DEN-2 cDNA inserts were obtained by the alkaline lysis method from 1.5 ml overnight cultures in LB broth (1% tryptone, 0.5% yeast extract, 0.17M NaCl) containing 100 µg/ml Amp (Sambrook *et al.*, 1989). Plasmid DNA to be used as template for sequencing reactions was purified from 5 ml overnight cultures in LB broth containing 100 µg/ml Amp using the Wizard *Plus* SV Minipreps DNA Purification System (Promega), according to the manufacturer's instructions.

2.5.7 Large scale preparation of plasmid DNA

Large scale preparations of plasmid DNA were prepared from 500 ml overnight cultures in LB broth containing 100 µg/ml Amp, using the QIAGEN Plasmid Midi Kit, as specified by the manufacturer.

2.6 Automated sequencing of DNA

Automated DNA sequencing reactions were performed according to the manufacturer's instructions, as described in the PRISM™ Big Dye™ Terminator Cycle Sequencing Ready Reaction Kit (Applied Biosystems). Resulting DNA sequences were analyzed using the GeneJockey II software program (BIOSOFT).

2.7 Plasmids used in this study

The plasmid containing the parental genomic length DEN-2 cDNA (NGC) is named pDVWS501 and is in a modified low copy number vector pWSK29 (described in Gualano *et al.,* 1998). For this study, virus derived from the parental plasmid pDVWS501 was named V2. Plasmids containing clustered charged-to-alanine mutations in the NS3 protein were named according to the NS3 amino acid numbers of regions mutagenized (e.g. pDVWS501NS3$_{63\text{-}66}$), and derived virus was designated with a V (e.g. V$_{63\text{-}66}$). Alternatively, plasmids containing amino acid substitutions within helicase motifs were named according to the residue mutated, its amino acid number within NS3, and the replacement residue (e.g. pDVWS501NS3$_{K199A}$), and derived virus was designated with a V (e.g. V$_{K199A}$). All nucleotide and amino acid

numbering refers to the DEN-2 NGC sequence published by Irie *et al.* (1989): GenBank accession number M19727.

2.8 Mutagenesis by overlap extension PCR

Site-directed mutagenesis was performed by overlap extension PCR (OE-PCR) (Ho *et al.*, 1989). The procedure is illustrated in Fig. 2.1. The procedure required two rounds of PCR. The first round of PCR involved two separate PCR reactions using flanking primers (a or d), and mutagenic primers (b or c) amplifying two precursor fragments from template DNA. The precursor fragments were analyzed by electrophoresis and the desired fragments were cut from the gel, and used as templates to produce the OE-PCR fragment, using the flanking primers a and d in the second round of PCR. This joins the two PCR fragments produced initially, via their complementary overlapping regions (Fig. 2.1).

Amplification of the two overlapping precursor fragments was performed using a Corbett Research Capillary FTS-1 Thermal Sequencer. The 50 µl reaction contained template DNA at a concentration of 5 ng, 0.5 µM of each primer, 50 µM of each dNTP, 2.5 units of PWO DNA polymerase (Boehringer Mannheim) and 5 µl of PWO 10X reaction buffer, supplied by the manufacturer. At 1X concentration, the reaction buffer contains 10 mM Tris-HCl pH 8.8, 25 mM KCl, 5 mM $(NH_4)_2SO_4$ and 2 mM $MgSO_4$. The PCR program was: 4 cycles of 94°C (10 sec), 55°C (30 sec), 72°C (1 min), 30 cycles of 94°C (5 sec), 55°C (5 sec), 72°C (40 sec), and 1 cycle of 94°C (5 sec), 55°C (5 sec) and 72°C (2 min).

The PCR products were analyzed by electrophoresis through 1% low melting point agarose (Progen) and the desired fragments were cut from the gel, placed in a microcentrifuge tube and incubated at 70°C for 5 min. A 1 µl aliquot of each of the precursor fragments was added to a new tube containing 100 µM dNTPs, 5 µM of each primer a and d, 5 units of PWO polymerase and 10 µl of 10X PWO buffer in a final volume of 100 µl. This second round PCR was performed in a Corbett Research FTS-320 Thermal Sequencer in 500 µl tubes overlayed with paraffin oil. The PCR program was 2 cycles of 94°C (2 min), 45°C (2 min), 72°C (2 min), 28 cycles of 94°C (1 min), 50°C (30 sec), 72°C (1 min), and 1 cycle of 72°C (4 min). Finally, OE-PCR products were purified by gel electrophoresis (see section 2.5.3).

2.9 Transcription of RNA from plasmids containing genomic length DEN-2

Procedures for transcription of RNA have been described previously by Gualano *et al.* (1998). In brief, parental and mutant pDVWS501 plasmids were linearized at a unique *Xba* I site at the 3' end of the DEN-2 insert, by digestion for 3 hr at 37°C. The DNA was purified by phenol/chloroform extraction and ethanol precipitation. The DNA pellet was resuspended in nuclease free water.

Transcription was carried out using the Promega T7 RiboMAX™ kit according to manufacturer's instructions. The 20 µl reaction contained 2.5 µg template DNA, 1 mM $m^7G(5')ppp(5')G$ cap analogue (New England Biolabs), 7.5 mM each of rATP, rCTP, rUTP and 2.5 mM rGTP. The reaction was incubated for 2 hr at 37°C. Transcript size and yield was analyzed by agarose gel electrophoresis. RNA was

stored at –70°C in 200 µl aliquots of approximately 10 µg RNA mixed with 5 µl of 3 M sodium acetate (pH 5.2) and 150 µl of ethanol. RNA for electroporation was pelleted, washed in 75% ethanol and resuspended in nuclease free water immediately prior to use.

2.10 Electroporation of genomic length RNA into BHK-21 cells

Conditions used to electroporate BHK-21 cells were described by Gualano *et al.* (1998). Briefly, BHK-21 cells were grown in 175 cm^2 flasks until the monolayers were 60-80% confluent (two days). Cells were then trypsinized, pooled and washed twice in cold PBS. The cells were resuspended in 2 ml of cold PBS and kept on ice while 20 µl of the cell suspension was counted in a haemocytometer. The cells were diluted in cold PBS to a concentration of 1 x 10^7 cells/ml, and 0.5 ml aliquots were dispensed into 0.4 cm GENE Pulser cuvettes (Bio-Rad). Approximately 50 µg of high grade yeast tRNA (Boehringer Mannheim) and 7-10 µg of transcribed virus RNA were added to each aliquot of cells. The cuvettes were kept on ice for 10 min and then cells were electroporated using a GENE pulser I apparatus (Bio-Rad), which was set to deliver a single pulse at 500 µF and 300-350 V. After electroporation, cells were kept on ice for 10 min prior to being recultured in two 60 mm^2 petri dishes containing 5 ml of growth medium (BME with 10% FCS), and incubated at 33°C or 37°C. A 15 µl aliquot of each sample of electroporated cells was also replated in duplicate in a chamber slide for later immunofluorescence (IF).

Growth medium was changed 16-24 hr post electroporation (p.e.). When monolayers were 70-80% confluent, growth medium was removed and replaced with

maintenance medium. Seven days p.e., the culture medium from the BHK-21 cells was harvested. For some samples, medium was harvested earlier than seven days p.e. (when most cells showed CPE) and kept at –70°C. For each sample, 250 µl of harvested medium was used undiluted as inoculum to infect C6/36 cells. The cells were incubated at 28°C for 1 hr with rocking every 15 min to redistribute the inoculum. The inoculum was removed and cells maintained in 5 ml of maintenance medium. Five days later, the culture medium from these C6/36 cells was used to set up a second passage in C6/36 cells. The medium from the second C6/36 passage was harvested when most of the cells showed CPE (between two and five days p.i.) or at day five if little or no CPE was evident. The titre of the virus twice passaged in C6/36 cells was determined by plaque assay in C6/36 cells, as described in section 2.2. Each virus was derived at least twice from its parental construct.

2.11 Indirect immunofluorescence

To determine the percentage of cells transfected by the RNA transcripts, the synthesis of viral protein was assayed by monitoring the production of E using a mix of anti-E monoclonal antibodies (Gruenberg & Wright, 1992).

At five or six days p.e., BHK-21 cells in chamber slides were washed with PBS and fixed in cold acetone for 2 min. Slides were kept for 1 hr at room temperature with 30 µl of a mixture of anti-E monoclonal antibodies added to each well. The slides were washed three times in PBS and 30 µl of a 1/50 dilution of fluorescein isothiocyanate conjugated anti-mouse immunoglobulin (Silenus) was added to each well. The slides were incubated in the dark for 1 hr at room

temperature, and washed three times in PBS. The slides were mounted in 20% glycerol in PBS and viewed using a Zeiss IM-35 inverted microscope.

2.12 RT-PCR of viral RNA

To confirm that the desired mutation was still present in viral RNA after electroporation and passaging, RNA was extracted from second passage infected C6/36 cells or culture medium, and RT-PCR and sequencing were performed.

The acid-guanidine isothiocyanate method (Lewis *et al.*, 1992) was used for RNA extraction. To extract RNA from infected cells, the cells were scraped from a 60 mm^2 petri dish into 1 ml of PBS. The cells were pelleted at 16000 g and resuspended in 250 µl of lysis buffer (4M guanidine isothiocyanate, 25 mM sodium citrate, 100 mM 2-mercaptoethanol, 0.5% sodium sarkosyl), 25 µl of 2 M sodium acetate (pH 4.0), 250 µl of phenol (pH 5.6), and 50 µl of chloroform/isoamyl alcohol (24:1). To extract RNA from the supernatant of infected cells, an initial 10000 g spin clarified the medium. RNA extracted from cell culture medium involved mixing 250 µl of medium with 100 µl of lysis buffer, 35 µl of 2 M sodium acetate (pH 4.0), 350 µl of phenol (pH 5.6), and 70 µl of chloroform/isoamyl alcohol (24:1).

The samples were vortexed and kept on ice for 15 min, and centrifuged at 16000 g at 4°C for 15 min. The aqueous phase was mixed with an equal volume of isopropanol and kept at –20°C for 1 hr before pelleting the preciptated RNA by a 20 min 16000 g spin at 4°C. The pellet was washed with 75% ethanol and air dried. The pellet was resuspended in 50 µl of nuclease free water and stored at –70°C.

A 10 µl sample of RNA was mixed with 3 pmol of a specific primer or 1 µl of 200 mM random primers (hexamers) synthesized with the Amplified Biosystems 394 DNA/RNA synthesizer [ABI] (by Mrs Khim Ho) in a final volume of 20 µl, followed by denaturation at 70°C for 10 min. Samples were immediately placed on ice and buffer containing 10 mM DTT, 0.5 mM dNTPs, 50 mM Tris-HCl, 75 mM KCl and 3 mM $MgCl_2$ was added. The reverse transcription (RT) reaction was initiated upon addition of 200 units of SuperScript™ II (Life Technologies) to each sample. After incubation at 42°C for 1 hr, the RT was inactivated by heating at 95°C for 5 min. PCR reactions were set up in a volume of 50 µl, using 5 µl of the RT reaction, 2.5 units of DynaZyme™ DNA polymerase (Finnzymes), 200 µM dNTPs and 0.5 µM of forward and reverse primers. The conditions for cDNA synthesis by PCR, were different to those in section 2.8. Amplification was performed using a Corbett Research Capillary FTS-1 Thermal Sequencer. The PCR program was: 1 cycle of 94°C (2 min), 48°C (1 min), 72°C (1 min), 4 cycles of 94°C (1 min), 48°C (1 min), 72°C (1 min), 30 cycles of 94°C (5 sec), 48°C (5 sec), 72°C (30 sec), and 1 cycle of 94°C (5 sec), 48°C (5 sec) and 72°C (2 min).

The complete NS2B and NS3 genes were sequenced to confirm the presence of the introduced mutation and the absence of any other changes that may have been introduced during virus passaging.

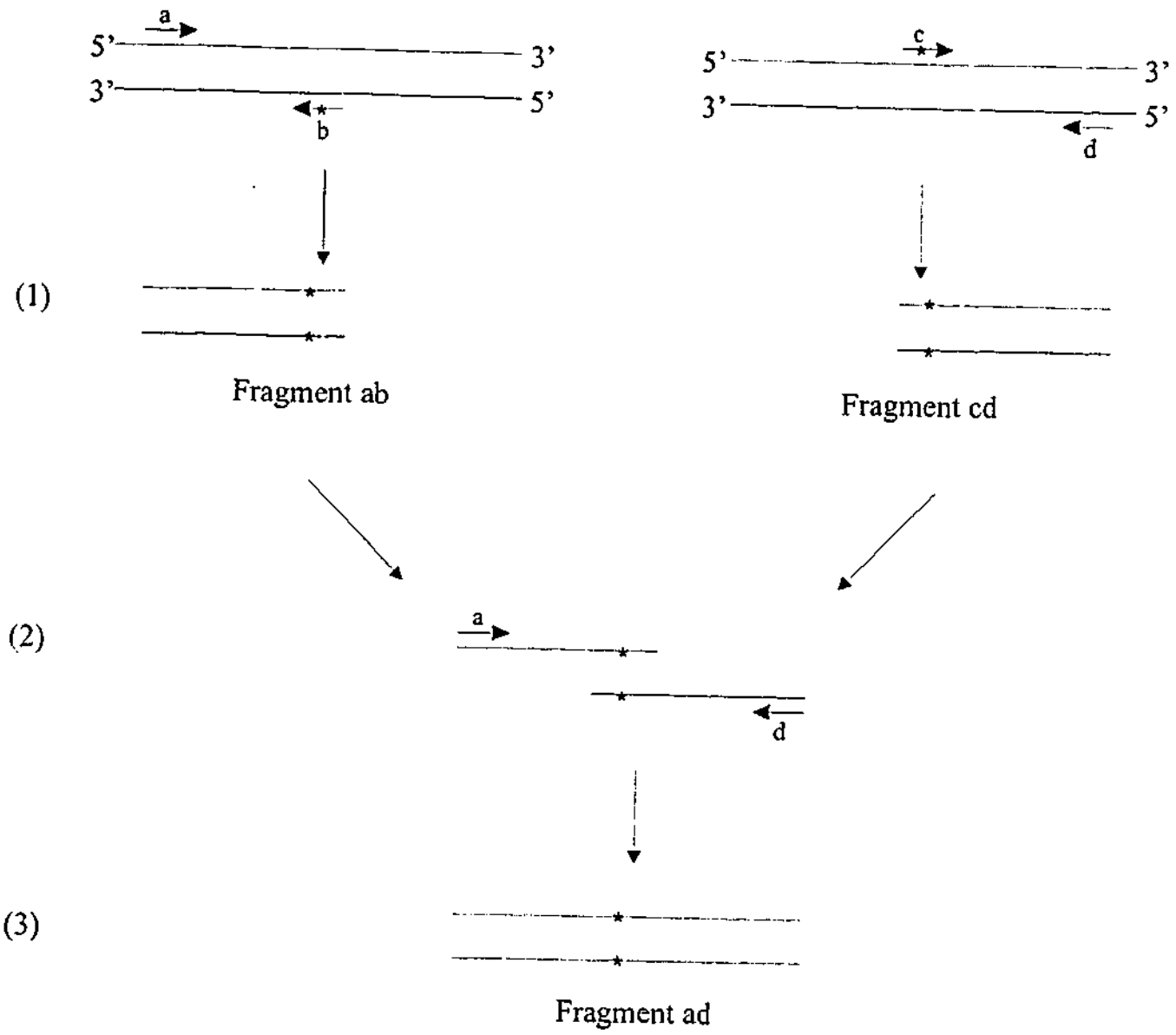

Fig. 2.1 Site-directed mutagenesis by overlap extension PCR. This involves a total of three separate PCR reactions and four oligonucleotide primers. Primers a and d are forward and reverse flanking primers respectively, primer b is the reverse mutagenesis primer and primer c is the forward mutagenesis primer. The asterisk signifies the introduced mutation. (1) In separate PCR reactions, two overlapping precursor products which contain the mutation are amplified. The products are purified by gel electrophoresis to remove the original template.

(2) The products are used in a third overlap PCR reaction.

(3) The final PCR product contains the introduced mutation.

CHAPTER THREE: MUTATIONAL ANALYSIS OF THE PROTEINASE REGION OF THE DEN-2 VIRUS NS3 PROTEIN

3.1 Introduction

The focus of this chapter is the DEN-2 viral proteinase, NS2B/3, that cleaves at the NS2A/NS2B, NS2B/NS3, NS3/NS4A and NS4B/NS5 junctions.

Mutations that restrict, but do not prevent, viral replication are candidates for incorporation into live virus vaccine strains including DEN-2 and other flaviviruses (Chambers *et al.*, 1997). The main aim of the experiments described in this chapter was to produce such mutations in the NS3 proteinase. Since previous studies on several flaviviruses have targeted the four conserved proteinase motifs and the cleavage sites (Chambers *et al.*, 1990*b*; Valle & Falgout, 1998), here locations outside these regions of NS3 were chosen. In particular, by avoiding motifs, it was reasoned that proteinase activity may be retained and that mutations may not be lethal.

Hydrophilic regions were targeted using clustered charged-to-alanine mutagenesis (Diamond & Kirkegaard, 1994; Wertman *et al.*, 1992). Charged amino acids are likely to occupy exposed positions in the tertiary structure and therefore interact with other proteins. Previous experiments with DEN-4 identified a 40 aa segment of NS2B that was largely hydrophilic and essential for proteinase activity (Falgout *et al.*, 1993). Therefore it was possible that changes to the hydrophilicity of NS3 might modify the interaction of NS3 with NS2B and the proteinase activity of the NS2B/3 complex.

The first 181 aa of NS3 were scanned for clusters of five residues which contained at least three charged amino acids, namely Asp, Glu, Lys and Arg (Bass *et al.*, 1991; Wertman *et al.*, 1992) (Fig. 3.1). Four such clusters ($\underline{K}_{63}\underline{R}\underline{I}\underline{E}_{66}$, $\underline{E}_{91}\underline{G}\underline{E}\underline{E}_{94}$, $\underline{E}_{169}\underline{K}\underline{S}\underline{I}\underline{E}_{173}$, and $\underline{E}_{179}\underline{D}\underline{D}_{181}$) outside proteinase motifs (Bazan & Fletterick, 1989) which also exhibited distinct peaks on a hydrophilicity plot (Hopp & Woods, 1981) (Fig. 3.2) were chosen for mutagenesis and the underlined charged residues were changed to Ala. Ala was chosen as the replacement amino acid since it removes the side chain beyond the beta carbon and also minimizes any steric effects within the polypeptide caused by the replacement (Cunningham & Wells, 1989). In addition, a hydrophobic region was chosen, $\underline{G}_{32}\underline{Y}SQI_{36}$ based on a hydropathy plot (Kyte & Doolittle, 1982) (Fig. 3.3) and conservation of sequence across the flaviviruses, with G_{32} being invariant at this position (Fig. 3.1) (Dalgarno *et al.*, 1986; Fu *et al.*, 1992; Osatomi & Sumiyoshi, 1990; Pletnev *et al.*, 1990; Westaway & Blok, 1997).

Previous work in our laboratory by Kelley (1996) had examined the effects of three of these mutations $\underline{G}_{32}\underline{Y}SNI_{36}$, $\underline{K}_{63}\underline{R}\underline{I}\underline{E}_{66}$ and $\underline{E}_{179}\underline{D}\underline{D}_{181}$ on *cis* cleavage at the internal NS3 and NS2B/NS3 sites, using a COS cell (Gluzman, 1981) transient expression system (Matusan *et al.*, 2001). All three mutants retained significant proteinase activity in COS cells.

Hence these three mutations and two additional charged-to-alanine mutations $K\underline{E}_{91}\underline{G}\underline{E}\underline{E}_{94}$ and $\underline{E}_{169}\underline{K}\underline{S}\underline{I}\underline{E}_{173}$ were incorporated into DEN-2 genomic length cDNA, to investigate their effects on virus replication and plaque forming ability (Fig. 3.4).

3.2 Materials and methods

Sections 3.2.1 and 3.2.2 describe the construction of genomic length DEN-2 clones (pDVWS501) containing mutations within the proteinase region of NS3. These constructs were needed to study the effects of the mutations on virus replication. A summary of the mutant constructs can be found in Fig. 3.4. A copy of Fig. 3.4 is removable for the reader's convenience from the pocket at the back of the thesis.

Table 3.1 summarizes the mutant constructs produced by OE-PCR and the sequences of primers used. After cloning of OE-PCR products was complete, each PCR derived region was completely sequenced, and the primers used for sequencing are listed in Table 3.2.

3.2.1 Construction of the proteinase mutant pDVWS501NS3$_{32\text{-}36}$

For cloning strategies, the locations of restriction enzyme sites cleaving in DEN-2 cDNA (Irie *et al.*, 1989) are shown in superscript, and sites present in plasmid vectors are not numbered. The plasmid pDVWS501, containing genomic length DEN-2 (NGC strain) cDNA in a modified low copy number vector pWSK29 has been described in detail (Gualano *et al.*, 1998).

cDNA encoding the mutation $\underline{G_{32}Y}SNI_{36}$ (underlined residues changed to Ala) in the NS3 hydrophobic region was cloned into pDVWS501 following the PCR synthesis of two fragments from two different templates, and the synthesis of the final fragment containing the mutation by OE-PCR (Fig. 3.5). The mutant was previously constructed in a pSV.SPORT 1 background in our laboratory by P. Kelley to test for

proteinase activity using transient expression of the pSV construct in COS cells. This mutation was present in the construct pSV.NS2B/$3_{32\text{-}36}$, however an additional I36V change at position 36 was also present, introduced during PCR (Matusan *et al.*, 2001). Both this construct and pDVWS501 were used as template DNAs for OE-PCR. The 2279 bp fragment, which contained the changes was generated using Amplitaq™ DNA polymerase (Perkin Elmer), rather than PWO DNA polymerase (Boehringer Mannheim) which due to its proofreading capabilities was used to generate all other PCR fragments (as described in section 2.8). In this instance, PWO DNA polymerase was unable to generate the desired fragment. The 2279 bp OE-PCR fragment was cleaved at the *Nhe* I and *Nsi* I sites located within the NS1 and NS3 genes respectively, and ligated into the plasmid pDVWS501 which had been digested with the same enzymes at these two unique sites. PCR derived regions were sequenced (Tables 3.1 and 3.2).

3.2.2 Construction of the charged-to-alanine mutants pDVWS501NS$3_{63\text{-}66}$, pDVWS501NS$3_{91\text{-}94}$, pDVWS501NS$3_{169\text{-}173}$ and pDVWS501NS$3_{179\text{-}181}$

Due to an absence of suitable restriction enzyme sites for cloning an appropriate fragment directly into pDVWS501, these four mutations were initially constructed in the plasmid pDVSO8298 prior to ligation of a subfragment into pDVWS501.

3.2.2(a) Construction of the plasmid pDVSO8298

The construction of pDVSO8298 is illustrated in Fig. 3.6. A 4243 bp *Kpn* I^{4497} – *Avr* II^{8740} DEN-2 fragment was isolated and cloned into *Xba* I/*Kpn* I-digested pSPORT 1 (Gibco BRL) to produce pDVSO8298. *Avr* II and Xb*a* I produce sticky ends that are complementary, enabling ligation.

3.2.2(b) Construction of the clustered charged-to-alanine mutants pDVWS501NS3$_{63\text{-}66}$ and pDVWS501NS3$_{179\text{-}181}$

Fragments of cDNA encoding mutations in the NS3 hydrophilic regions, $\underline{K_{63}}R\underline{IE_{66}}$ or $\underline{E_{179}}\underline{DD_{181}}$ were cloned into pDVSO8298 by removing the mutagenized *Nsi* I – *Ppu* MI fragments from the corresponding pSV.NS2B/3 plasmids (Kelley, 1996), and ligating them into pDVSO8298 digested with *Nsi* I and *Ppu* MI (Fig. 3.7). To introduce these mutants into the genomic length DEN-2 clone, *Nsi* I – *Stu* I mutated fragments were then removed from the appropriate pDVSO8298 plasmid and ligated into pDVWS501 cleaved with *Nsi* I^{4700} and *Stu* I^{7874} at these unique sites (Fig. 3.7).

3.2.2(c) Construction of the clustered charged-to-alanine mutants pDVWS501NS3$_{91\text{-}94}$ and pDVWS501NS3$_{169\text{-}173}$

The two remaining charged-to-alanine mutations, $\underline{E_{91}}G\underline{EE_{94}}$ and $\underline{E_{169}}\underline{K}SI\underline{E_{173}}$, were introduced into *Nsi I/Ppu* MI-digested pDVSO8298 as OE-PCR fragments. For both mutations, *Nsi* I – *Stu* I fragments were then removed from the appropriate

pDVSO8298 plasmid and ligated into *Nsi* I^{4700}/*Stu* I^{7874}-digested pDVWS501 (Fig. 3.8 A and B).

3.2.3 RT-PCR of viral RNA

To confirm that the desired mutation was present in viral RNA obtained as described in section 2.10, RNA was extracted from infected C6/36 cells or culture medium. The cells were infected with virus obtained by electroporation of RNA into BHK-21 cells (maintained at 33°C or 37°C) and in previous passages in C6/36 cells (section 2.10). RT-PCR and sequencing was performed as described in section 2.12. Table 3.3 shows the primers used in reverse transcription (random hexamers were also used), PCR and sequencing of each virus. The sequence of each primer is shown in Table 3.2.

3.2.4 Growth curves of parental and mutant DEN-2 viruses

C6/36 cells were seeded into 30 mm^2 petri dishes and infected with parental and mutant viruses at an MOI of 1.0 when cells reached 70-80% confluency. Following a 1 hr incubation at 28°C, the virus inoculum was removed, and the cells washed twice with PBS. To each petri dish, 3 ml of maintenance medium was added. Supernatant from a petri dish for each virus at each time point (0 hr, 24 hr, 48 hr, 72 hr and 96 hr p.i.) was harvested and titred by plaque assay in C6/36 cells (see section 2.2).

3.2.5 Serial passage of V_{32-36} and V_{91-94} in C6/36 cells

C6/36 cells were seeded into 60 mm^2 petri dishes and infected with 250 µl aliquots of first passage supernatant stocks of each mutant virus. Following a 1 hr incubation at 28°C, the virus inoculum was removed, and 5 ml of maintenance medium was added. The cells were maintained at 28°C for five days (or until cell monolayers exhibited extensive CPE). On day 5, 250 µl of supernatant was then removed form the appropriate petri dish and fresh C6/36 cells were infected. Virus was serially passaged up to 12 times in C6/36 cells.

3.2.6 Coordinates and calculations

The crystal structures of the DEN-2 NS3 serine proteinase (protein data bank identifier 1BEF; Murthy *et al.*, 1999) and the HCV NS3/NS4A proteinase/cofactor complex (protein data bank identifier 1NS3; Yan *et al.*, 1998) were obtained from the protein data bank (Berman *et al.*, 2000; Bernstein *et al.*, 1977) by Dr. J. Whisstock (Department of Biochemistry and Molecular Biology, Monash University).

The model between the DEN-2 NS3 proteinase and a portion of the NS2B cofactor was generated by Dr. J. Whisstock using the Quanta/CHARMm suite of software (M.S.I. Inc., San Diego). The sequence G_{69}SSPILSITISE$_{80}$ within NS2B corresponds to the portion of the NS4A cofactor seen in the structure of the HCV proteinase (Brinkworth *et al.*, 1999) (Fig. 1.2). The DEN-2 and HCV proteinases were superposed and the NS4A peptide within the HCV proteinase structure used as a template to homology model the NS2B sequence (GSSPILSITISE) into the DEN-2

NS3 proteinase. The model was subjected to rounds of CHARMm minimization, initially with constraints applied to the proteinase and the co-factor allowed to move freely. Later rounds were performed to convergence with no constraints. Dihedral constraints were applied to four residues in non-allowed conformations. A Ramachandran plot of the final model indicated that all residues were in allowed conformations. The position of the mutations described in Fig. 3.4 were examined with respect to the crystal structure of the DEN-2 NS3 proteinase and the model between the NS3 proteinase and the NS2B cofactor.

3.3 Results

3.3.1 Analysis of virus replication

Previous experiments showed that mutations which abolished or strongly reduced YFV NS2B/3 proteinase activity usually prevented or greatly reduced viral replication (Amberg & Rice, 1999; Chambers *et al.*, 1993; Chambers *et al.*, 1995; Nestorowicz *et al.*, 1994), whereas mutations with less severe effects on cleavage generally allowed the recovery of infectious virus, albeit with reduced plaque titres and small plaque phenotypes (Amberg & Rice, 1999; Chambers *et al.*, 1995; Nestorowicz *et al.*, 1994).

Previous work by Kelley (1996) showed that the charged-to-alanine mutants, $\underline{K}_{63}\underline{R}\underline{I}\underline{E}_{66}$, $\underline{E}_{179}\underline{D}\underline{D}_{181}$, and the mutation within the hydrophobic region, $\underline{G}_{32}\underline{Y}SNI_{36}$, did not show severe inhibition of proteinase activity when tested using transient expression of parental and mutant pSV.SPORT 1 constructs in COS cells. Hence

these mutations and a further two of the charged-to-alanine-type (without prior testing in COS cells) were chosen for incorporation into genomic length cDNA.

Virus was produced from genomic length cDNA cloned in the pDVWS501 series of plasmids (Fig. 3.4) by established procedures (Gualano *et al.*, 1998) (sections 2.9 and 2.10) as follows. RNA was transcribed and electroporated into BHK-21 cells and the cells were incubated at 33°C or 37°C. BHK-21 cells were tested for immunofluorescence with anti-E monoclonal antibodies. Medium from the transfected BHK-21 cells was passaged twice in C6/36 cells at 28°C, and the virus titre determined after the second passage by plaque assay in C6/36 cells (Table 3.4). Viral RNA was then amplified by RT-PCR and sequenced to check that the mutation was retained during the passaging. For the four charged-to-alanine mutant viruses, the entire NS2B and NS3 genes were sequenced and no additional changes were detected. Due to the low virus yield of $V_{32\text{-}36}$, RNA levels were very low, and although sufficient RNA was obtained at 33°C to confirm the presence of the mutation, more extensive sequencing was difficult and not pursued. These procedures were completed at least twice for each construct, and the results are summarized in Table 3.4.

The parental virus V2 and mutant viruses $V_{63\text{-}66}$, $V_{169\text{-}173}$, and $V_{179\text{-}181}$ grew to comparable titres of 10^5 to 10^6 pfu/ml following initial electroporation at 33°C or 37°C (Table 3.4). All three mutant viruses showed a small plaque phenotype (Fig. 3.9). For viruses $V_{32\text{-}36}$ and $V_{91\text{-}94}$, detectable virus was recovered following electroporation at 33°C only, and at low titres (3×10^1 and 2.4×10^3 pfu/ml respectively). These results suggested that $V_{32\text{-}36}$ and $V_{91\text{-}94}$ were severely restricted in replication and possibly heat sensitive.

To examine further the properties of these viruses, more concentrated stocks were prepared by PEG precipitation (section 2.3). We wished to obtain titres sufficiently high to enable infection of cells at an MOI of 1.0. This proved possible only for V2, V_{63-66}, $V_{169-173}$, and $V_{179-181}$.

3.3.2 Growth of viruses V2, V_{63-66}, $V_{169-173}$, and $V_{179-181}$ in C6/36 and BHK-21 cells

C6/36 cells were infected with recombinant viruses V2, V_{63-66}, $V_{169-173}$, or $V_{179-181}$, at an MOI of 1.0, maintained at 28°C and sampled at 24 hr intervals up to 96 hr p.i.. Virus titres were determined by plaque assay in C6/36 cells. The resulting growth curves are shown (Fig. 3.10). The two viruses with small plaque size (Table 3.4, V_{63-66} and $V_{179-181}$) initially lagged in replication, although by 48 hr p.i., their titres had reached 1 to 8 $\times$ 10^4 pfu/ml, and by 72 hr p.i., the yields of all four viruses were comparable (Fig. 3.10). The presence of the respective mutations in the recovered viruses was confirmed by RT-PCR and sequencing.

To analyze the effect of temperature on the replication of V2, V_{63-66}, $V_{169-173}$, and $V_{179-181}$ in a more rigorous manner than in the experiments summarized in Table 3.4, BHK-21 cells were infected at an MOI of 1.0 and cells were incubated at 33°C or 37°C. Experiments maintaining the BHK-21 cells at 39°C were unsuccessful because of poor cell survival. The culture medium was sampled at 72 hr p.i. and virus titres were determined by plaque assay in C6/36 cells (Fig. 3.11). All four viruses showed no significant temperature sensitivity, as defined by a 50-fold or greater difference in titre between temperatures (Fig. 3.11). The integrity of each mutation was reconfirmed by RT-PCR and sequencing.

3.3.3 Serial passage of V_{32-36} and V_{91-94} in C6/36 cells

The viruses V_{32-36} and V_{91-94} which were severely restricted in replication and possibly heat sensitive (Table 3.4), were serially passaged in C6/36 cells at 28°C. It was hypothesized that ongoing passaging of these viruses may select a reversion or second site mutation that enabled these viruses to replicate more efficiently.

For mutant viruses V_{32-36} and V_{91-94}, virus was passaged up to 12 times in C6/36 cells (as described in section 3.2.5). The cells were maintained at 28°C for five days at each passage (or until cell monolayers exhibited extensive CPE). The virus V_{32-36} did not show any significant increase in CPE or virus titre over 10 passages (Table 3.5). However, following eight passages, on day five of passage number nine, cells infected with the virus V_{91-94} exhibited low levels of CPE. Over the next three passages, the onset of CPE was more rapid, and the levels of CPE increased until passage number 12. The titre of virus in the supernatant was determined for several passages (Table 3.5).

To detect one or more mutations that may be restoring virus replication, genome sequencing of passage 11 virus was commenced. Initially, RT-PCR and sequencing directly across the site mutated showed it had not reverted during passaging. Then, in conjunction with Dr. M. Pryor, further sequencing of nucleotides 2180 (in E gene) to 10400 (in the 3′ UTR) of V_{91-94} passage 11 virus was performed to look for potential supressor mutations in other regions of the genome. The full-length of the NGC DEN-2 genome is 10,723 nucleotides.

Apart from the introduced mutations, no other differences between $V_{91\text{-}94}$ and parental virus V2 were detected in the nonstructural gene sequence. An A to C nucleotide change was observed in the 3′ UTR at position 10344.

3.4 Discussion

Five sites distributed through the amino terminal proteinase region of DEN-2 NS3, and outside conserved enzyme motifs, were mutagenized in these experiments. They were selected before the publication of the model (Brinkworth *et al.*, 1999) and X-ray crystal structures (Brinkworth *et al.*, 1999; Kim *et al.*, 1996; Love *et al.*, 1996; Murthy *et al.*, 1999; Yan *et al.*, 1998) of NS3 proteinase became available. Four sites were rich in charged amino acids (Fig. 3.2), and were considered possible sites of interaction with regions of the 40 aa fragment of NS2B essential for activity (Chambers *et al.*, 1991; Falgout *et al.*, 1993; Falgout *et al.*, 1991; Preugschat *et al.*, 1990).

Of the four charged sites mutated to Ala in DEN-2 NS3, two were previously examined by transient expression in COS cells and shown to retain proteinase activity ($K_{63}RIE_{66}$ and $E_{179}DD_{181}$) (Kelley, 1996). Mutations related, but not identical, to those at $K_{63}RIE_{66}$ ($K_{65}K_{66}$ in YFV), $E_{91}GEE_{94}$ ($E_{94}EE_{96}$ in YFV) and $E_{169}KSIE_{173}$ ($E_{171}VK_{173}$ in YFV), were tested for their effect on the activity of YFV NS2B/3 proteinase (Droll *et al.*, 2000). None reduced proteinase activity significantly. This indicates that these charged regions individually are not critical for NS2B-NS3 protein-protein interactions and proteinase activity *in vitro*. However as shown here, these mutations result in DEN-2 viruses displaying reduced plaque size and hence growth restriction.

3.4.1 Virus production

None of the five mutations inserted into the DEN-2 infectious clone abolished virus production. Five viruses with reduced plaque size on C6/36 cells were obtained; two of these, $V_{32\text{-}36}$ and $V_{91\text{-}94}$, were possibly *ts* but did not grow sufficiently well for adequate testing (Table 3.4). The remaining three viruses grew to good titres (Figs. 3.10 and 3.11), displayed small plaques (Fig. 3.9), but did not show the *ts* phenotype that has been observed for some viruses with charged-to-alanine mutations in nonstructural genes (Diamond & Kirkegaard, 1994; Gavin *et al.*, 1999; Huang *et al.*, 1998; Muylaert *et al.*, 1997; Parkin *et al.*, 1996). In previous studies of flavivirus NS2B/3 proteinase, the enzyme motifs in NS3 (Chambers *et al.*, 1991; Chambers *et al.*, 1990*b*; Pugachev *et al.*, 1993; Valle & Falgout, 1998; Wengler & Wengler, 1991), the NS2B/NS3 cleavage site (Chambers *et al.*, 1995) and parts of NS2B (Chambers *et al.*, 1993; Falgout *et al.*, 1993; Falgout *et al.*, 1991) were mutated, whereas here, regions outside the motifs were targeted. Four sites were rich in charged amino acids (Fig. 3.2), and were considered possible sites of interaction with either NS2B (Chambers *et al.*, 1991; Falgout *et al.*, 1991; Preugschat *et al.*, 1990) or NS5 (Chen *et al.*, 1997*a*; Kapoor *et al.*, 1995).

The approach of charged-to-alanine mutagenesis was first used successfully with *Poliovirus* to isolate *ts* polymerase mutants (Diamond & Kirkegaard, 1994). Ten *ts* mutants were obtained following mutagenesis of 27 sites and the recovery of 12 viruses. Fewer *ts* mutants have been reported for other viruses following charged-to-alanine mutagenesis. Single *ts* mutants have been described for *Human immunodeficiency virus* (HIV) with mutations located in the reverse transcriptase and integrase genes (Huang *et al.*, 1998; Wiskerchen & Muesing, 1995), and *Adeno-*

associated virus type 2 following mutagenesis of the Rep78/68 helicase genes (Gavin *et al.*, 1999). Mutagenesis of the *Influenza A virus* polymerase subunit PB2 generated three *ts* mutants following mutagenesis of ten sites (Parkin *et al.*, 1996). The only reported *ts* mutant for the flaviviruses was obtained following charged-to-alanine mutagenesis of the YFV NS1 protein (Muylaert *et al.*, 1997). No analyses of flavivirus replication following mutagenesis of the viral proteinase by this method have been reported.

Virus $V_{32\text{-}36}$ replicated too poorly to be of further use, and therefore the viruses of most interest with respect to growth restriction were $V_{63\text{-}66}$ and $V_{91\text{-}94}$. Both viruses replicated less well than parental virus and showed small plaque phenotypes. The mutations contained in these viruses may be suitable for incorporation into growth-restricted vaccine strains. It may be possible to enhance the yield of $V_{91\text{-}94}$ by reducing the number of charged residues changed to Ala in the sequence $E_{91}GEE_{94}$ while retaining some growth restriction and a small plaque phenotype.

3.4.2 Virus stability on passaging

The mutations that were introduced here required multiple nucleotide and codon changes. In theory, multiple changes reduce the probability of reversion to parental phenotype when introduced into a potential vaccine strain. The $V_{32\text{-}36}$ virus stock was stable over 10 passages, with no increase in titre, or CPE. The $V_{91\text{-}94}$ virus stock was less stable, with increased titre by serial passage number nine. Further examination of the high passage $V_{91\text{-}94}$ virus stock with the additional 3′ UTR change would be of interest. The incorporation of the second-site 3′UTR change into genomic length DEN-2 cDNA with the original NS3 mutation would enable analysis of the

contribution of the second-site mutation to the restoration of parental levels of virus replication. Further sequencing of the 3′ UTR and the 5′ UTR and structural genes may reveal additional changes contributing to the improved replication of this mutant.

A study by Ryan *et al.* (1998) showed that sequential passaging of two slow growing Sindbis viruses, each containing different single amino acid changes in the envelope E2 protein, resulted in the production of viruses with faster growth rates. Sequence analysis of these viruses revealed that the original E2 mutations were retained and that there were additional amino acid changes in the virus capsid protein, suppressing the effects of the original E2 mutations.

A recent study by Lee *et al.* (2000) examined the effect of mutagenesis of the signal sequence of the YFV prM protein on virus replication. The authors isolated ten mutant virus stocks following five independent transfections of the same genomic length RNA which contained mutations in the prM signal sequence. Transcripts containing the prM signal sequence mutations (which enhanced signal peptidase cleavage *in vitro*) did not allow virus replication. Ten viruses were recovered from cells transfected with mutant RNA transcripts however, for all viruses, reversions or second-site mutations restoring the replication of virus were located in the prM signal sequence. This work demonstrated the importance of the prM signal sequence in virus replication and the strong selective pressures for second-site mutations in this region. Only the C and prM coding regions of the mutant virus genomes were sequenced, and therefore additional mutations within the remainder of the genome affecting virus replication may have been missed. In comparison the two proteinase mutant viruses passaged here were comparatively stable with only one virus, $V_{91\text{-}94}$, appearing to alter upon several passages. A large region of the genome was sequenced before any

changes were identified. The entire proteinase region (NS2B/NS3) did not contain any second-site mutations.

As mentioned in section 1.11, serial passage of flaviviruses can lead to an accumulation of multiple changes in the viral genome which can attenuate the virus. The best known example is that of the YFV vaccine strain YF 17D, which was obtained following 236 serial passages of the virulent Asibi strain in mouse embryonic tissue and primary chick embryo cultures (Theiler & Smith, 1937). The vaccine strain was shown to be largely homogeneous and extremely stable (Xie *et al.*, 1998). However, another YFV vaccine strain, FNV-1P, derived from the parental strain FVV, was recently plaque purified and passaged eight times in Vero cells. Virus passaged twice and eight times in Vero cells was fully sequenced and compared to the vaccine strain. A total of 37 nt and 10 aa changes were identified, 11 nt changes were direct reversions back to the parental FVV sequence (Holbrook *et al.*, 2000). The reason for the instability of this vaccine strain, which is less homogeneous than the 17D strain, is not clear.

Therefore just as serial passaging of flaviviruses may generate attenuated viruses, passaging of mutant viruses may lead to reversion or the introduction of second site suppressor mutations.

3.4.3 Structural interpretation

Murthy *et al.* (1999) reported the X-ray crystal structure of the DEN-2 NS3 proteinase. This structure provides the opportunity to interpret the effects of mutations within the NS3 proteinase on the structure of the protein. It is also a useful tool for the more informed selection of amino acid residues for mutation based on their location in

the crystal structure, e.g. residues predicted to be important for NS2B-NS3 interactions. The model of NS2B/3 in Fig. 3.12 means residues can be more accurately selected to verify the model and also alter NS2B-NS3 interactions, proteinase activity and/or generate growth-restricted viruses.

The locations of the four charged sites are shown mapped onto the model of NS2B/3 in Fig. 3.12 (modelled by Dr. J. Whisstock, who also contributed to the interpretations given below) which is based on the crystal structure of DEN-2 NS3 proteinase (Murthy *et al.*, 1999) and a fragment of NS2B corresponding to the fragment of NS4A seen in the structure of HCV proteinase (Brinkworth *et al.*, 1999).

The X-ray crystal structure of DEN-2 NS3 reveals that region $E_{91}GEE_{94}$, mutated in the low yielding virus $V_{91\text{-}94}$, does not form part of the active site cleft, nor does it interact with the fragment of NS2B in the model. E_{91} and E_{93} form salt bridges to R_{107}. The loss of two salt bridges in the $A_{91}GAA_{94}$ mutation would be predicted to have a deleterious effect upon proteinase stability and possibly virus yield, however, we cannot exclude the possibility that $E_{91}GEE_{94}$ interacts with the full length NS2B. In HCV the loops equivalent to residues 90-94 and 140-145 in DEN-2 NS3 are linked via interactions with a zinc ion. Interestingly, in the DEN-2 NS3 structure, the primary interaction between these loops is a hydrogen bond between the carbonyl oxygen of E_{94} and the side chain of K_{142}. These data are in conflict with the prediction of Brinkworth *et al.* (1999) that E_{93} forms a salt bridge with K_{145}. However, this prediction was based on a homology model developed from the HCV NS3 protein X-ray crystal structure before the availability of the DEN-2 NS3 proteinase structure.

The residues $K_{63}RIE_{66}$ (virus $V_{63\text{-}66}$) are located at the amino terminal end of the NS2B binding cleft. K_{63}, R_{64} and E_{66} are solvent exposed residues located at one end of the the NS2B binding cleft. In the X-ray crystal structure of NS3, R_{64} and E_{66}

form a salt bridge. The model of the NS3/NS2B complex predicts that R_{64} makes a hydrogen bond to the carbonyl oxygen of the first residue in the NS2B peptide. More extensive interactions between R_{64} and E_{66} may be made with the full-length NS2B protein. The disruption of any one of these interactions, either alone or in combination, may explain the observed reduction in yield of virus $V_{63\text{-}66}$.

The residues $E_{169}KSIE_{173}$ and $E_{179}DD_{181}$ lie at the carboxy terminus of the proteinase, at its junction with the helicase domain of NS3. Both sites are excluded from the minimal proteinase domain, defined as the amino terminal 167 aa of NS3 by Li *et al.* (1999) using *in vitro* transcription and translation. Residues $E_{169}KSIE_{173}$ form an α-helix (Fig. 3.12), and the individual residues form hydrogen bonds with solvent molecules, apart from K_{170} which forms a hydrogen bond to the carbonyl oxygen of E_{167}. These residues are located at the end of the substrate binding cleft (on the P side; Schechter & Berger, 1967) and thus may be important for determining substrate specificity. For $E_{179}DD_{181}$, the structure of NS3 reveals that E_{179} and D_{181} make hydrogen bonds to solvent molecules. D_{180} also forms a hydrogen bond to the sidechain of W_{69}. The interaction with W_{69} is of particular interest as this residue is located six residues amino terminal to the catalytic D_{75}. Disruption of this hydrogen bond by the introduction of an Ala at position 180 may affect the conformation of the β-strand containing the catalytic Asp and thus impair proteinase activity.

In addition to the mutagenesis of the four charged sites, substitutions were made in the hydrophobic region $G_{32}YSQI_{36}$. The residue G_{32} lies outside the enzyme motifs but is highly conserved in members of the genus *Flavivirus* (Fig. 3.1) (Chang, 1997). The respective mutant protein had autocatalytic activity as determined by Kelley (1996), but the yield of $V_{32\text{-}36}$ was the lowest recorded. G_{32} and Y_{33} line the amino terminal end of the NS2B binding cleft. Interestingly, the crystal structure of

NS3 reveals that Y_{33} bridges across the cleft, forming a hydrogen bond to the carbonyl oxygen of P_{10}. Mutation at this position may affect NS2B binding. G_{32} forms part of a pocket which contains S_3 from the NS2B peptide. Mutation of this residue will probably affect the size of this pocket.

Overall, the five sites mutagenized were distributed over the primary sequence of the NS3 proteinase and represented distinct regions in the model of NS3 complexed with the NS2B cofactor peptide. Two were located at the amino terminus of the NS2B binding cleft ($K_{63}RIE_{66}$ and $G_{32}YSQI_{36}$), two at the carboxy terminus of the proteinase domain ($E_{169}KSIE_{173}$ and $E_{179}DD_{181}$), and one ($E_{91}GEE_{94}$) was solvent exposed. The charged region ($K_{63}RIE_{66}$) was adjacent to the NS2B binding cleft. At present it is unknown whether any of the other three charged regions interact with full length NS2B. It is also possible that the basis for their effect on viral replication is unrelated to proteinase activity, and may lie, for example, in the interaction of NS3 with other viral proteins such as NS5 (Chen *et al.*, 1997*a*; Kapoor *et al.*, 1995). The substitutions to Ala in the conserved hydrophobic region were more disruptive to virus production (virus $V_{32\text{-}36}$), than changes at hydrophilic sites by charged-to-alanine mutagenesis.

3.5 Concluding remarks

The results demonstrated that charged-to-alanine mutagenesis has potential for obtaining growth-restricted viruses of DEN-2 and other flavivirus species, by the introduction of mutations in the proteinase and perhaps in other nonstructural proteins. Infectious virus was recovered for all mutants described in this chapter, and the viruses displayed a useful range of growth restriction. Comparisons of the deduced amino acid sequences of flaviviruses show high conservation of hydrophilicity and

hydrophobicity across the viral polyprotein, regardless of considerable variation in primary sequence (Westaway & Blok, 1997), and thus it may be possible to extend these results to the other dengue serotypes and encephalitic flaviviruses.

The model of the NS3 complexed with an NS2B peptide cofactor enabled the definition of some individual residues important in the interaction between the two proteins.

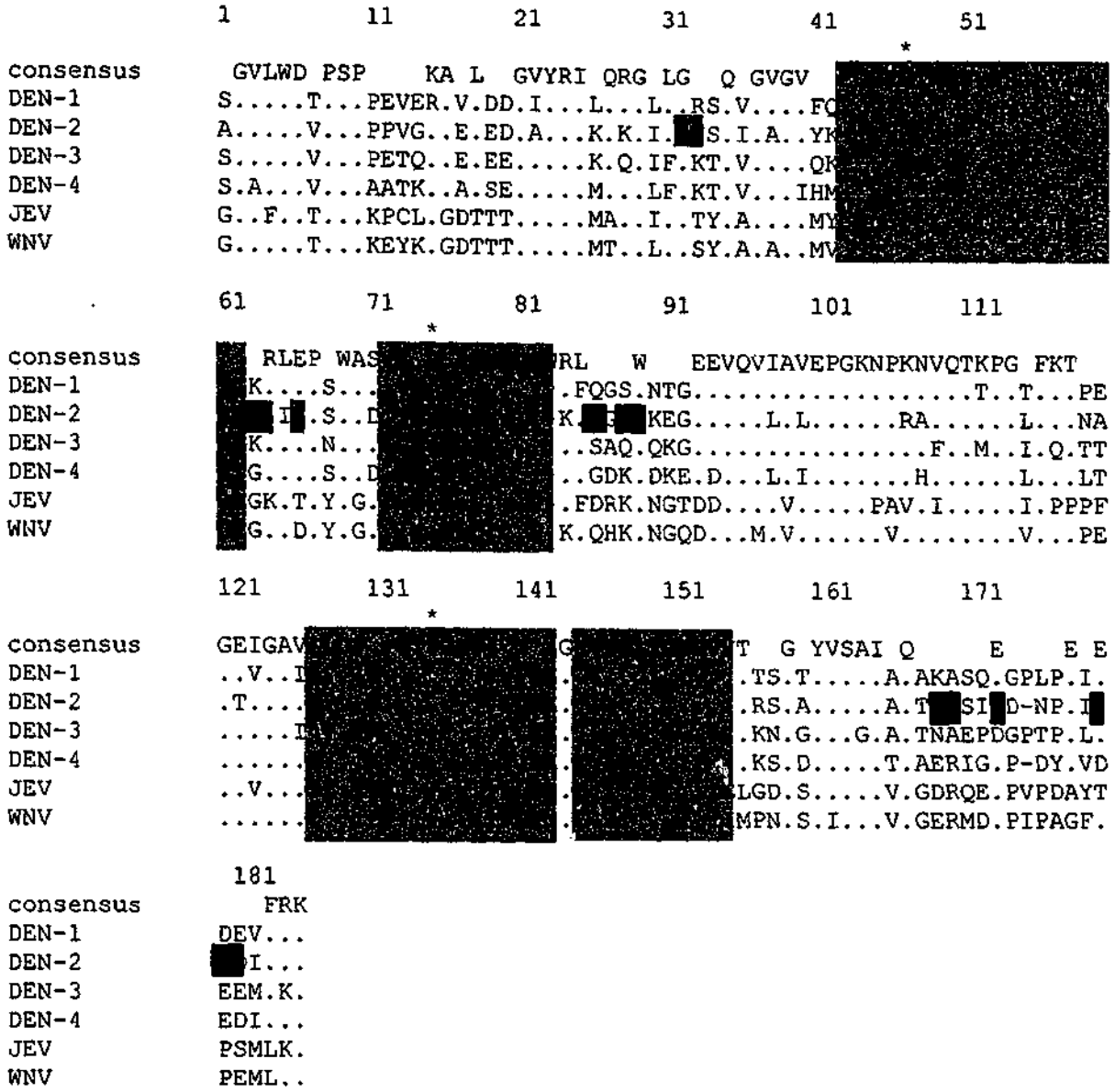

Fig. 3.1 Alignment of several flavivirus NS3 proteinase amino acid sequences and mutations introduced into DEN-2 NS3. Dots stand for identical amino acid residues while dashes represent gaps introduced to allow maximal homology. The four proteinase motifs are shown as blue boxes, the catalytic triad is indicated with asterisks. Each mutant is colour coded, and each colour will be used throughout the chapter to designate a particular mutant virus. The position of amino acids within DEN-2 NS3 are shown above the sequence. The same virus GenBank accession numbers were used for this NS3 alignment as for the NS2B alignment (Fig. 1.2).

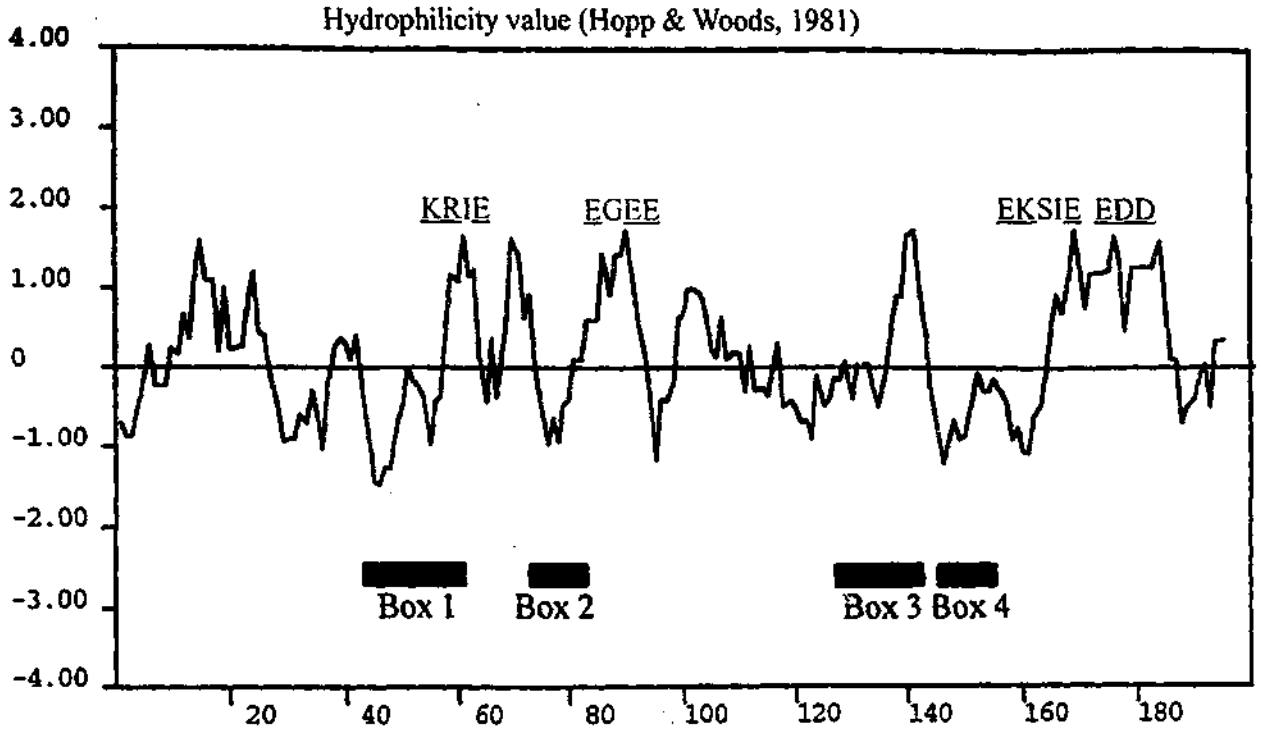

Fig. 3.2 Hydrophilicity plot of the first 200 amino acids of NS3. The positions of the four serine proteinase boxes and the four hydrophilic regions mutated are shown.

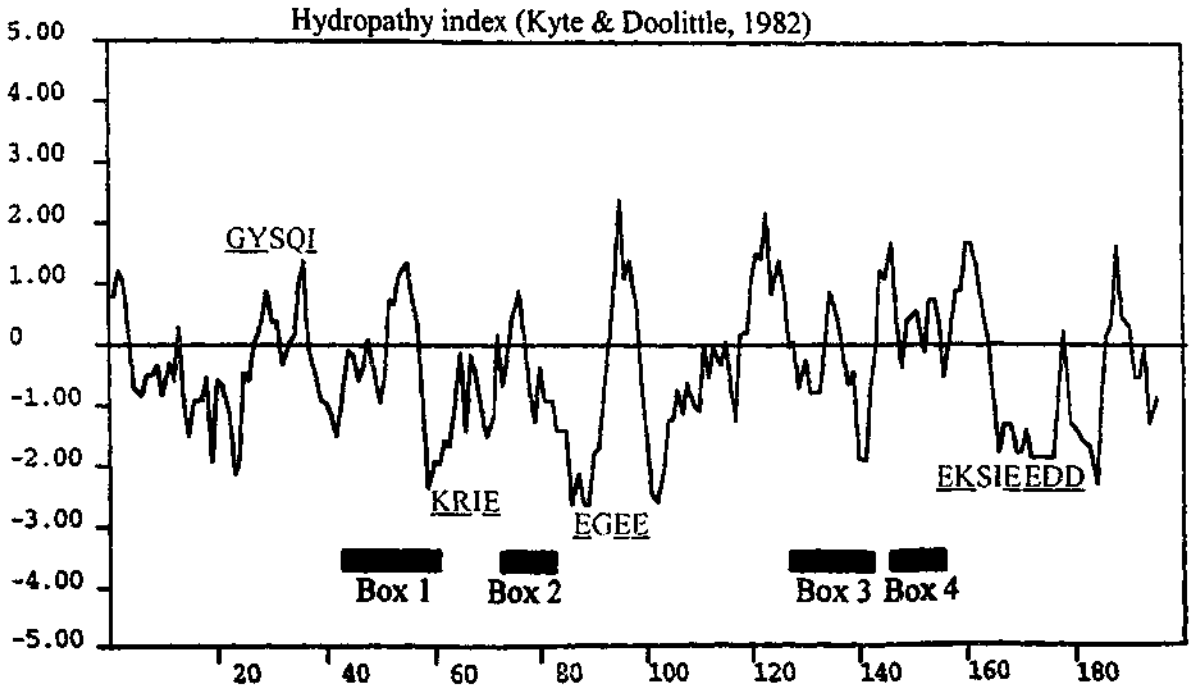

Fig. 3.3 Hydropathy plot of the first 200 amino acids of NS3. The positions of the four serine proteinase boxes and the single hydrophobic and four hydrophilic regions mutated are shown.

Fig. 3.4 Genomic map of DEN-2 and NS3 mutations incorporated into genomic length cDNA. The catalytic residues H, D and S and the serine proteinase motifs (shaded) are shown (Bazan & Fletterick, 1989); residue numbers within NS3 are given. On the right are the names of the plasmids containing genomic length cDNA (pDVWS) and derived virus (V). The various mutations are shown in their respective colour coding. Underlined residues were mutated to Ala (with the exception of $I_{36}V$). Asterisks denote mutants which were tested for proteinase activity by P. Kelley (Matusan *et al.*, 2001).

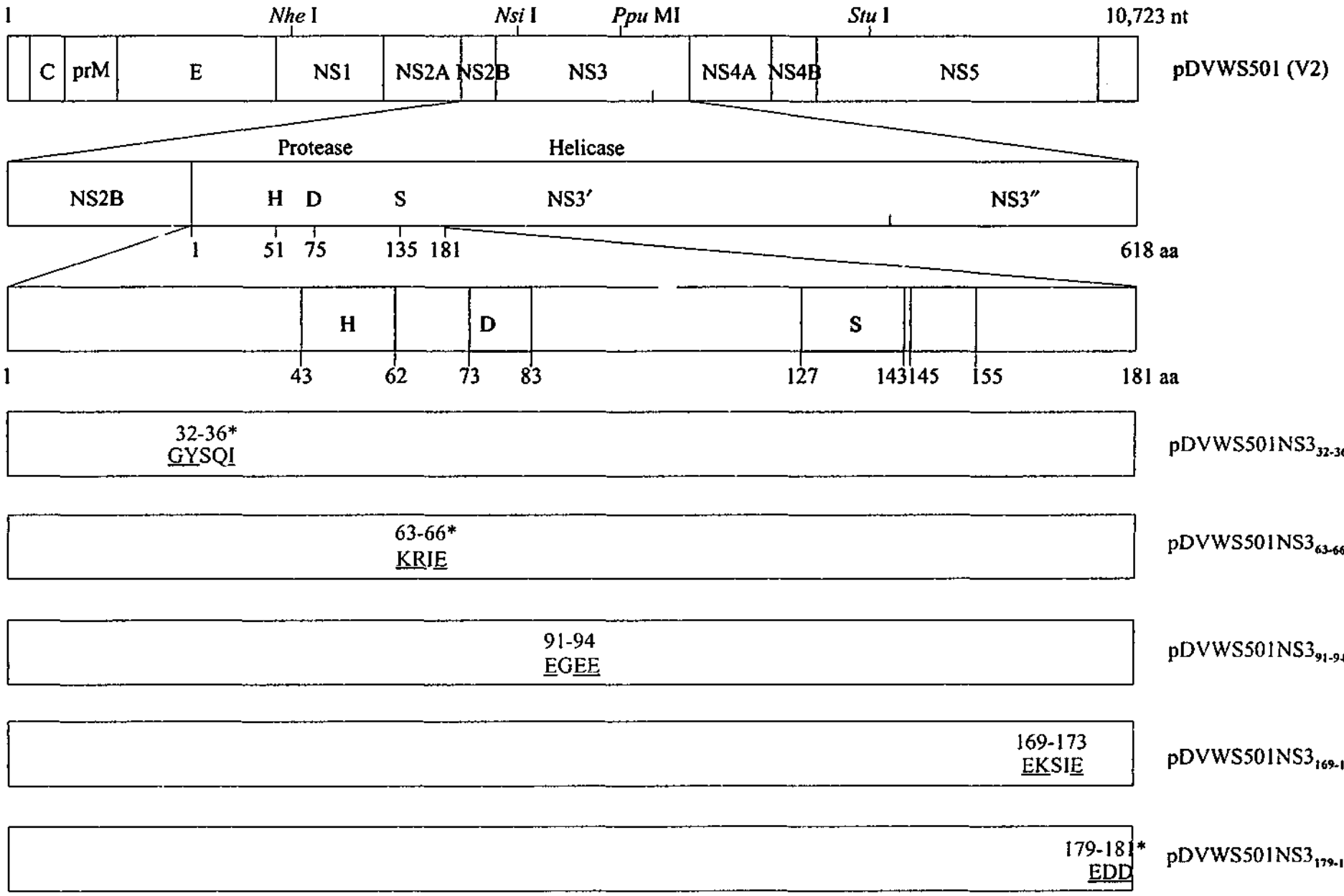
1
Nhe I
Nsi I
Ppu MI
Stu I
10,723 nt
C
prM
E
NS1
NS2A
NS2B
NS3
NS4A
NS4B
NS5
pDVWS501 (V2)
Protease
Helicase
NS2B
H
D
S
NS3′
NS3″
1
51
75
135
181
618 aa
H
D
S
1
43
62
73
83
127
143
145
155
181 aa
32-36*
GYSQI
pDVWS501NS3$_{32-36}$(V$_{32-36}$)
63-66*
KRIE
pDVWS501NS3$_{63-66}$(V$_{63-66}$)
91-94
EGEE
pDVWS501NS3$_{91-94}$(V$_{91-94}$)
169-173
EKSIE
pDVWS501NS3$_{169-173}$(V$_{169-173}$)
179-181*
EDD
pDVWS501NS3$_{179-181}$(V$_{179-181}$)

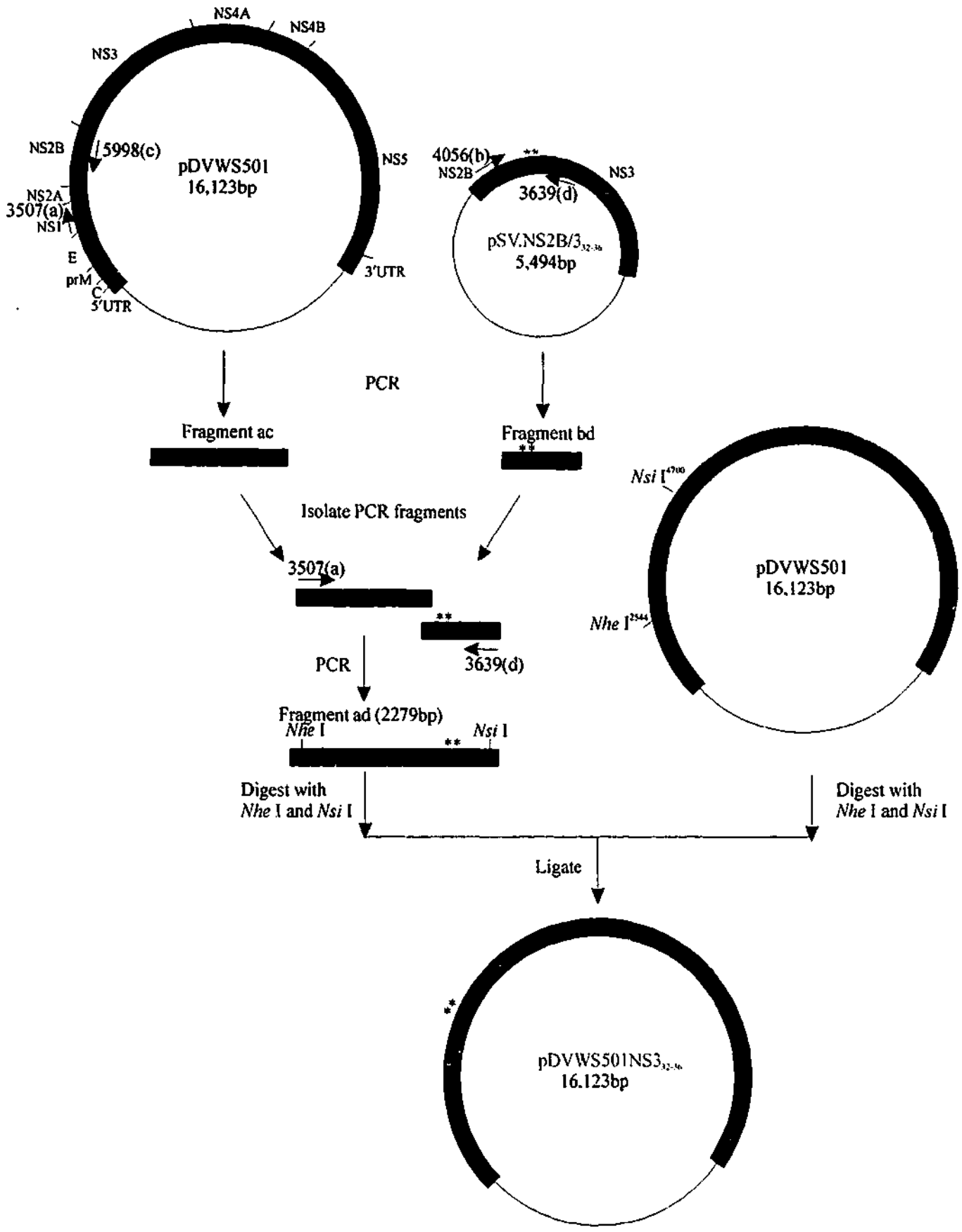

Fig. 3.5 Construction of the plasmid pDVWS501NS3$_{32-36}$. OE-PCR was used to insert the $G_{32}YSQI_{36}$ (parental) to $A_{32}ASQV_{36}$ (mutant) change within NS3. The $I_{36}\rightarrow V_{36}$ change was present in the plasmid pSV.NS2B/3$_{32-36}$. The 2156bp *Nhe* I – *Nsi* I fragment containing the mutation was directly cloned into pDVWS501.

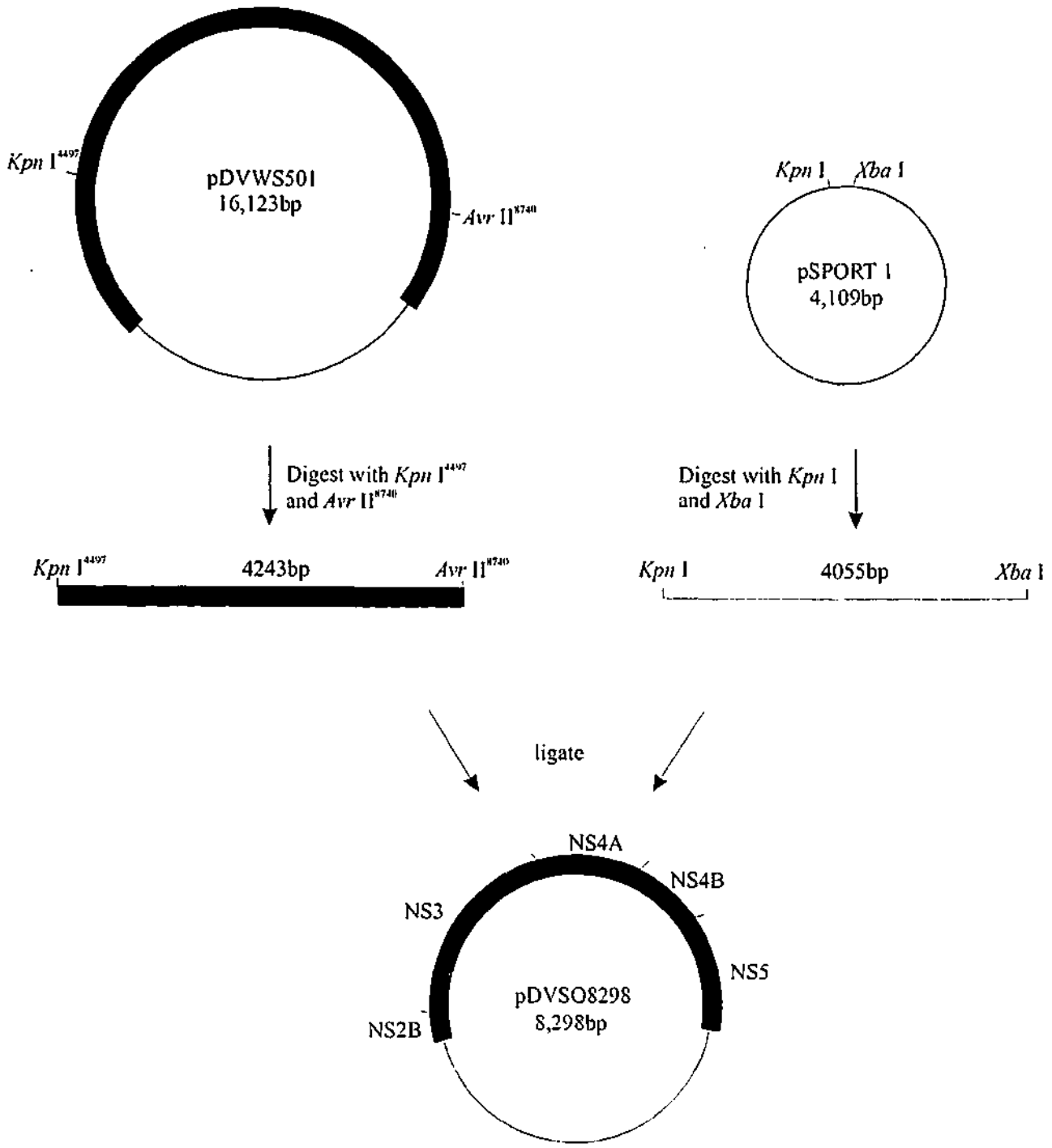

Fig. 3.6 Construction of the plasmid pDVSO8298. To produce the plasmid pDVSO8298, a 4243bp *Kpn* I[4497] - *Avr* II[8740] fragment was removed from pDVWS501 and ligated into *Kpn* I/*Xba* I-digested pSPORT 1. *Avr* II and *Xba* I produce sticky ends that are complementary.

Fig. 3.7 Construction of the plasmids pDVWS501NS3$_{63-66}$ and pDVWS501NS3$_{179-181}$. To produce the plasmids pDVWS501NS3$_{63-66}$ and pDVWS501NS3$_{179-181}$, fragments of cDNA encoding these mutations were cloned into pDVSO8298 by removing the 1152bp mutagenized *Nsi* I – *Ppu* MI fragments from the corresponding pSV.NS2B/3 plasmids (previously constructed by P. Kelley), and ligating them into *Nsi* I/*Ppu* MI-digested pDVSO8298. To introduce these mutations into the genomic length DEN-2 clone, 3174bp *Nsi* I – *Stu* I mutated fragments were then removed from the appropriate pDVSO8298 plasmid and ligated into *Nsi* I^{4700}/*Stu* I^{7874}-digested pDVWS501.

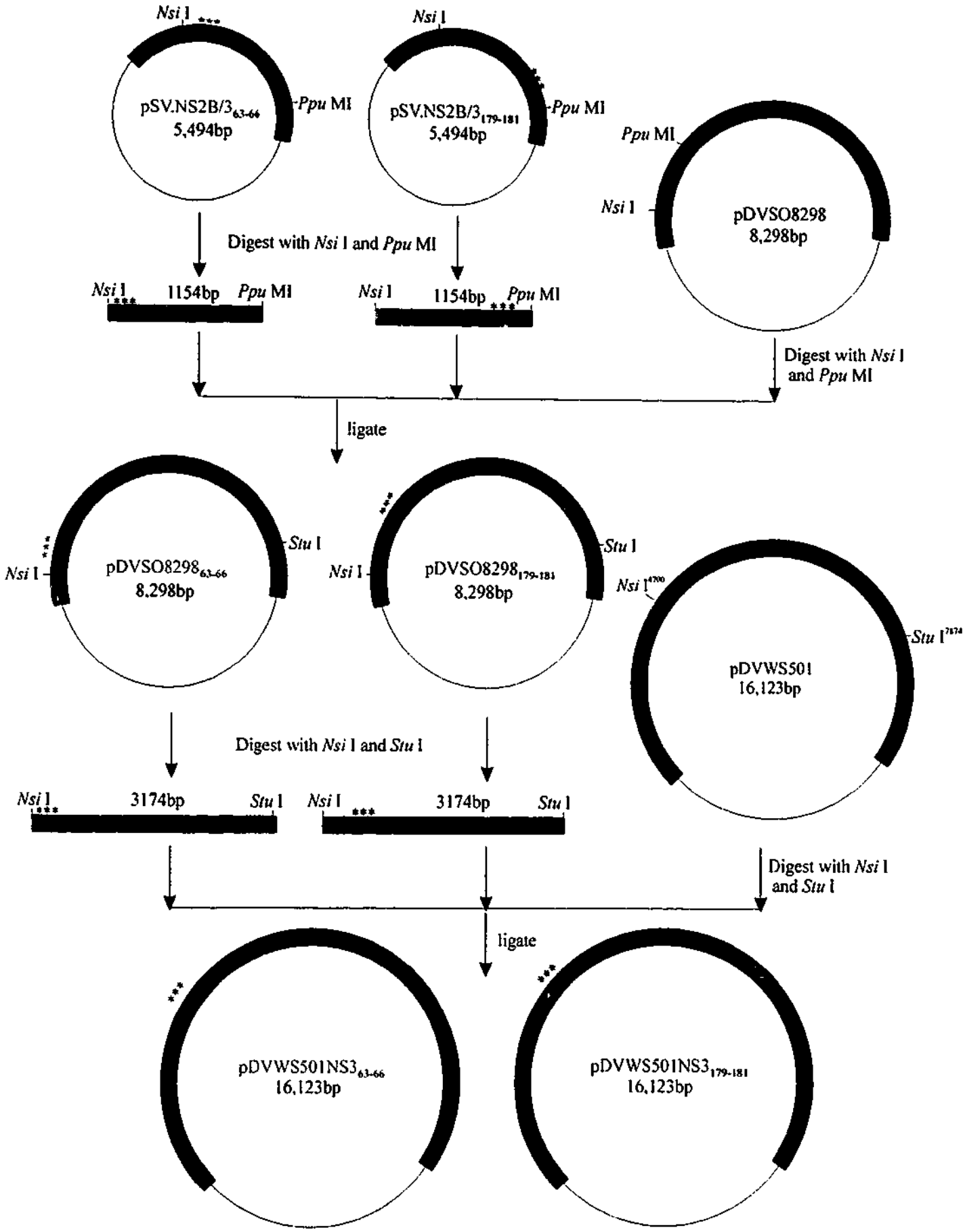
Nsi I
pSV.NS2B/3 63-66
5,494bp
Ppu MI
Nsi I
pSV.NS2B/3 179-181
5,494bp
Ppu MI
Ppu MI
Nsi I
pDVSO8298
8,298bp
Digest with Nsi I and Ppu MI
Nsi I
1154bp
Ppu MI
Nsi I
1154bp
Ppu MI
Digest with Nsi I and Ppu MI
ligate
Nsi I
pDVSO8298 63-66
8,298bp
Stu I
Nsi I
pDVSO8298 179-181
8,298bp
Stu I
Nsi I 4700
Stu I 7874
pDVWS501
16,123bp
Digest with Nsi I and Stu I
Nsi I
3174bp
Stu I
Nsi I
3174bp
Stu I
Digest with Nsi I and Stu I
ligate
pDVWS501NS3 63-66
16,123bp
pDVWS501NS3 179-181
16,123bp

Fig. 3.8 (A) Construction of the plasmid, pDVWS501NS3$_{91\text{-}94}$. A 1356bp OE-PCR fragment containing the mutation (as indicated by the asterisks) was digested with *Nsi* I and *Ppu* MI and the resulting 1152bp mutagenized fragment was ligated into *Nsi* I/*Ppu* MI-digested pDVSO8298. To produce the plasmid pDVWS501NS3$_{91\text{-}94}$, a 3174bp *Nsi* I–*Stu* I fragment was removed from pDVSO8298$_{91\text{-}94}$ and ligated into *Nsi* I^{4700}/*Stu* I^{7874}-digested pDVWS501.

A

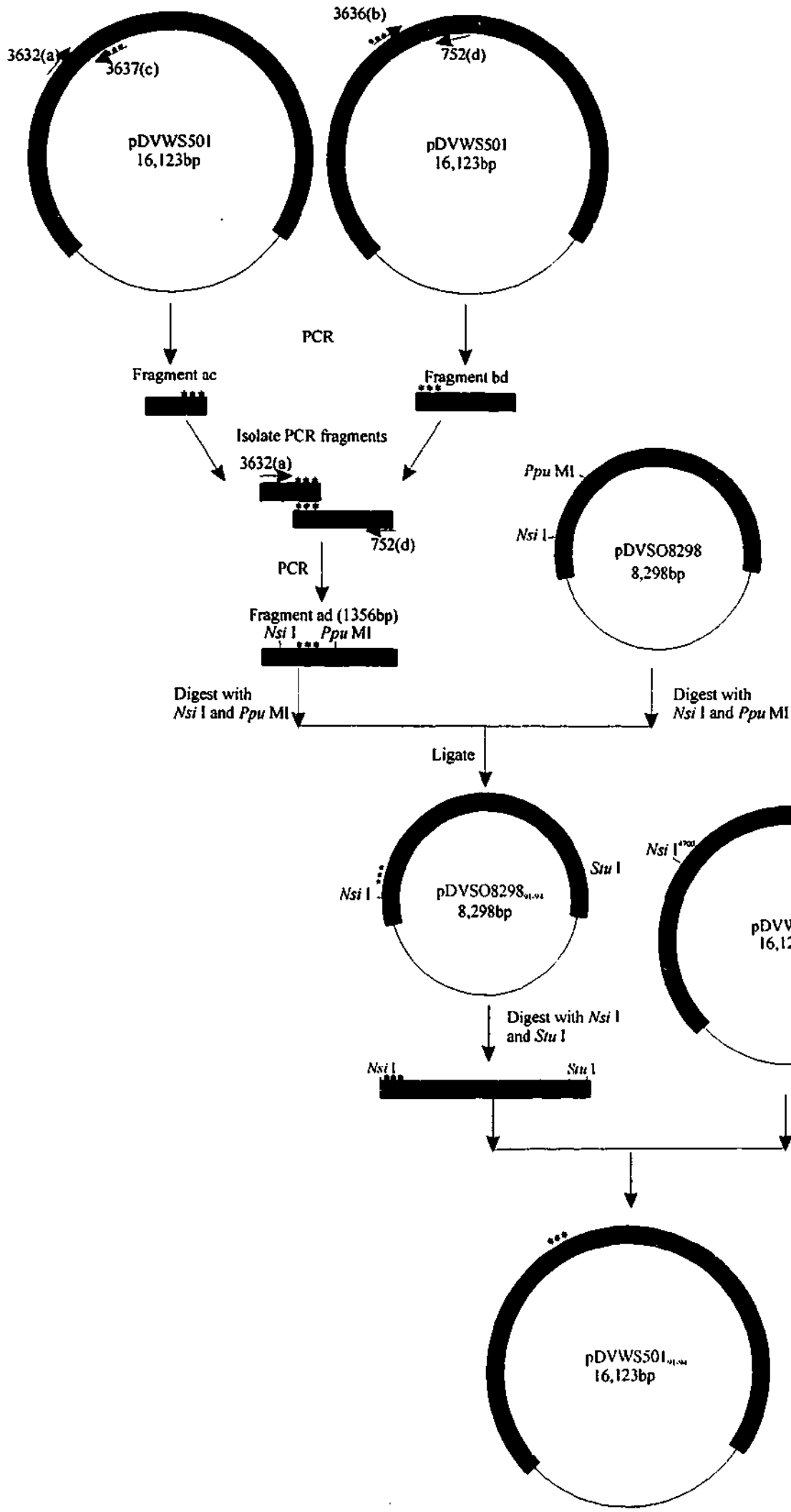
3632(a)
3637(c)
pDVWS501
16,123bp
3636(b)
752(d)
pDVWS501
16,123bp
PCR
Fragment ac
Fragment bd
Isolate PCR fragments
3632(a)
752(d)
PCR
Fragment ad (1356bp)
Nsi I
Ppu MI
Ppu MI
Nsi I
pDVSO8298
8,298bp
Digest with
Nsi I and Ppu MI
Digest with
Nsi I and Ppu MI
Ligate
Nsi I
Stu I
pDVSO8298
8,298bp
Nsi I
Stu I
pDVWS501
16,123bp
Digest with Nsi I
and Stu I
Nsi I
Stu I
Digest with Nsi I
and Stu I
pDVWS501
16,123bp

Fig. 3.8 (B) Construction of the plasmid, pDVWS501NS3$_{169\text{-}173}$. A 1356bp OE-PCR fragment containing the mutation (as indicated by the asterisks) was digested with *Nsi* I and *Ppu* MI and the resulting 1152bp mutagenized fragment was ligated into *Nsi* I/*Ppu* MI-digested pDVSO8298. To produce the plasmid pDVWS501NS3$_{169\text{-}173}$, a 3174bp *Nsi* I–*Stu* I fragment was removed from pDVSO8298$_{169\text{-}173}$ and ligated into *Nsi* I^{4700}/*Stu* I^{7874}-digested pDVWS501.

B

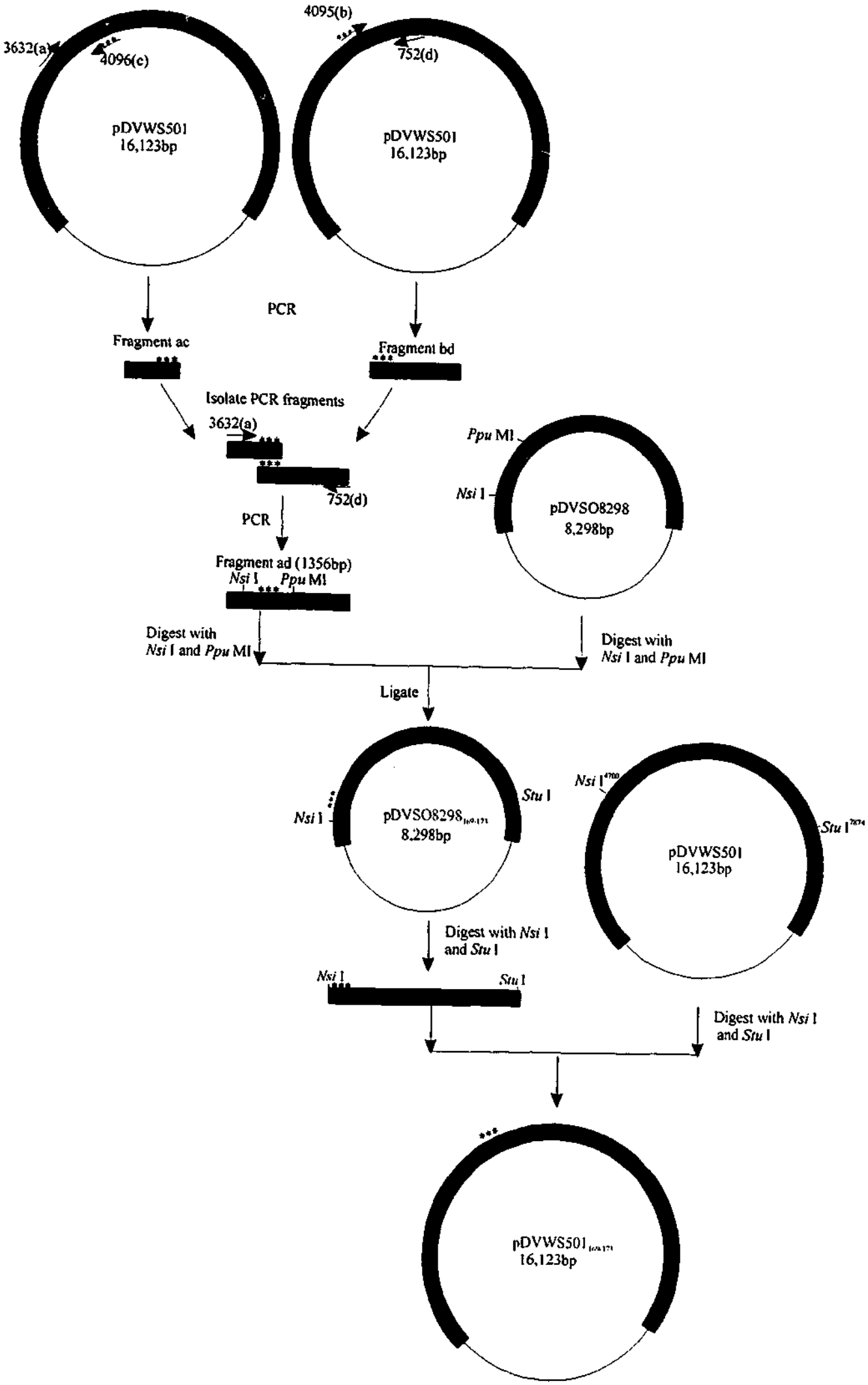
3632(a)
4096(c)
4095(b)
752(d)
pDVWS501
16,123bp
pDVWS501
16,123bp
PCR
Fragment ac
Fragment bd
Isolate PCR fragments
3632(a)
752(d)
PCR
Fragment ad (1356bp)
Nsi I
Ppu MI
Ppu MI
Nsi I
pDVSO8298
8,298bp
Digest with
Nsi I and Ppu MI
Digest with
Nsi I and Ppu MI
Ligate
Nsi I
Stu I
pDVSO8298
8,298bp
Nsi I
Stu I
pDVWS501
16,123bp
Digest with Nsi I
and Stu I
Nsi I
Stu I
Digest with Nsi I
and Stu I
pDVWS501
16,123bp

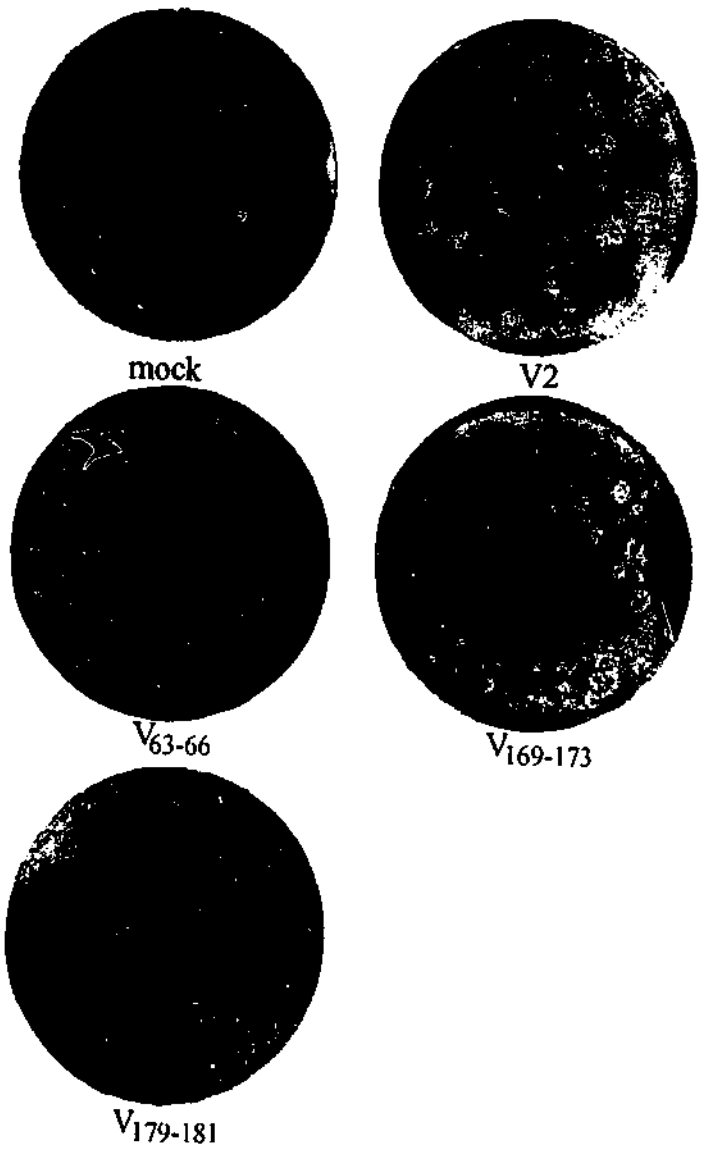

Fig. 3.9 Plaques of mutant viruses in C6/36 cells at 28°C.

The plaque morphologies of three mutant viruses compared with parental virus V2.

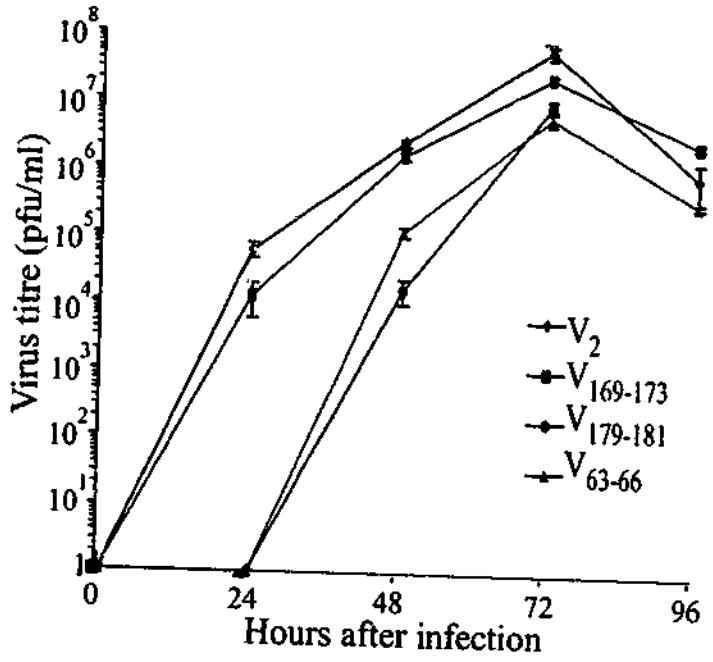

Fig. 3.10 Replication of mutant viruses in C6/36 cells at 28°C.

Cells were infected at an MOI of 1.0 and the culture medium was sampled at the times indicated; virus titres were determined by plaque assay in C6/36 cells.

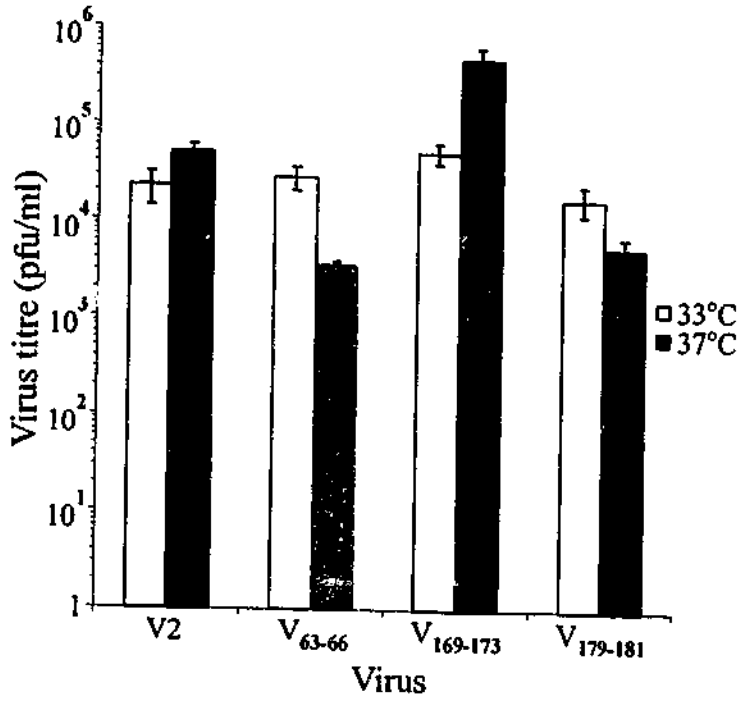

Fig. 3.11 Replication of selected mutant viruses in BHK-21 cells at 33°C and 37°C. Cells were infected at an MOI of 1.0 and the culture medium was sampled at 72hr p.i.; virus titres were determined by plaque assay on C6/36 cells (28°C). Error bars show one standard deviation of the plaque titre.

Fig. 3.12 X-ray crystal structure of the DEN-2 NS3 proteinase (blue) with the NS2B peptide (pink) modelled into the binding cleft. The active site triad , H51, D75 and S135, is shown in green stick. Charged residues that were mutated to alanine are labelled in their respective colour code and shown on the ribbon diagram in red. The hydrophobic region mutated is shown in yellow.

Table 3.1: Sequence of the primers used in OE-PCR.

Construct	Primer number	Primer designation[1]	Sequence[2] 5' to 3'	Primers used for sequencing of OE-PCR products[3]
pDVWS501$_{32\text{-}36}$	3507	a	^{2536}CCTTCAAAACTAGCTTCAG^{2554}	3632, 4056, 838, 3496, 1208, 179, 1921, 60, 1260, 775, 461, 3639
	4056	b	^{4132}AGCTGGCCACTAAATGAGGCTATC^{4155}	
	5998	c	^{4235}CCAGCCACTAATGGTCCTGTCATGGG^{4210}	
	3639	d	^{4815}CAAGACCGCGGCTTCTTCTCCTTCCTTCCATTC^{4783}	
pDVWS501$_{91\text{-}94}$	3632	a	^{4609}ATTCTTGCAGCTTCCCAGATCGGAGCCGGAG^{4639}	3632, 752, 3682
	3636	b	^{4786}TGGAAGGcAGGAGcAGcAGTCCAGGTCTTGGC^{4818}	
	3637	c	^{4809}CTGGACTgCTgCTCCTgCCTTCCATTCTCC^{4780}	
	752	d	^{5964}ATTTTCCAGAGGTTCCCC^{5947}	
pDVWS501$_{169\text{-}173}$	3632	a	^{4609}ATTCTTGCAGCTTCCCAGATCGGAGCCGGAG^{4639}	3632, 752, 3682
	4095	b	^{5020}CAGACTGcAgcAAGTATTGcAGACAATCCAGAGAT^{5055}	
	4096	c	^{5045}TTGTCTgCAATACTTgcTgCAGTGTGGGCTATAGCA^{5010}	
	752	d	^{5964}ATTTTCCAGAGGTTCCCC^{5947}	

[1] See Fig. 2.1 for the a-d designation of primers.

[2] All sequences are listed 5′ to 3′, and the substituted nucleotides are written in lower case. Nucleotide numbering refers to the NGC DEN-2 sequence of Irie *et al.* (1989).

[3] For sequence of primers see Table 3.2.

Table 3.2: Primers used for sequencing of OE-PCR and RT-PCR products.

Primer number	Sequence 5′ to 3′[1]
60	^{3462}CTCCTTGGCCACAGCCGGAC^{3481}
179	^{3654}GGTGGGCGCTACTATGACG^{3672}
461	^{2823}AGAAAGGTCTGGGCATGAGACTCTG^{2798}
752	^{5964}ATTTTCCAGAGGTTCCCC^{5947}
775	^{3263}TCGCAGAAATCAAAGTCC^{3246}
838	^{3099}TGGCCAGTGGGCGCTTTTAACT^{3078}
1146	^{6828}GTTTGCCATGGTTGCGGCCGCCACTGTGAG^{6799}
1208	^{3391}AGAGGTGAGGACGGAGCCTGGTACGGGATG^{3420}
1260	^{3348}AGAATGGTGCGCCCGATCTGCCACATTACCAC^{3379}
1396	^{4837}CCAAGAGCCGTCCAAACAAAACCT^{4860}
1921	^{2856}GTTGGGGCATTCTGGTGTTTCGGG^{2833}
2620	^{5107}GGAGCGGCTAAGACGAAGAGATACCTTCCG^{5136}
2621	^{5126}CTCTTCGTCTTAGCCGCTCCTGGGTGGAGG^{5096}
2626	^{5374}CGTCGAAGATGATCAGGTTGTAATTTGGC^{5346}
3496	^{3016}GGTTATTGGATAGAAAGTGC^{3035}
3630	^{4565}AGGCTGCACTGGCAGCTGGAGCCTATAGAATC^{4596}
3632	^{4609}ATTCTTGCAGCTTCCCAGATCGGAGCCGGAG^{4639}
3633	^{4626}CTGGGAAGCTGCAAGAATCCCTTTTTGCTTG^{4596}
3639	^{4816}CAAGACCGCGGCTTCTTCTCCTTCCTTCCATTC^{4783}
3682	^{8177}CTCCATATTTCCTTTGTAGTGC^{8156}
4056	^{4132}AGCTGGCCACTAAATGAGGCTATC^{4155}
4096	^{5045}TTGTCTGCAATACTTGCTGCAGTGTGGGCTATAGCA^{5010}
4099	^{5516}TCATGGCTGCAGCAAGAGAAATCCCTGAACG^{5546}
4105	^{5666}ACTTTCGCTCCATTTGCTGCCAGGCAAGCTGCTATATC^{5629}
4106	^{5821}CTAACAGCTGGTGCAGCGCGGGTGATCCTGGC^{5852}
4318	^{6123}CACAAAGGTTGCCGCTGCTGCTCCTCTCAAGCG^{6090}
5998	^{4235}CCAGCCACTAATGGTCCTGTCATGGG^{4210}

[1] Nucleotide numbering refers to the NGC DEN-2 sequence of Irie *et al.* (1989).

Table 3.3: Primers used to amplify and sequence RT-PCR products from C6/36 cells infected with second passage mutant virus.

Virus	RT primer	PCR primers	Location[1] of amplified cDNA 33°C[2]	37°C[2]	Region sequenced[3]	Sequencing primer[4]
V_{32-36}	4096	4096, 4056	nt 4132-5046	no product	nt 4431-5006	4096
V_{63-66}	Random hexamers	179, 3633, 3630, 2626, 2620, 4318, 4106, 1146	nt 4132-6375	nt 4132-5374	NS2B and NS3 nt 4132-6375	5998, 4056, 4105, 4099 1146, 4106, 2621,1396
V_{91-94}	4096	4096, 4056	nt 4132-5046	no product	nt 4548-5007	4096
$V_{169-173}$	Random hexamers	179, 3633, 3630, 2626, 2620, 4318, 4106, 1146	nt 4132-6375	nt 4609-5374	NS2B and NS3 nt 4132-6375	5998, 4056, 4105, 4099 1146, 4106, 2621,1396
$V_{179-181}$	Random hexamers	179, 3633, 3630, 2626, 2620, 4318, 4106, 1146	nt 4132-6375	nt 4565-5374	NS2B and NS3 nt 4132-6375	5998, 4056, 4105, 4099 1146, 4106, 2621,1396

[1] Numbering follows the sequence of Irie *et al.* (1989).

[2] All sequenced products were from viral RNA obtained following electroporation of RNA into BHK-21 cells (maintained at 33°C or 37°C) and two passages of virus in C6/36 cells at 28°C.

[3] For products obtained from viruses maintained at 37°C, only the region spanning the mutation was sequenced. For viruses V_{63-66}, $V_{169-173}$, and $V_{179-181}$ maintained at 33°C, RT-PCR products covering the entire NS2B and NS3 genes were sequenced.

[4] For sequence of primers see Table 3.2.

Table 3.4: Yields of mutant viruses following electroporation of RNA into BHK-21 cells and two passages of virus in C6/36 cells.

Site mutated	Virus		IF[1]	Virus titre[3] (pfu/ml)	Approximate Plaque size (mm)	RT-PCR[4]
	V2	33°C[2]	++++	$(1.1 \pm 0.1) \times 10^6$	4	yes
		37°C	++++	$(7.3 \pm 0.8) \times 10^6$	4	yes
GYSQI	$V_{32\text{-}36}$	33°C	+	$(3.0 \pm 0.9) \times 10^1$	1	yes
		37°C	–	none detected		no
KRIE	$V_{63\text{-}66}$	33°C	++++	$(4.6 \pm 0.9) \times 10^5$	1	yes
		37°C	+++	$(7.0 \pm 1.5) \times 10^5$	1	yes
EGEE	$V_{91\text{-}94}$	33°C	+	$(2.4 \pm 0.3) \times 10^3$	1	yes
		37°C	–	none detected		no
EKSIE	$V_{169\text{-}173}$	33°C	++++	$(2.7 \pm 0.2) \times 10^6$	3	yes
		37°C	++++	$(2.2 \pm 0.5) \times 10^6$	3	yes
EDD	$V_{179\text{-}181}$	33°C	+++	$(4.9 \pm 1.0) \times 10^5$	1	yes
		37°C	+++	$(1.4 \pm 0.2) \times 10^6$	1	yes

[1] Immunofluorescence (IF) in BHK-21 cells at 5-6 days p.e.. IF was scored (–) no positive cells, (+) 0-25% positive cells, (++) 25-50% positive cells, (+++) 50-75% positive cells, (++++) 75-100% positive cells.

[2] Temperature at which BHK-21 cells were incubated immediately after electroporation i.e. 33°C or 37°C.

[3] Plaque titres are expressed in pfu/ml ± one standard deviation. Each virus was derived at least twice from RNA transcripts, therefore the result shown for each virus is the average of two or more experiments.

[4] Detection and sequence confirmation of product after RT-PCR. All positive samples retained the required mutation.

Table 3.5: Serial passage of the low titre viruses $V_{32\text{-}36}$ and $V_{91\text{-}94}$.

Passage number	$V_{32\text{-}36}$		$V_{91\text{-}94}$	
	CPE[1]	Plaque titre[3]	CPE	Plaque titre
2	–	$(8.0 \pm 1.6) \times 10^1$	–	$(2.8 \pm 0.2) \times 10^2$
3	–	n.t.	–	$(1.3 \pm 0.6) \times 10^2$
4	–	n.t.	–	n.t.
5	–	$(1.3 \pm 0.6) \times 10^1$	–	$(2.0 \pm 0.3) \times 10^2$
6	–	n.t.	–	n.t.
7	–	n.t.	–	$(3.0 \pm 1.0) \times 10^2$
8	–	n.t.	–	n.t.
9	–	n.t.	+ (day 5)	$(2.3 \pm 0.9) \times 10^3$
10	–	$< 1 \times 10^1$	+ (day 3)	$(1.1 \pm 0.2) \times 10^4$
11	n.t.[2]	n.t.	+ (day 2)[4]	$(1.4 \pm 0.2) \times 10^6$
12	n.t.	n.t.	+ (day 2)[4]	$(5.7 \pm 0.3) \times 10^5$

[1] CPE of infected C6/36 cells was scored as (–) no CPE, (+) up to 20% of the cell monolayer showing CPE.

[2] n.t., not tested.

[3] Plaque titres are expressed in pfu/ml ± one standard deviation.

[4] By day three of passage 11 and 12, $V_{91\text{-}94}$ infected cells demonstrated extensive (>70%) cell monolayer destruction.

CHAPTER FOUR: MUTATIONAL ANALYSIS OF THE HELICASE REGION OF THE DEN-2 VIRUS NS3 PROTEIN

4.1 Introduction

The flavivirus genome encodes at least seven nonstructural proteins NS1-NS2A-NS2B-NS3-NS4A-NS4B-NS5. Biochemical functions have been demonstrated for some nonstructural proteins. NS5 possesses RdRp activity (Tan *et al.*, 1996). A complex of NS2B and NS3 acts as a chymotrypsin-like serine proteinase; the amino terminal one-third of NS3 is sufficient for this activity (Chambers *et al.*, 1990*b*; Falgout *et al.*, 1991; Preugschat *et al.*, 1990). The carboxy terminal two-thirds of NS3 has seven motifs characteristic of RNA helicases of the DExH subfamily. Several forms of recombinant proteins containing the carboxy terminal helicase region of NS3 have been shown to possess NTPase activity (Cui *et al.*, 1998; Li *et al.*, 1999; Takegami *et al.*, 1994; Warrener *et al.*, 1993) and RNA helicase activity (Li *et al.*, 1999; Utama *et al.*, 2000*b*).

RNA helicases catalyze the unidirectional unwinding of duplex RNAs (containing a ssRNA region of at least 3 nt) in the presence of a divalent cation and require the hydrolysis of the β-γ bond of a suitable deoxy-NTP or NTP (usually ATP) as an energy source (Lain *et al.*, 1990; Paolini *et al.*, 2000*a*). Known and putative RNA helicases of viral origin possess conserved amino acid sequence motifs enabling their classification into three distinct superfamilies (Koonin & Dolja, 1993). The helicase of the flavivirus DEN-2 is a member of superfamily 2 which includes the helicases of the pestivirus BVDV and the hepacivirus HCV. Helicases can be further

classified into DEAD, DExH and DExx subfamilies based on the sequence of motif II (Luking *et al.*, 1998; Schmid & Linder, 1992). The multifunctional flavivirus NS3 helicase protein is believed to be a component of the viral RNA replication complex with the RdRp NS5 protein (Kapoor *et al.*, 1995). There is evidence that NS3 interacts with both NS5 and stem-loop structures in the 3′ UTR, possibly playing an important role in the initiation of negative strand RNA synthesis (Chen *et al.*, 1997*a*; Kapoor *et al.*, 1995).

Several X-ray crystal structures of the HCV NS3 helicase domain have been determined (Cho *et al.*, 1998; Kim *et al.*, 1998; Yao *et al.*, 1997), and together with site-directed mutagenesis have helped to define the function of some helicase motifs. The first reported mutagenesis studies of HCV and other positive strand viruses targeted the helicase motifs I, II, III and VI. Motif I (GxGKT), conserved in all three superfamilies, is involved in binding the β and γ phosphate groups of NTPs. Motif II (DExH in DEN-2), also present in all three superfamilies, is predicted to bind Mg^{2+}, making a complex with the terminal phosphates of the NTP. Several residues and motifs have been implicated in the coupling of NTP hydrolysis with RNA unwinding; they are the His residue of motif II, motif III (TAT box), and the glutamine and Arg residues of motif VI ([Q/x]RxGRxxR) (Grassmann *et al.*, 1999; Gross & Shuman, 1996*a*; Gu *et al.*, 2000; Kim *et al.*, 1997*b*; Paolini *et al.*, 2000*b*; Utama *et al.*, 2000*a*; Wardell *et al.*, 1999; Yao *et al.*, 1997).

The initial studies of viral helicase by mutagenesis targeted the helicase motifs I, II, III and VI, and showed that highly conserved residues within these motifs are essential for enzymatic activity (Grassmann *et al.*, 1999; Gross & Shuman, 1996*a*; Gu

et al., 2000; Kim *et al.*, 1997*b*; Paolini *et al.*, 2000*b*; Utama *et al.*, 2000*a*; Wardell *et al.*, 1999). More recently, the roles of residues outside motifs were examined using site-directed mutagenesis and a crystal structure of the HCV NS3 helicase-$(dU)_8$ complex (Kim *et al.*, 1998; Lin & Kim, 1999; Paolini *et al.*, 2000*b*). Several conserved HCV helicase residues which contact the oligonucleotide were shown to be involved in RNA binding, duplex unwinding and polynucleotide stimulated ATPase activity.

This study investigated the importance of selected residues in the DEN-2 NS3 helicase region for enzyme activity and viral replication. Two types of mutations were introduced. One type was the substitution of residues within motifs I (G198A and K199A), II (M283F) and VI (R457A,R458A), and the second type was the replacement with Ala of amino acids in clusters of charged amino acids outside motifs. Amino acids 161 to 462 of NS3 were scanned for clusters of five residues which contained at least three charged amino acids, namely Asp, Glu, Lys and Arg (Bass *et al.*, 1991, Wertman *et al.*, 1992) (Fig. 4.1). Six such clusters ($E_{169}KSIE_{173}$, $E_{179}DD_{181}$, $R_{184}KR_{186}$, $D_{334}EE_{336}$, $R_{376}KNGK_{380}$, and $D_{436}GEE_{439}$) outside helicase motifs (Koonin & Dolja, 1993) which also exhibited distinct peaks on a hydrophilicity plot (Hopp & Woods, 1981) (Fig. 4.2) were chosen for mutagenesis and the charged residues were changed to Ala (Fig.4.3). Mutant proteins were synthesized as amino terminal truncated fusion proteins in *E. coli*, purified and assayed for ATPase and RNA helicase activities. Mutations were also incorporated into genomic length DEN-2 cDNA to investigate the effects of changes to the hydrophilicity of NS3 (which may modify the interaction of NS3 with other proteins within the viral replication complex) on viral yield, and to study the role of both conserved and non conserved residues within helicase motifs in viral replication.

4.2 Materials and methods

4.2.1 The pGEX-3X expression vector

The pGEX-3X plasmid (Pharmacia Biotech) (Fig. 4.4) features a *tac* promoter for chemically inducible, high-level expression of genes or gene fragments as fusions with *Schistosoma japonicum* glutathione *S*-transferase (GST). The plasmid contains a selective marker for ampicillin resistance.

The fusion proteins made in this study contain mutations within the helicase region of NS3, to study their effects on *in vitro* ATPase and RNA helicase activities. A summary of the mutant constructs can be found in Fig. 4.3. A copy of Fig. 4.3 is removable for the reader's convenience from the pocket at the back of the thesis.

Table 4.1 summarizes the mutant constructs produced by OE-PCR and the sequences of primers used. After cloning of OE-PCR products was complete, each PCR derived region was completely sequenced, and the primers used for sequencing are also listed.

4.2.2 Construction of the parental plasmid pGX74%NS3

To obtain a plasmid encoding the carboxy terminal region of the DEN-2 NS3 protein, a *Nde* I^{5002}-*Spe* I cDNA fragment (containing nucleotides 5002-6375 of the DEN-2 NGC genome) was excised from the vector pSV.NS3, which encodes full length NS3 and contains a stop codon at the 3′ end of the NS3 gene (Teo & Wright, 1997). Blunt ends were generated using Klenow DNA polymerase I (section 2.5.1), which allowed ligation into the *Sma* I site of pGEX-3X (Fig. 4.5). This plasmid was

constructed by Dr. Catherine Agius. The resulting plasmid pGX74%NS3 (G2) encodes the GST protein fused to residues 161-618 of DEN-2 NS3.

In this study, protein derived from the parental plasmid pGX74%NS3 was named G2. Plasmids containing clustered charged-to-alanine mutations in the truncated NS3 protein were named according to the NS3 amino acid numbers of regions mutated (e.g. pGX74%NS3$_{169\text{-}173}$), and derived protein was designated with a G (e.g. G$_{169\text{-}173}$). Alternatively, plasmids containing amino acid substitutions within helicase motifs were named according to the residue mutated, its amino acid number within NS3, and the replacement residue (e.g. pGX74%NS3$_{K199A}$), and derived protein was designated with a G (e.g. G$_{K199A}$).

4.2.3 Mutagenesis of the parental plasmid pGX74%NS3

4.2.3(a) Construction of the charged-to-alanine mutants pGX74%NS3$_{169\text{-}173}$, pGX74%NS3$_{179\text{-}181}$ and pGX74%NS3$_{184\text{-}186}$

The three charged-to-alanine mutations, E$_{169}$KSIE$_{173}$, E$_{179}$DD$_{181}$ and R$_{184}$KR$_{186}$ (underlined residues changed to Ala) (Fig. 4.3) were derived from pGX74%NS3 by replacing the *Bam* HI-*Xho* I[5426] fragment (*Bam* HI is located in the pGEX-3X multiple cloning site immediately upstream of *Sma* I) with a mutated fragment prepared by OE-PCR (Fig. 4.6). PCR-derived regions were sequenced (Table 4.1).

4.2.3(b) Construction of the motif I and II mutants pGX74%NS3$_{G198A}$, pGX74%NS3$_{K199A}$ and pGX74%NS3$_{M283F}$

The three motif mutations, G198A and K199A (motif I) and M283F (motif II) (Fig. 4.3) were constructed as described above in section 4.2.3(a), by replacing the *Bam* HI-*Xho* I^{5426} fragment of pGX74%NS3 with a mutated fragment prepared by OE-PCR (Fig. 4.7). PCR-derived regions were sequenced (Table 4.1).

4.2.3(c) Construction of the motif VI mutant pGX74%NS3$_{R457A,R458A}$

The plasmid pGX74%NS3$_{R457A,R458A}$ (G$_{R457A,R458A}$) was constructed by removing the mutated *Xho* I^{5426}-*Sna* BI fragment from the plasmid pSV.NS2B/3$_{457,458}$ (Teo & Wright, 1997) which contains the double Arg to Ala mutations at amino acid positions 457 and 458 of motif VI, and ligating this into *Xho* I^{5426}/*Bsa* AI-digested pGX74%NS3 (Fig. 4.8). Both *Sna* BI and *Bsa* AI restriction enzymes generate blunt ends.

4.2.3(d) Construction of the charged-to-alanine mutants pGX74%NS3$_{334-336}$, pGX74%NS3$_{376-380}$ and pGX74%NS3$_{436-439}$

The three remaining charged-to-alanine mutations, D$_{334}$EE$_{336}$, R$_{376}$KNGK$_{380}$, and D$_{436}$GEE$_{439}$ were introduced into *Xho* I^{5426}/*Ppu* MI^{5852}-digested pGX74%NS3 as mutated OE-PCR fragments (Fig. 4.9). PCR-derived regions were sequenced (Table 4.1).

4.2.4 Synthesis and purification of NS3 proteins

The recombinant proteins containing an amino terminal GST tag were expressed in *E. coli* DH5α cells grown at 37°C in LB medium containing 100 µg/ml ampicillin. Synthesis of the recombinant proteins was induced by the addition of 0.1 mM isopropyl-β-D-thiogalactopyranoside. Two hours later, the cells were collected by centrifugation, and resuspended in ice-cold PBS containing 33 µg/ml lysozyme, and held on ice for 10 min. Triton X-100, at a final concentration of 0.1%, was added to the cells prior to their sonication on ice for 2 min. The cell lysate was clarified by centifugation at 12,000g for 10 min. The soluble fraction was mixed with Glutathione Sepharose 4B beads (Pharmacia Biotech) and gently mixed at 4°C for 30 min. The beads were washed three times with PBS and bound protein was eluted in 1 ml of elution buffer (10 mM glutathione and 50 mM Tris-HCl [pH 8.0]) at 25°C for 15 min. The elution was repeated with 0.5 ml of the same buffer. All protein preparations were adjusted to 10% glycerol and stored at -70°C. Protein concentrations were estimated by densitometer scanning (LKB Ultrascan) of Coomassie blue stained acrylamide gels with co-electrophoresed bovine serum albumin (BSA) standards of known concentration, and by Bradford assay (Bio-Rad).

4.2.5 Polyacrylamide gel electrophoresis (SDS-PAGE) of recombinant proteins

Protein samples were mixed with an equal volume of double strength reducing buffer (62.5 mM Tris-HCl [pH 6.8], 2% SDS, 10% glycerol, 5% 2 mercaptoethanol, 0.25% bromophenol blue [BPB]). The mix was heated at 100°C for 2 min prior to

analysis by electrophoresis through discontinuous 10% SDS-polyacrylamide gels (Laemmli, 1970). SDS-6H protein molecular weight markers (Sigma) were co-electrophoresed to serve as standards. The markers were: myosin (M_r 200,000), β-galactosidase (M_r 116,000), phosphorylase b (M_r 97,400), bovine serum albumin (M_r 66,000), ovalbumin (M_r 45,000), carbonic anhydrase (M_r 29,000).

To visualize proteins, gels were stained by incubation for 30 min at room temperature in Coomassie blue stain (0.25% Coomassie brilliant blue, 45% methanol and 10% acetic acid), and destained in a solution of 10% acetic acid and 25% methanol.

4.2.6 Immunoblots

After electrophoresis through polyacrylamide gels, proteins were transferred to 0.45 μm nitrocellulose membranes overnight at 250 mA using a trans-blot apparatus (Bio-Rad) The transfer buffer consisted of 25 mM Tris, 190 mM glycine and 20% methanol. The membranes were blocked in 2% (w/v) skim milk made in PBS for 2 hr before incubating with the appropriate rabbit antiserum at 37°C for another 2 hr. The membranes were then washed in PBS-0.05% Tween 20 and incubated with sheep anti-rabbit IgG antiserum conjugated with horseradish peroxidase (Silenus) for 1 hr. Finally the proteins were detected by ECL™ (Amersham) on Fuji film.

4.2.7 ATPase assay

The assay was a modified procedure of Warrener *et al.* (1993). The final volume of the standard assay used to test mutant proteins was 10 µl, containing 50 mM Tris-HCl (pH 8.0), 10 mM NaCl, 2.5 mM $MgCl_2$, 1 µCi [α-^{32}P] ATP (800 Ci/mmol, DuPont) and 0.4 pmol of protein sample. Reaction mixes were incubated for 1 hr at 25°C, and the reactions terminated by the addition of EDTA to a final concentration of 20 mM. A 0.5 µl sample of the reaction mixture was spotted onto plastic-backed polyethyleneimine-cellulose sheets and ^{32}P-labelled ATP and ADP were separated by ascending chromatography in 0.375 M potassium phosphate (pH 3.5). The sheets were dried and exposed to X-ray film. The percentage conversion of ATP to ADP was estimated by measuring the radioactivity in separated nucleotides by liquid scintillation counting.

The values of K_m and k_{cat} were calculated from a Lineweaver-Burk plot of ATP hydrolysis activity over a range of ATP concentrations from 1 to 5 mM. The concentration of poly(A), if present, was 0.17 µg/µl (0.5 mM measured as mononucleotide equivalents).

4.2.8 Helicase assay

A partial dsRNA substrate was prepared by using a modified pGEM-4Z (Promega) plasmid. A 24 bp region of the polylinker was removed by digestion with *Eco* RI and *Hind* III, fill in of recessed ends with Klenow DNA polymerase, and blunt-end ligation to generate the plasmid pGEM-4ZΔ24 (Fig. 4.10).

Nde I digested plasmid pGEM-4ZΔ24 was transcribed with T7 RNA polymerase to produce a 259 nt strand. *Ban* I digested plasmid pGEM-4ZΔ24 was transcribed with SP6 RNA polymerase in the presence of [α-^{32}P] ATP to produce a radiolabelled 144 nt strand (Fig. 4.10). Reaction mixes were treated with RQI RNase-Free DNase (Promega), extracted with phenol/chloroform and the RNA was precipitated with ethanol. Transcripts were combined in annealing buffer containing 10 mM Tris-HCl (pH 7.5), 0.1 mM EDTA and 200 mM NaCl. The mixture was heated for 5 min at 95°C and 1 hr at 65°C and then allowed to cool to room temperature over 3 hr. 5X RNA sample buffer (25 mM EDTA, 0.25% BPB, 50% glycerol and 0.5% SDS) was added to the hybridization mixture, which was then electrophoresed through a 6% polyacrylamide gel (acrylamide-bisacrylamide [30:0.8], 0.5X TBE [90 mM Tris borate pH 7.5, 2 mM EDTA] and 0.1% SDS). The region of the gel containing the RNA duplex was localized by autoradiography, excised from the gel, pulverized and RNA eluted overnight at 37°C with 500 mM ammonium acetate, 10 mM magnesium acetate, 1 mM EDTA and 0.1% SDS. The eluted RNA was precipitated with ethanol and resuspended in water.

The RNA helicase assay was carried out in a total volume of 20 µl containing 25 mM MOPS-KOH (pH 6.5), 5 mM ATP, 3 mM $MnCl_2$, 2 mM dithiothreitol, 100 µg/ml BSA, 5U RNasin (Promega), approximately 1500 cpm of radiolabelled substrate and 1 pmol of protein. Reaction mixtures were incubated for 30 min at 37^{0}C and terminated by the addition of 5X RNA sample buffer. The reaction mixture was analyzed by electrophoresis through a 6% polyacrylamide gel. Gels were dried and exposed to the storage phosphor screen (Molecular Dynamics). The phosphor screen was analyzed using a STORM Phosphoimager™ system and ImageQuant image

analysis software® (Molecular Dynamics) was used to estimate the percentage of ^{32}P-labelled fragment unwound.

The mutated NS3 helicase fusion proteins were examined for ATPase and RNA helicase activity, and then the mutations were inserted into genomic length DEN-2 cDNA (described in sections 4.2.9 to 4.2.11) to study their effects on virus replication (except the G198A mutant). A summary of the mutant constructs can be found in Fig. 4.3 and at the back of this thesis.

4.2.9 Construction of the charged-to-alanine mutants pDVWS501NS3$_{169\text{-}173}$, pDVWS501NS3$_{179\text{-}181}$ and pDVWS501NS3$_{184\text{-}186}$

Due to an absence of suitable restriction enzyme sites for cloning an appropriate fragment directly into pDVWS501, these three mutations were initially constructed in the plasmid pDVSO8298 (Section 3.2.2(a)) prior to ligation of a subfragment into pDVWS501.

The insertion of the mutations E$_{169}$KSIE$_{173}$ and E$_{179}$DD$_{181}$ into pDVWS501 was described in sections 3.2.2 (b and c). The additional change R$_{184}$KR$_{186}$ was also initially cloned into pDVSO8298 prior to insertion into pDVWS501. This mutation was introduced into *Nsi* I/*Ppu* MI-digested pDVSO8298 as an OE-PCR fragment using flanking primers 3632 (a) and 752 (d), and mutagenic primers 4097 (b) and 4098 (c) (primer sequences are listed in Tables 3.2 and 4.1). Subsequently an *Nsi* I-*Stu* I mutated fragment was removed from the pDVSO8298$_{184\text{-}186}$ plasmid and ligated into *Nsi* I^{4700}/*Stu* I^{7874}-digested pDVWS501 (Fig. 4.11). PCR-derived regions were sequenced.

4.2.10 Construction of the motif I, II and VI mutants pDVWS501NS3$_{K199A}$, pDVWS501NS3$_{M283F}$ and pDVWS501NS3$_{R457A,R458A}$

The plasmids pDVWS501NS3$_{K199A}$, pDVWS501NS3$_{M283F}$, and pDVWS501NS3$_{R457A,R458A}$ were prepared by removal of the mutated *Bst* BI^{5069}-*Bst* BI^{6046} fragments from the corresponding pGX74%NS3 plasmids, and ligation into *Bst* BI digested pDVWS501 (Fig. 4.12).

4.2.11 Construction of the charged-to-alanine mutants pDVWS501NS3$_{334-336}$, pDVWS501NS3$_{376-380}$ and pDVWS501NS3$_{436-439}$

The plasmids pDVWS501NS3$_{334-336}$, pDVWS501NS3$_{376-380}$ and pDVWS501NS3$_{436-439}$ were prepared by replacing the *Bst* BI^{5069}-*Bst* BI^{6046} fragment of pDVWS501 with a mutated fragment prepared by OE-PCR using flanking primers 3638 (a) and 4318 (d), and mutagenic primers 4099 (b) and 4100 (c): 4104 (b) and 4105 (c): and 4106 (b) and 4107 (c) respectively. Primer sequences are listed in Table 4.1 (mutagenic primers were the same for generating OE-PCR fragments for ligation into both pGX74%NS3 and pDVWS501) (Fig. 4.13).

4.2.12 RT-PCR of viral RNA

To confirm that the desired mutation was present in viral RNA obtained as described in section 2.10, RNA was extracted from infected C6/36 cells or culture medium. The cells were infected with virus obtained by electroporation of RNA into BHK-21 cells (maintained at 33°C or 37°C) and previous passage in C6/36 cells

(section 2.10). RT-PCR and sequencing was performed as described in section 2.11. Table 4.2. shows the primers used in reverse transcription (random hexameric primers were used), PCR and sequencing of each virus. The sequence of each primer is shown in Table 3.2.

4.2.13 Temperature shift experiments

BHK-21 cells were seeded into 30 mm^2 petri dishes and infected with the parental V2 or mutant V_{M283F} virus at an MOI of 10 when cells reached 70-80% confluency. Following a 1 hr incubation at 33°C, the virus inoculum was removed, and the cells washed twice with PBS. To each petri dish, 3 ml of maintenance medium was added and cells were incubated for 48 hr at 33°C. At 48 hr after infection, incubations were continued at 33°C or shifted to 37°C. At 0 hr, 16 hr and 24 hr post shift, supernatant from a petri dish for each virus was harvested and titred by plaque assay in C6/36 cells (see section 2.2). At the same time points, RNA extracts of infected cells were prepared using RNeasy columns (Qiagen) for analysis of viral RNA content by dot blot hybridization.

4.2.13(a) Dot blot hybridizations

RNA samples for dot blot hybridization analysis (prepared as described in section 4.2.13 above) were diluted in RNA dilution buffer (DEPC-treated H_2O:20X SSC:formaldehyde, 5:3:2) and held at 65°C for 15 min to remove RNA secondary structure. The samples were applied to a Hybond-N+ nylon membrane (Amersham),

presoaked in 10X SSC, using an SRC 96 D Minifold I dot blotter (Schleicher and Schuell). The membrane was allowed to dry at room temperature (15 min), cross-linked with UV light (3 min) and prehybridized at 68°C for 2 hr in hybridization solution (5X SSC, 1% SDS and 1% BSA).

A ^{32}P-labelled DNA probe spanning nucleotides 5364-6123 of the DEN-2 genome was produced by random primed labelling using [α-^{32}P]dATP (3000 Ci/mmol), labeling mix-dCTP and pd(N)$_6$ (Pharmacia Biotech) and the Klenow fragment of DNA polymerase I (New England Biolabs) at 37°C for 1 hr. ^{32}P-labelled DNA was purified by chromatography through Sephadex G-50. Labelled DNA probe, at 10^7 cpm/ml, was heated at 95°C and added to fresh hybridization solution, and the membrane was incubated for a further 16 hr in the presence of the probe. The membrane was then washed twice for 5 min at room temperature in 2X SSC and 0.1% SDS, followed by two 15 min washes at 68°C in 0.1X SSC and 0.1% SDS. Bound radioactivity was detected using the STORM Phosphoimager™ system (Molecular Dynamics).

4.2.13(b) Radiolabelling of infected cells and radioimmunoprecipitation (RIP)

To assess the effect of temperature shift on viral protein synthesis, BHK-21 cells were infected with parental V2 or mutant V_{M283F} viruses and temperature shift was performed as described in section 4.2.10. At 0 hr and 24 hr post shift, the cells for each virus at each temperature were washed in PBS and incubated for 2 hr in 2.5 ml per dish of methionine and cysteine deficient Dulbecco's modified Eagle's medium (DMEM; ICN) supplemented with 1/50 volume of 200 mM glutamine. The cells were

labelled for 2 hr with 50 µCi per dish of TRAN[^{35}S] LABEL™ (ICN; specific activity 1150-1250 Ci/mmol), in 0.5 ml of methionine deficient DMEM. For harvesting, the dishes were chilled on ice and washed twice in cold PBS. The cells in each dish were scraped off with a bent pasteur pipette into 0.5 ml of cold PBS, after which the cells were pelleted at 16000 g at 4°C. The cells were lysed by vortexing in 0.5 ml of lysis buffer (150 mM NaCl, 0.5% Na deoxycholate, 1% Triton X-100, 0.1% SDS, 15 mM Tris-HCl [pH 7.5]). The lysates were passed three times through a 26G needle and stored at -70°C.

BHK-21 cells that had been mock infected, incubated and radiolabelled (as described above) were used as negative controls.

The antiserum against NS3 used throughout this chapter for the detection of NS3 was prepared by Dr. K. F. Teo. DEN-2 cDNA corresponding to nucleotides 5584-6302 was cloned into pGEMEX-2 for production of a bacterial fusion protein which was used as an antigen to raise anti-NS3 antibodies in rabbits as described previously (Teo & Wright, 1997). For the following experiment, 5 µl of the anti-NS3 antiserum was used in each RIP.

Protein A-Sepharose CL-4B beads (Pharmacia) were prepared as a 50% (v/v) solution in RIP wash buffer (150 mM NaCl, 0.25% Na deoxycholate, 0.5% Triton X-100, 0.05% SDS, 15 mM Tris-HCl [pH 7.5]). For each RIP, a 100 µl aliquot of cell lysate was incubated for 1 hr at 4°C with 2 µl of 1 µg/µl aprotinin, 1 µl of 100 mM phenylmethylsulfonyl fluoride and 30 µl of Protein A. The beads were pelleted at 16000 g in a microfuge for 5 min at 4°C. The cleared cell lysate was then mixed with rabbit anti-NS3 antiserum (Teo & Wright, 1997) and incubated overnight at 4°C with gentle rotation.

The antigen-antibody complexes were captured by adding 50 µl of Protein A and incubating for 45 min at room temperature with gentle rotation. The suspension was then layered onto 400 µl of a 10% solution of sucrose in wash buffer, and the beads were left to settle on ice for 10 min. The supernatant was discarded and the beads were washed three times in wash buffer. The proteins were eluted in 30 µl of double strength reducing buffer (62.5 mM Tris-HCl [pH 6.8], 2% SDS, 10% glycerol, 5% 2 mercaptoethanol, 0.25% BPB) by heating at 100°C for 5 min.

4.2.13(c) SDS-PAGE of radiolabelled proteins

Radioimmunoprecipitated protein samples were analyzed by electrophoresis through 10% discontinuous SDS-polyacrylamide gels. Gels were fixed by incubation for 30 min at room temperature in a solution of 10% acetic acid and 25% methanol. Gels were then fluorographed with the Amplify reagent (Amersham), which was used according to manufacturer's instructions. Dried protein gels were autoradiographed using Fuji Film. A mixture of [^{14}C] methylated proteins (Amersham) were electrophoresed with the radiolabelled protein samples. The markers were: myosin (M_r 200,000), phosphorylase b (M_r 97,400), bovine serum albumin (M_r 69,000), ovalbumin (M_r 46,000), carbonic anhydrase (M_r 30,000) and lysozyme (M_r 14,300).

4.2.14 Serial passage of $V_{334\text{-}336}$ in C6/36 cells

C6/36 cells were seeded into 60 mm^2 petri dishes and infected with 250 µl aliquots of first passage supernatant stock of the mutant virus $V_{334\text{-}336}$. Following a 1

hr incubation at 28°C, the virus inoculum was removed, and 5 ml of maintenance medium was added. The cells were maintained at 28°C for five days (or until cell monolayers exhibited extensive CPE). On day 5, 250 µl of supernatant was then removed from the appropriate petri dish and fresh C6/36 cells were infected. Virus was serially passaged up to 11 times in C6/36 cells.

4.3 Results

4.3.1 Mutagenesis of the helicase region of NS3

In order to test the importance of selected residues in the helicase region of DEN-2 NS3 for enzyme activity and virus replication, two types of mutations were introduced. First, changes were made in motifs I, II and VI. These were single Ala substitiutions G198A and K199A (motif I) and a double change at R457A,R458A (motif VI). In motif II, the substitution was M283F; Phe is the second most common residue (after Met) at this position in positive strand viruses (Koonin & Dolja, 1993). Based on previous mutational studies and X-ray crystallography data of related viral RNA helicases (Grassmann *et al.*, 1999; Gross & Shuman, 1996*a*; Gu *et al.*, 2000; Kim *et al.*, 1997*b*; Paolini *et al.*, 2000*b*; Utama *et al.*, 2000*a*; Wardell *et al.*, 1999), these motifs are known to be involved in the binding and hydrolysis of ATP and/or the coupling of helicase and ATPase activities. Thus for the first three mutations, a reduction in enzyme activity and virus replication was predicted, although there are no previous studies on the replication of flaviviruses carrying these types of mutations. The possible effect of the substitution M283F was unknown.

The second type of mutation was the replacement with Ala of three amino acids in clusters of charged amino acids. Charged amino acids are likely to occupy exposed positions in the tertiary structure and therefore interact with other proteins (as mentioned in sections 1.12 and 3.1). Several studies have demonstrated an association between the flavivirus NS3 protein and other viral nonstructural proteins including NS2B and NS5, both *in vitro* and during viral replication (Chambers *et al.*, 1991; Chambers *et al.*, 1993; Chen *et al.*, 1997*a*; Falgout *et al.*, 1993; Falgout *et al.*, 1991; Kapoor *et al.*, 1995; Westaway *et al.*, 1997*b*). It was of interest to determine whether these changes in hydrophilicity outside helicase motifs modified the enzyme activity of NS3 in the absence of any other viral protein, or whether any effects of the changes could be detected only by examining virus replication, when not only helicase activity but also interactions between NS3 and other viral or host proteins may be required.

4.3.2 Synthesis of truncated parental and mutant NS3 in *E. coli*

To provide a source of flavivirus NS3 protein for biochemical studies, truncated (amino acids 161-618) parental and mutant polypeptides were synthesized as GST fusion proteins in *E. coli* DH5α cells. Proteins were purified from the cell lysate by affinity chromatography, and purified parental GST:74% NS3 fusion protein (G2) of 78 kDa was detected following SDS-PAGE (Fig. 4.14A, lane 2). In addition to the G2 protein, several proteins of lower molecular weight were also detected. These were possibly generated by either proteolytic degradation or premature translational termination, as they were recognised by anti-GST and anti-NS3 antibodies (Fig. 4.14B, lane 1; Fig. 4.14C, lane 1). GST (26 kDa) was also synthesized in *E.coli* to use as a negative control for the *in vitro* enzyme assays (Fig.

4.14A, lane 3; Fig. 4.14B, lane 2). Preparations of all mutant fusion proteins used for enzyme assays are shown in Fig. 4.15.

4.3.3 NS3-mediated ATPase activity

The ATPase activity of increasing amounts of the parental NS3 fusion protein G2 was first measured over 45 min in the presence of 5 mM ATP (Fig. 4.16A). The rate of hydrolysis was directly proportional to the amount of enzyme. Using 1 pmole of enzyme and 5 mM ATP, the rate of hydrolysis was linear from 15 to 90 min (Fig. 4.16B). To determine K_m of G2, the ATPase activity of 1 pmole of G2 was measured at ATP concentrations from 1 to 5 mM for 60 min in the presence or absence of poly(A). The Lineweaver-Burk plots were linear in this range (Fig. 4.16C). The K_m values for the parental protein were 3.0 mM or 2.6 mM in the absence or presence of poly(A) respectively. Corresponding k_{cat} values were 1.2 and 1.5 sec^{-1}. The measure of catalytic efficiency k_{cat}/K_m increased from 4.0 x 10^2 $(mol/l)^{-1}s^{-1}$ in the absence of poly(A) to 5.8 x 10^2 $(mol/l)^{-1}s^{-1}$ in the presence of poly(A). Thus the stimulation of ATPase activity (1.45 fold) by poly(A) was low.

The results of testing the ATPase activity of the mutant NS3 fusion proteins are shown in Fig. 4.17. The chromatographic analyses of a typical experiment are displayed in Fig. 4.17A, the means of three experiments in Fig. 4.17B, and an overall summary in Table 4.3. As expected, mutation of the highly conserved G198 and K199 residues within the ATP binding motif I abolished ATPase activity (Fig. 4.17A, lanes 7 and 8). Mutation of the less conserved residues in motifs II and VI, also reduced ATPase activity (Fig. 4.17A, lanes 9 and 13), although to a lesser extent than the motif I mutants. The clustered charged-to-alanine mutants located outside

helicase motifs demonstrated a range of ATPase activities, from levels lower (Fig. 4.17A, lanes 10 and 11) to higher (Fig. 4.17A, lanes 4, 5, 6 and 12) than that of the parental protein (Fig. 17A, lane 3). It is interesting to note that mutated clusters located within the linker region (residues 161-188) between the final proteinase box 4 (residues 145-155) (Bazan & Fletterick, 1989) and upstream of the first helicase motif I (residues 188-205), stimulated ATPase activity. Previous studies have also shown increased ATPase activity for helicase mutants; Li *et al.* (1999) produced a comparable DEN-2 NS3 mutant ($R_{184}KRK_{187}$ to $Q_{184}NGN_{187}$) and demonstrated that it had a 2-fold increase in basal ATPase activity.

4.3.4 RNA helicase activity of NS3 mutants

Helicase activity was tested by using an RNA substrate which consisted of a 259 nt RNA strand hybridized to a 144 nt radiolabelled RNA strand to produce a partially duplex RNA substrate containing 3′ single stranded regions with a 24 bp duplex region (Fig. 4.10). The G2 protein had RNA helicase activity in the presence of Mn^{2+} and ATP shown by the release of the radiolabelled strand (Fig. 4.18, lane 3). In the absence of the G2 protein (lane 2), or Mn^{2+} and ATP (lane 4), no activity was detected.

Next the mutant NS3 proteins were examined in the RNA helicase assay, with results of a typical experiment shown in Fig. 4.19A (summary shown in Table 4.3). As expected, mutation of the ATP-binding motif I abolished RNA helicase activity (Fig. 4.19A, lanes 8 and 9); the extent of unwinding was the same as for GST alone (lane 3), confirming that no RNA helicase activity was detected in the absence of ATPase activity. Interestingly, mutation M283F in motif II demonstrated reduced

ATPase activity (Fig. 4.17A, lane 9) and increased helicase activity (Fig. 4.19A, lane 10) compared to the parental G2 protein (Fig. 4.17A, lanes 3 and 4). Also, the protein with changes R457A and R458A in motif VI which retained ATPase activity (Fig. 4.17A, lane 13) showed no detectable RNA unwinding (Fig. 4.19A, lane 14). These results demonstrate that the NTPase and RNA helicase activities of the DEN-2 NS3 protein can be functionally uncoupled by mutations within motifs.

Mutation of the clustered charged regions external to the helicase motifs had variable effects on RNA unwinding. The three mutants $G_{169\text{-}173}$, $G_{179\text{-}181}$, and $G_{184\text{-}186}$, located upstream of motif I, demonstrated a large increase in RNA unwinding (Fig. 4.19A, lanes 5, 6, and 7) compared with parental NS3, which corresponded to their increased ATPase activity (Fig. 4.17). However, the $G_{436\text{-}439}$ mutant, which also exhibited enhanced ATP hydrolysis, showed only a slight increase in helicase activity over parental G2 (Fig. 4.19B, lane 13). The remaining two mutants $G_{334\text{-}336}$ and $G_{376\text{-}380}$ each demonstrated ATPase activity, but low or no RNA unwinding (lanes 11 and 12). These results show uncoupling of ATPase and helicase activity by mutagenesis outside enzyme motifs. This indicates that other regions external to enzyme motifs may also be critical in the complexity of NS3 enzymatic activities.

4.3.5 Analysis of virus replication

To test the effects of the mutations described above on virus replication, all mutants except G198A were incorporated into DEN-2 genomic length cDNA. It was considered unnecessary to test both the motif I mutants, G198A and K199A.

Virus was produced from genomic length cDNA by established procedures (Gualano *et al.*, 1998) as described in sections 2.9 and 2.10. RNA was transcribed and

electroporated into BHK-21 cells and the cells were incubated at 33°C or 37°C. BHK-21 cells were tested for immunofluorescence with anti-E antibodies. Medium from the transfected BHK-21 cells was passaged twice in C6/36 cells at 28°C, and the virus titre determined after the second passage by plaque assay in C6/36 cells. Viral RNA was then amplified by RT-PCR and the entire NS2B and NS3 genes were sequenced to check that the mutation was retained during the passaging, and that no other changes were present within this region. These procedures were completed at least twice for each construct, and the results are summarized in Table 4.3.

The parental virus V2 and mutant viruses, $V_{169\text{-}173}$, and $V_{179\text{-}181}$ grew to comparable titres of 10^5 to 10^6 pfu/ml following initial electroporation at 33°C or 37°C (Table 4.3), although both mutant viruses showed a small plaque phenotype (Fig. 4.20). These viruses were described in chapter three with respect to their proteinase activity and viral replication, and will be discussed within this chapter with respect to their effects on helicase activity and viral replication. The corresponding NS3 fusion proteins G2 and mutants $G_{169\text{-}173}$, and $G_{179\text{-}181}$ all possessed *in vitro* ATPase and RNA helicase activities. For viruses V_{M283F} and $V_{334\text{-}336}$, virus was detected following electroporation at 33°C only, and at reduced titres (4.7×10^5 and 7.3×10^2 pfu/ml respectively), and with a small plaque phenotype (Table 4.3, Fig. 4.20). These results suggested that V_{M283F} and $V_{334\text{-}336}$ were restricted in replication and possibly heat sensitive. The G_{M283F} and $G_{334\text{-}336}$ fusion proteins both had reduced ATPase activity *in vitro* (Fig.4.17B), and helicase activity that was either increased or reduced respectively (Fig. 4.19B).

No virus was detected for five constructs. The lack of virus from the three constructs containing K199A (motif I), R457A.R458A (motif VI) or clustered charged-to-alanine changes $R_{376}KNGK_{380}$ corresponded to the lack of helicase activity

detected for the corresponding fusion proteins. However, clustered changes at $R_{184}KR_{186}$ and $D_{436}GEE_{439}$ did not reduce helicase activity of the fusion proteins, and yet no virus was recovered. Therefore these residues may be required for other NS3 functions, such as the interaction with proteins in the viral replication complex.

4.3.6 Growth of viruses V2, $V_{169\text{-}173}$, $V_{179\text{-}181}$ and V_{M283F} in BHK-21 cells

To examine further the properties of the viruses, more concentrated stocks were prepared by PEG precipitation of all viruses except $V_{334\text{-}336}$. Virus $V_{334\text{-}336}$ did not replicate adequately to obtain sufficient titres for further experiments.

BHK-21 cells were infected at an MOI of 1 and cells were incubated at 33°C or 37°C. Experiments maintaining the BHK-21 cells at 39°C were unsuccessful because of poor cell survival. The culture medium was sampled at 72 hr after infection and virus titres were determined by plaque assay in C6/36 cells (Fig. 4.21). The results for V2, $V_{169\text{-}173}$, $V_{179\text{-}181}$ have also been presented in chapter three. Of the four viruses, only V_{M283F} showed significant temperature sensitivity. At 72 hr after infection, supernatant from cells infected with virus V_{M283F} and maintained at 33°C contained $(3.0 \pm 0.4) \times 10^4$ pfu/ml, whereas cells maintained at 37°C contained $(5.7 \pm 0.4) \times 10^2$ pfu/ml (Fig. 4.21). The presence of each mutation in recovered virus was reconfirmed by RT-PCR and sequencing.

4.3.7 Temperature shift experiments with virus V_{M283F}

To assess the effect of temperature shift on viral RNA synthesis and replication of V_{M283F}, duplicate BHK-21 cell monolayers were infected with the parental V2 or mutant V_{M283F} viruses at an MOI of 10 and incubated for 48 hr at 33°C. At this time monolayers were maintained at 33°C or shifted to 37°C. At 0 hr, 16 hr and 24 hr after the shift, culture fluid was removed for analysis of virus production by plaque assay, and RNA extracts of the infected cells were prepared for analysis of viral RNA content by dot blot hybridization.

At 24 hr after the shift (72 hr after infection) the cell culture medium was assayed for virus yield (Fig. 4.22A). The titres for the mutant and parental viruses were both higher at 33°C than at 37°C. However, the shift to 37°C clearly had a greater effect on mutant V_{M283F} than on V2. The reductions in titre (log_{10}) were 1.9 and 0.7 respectively.

The results of the analysis of RNA accumulation by dot blots (Fig. 4.22B) correlated with the titre of released virus described above. Overall, the V2 infected cells contained more viral RNA than those infected with the mutant V_{M283F} (Fig. 4.22B), consistent with the higher yield of virus from the former (Fig. 4.22A). Following the shift, V2 infected cells showed similar viral RNA content at the two temperatures at 64 hr and 72 hr, whereas for the mutant V_{M283F}, the cells maintained at 33°C clearly had more viral RNA than at 37°C. Both positive and negative strand viral RNA were detected by the dsDNA probe.

To assess the effect of the temperature shift on viral protein synthesis, the accumulation of labelled proteins at the permissive (33°C) and non-permissive (37°C)

temperatures was compared. The timing of the experiment was similar to that described above for the dot blot. BHK-21 cell monolayers were infected with the V2 or mutant V_{M283F} viruses at an MOI of 10 and incubated for 48 hr at 33°C. At 48 hr after infection monolayers were maintained at 33°C or shifted to 37°C. At 0 hr and 24 hr post shift, media was replaced with fresh medium lacking methionine for 2 hr. Proteins were then radiolabelled with [^{35}S]methionine for a further 2hr. As a measure of overall viral protein synthesis, the amount of NS3 protein was assessed by RIP of cell lysates using anti-NS3 polyclonal antiserum (Fig. 4.23). As for viral RNA, less NS3 was detected in the cells infected by the mutant virus V_{M283F} than by V2. In addition, cells infected by the mutant contained less NS3 at the higher temperature (Fig. 4.23A, lanes 7 and 8 compared with lanes 9 and 10), whereas V2 infected cells, (lanes 11 and 12), were more similar in NS3 content.

Fig. 4.23B shows that the amount of protein in cell lysates before immunoprecipitation varied little. This demonstrated that the differences in levels of NS3 seen following RIP were probably due to the availability of template viral RNA for protein synthesis and not to variation in the number of cells in the monolayer or efficiency of lysis. Therefore the mutant virus V_{M283F} was temperature (heat) sensitive in RNA synthesis, protein synthesis and virus yield.

4.3.8 Serial passage of $V_{334\text{-}336}$ in C6/36 cells

The virus $V_{334\text{-}336}$ was severely restricted in replication and possibly heat sensitive (Table 4.3), and was serially passaged in C6/36 cells at 28°C. It was

hypothesized that ongoing passaging may select a reversion or second site mutation that enabled this virus to replicate more efficiently.

An aliquot of virus was passaged up to 11 times in C6/36 cells (see section 4.2.14 for method details). The cells were maintained at 28°C for five days at each passage (or until cell monolayers exhibited extensive CPE). On day five of passage number seven, cells infected with $V_{334\text{-}336}$ exhibited low levels of CPE. Over the next three passages, the onset of CPE was more rapid, and the levels of CPE increased until passage number ten. The titre of virus in the supernatant was determined for several passages (Table 4.4).

To detect one or more mutations that may be restoring virus replication, initial RT-PCR and sequencing directly across the site mutated showed it had not reverted during passaging Then, further sequencing of nucleotides 4132 (in NS2B) to 6375 (in NS3) of $V_{334\text{-}336}$ passage 10 virus was performed to look for potential suppressor mutations.

An A to G nucleotide change was observed in NS2B at position 4573, which resulted in a Ile to Met amino acid change. This amino acid residue is not located within the 40 amino acid hydrophilic region of NS2B shown to be important for NS2B/3 interactions.

4.4 Discussion

Ten sites distributed through the helicase region of DEN-2 NS3 were mutated in these experiments. Four were located in enzyme motifs, and a further six that were rich in charged amino acids were altered by charged-to-alanine mutagenesis of three residues (Fig. 4.3).

4.4.1 NS3-mediated ATPase and RNA helicase activity

Ten mutant proteins were synthesized in *E. coli* and tested *in vitro* for their effects on ATPase and RNA helicase activities. The ATPase activity of the parental protein G2 was stimulated only modestly by poly(A) in these experiments. The increase in k_{cat}/K_m was 1.45 fold, corresponding to an increase in V_{max} of 1.25 fold. This was in contrast to the results obtained by Li *et al.* (1999) who showed a 9.7 fold increase in V_{max} for a DEN-2 NS3 in the presence of poly(A), using a protein with a similar amino terminal truncation but containing a carboxy terminal His tag rather than the much larger amino terminal GST tag of these experiments. Other significant differences in NTPase activities among NS3 proteins in the presence of polynucleotides have also been described (Borowski *et al.*, 2001; Kuo *et al.*, 1996; Suzich *et al.*, 1993; Tamura *et al.*, 1993; Warrener *et al.*, 1993). The reasons for the differences have not been identified, but probably reflect variation in the types, sizes and locations of fused peptides, the degree of truncation of the enzymes, the methods of expression (e.g. in bacteria, insect or mammalian cells), the purification procedures, and the assay conditions.

Truncated NS3 synthesized as an amino terminal GST fusion remained largely soluble and was functional as an ATPase and RNA helicase. Enzymatic activity was absent/minimal for GST expressed in *E.coli* from pGEX-3X. This implied that these activities were authentic functions of NS3 and not those of an *E. coli* derived contaminant.

Previous research has focused on either the helicase motifs or the amino acid residues external to helicase motifs predicted to interact with single stranded nucleic acids. The findings were related to the proposed mechanism of ATPase and helicase

activities (Grassmann *et al.*, 1999; Gu *et al.*, 2000; Kim *et al.*, 1998; Lin & Kim, 1999; Min *et al.*, 1999; Paolini *et al.*, 2000*b*; Utama *et al.*, 2000*a*; Wardell *et al.*, 1999). The majority of these mutations were of HCV NS3, and were only tested in *in vitro* assays due to a lack of tissue culture systems permisssive of HCV replication.

In these experiments, both ATPase and helicase activity were tested *in vitro*. Five patterns of activity were observed and they are discussed in turn below: (i) no ATPase and no helicase, (ii) enhanced ATPase and enhanced helicase, (iii) reduced ATPase and no helicase, (iv) reduced ATPase and reduced helicase and (v) reduced ATPase and enhanced helicase.

(i) No ATPase and no helicase. Only two of the ten mutant fusion proteins assayed for enzymatic activity in this study lacked both *in vitro* ATPase and RNA helicase activities. They contained a substitution of the invariant G_{198} or K_{199} residue in the NTP-binding motif I. Substitution of the residue corresponding to K_{199} in BVDV and HCV was previously shown to greatly reduce ATPase and RNA helicase activities (Gu *et al.*, 2000; Heilek & Peterson, 1997; Kim *et al.*, 1997*b*; Min *et al.*, 1999; Wardell *et al.*, 1999).

(ii) Enhanced ATPase and enhanced helicase. All six proteins with charged-to-alanine mutations had ATPase activity. Of these, four proteins $G_{169\text{-}173}$, $G_{179\text{-}181}$, $G_{184\text{-}186}$ and $G_{436\text{-}439}$ were more active than parental G2 (Fig. 4.17). Increased ATPase corresponded to increased helicase activity (Fig. 4.19). Previous studies have also shown enhanced NTPase activity for some flavivirus and poxvirus enzyme mutants. Li *et al.* (1999) generated a DEN-2 NS3 mutant $Q_{184}NGN_{187}$, comparable to the $R_{184}KRK_{187}$ mutant, and demonstrated that it had a 2-fold increase in ATPase activity in the absence of poly(A). Substitution of the conserved His residue of motif II with Ala in NS3 of HCV and JEV, and in the NPH-II of *Vaccinia virus*, also caused an

increase in NTPase activity in the absence of poly(A) compared with parental protein (Gross & Shuman, 1995; Heilek & Peterson, 1997; Utama *et al.*, 2000*a*).

(iii) Reduced ATPase and no helicase. In this study, the motif VI mutant $G_{R457A,R458A}$ and the charged-to-alanine mutant $G_{376\text{-}380}$ had reduced ATPase activity and no helicase activity, identifying two regions required for coupling of the two activities. The role of the Arg residues of motif VI have been examined in *Vaccinia virus* NPH-II and HCV NS3 helicases. In the X-ray crystal structure of the related HCV NS3 helicase of Kim *et al.* (1998), residues in motif VI are located in the cleft between domains one and two. The first Arg (R_{457} in DEN-2) points away from the cleft and is hydrogen bonded to HCV D_{412} and D_{427} (Kim *et al.*, 1998). Mutation of this first Arg residue in NPH-II and HCV helicase leads to a decrease in RNA binding (Gross & Shuman, 1996*a*; Kim *et al.*, 1997*b*), possibly as a consequence of an alteration in the conformation of D_{412} which lines the RNA binding channel in HCV (Kim *et al.*, 1998). An alternative explanation is provided by Chang *et al.* (2000) who demonstrated by mutagenesis that for HCV only the second Arg (R_{458} in DEN-2) is involved in RNA binding. Thus by comparison with these viruses, the lack of detectable helicase activity of the $G_{R457A,R458A}$ double mutant protein was probably due to inhibition of RNA binding. In contrast to $G_{R457A,R458A}$, mutagenesis of the region corresponding to $G_{376\text{-}380}$ has not been reported, and analysis of the HCV structure at this location provides no understanding on the role of these residues in enzyme activity. However, the substitution of basic residues by Ala may also have an adverse effect on RNA binding. Recent structure based mutagenesis of HCV NS3 helicase demonstrated that substitution with Ala of several residues (external to helicase motifs) proposed to interact with RNA based on an X-ray crystal structure of

a binary complex of the HCV helicase with a $(dU)_8$ oligonucleotide, also uncoupled the two enzyme activities (Lin & Kim, 1999).

(iv) Reduced ATPase and reduced helicase. The remaining charged-to-alanine mutant $G_{334\text{-}336}$ showed reduced levels of both ATPase and RNA helicase activities.

(v) Reduced ATPase and enhanced helicase. The only protein which demonstrated reduced ATPase activity and increased helicase activity with respect to parental G2 was the motif II mutant G_{M283F}. The mutation in this protein was of particular interest because the residue at this position (Met in DEN-2 motif II L_{280}IIMDEAH$_{287}$) (Koonin & Dolja, 1993), adjacent to the invariant acid residues D_{284} and E_{285}, has not been previously mutated for any virus. Phe commonly occurs at this position in positive strand viruses (Koonin & Dolja, 1993). Analysis of the HCV NS3 crystal structure indicates that the adjoining Asp and Glu residues potentially interact with the bound ATP γ phosphate and amino acid residues in motif I via Mg^{2+} binding (Kim *et al.*, 1998) and both residues are required for NTPase and helicase activities (Utama *et al.*, 2000*a*; Wardell *et al.*, 1999). However, the reason for the increased helicase activity observed in this study is unknown. Analysis of the HCV helicase structure demonstrates that the residue equivalent to DEN-2 M_{283} is buried within the secondary structure, suggesting that it is not directly involved in ATPase or helicase activity (J. C. Whisstock, personal communication).

4.4.2 Virus production

With the availability of genomic length cDNA, the effect on virus replication of nine mutations modifying ATPase and helicase activity *in vitro* was tested. As

described above, the mutations produced five patterns of enzyme activity *in vitro*, and their effects on replication were of considerable interest. The introduction of helicase mutations into viral genomes has been reported for only one positive strand RNA virus, BVDV (Gu *et al.*, 2000). For BVDV, three mutations, two point mutations in motifs I and II and a deletion mutant in motif VI, abolished helicase activity and virus replication (Gu *et al.*, 2000). Likewise for DEN-2, the mutations in motifs I (K199A) and VI (R457A,R458A) that abolished helicase activity also prevented virus replication. In addition, the charged-to-alanine mutation at $R_{376}KNGK_{380}$ in DEN-2 NS3 also stopped helicase activity and virus replication. Thus for both these members of the family *Flaviviridae*, lack of helicase *in vitro* correlated directly with no detectable virus replication.

On the other hand, mutations permitting helicase activity *in vitro* did not necessarily permit virus replication. There were four mutations that allowed replication i.e. $E_{169}KSIE_{173}$, $E_{179}DD_{181}$, M283F and $D_{334}EE_{336}$ (although with smaller plaque phenotype and in two instances temperature sensitivity), and two that did not i.e. $R_{184}KR_{186}$ and $D_{436}GEE_{439}$. With the exception of M283F (motif II mutant), these mutations were all of the charged-to-alanine type and therefore likely to be located on the surface of NS3 and involved in protein-protein or RNA-protein interactions (Alber, 1989; Diamond & Kirkegaard, 1994). NS3 has been identified in NS3/NS5 complexes (Chen *et al.*, 1997*a*; Kapoor *et al.*, 1995) and associated with the nonstructural proteins NS1, NS2A, NS4A and NS5 in replication complexes (Khromykh *et al.*, 1999*a*; Khromykh *et al.*, 1999*b*; Mackenzie *et al.*, 1998; Westaway *et al.*, 1997*b*). It is therefore likely that subtle or substantial changes in these interactions led to the observed range of phenotypes. In particular, the charged residues at $R_{184}KR_{186}$, $D_{334}EE_{336}$, and $D_{436}GEE_{439}$ are worthy of further investigation.

Less severe mutagenesis of these sites would establish the relative contribution of individual residues to enzyme activity and virus replication. Additional experiments which may assist in determining the roles of residues, are binding assays *in vitro* for analysis of protein-protein and RNA-protein interactions (Cui *et al.*, 1998). Since the hydrophilicity profiles of proteins specified by viruses within the genus *Flavivirus* are highly conserved (Westaway & Blok, 1997), the results obtained using DEN-2 would be potentially applicable across the genus.

Upon serial passage, virus $V_{334\text{-}336}$ showed evidence of improved replication (CPE) by passage number seven (Table 4.4). The high passage virus stock was sequenced across the NS2B and NS3 regions, and a second-site change was discovered in NS2B. Although not located within the predicted 40 amino acid region required for NS2B-NS3 interaction and proteinase activity, this residue may be involved in this or other protein-protein interactions, and therefore have an effect on proteinase activity or even other replicative requirements. An X-ray crystal structure of the complex of full-length NS2B-NS3 (currently not available) would also help to determine the role of both the original NS3 mutation and the second-site NS2B change in protein-protein interactions and possibly enzymatic function.

Further sequencing of the remainder of the genome would also be required to determine whether there were any other changes introduced during passaging which may have contributed to the improved replication of this mutant. The original $V_{334\text{-}336}$ low passage virus would also need to be fully sequenced to ensure that any additional second-site changes are unique to the high passage virus stock (the entire NS2B region of the low passage $V_{334\text{-}336}$ virus stock was sequenced and the second-site NS2B change was not present). The high passage $V_{334\text{-}336}$ virus stock may be further characterized by analysis of any altered replicative properties in C6/36 or BHK-21

cells. The incorporation of the second-site NS2B change into genomic length DEN-2 cDNA both with and without the original NS3 mutation would also enable analysis of the contribution of the second-site mutation to the restoration of parental levels of virus replication.

There was limited success in producing *ts* mutants by charged-to-alanine mutagenesis. Here one potential mutant ($V_{334\text{-}336}$) was obtained after mutagenesis of six different sites however, this virus replicated too poorly for further studies (Table 4.3). Only one *ts* mutant produced by this technique has been reported for the flaviviruses, in NS1 of YFV (Muylaert *et al.*, 1997). However, a *ts* mutant, V_{M283F}, with the M283F substitution in motif II was produced. As noted above for the hydrophilicity profiles, the conservation of the sequence MDEAH in motif II suggests the results with V_{M283F} may hold for other flaviviruses. The data shown in Fig. 4.22B demonstrated that cells infected with this virus were defective in RNA synthesis at the non-permissive temperature (37°C). Further experiments would be required to determine the basis of this defect.

4.5 Concluding remarks

This study identified residues in the NS3 helicase region of DEN-2 within and outside motifs that modify enzyme activities *in vitro* and alter virus phenotype. Mutations that abolished helicase but not ATPase activity were identified. In some instances enhancement of enzyme activities was observed. Absence of helicase activity *in vitro* correlated directly with lack of virus replication. Substitutions to conserved motifs were more disruptive to ATPase and helicase activities *in vitro* than changes at hydrophilic sites by charged-to-alanine mutagenesis. Of the nine mutant

viruses tested, five were lethal (Table 4.3), reflecting the importance of NS3 in viral replication. The mutations contained within the four viruses which did replicate may be suitable for incorporation into growth-restricted vaccine strains. It may be possible to enhance the yield of $V_{334\text{-}336}$ by reducing the number of charged residues changed to Ala in the sequence $D_{334}EE_{336}$ while retaining some growth restriction and a small plaque phenotype.

The results demonstrate that mutagenesis in the helicase region or perhaps in other nonstructural proteins has potential for obtaining growth-restricted and *ts* viruses of other flavivirus species. In our studies with DEN-2 NS3, we recovered infectious virus for 50% of charged-to-alanine mutants tested. Comparisons of the deduced amino acid sequences of flaviviruses show high conservation of hydrophilicity and hydrophobicity across the viral polyprotein, regardless of considerable variation in primary sequence (Westaway & Blok, 1997), and thus it may be possible to extend these results to the other dengue serotypes and encephalitic flaviviruses. The mutations that were introduced here required multiple nucleotide and codon changes. In theory, multiple changes reduce the risk of reversion to parental phenotype when introduced into a potential vaccine strain.

The continued analysis of the biological role of the NS3 helicase in viral replication will aid in the development of anti-viral compounds which may inhibit (i) NTP binding, (ii) RNA binding, (iii) the coupling of NTPase and RNA helicase activities, (iv) inhibition of the translocation of the helicase along the polynucleotide, or (v) block protein-protein interactions within the replication complex, and also expand our understanding of the role of the NS3 RNA unwinding function in the virus life cycle.

Fig. 4.1 Alignment of several NS3 helicase amino acid sequences and mutations introduced into DEN-2 NS3. Dots stand for identical amino acid residues while dashes represent gaps introduced to allow maximal identity. The seven helicase motifs (I-VI) are shown as pink boxes. Each of the ten mutations is colour coded, and each colour will be used throughout the chapter to designate a particular mutant virus. Residues at four sites within motifs I, II and VI were substituted, in addition to six sites outside motifs. The position of amino acids within DEN-2 NS3 are shown above the sequence. The same virus GenBank accession numbers were used for this NS3 helicase alignment as for the NS2B alignment (Fig. 1.2).

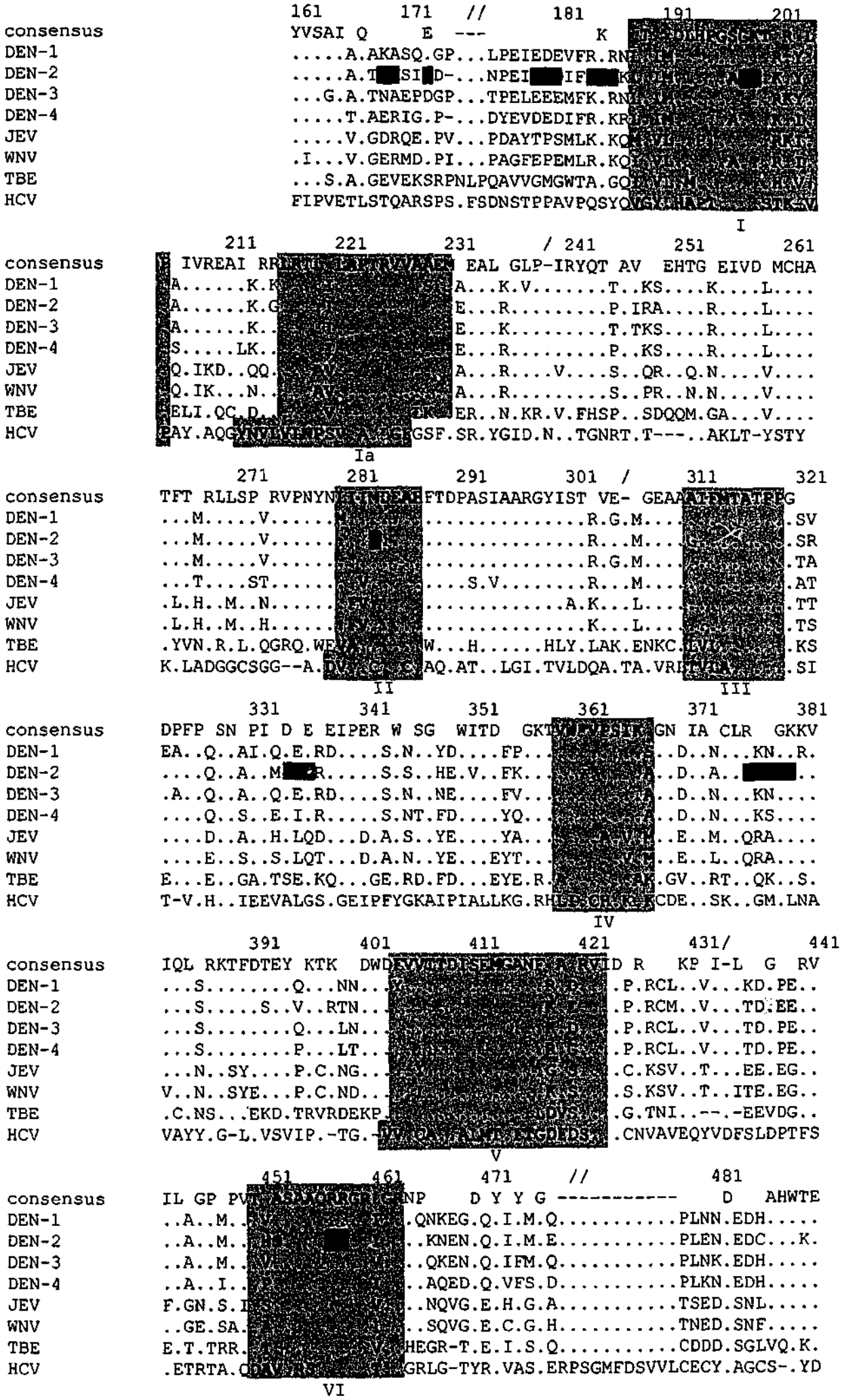
161 171 // 181 191 201
consensus YVSAI Q E --- K
DEN-1 .....A.AKASQ.GP...LPEIEDEVFR.RN
DEN-2 .....A.T SI D-...NPEI IF K
DEN-3 ...G.A.TNAEPDGP...TPELEEEMFK.RN
DEN-4 .....T.AERIG.P-...DYEVDEDIFR.KR
JEV .....V.GDRQE.PV...PDAYTPSMLK.KQ
WNV .I...V.GERMD.PI...PAGFEPEMLR.KQ
TBE ...S.A.GEVEKSRPNLPQAVVGMGWTA.GQ
HCV FIPVETLSTQARSPS.FSDNSTPPAVPQSYQ
I
211 221 231 / 241 251 261
consensus IVREAI RR EAL GLP-IRYQT AV EHTG EIVD MCHA
DEN-1 A.....K.K A...K.V.....T..KS....K....L....
DEN-2 A.....K.G E...R.....P.IRA....R....L....
DEN-3 A.....K.. E...K.....T.TKS....R....L....
DEN-4 S.....LK.. E...R.....P..KS....R....L....
JEV Q.IKD..QQ. A...R....V....S..QR..Q.N....V....
WNV Q.IK...N.. A...R.....S..PR..N.N....V....
TBE ELI.QC.D. ER..N.KR.V.FHSP..SDQQM.GA...V....
HCV PAY.AQG GSF.SR.YGID.N..TGNRT.T---..AKLT-YSTY
Ia
271 281 291 301 / 311 321
consensus TFT RLLSP RVPNYN FTDPASIAARGYIST VE- GEA
DEN-1 ...M.....V..... .....R.G.M.....SV
DEN-2 ...M.....V..... .....R...M.....SR
DEN-3 ...M.....V..... .....R.G.M.....TA
DEN-4 ...T....ST..... ....S.V.....R...M.....AT
JEV .L.H..M..N..... .....A.K...L.....TT
WNV .L.H..M..H..... .....K...L.....TS
TBE .YVN.R.L.QGRQ.WF W...H.....HLY.LAK.ENKC.....KS
HCV K.LADGGCSGG--A.DV AQ.AT..LGI.TVLDQA.TA.VR.....SI
II III
331 341 351 361 371 381
consensus DPFP SN PI D E EIPER W SG WITD GK GN IA CLR GKKV
DEN-1 EA..Q..AI.Q.E.RD....S.N..YD....FP.....D..N...KN..R.
DEN-2 ....Q..A..M R.....S.S..HE.V..FK.....D..A.. ..
DEN-3 .A..Q..A..Q.E.RD....S.N..NE....FV.....D..N...KN....
DEN-4 ....Q..S..E.I.R.....S.NT.FD....YQ.....D..N...KS....
JEV ....D..A..H.LQD...D.A.S..YE....YA.....E..M..QRA....
WNV ....E..S..S.LQT...D.A.N..YE...EYT.....E..L..QRA....
TBE E...E..GA.TSE.KQ...GE.RD.FD...EYE.R.....GV..RT..QK..S.
HCV T-V.H..IEEVALGS.GEIPFYGKAIPIALLKG.RH CDE..SK..GM.LNA
IV
391 401 411 421 431/ 441
consensus IQL RKTFDTEY KTK DWD R KP I-L G RV
DEN-1 ...S.....Q...NN.. .P.RCL..V...KD.PE..
DEN-2 ...S.....S..V..RTN.. .P.RCM..V...TD.EE..
DEN-3 ...S.....Q...LN.. .P.RCL..V...TD.PE..
DEN-4 ...S.....P...LT.. .P.RCL..V...TD.PE..
JEV ...N..SY....P.C.NG.. .C.KSV..T...EE.EG..
WNV V..N..SYE...P.C.ND.. .S.KSV..T..ITE.EG..
TBE .C.NS...EKD.TRVRDEKP .G.TNI..--.-EEVDG..
HCV VAYY.G-L.VSVIP.-TG. .CNVAVEQYVDFSLDPTFS
V
451 461 471 // 481
consensus IL GP PV NP D Y Y G ---------- D AHWTE
DEN-1 ..A..M..V .QNKEG.Q.I.M.Q.....PLNN.EDH.....
DEN-2 ..A..M..H ..KNEN.Q.I.M.E.....PLEN.EDC...K.
DEN-3 ..A..M..V ..QKEN.Q.IFM.Q.....PLNK.EDH.....
DEN-4 ..A..I..T ..AQED.Q.VFS.D.....PLKN.EDH.....
JEV F.GN.S.I ..NQVG.E.H.G.A.....TSED.SNL.....
WNV ..GE.SA. ..SQVG.E.C.G.H.....TNED.SNF.....
TBE E.T.TRR. HEGR-T.E.I.S.Q.....CDDD.SGLVQ.K.
HCV .ETRTA.Q GRLG-TYR.VAS.ERPSGMFDSVVLCECY.AGCS-.YD
VI

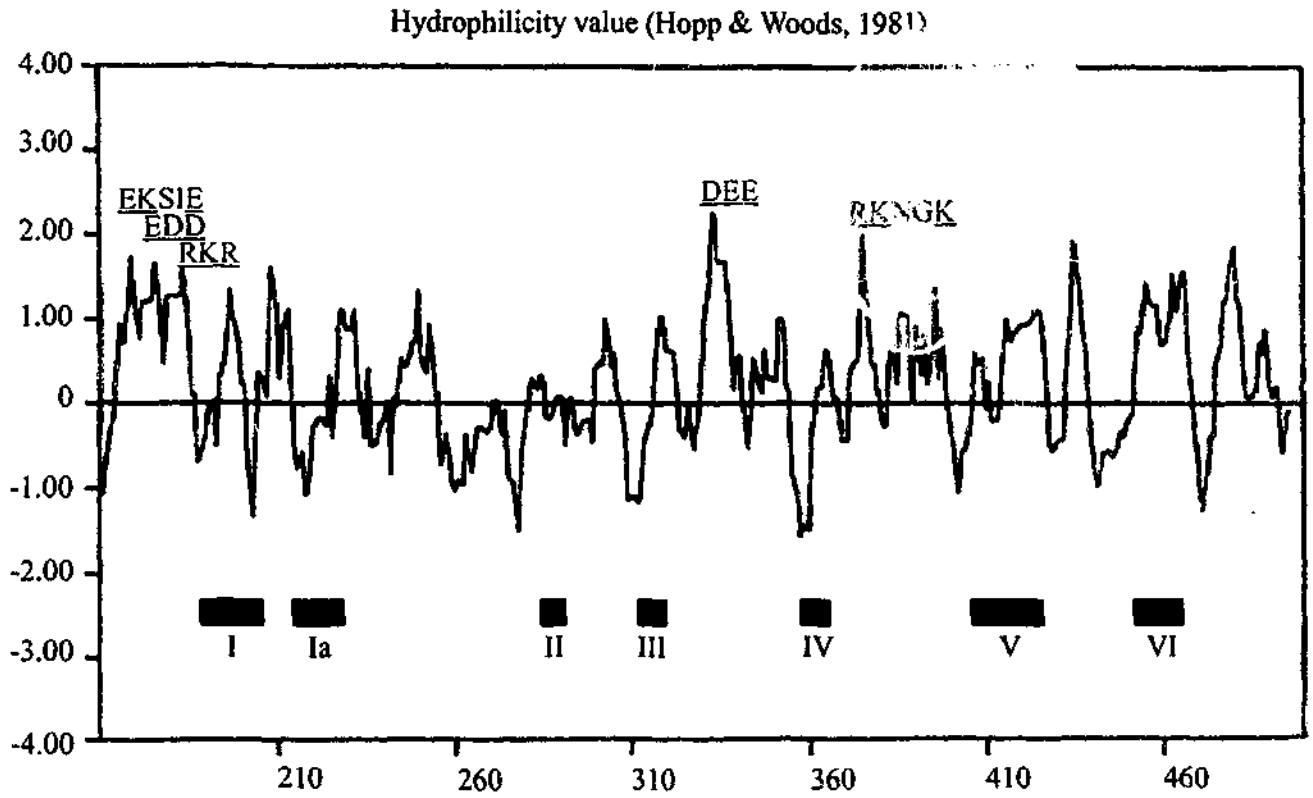

Fig. 4.2 Hydrophilicity plot of the central helicase region of NS3. The positions of the seven helicase motifs and the five hydrophilic regions mutated are shown. The underlined residues were mutated to Ala. Amino acid numbers within NS3 are shown below the plot.

Fig. 4.3 Constructs used to synthesize NS3 fusion proteins and prepare mutated viruses. The seven helicase motifs are shaded (Koonin & Dolja, 1993); residue numbers within NS3 are given. On the left are the full (pGX) and abbreviated (G) designations of the truncated NS3 gene constructs in pGEX-3X. The G designations are also used for the corresponding encoded mutant fusion proteins where appropriate. On the right are the names of the plasmids containing genomic-length cDNA (pDVWS) and derived virus (V). Antiserum raised in rabbits against a bacterial fusion protein (Teo and Wright, 1997) was directed against a segment of NS3 (vertical stripes). For clustered charged-to-alanine mutants, the underlined residues were mutated to Ala.

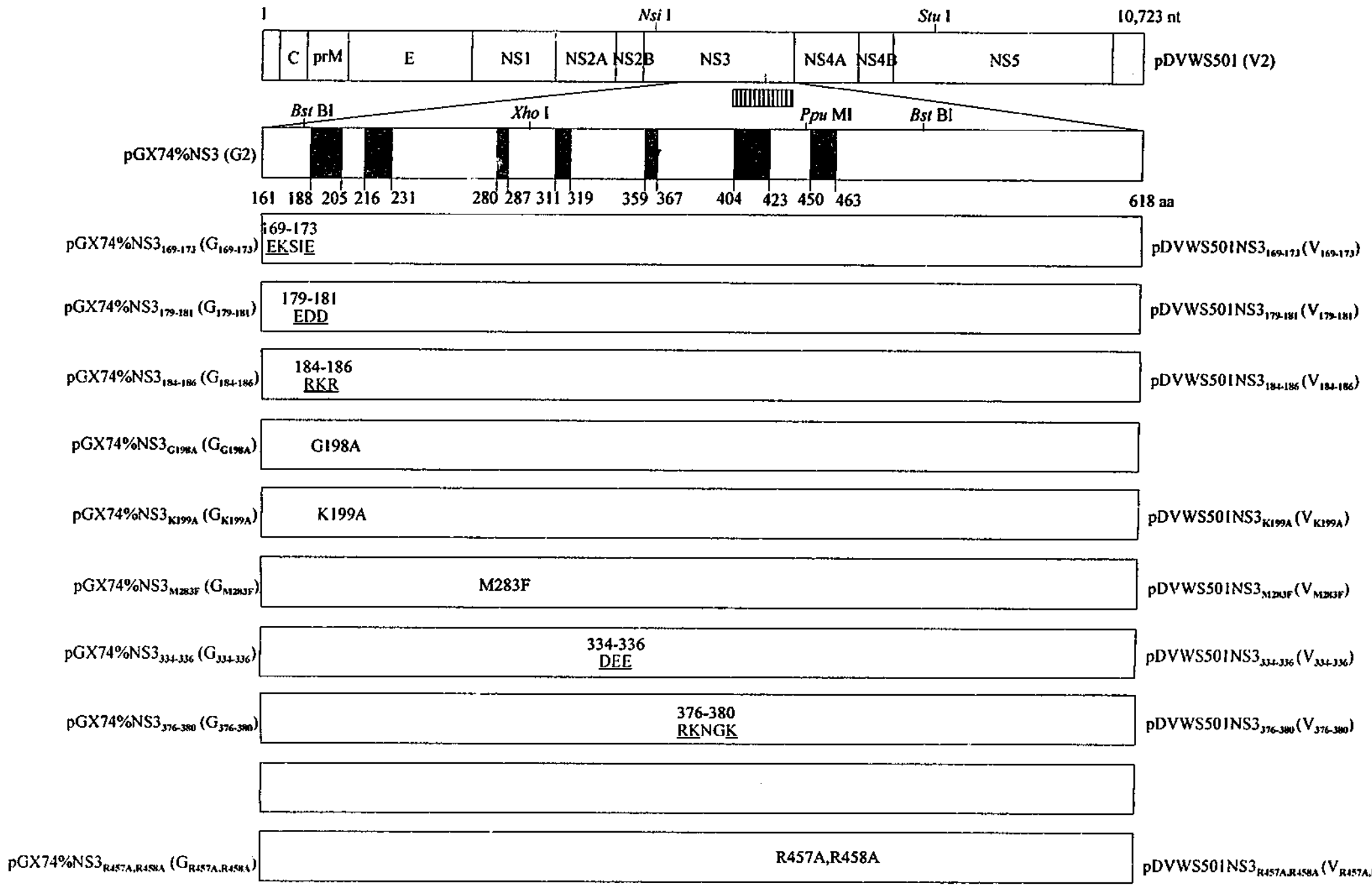
1
Nsi I
Stu I
10,723 nt
C
prM
E
NS1
NS2A
NS2B
NS3
NS4A
NS4B
NS5
pDVWS501 (V2)
Bst BI
Xho I
Ppu MI
Bst BI
pGX74%NS3 (G2)
161 188 205 216 231 280 287 311 319 359 367 404 423 450 463
618 aa
pGX74%NS3169-173 (G169-173)
169-173
EKSIE
pDVWS501NS3169-173(V169-173)
pGX74%NS3179-181 (G179-181)
179-181
EDD
pDVWS501NS3179-181(V179-181)
pGX74%NS3184-186 (G184-186)
184-186
RKR
pDVWS501NS3184-186(V184-186)
pGX74%NS3G198A (GG198A)
G198A
pGX74%NS3K199A (GK199A)
K199A
pDVWS501NS3K199A(VK199A)
pGX74%NS3M283F (GM283F)
M283F
pDVWS501NS3M283F(VM283F)
pGX74%NS3334-336 (G334-336)
334-336
DEE
pDVWS501NS3334-336(V334-336)
pGX74%NS3376-380 (G376-380)
376-380
RKNGK
pDVWS501NS3376-380(V376-380)
pGX74%NS3R457A,R458A (GR457A,R458A)
R457A,R458A
pDVWS501NS3R457A,R458A(VR457A,R458A)

A

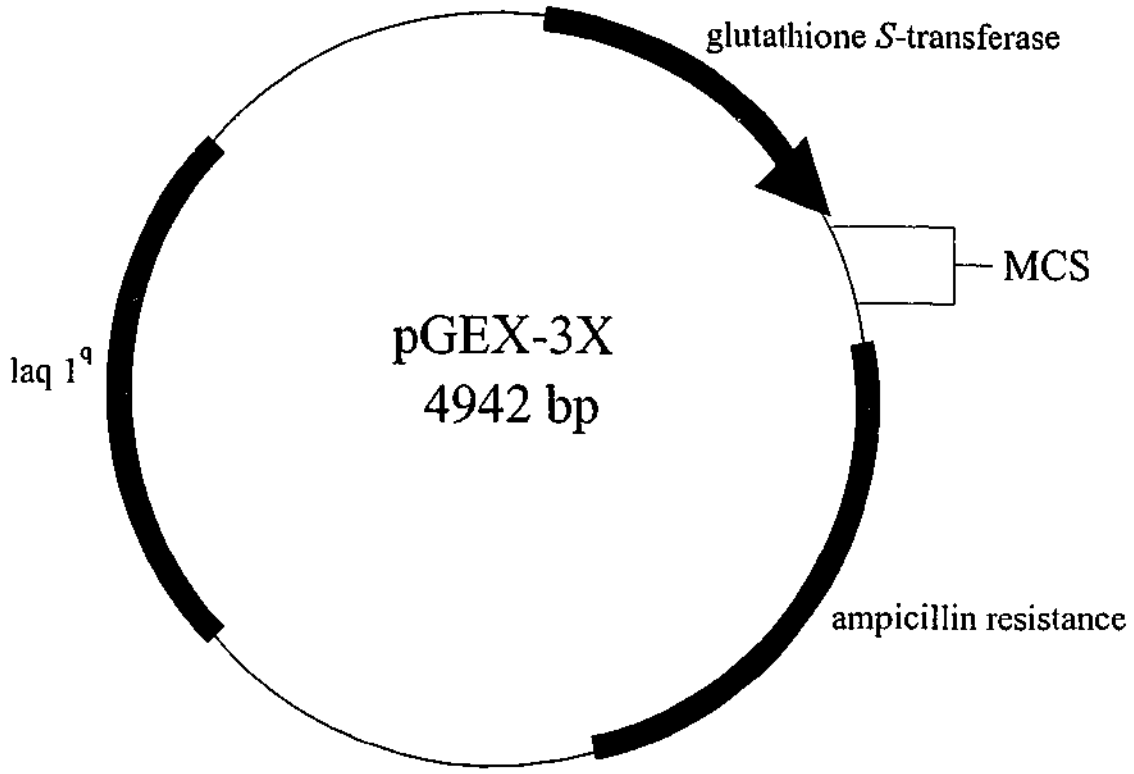

B

Factor Xa

ATC GAA GGT CGT GGG ATC CCC GGG AAT TCA TCG TGA CTG ACT GAC

Bam HI *Sma* I *Eco* RI stop codons

Fig. 4.4 (A) Simplified map of the expression vector pGEX-3X. The multiple cloning site is located immediately downstream of the GST gene enabling the gene of interest to be expressed as a GST fusion protein. (B) Map of the MCS containing the three available stop codons.

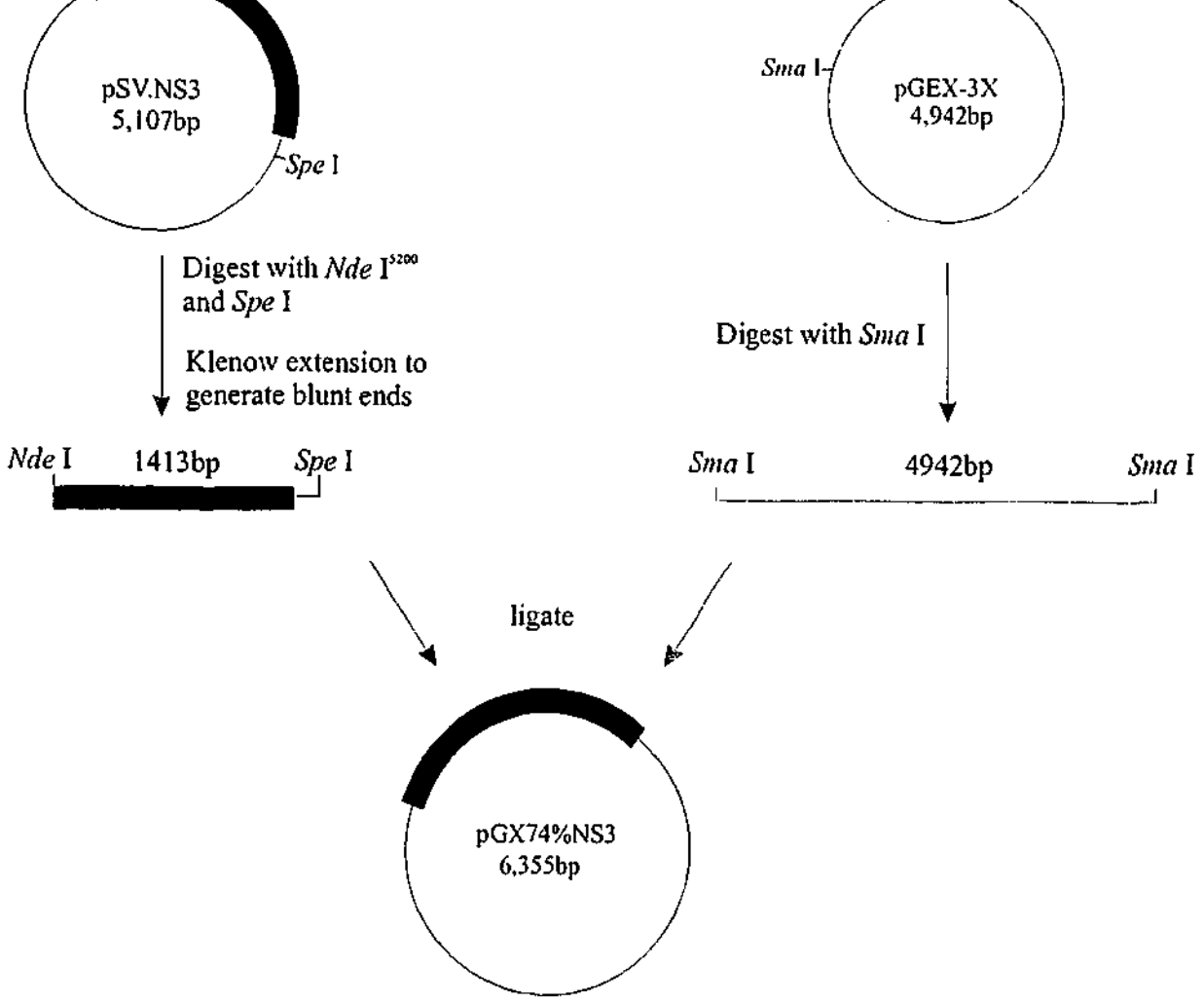

Fig. 4.5 Construction of the plasmid pGX74%NS3. To produce the plasmid pGX74%NS3, a 1413bp *Nde* I^{5200} - *Spe* I fragment was removed from pSV.NS3, recessed ends were filled in using Klenow DNA polymerase I, and the fragment was ligated into *Sma* I digested pGEX-3X. The final construct contained 1373bp of DEN-2 sequence.

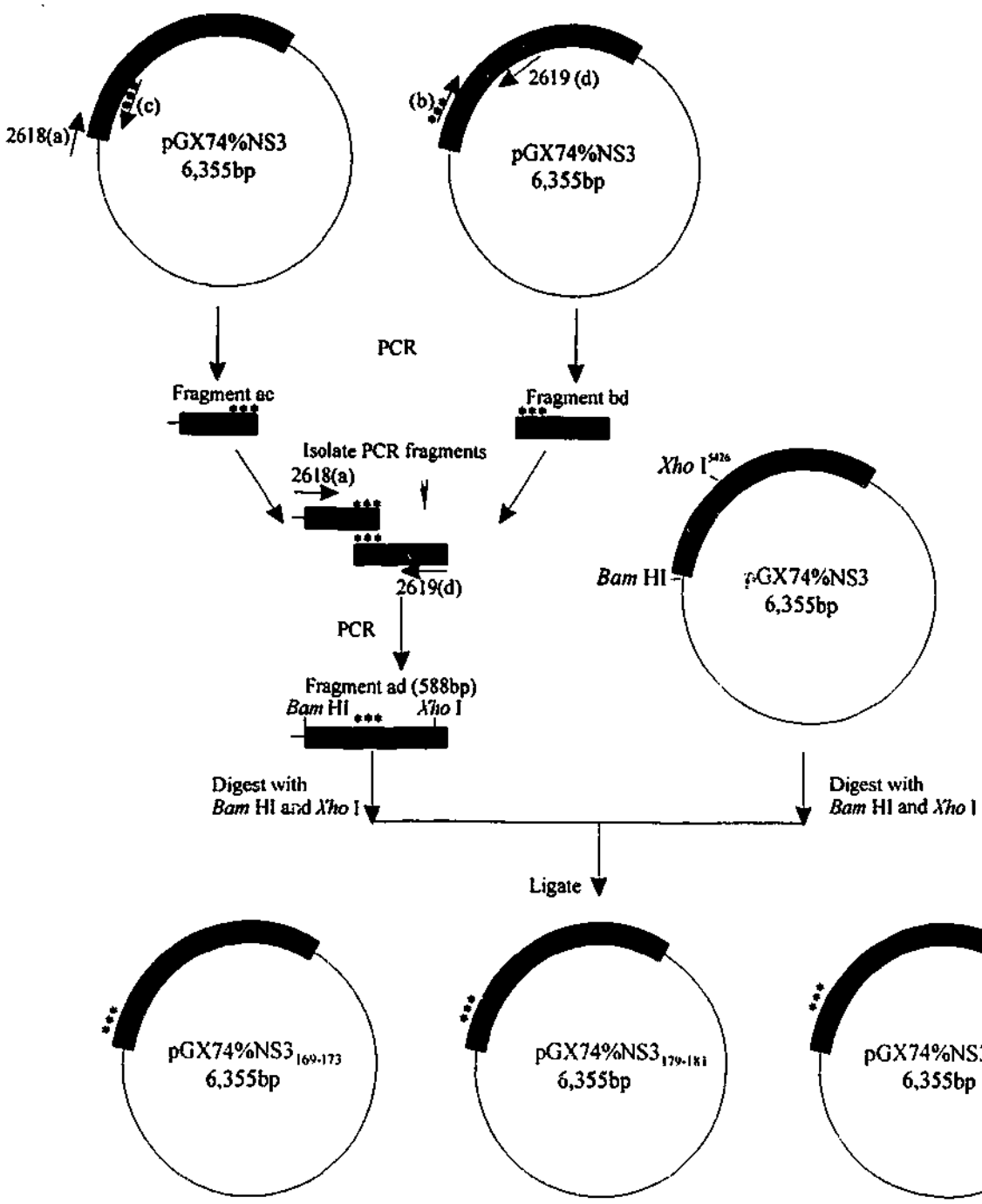

Fig. 4.6 Construction of plasmids pGX74%NS3$_{169\text{-}173}$, pGX74%NS3$_{179\text{-}181}$ and pGX74%NS3$_{184\text{-}186}$. OE-PCR was used to insert the changes $E_{169}KSIE_{173}$ (parental) to $A_{169}ASIA_{173}$ (mutant), $E_{179}DD_{181}$ to $A_{179}AA_{181}$ and $R_{184}KR_{186}$ to $A_{184}AA_{186}$ within NS3. The mutagenic primers used (primers b and c) are listed for each mutant in Table 4.1. Each respective 432bp *Bam* HI- *Xho* I fragment containing the mutation was directly cloned into pGX74%NS3.

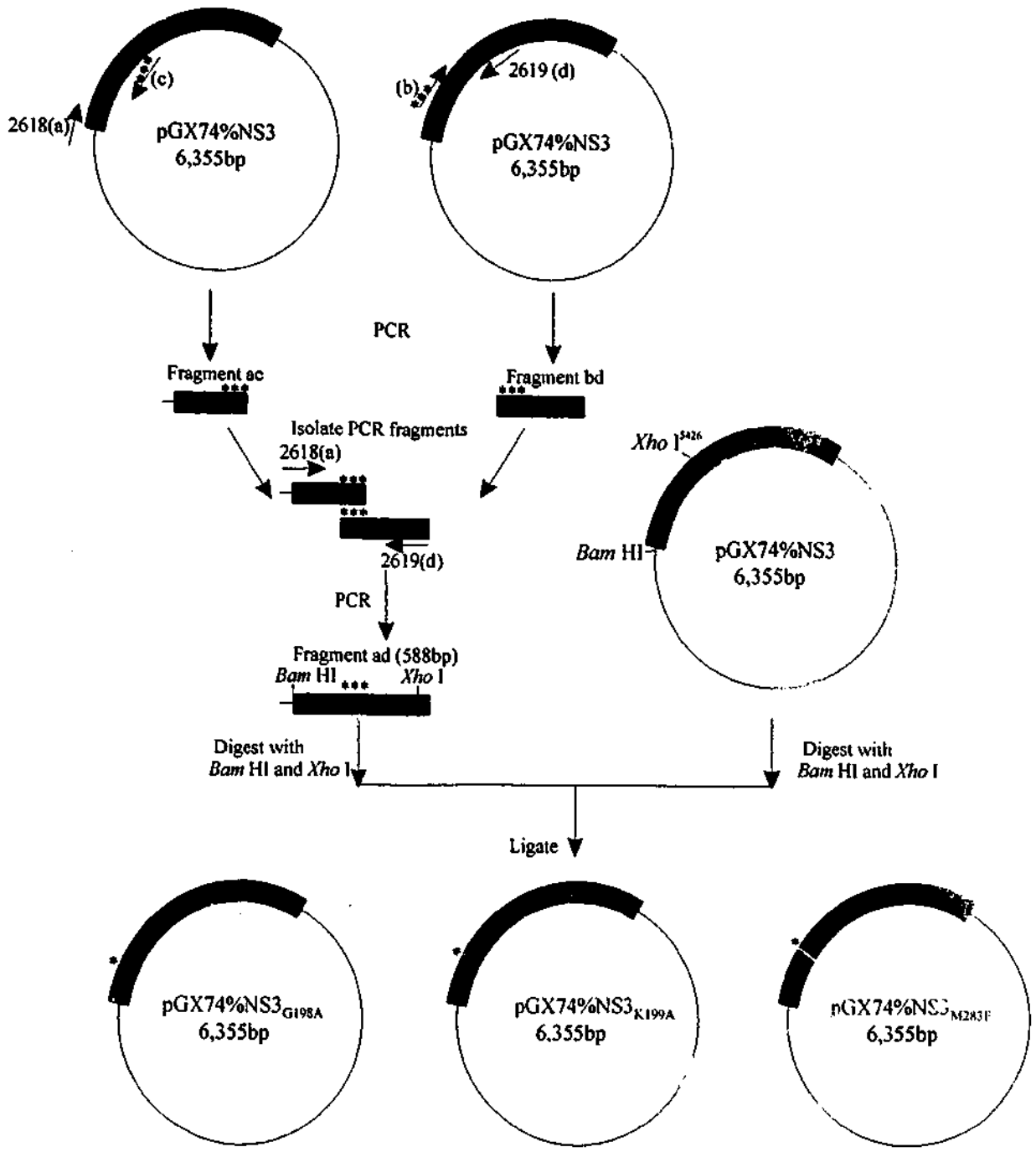

Fig. 4.7 Construction of plasmids pGX74%NS3$_{G198A}$, pGX74%NS3$_{K199A}$ and pGX74%NS3$_{M283F}$. OE-PCR was used to insert the changes within NS3. The mutagenic primers used (primers b and c) are listed for each mutant in Table 4.1. Each respective 432bp *Bam* HI- *Xho* I fragment containing the mutation was directly cloned into pGX74%NS3.

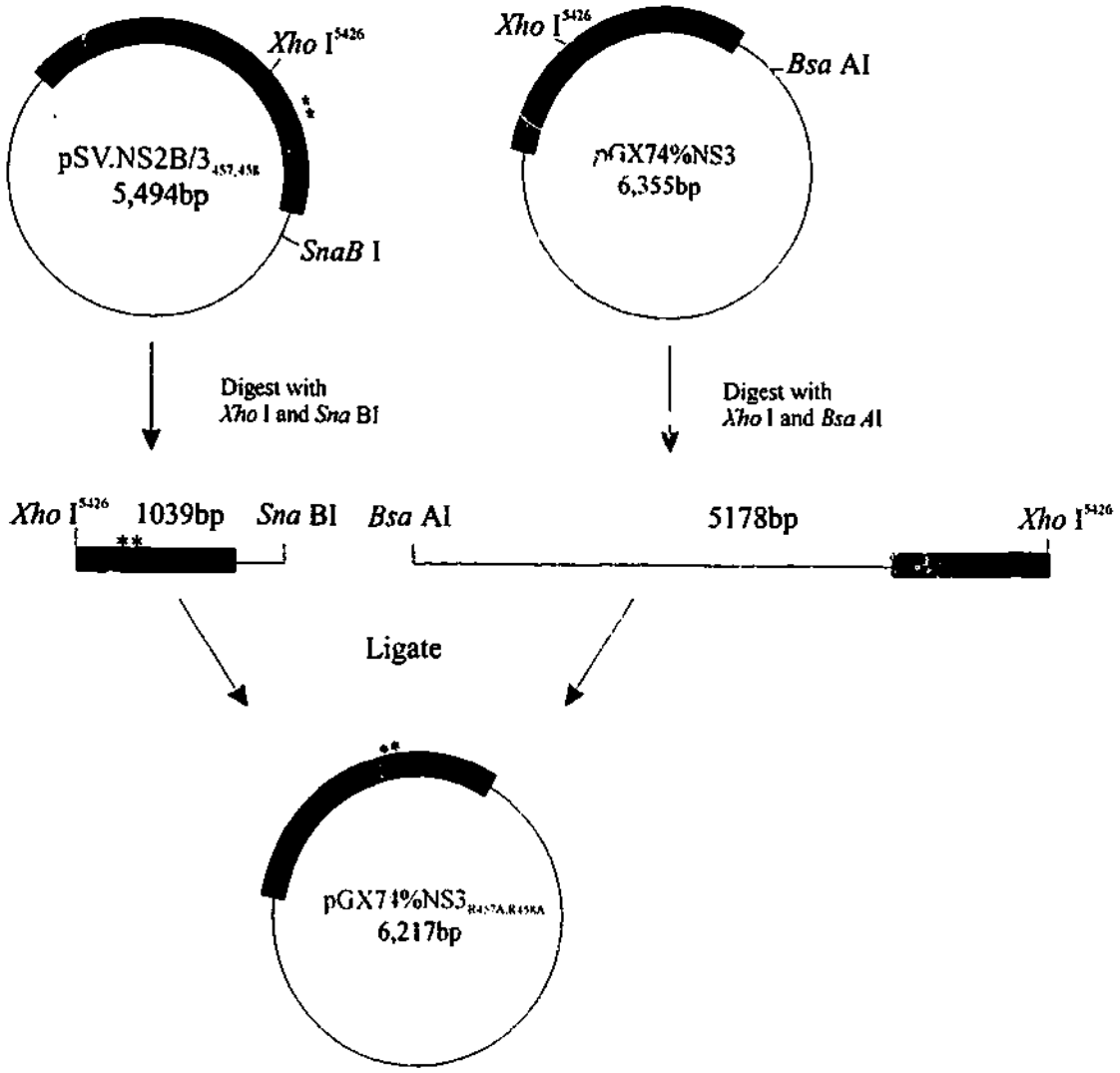

Fig. 4.8 Construction of the plasmid pGX74%NS3$_{R457A,R457A}$. To produce the plasmid pGX74%NS3$_{R457A,R458A}$, a 1039bp *Xho* I^{5426} - *Sna* BI fragment was removed from pSV.NS2B/3 and ligated into pGEX-3X digested *Xho* I^{5426}/*Bsa* AI. Both *Sna* BI and *Bsa* AI restriction enzymes generate blunt ends. The final construct contained 1147bp of DEN-2 sequence.

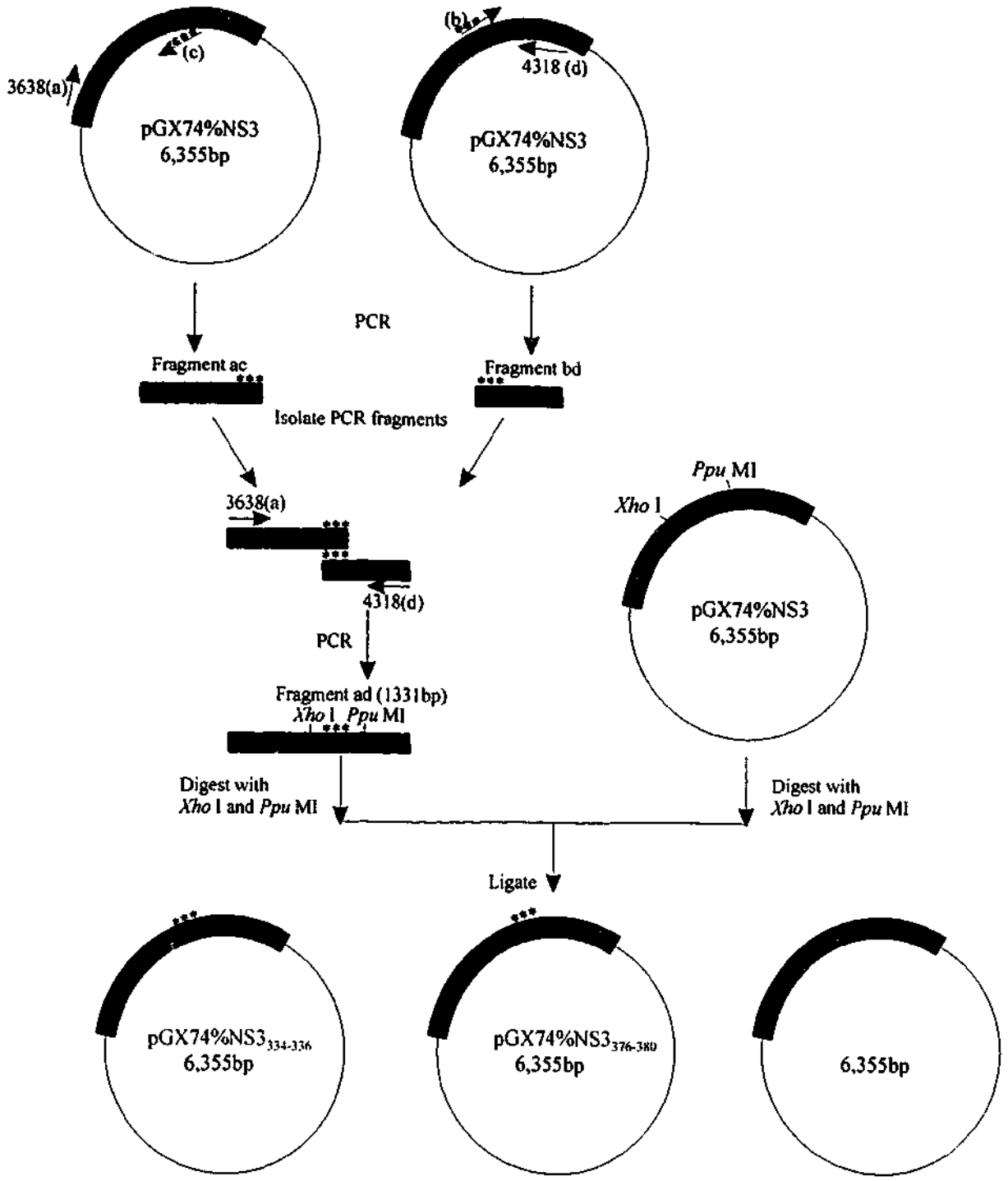

Fig. 4.9 Construction of plasmids pGX74%NS3$_{334\text{-}336}$, pGX74%NS3$_{376\text{-}380}$ and pGX74%NS3$_{436\text{-}439}$. OE-PCR was used to insert the changes $D_{334}EE_{336}$ (parental) to $A_{334}AA_{336}$ (mutant), $R_{376}KNGK_{380}$ to $A_{376}ANGA_{380}$ and $D_{436}GEE_{439}$ to $A_{436}GAA_{439}$ within NS3. The mutagenic primers used (primers b and c) are listed for each mutant in Table 4.1. Each respective 426 bp *Xho* I^{5426}-*Ppu* MI^{5852} fragment containing the mutation was directly cloned into pGX74%NS3.

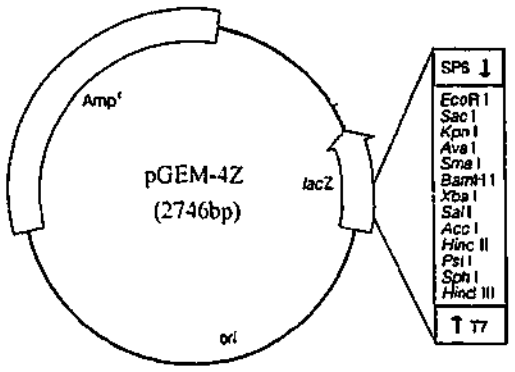

1. Digest with *Eco* RI and *Hind* III
2. Klenow fill-in to produce blunt ends
3. Ligate

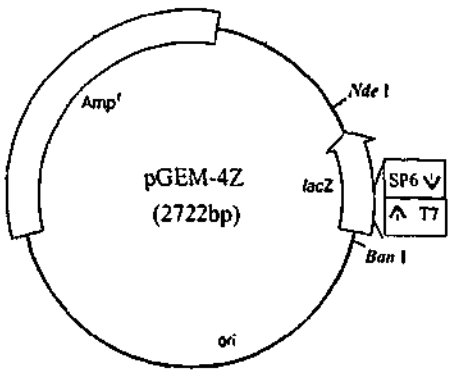

4. Digest with *Nde* I and transcribe with T7 polymerase
OR
4. Digest with *Ban* I and transcribe with SP6 polymerase in the presence of [α^{32}P] ATP
5. Hybridize

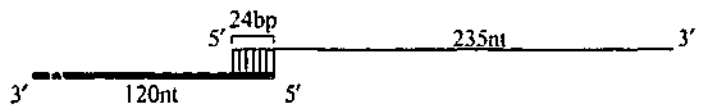

Fig. 4.10 Construction of the 3′-tailed dsRNA substrate. Initially the plasmid pGEM-4ZΔ24 was constructed by digestion of the plasmid pGEM-4Z with *Eco* RI and *Hind* III. The resultant plasmid was then used for *in vitro* transcriptions to produce RNA for subseqent hybridization.

Fig. 4.11 Construction of the plasmid, pDVWS501NS3$_{184\text{-}186}$. Initially, a 1356bp OE-PCR fragment containing the mutation (as indicated by the asterisks) was digested with *Nsi* I and *Ppu* MI and the resulting 1152bp mutated fragment was ligated into *Nsi* I/*Ppu* MI-digested pDVSO8298. To produce the plasmid pDVWS501NS3$_{184\text{-}186}$, a 3174bp *Nsi* I – *Stu* I fragment was removed from pDVSO8298$_{184\text{-}186}$ and ligated into *Nsi* I^{4700}/*Stu* I^{7874}-digested pDVWS501.

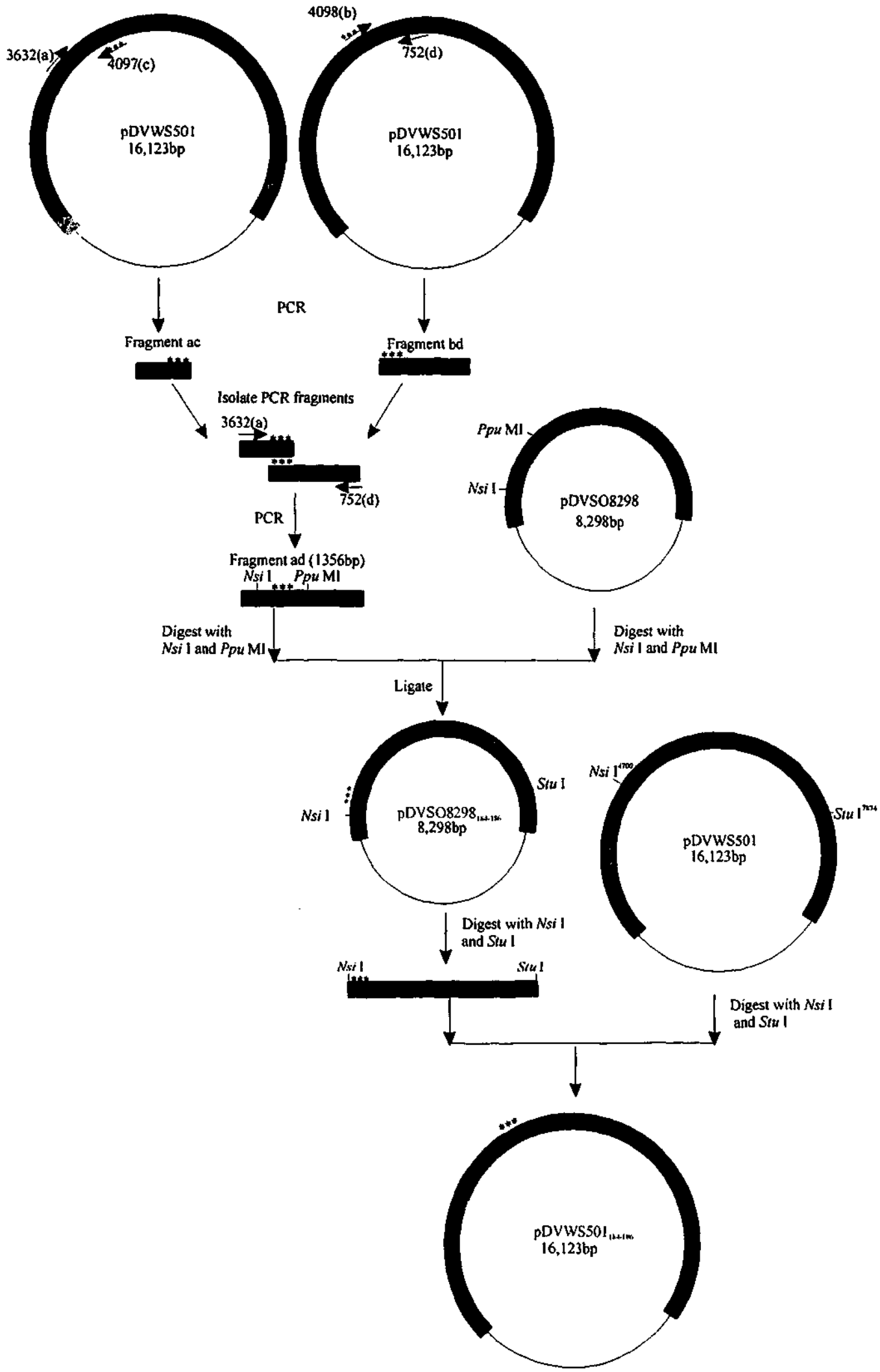
4098(b)
3632(a)
4097(c)
752(d)
pDVWS501
16,123bp
pDVWS501
16,123bp
PCR
Fragment ac
Fragment bd
Isolate PCR fragments
3632(a)
752(d)
PCR
Fragment ad (1356bp)
Nsi I
Ppu MI
Ppu MI
Nsi I
pDVSO8298
8,298bp
Digest with
Nsi I and Ppu MI
Digest with
Nsi I and Ppu MI
Ligate
Stu I
Nsi I
pDVSO8298
8,298bp
Nsi I
Stu I
pDVWS501
16,123bp
Digest with Nsi I
and Stu I
Nsi I
Stu I
Digest with Nsi I
and Stu I
pDVWS501
16,123bp

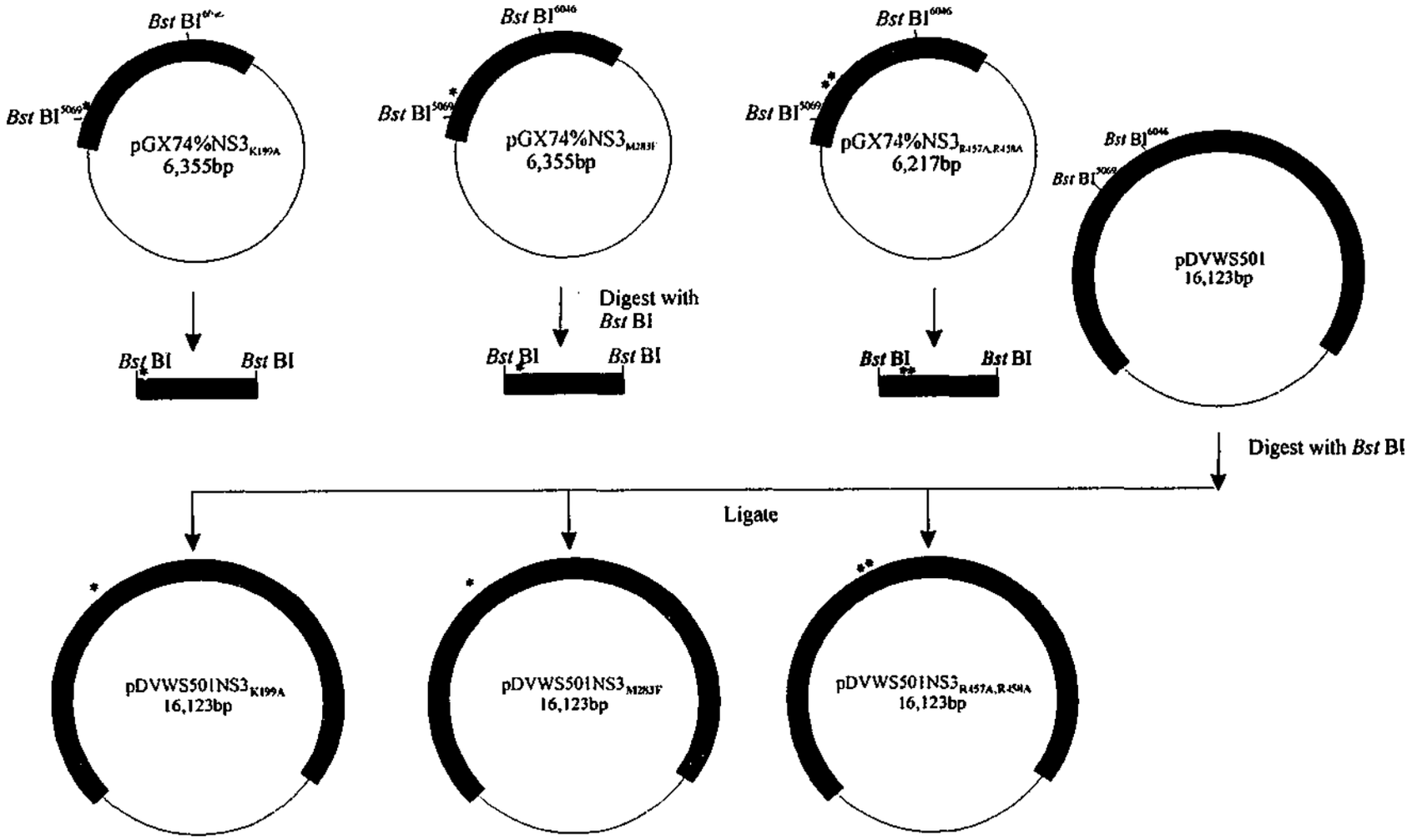

Fig. 4.12 Construction of plasmids pDVWS501$_{K199A,}$ pDVWS501NS3$_{M283F}$ and pDVWS501NS3$_{R457A,R458A}$. To produce the plasmids pDVWS501NS3$_{K199A}$, pDVWS501NS3$_{M283F}$ and pDVWS501NS3$_{R457A,R458A}$, cDNA encoding these mutations was cloned into pDVWS501 by removing the 977bp mutated *Bst* BI^{5069}/*Bst* BI^{6046} fragment from the corresponding pGX74%NS3 plasmid, and ligating this into *Bst* BI^{5069}/*Bst* BI^{6046}-digested pDVWS501.

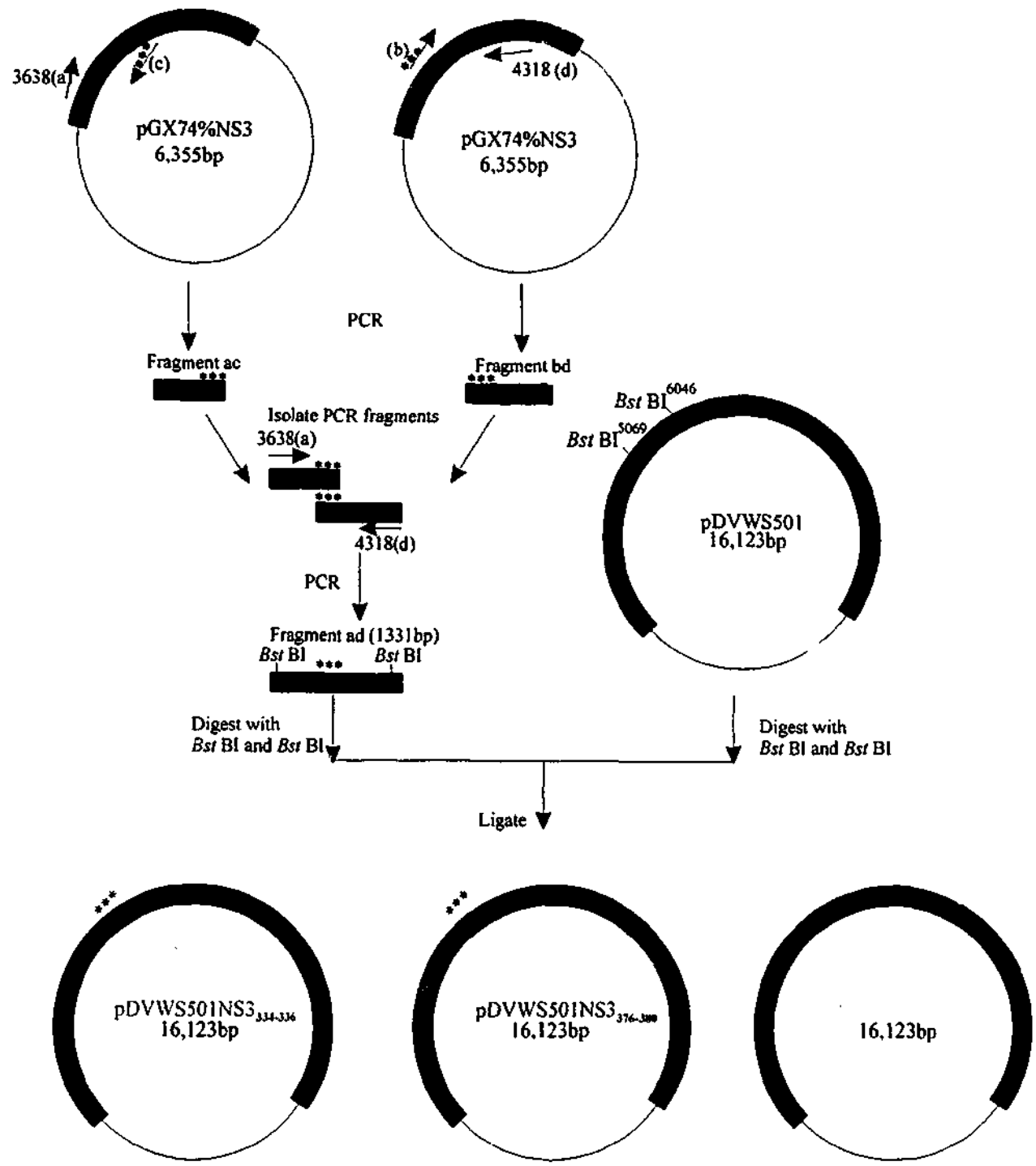

Fig. 4.13 Construction of plasmids pDVWS501NS3$_{334-336}$, pDVWS501NS3$_{376-380}$ and pDVWS501NS3$_{436-439}$. OE-PCR was used to insert the changes within NS3. The mutagenic primers used (primers b and c) are listed for each mutant in Table 4.1. Each respective 977bp *Bst* BI^{5069} - *Bst* BI^{6046} fragment containing the mutation was directly cloned into pDVWS501.

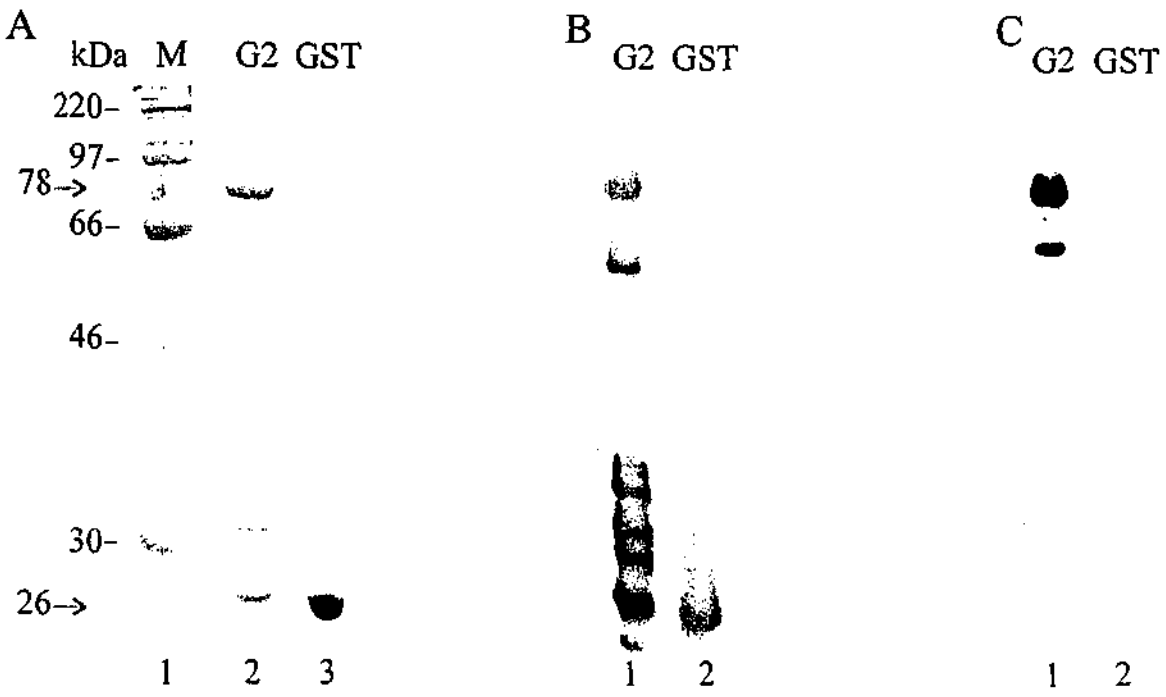

Fig. 4.14 Analysis on 10% polyacrylamide gels of partially purified parental G2 protein. (A) Coomassie blue staining. (B) Immunoblot using anti-GST antibodies (Pharmacia Biotech). (C) Immunoblot using anti-NS3 antiserum. Size markers are shown on the left.

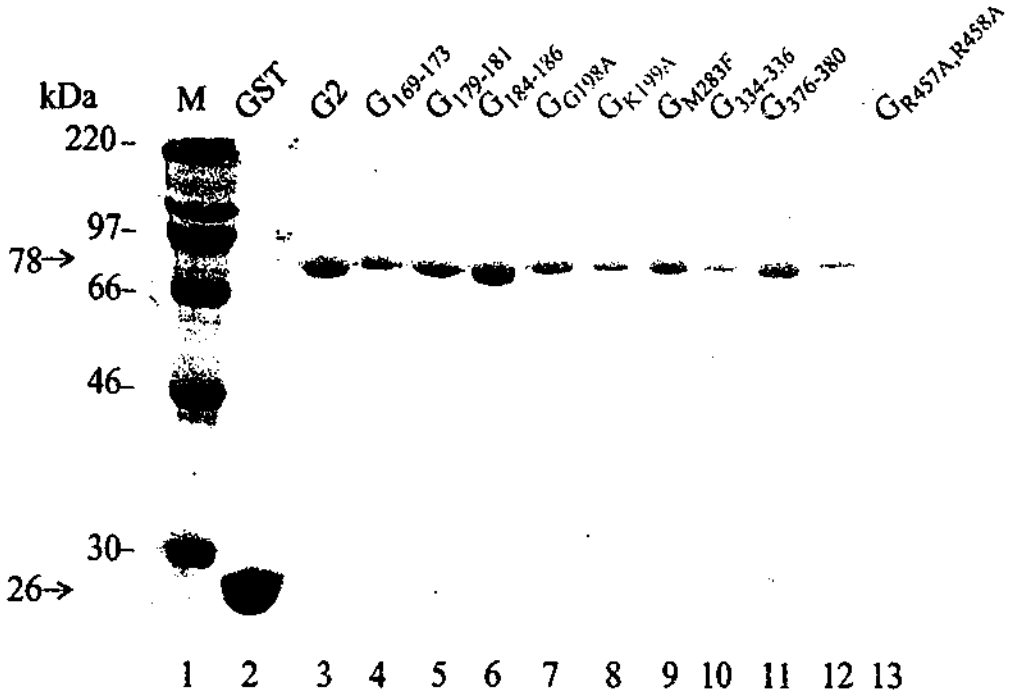

Fig. 4.15 Analysis of partially purified parental and mutant GST:74%NS3 fusion proteins. Coomassie blue staining of the GST:74%NS3 mutant fusion proteins. Size markers are shown on the left.

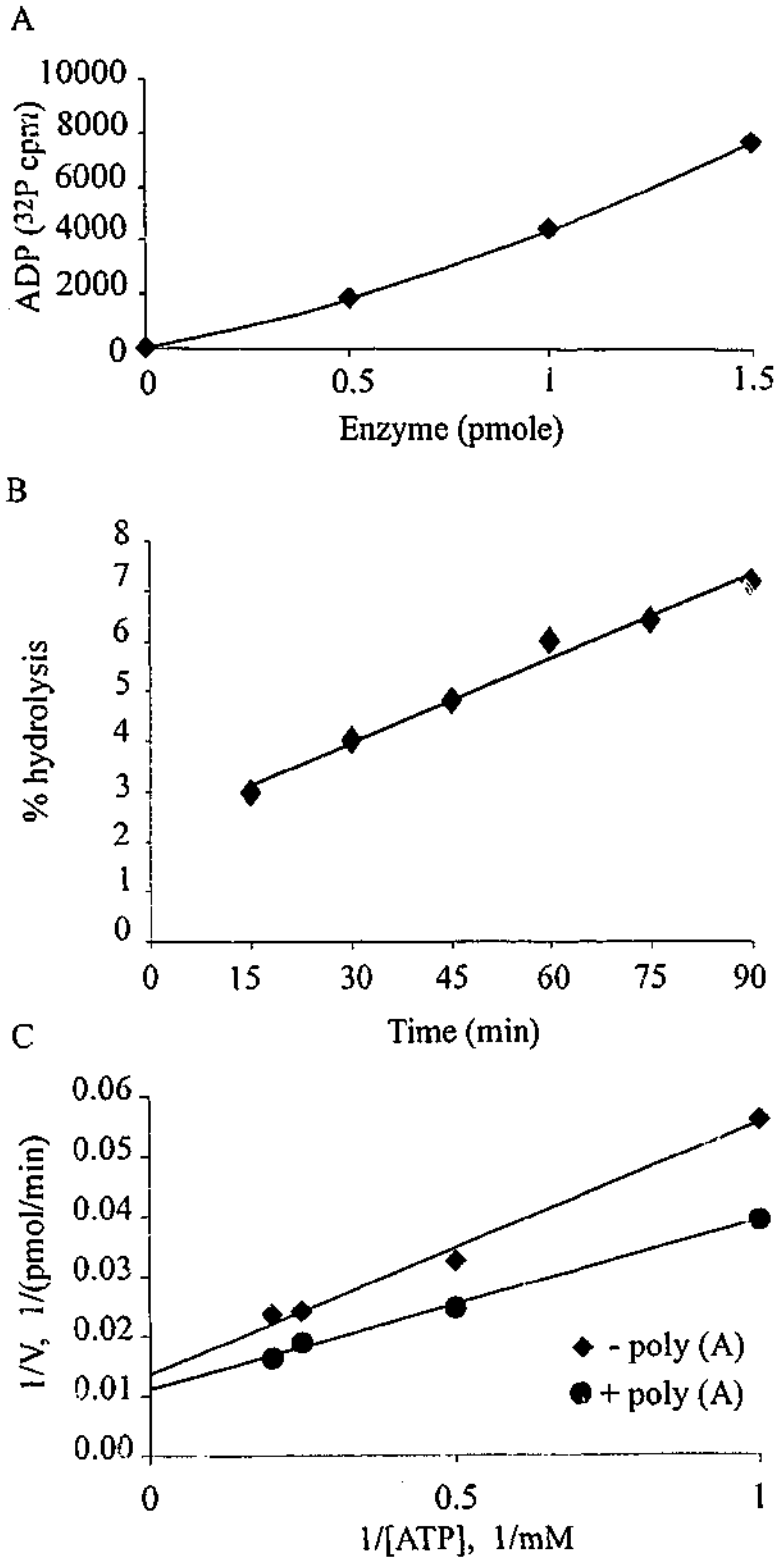

Fig. 4.16 ATPase activity of parental G2 fusion protein. (A) ATPase activity of increasing amounts of parental GST:74%NS3 fusion protein measured by the production of [α^{32}P] ADP. (B) Rate of ATP hydrolysis using 1 pmol of protein and 5 mM ATP. (C) Lineweaver-Burk plots of ATPase activity in the presence or absence of 0.5 mM poly(A). Reaction volume of 10 µl contained 1 pmol of enzyme.

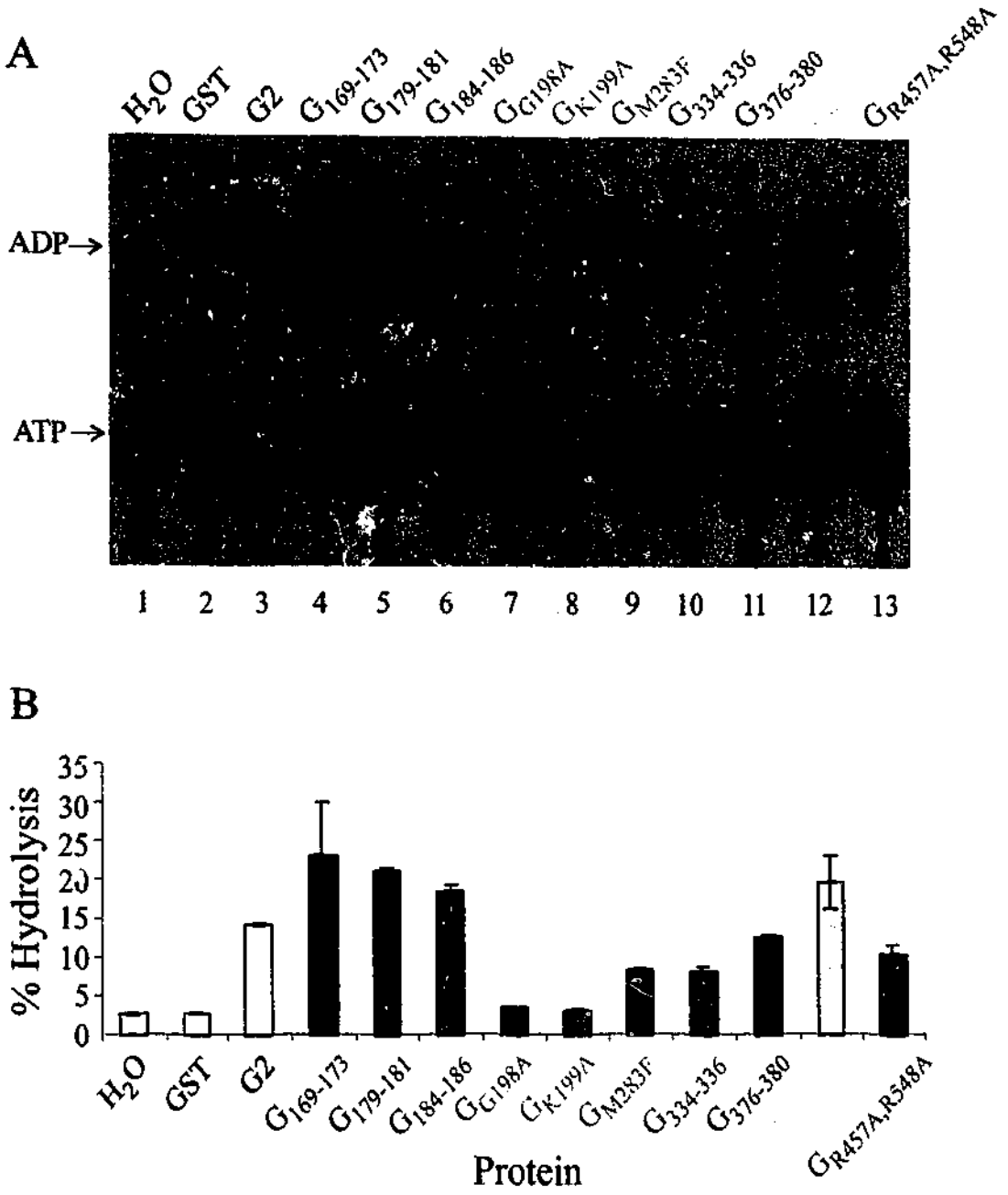

Fig. 4.17 ATPase activities of wild-type and mutant 74%NS3 fusion proteins. (A) Radioactive ADP and ATP were separated by TLC. (B) Percent hydrolysis of ATP to ADP. Means (columns) and range of values (single line bars) from three independent experiments are shown.

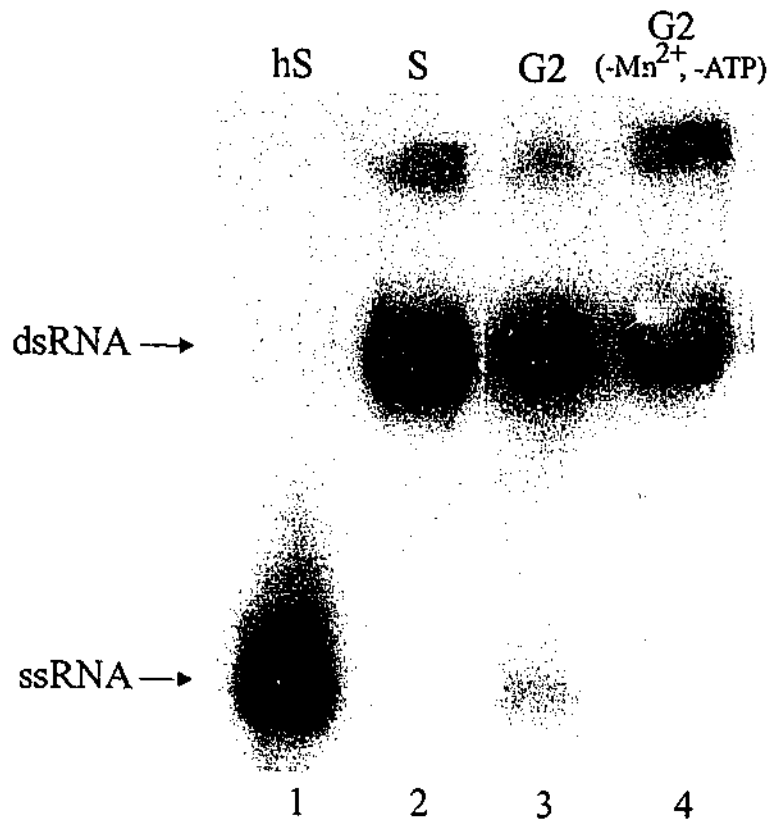

Fig. 4.18 RNA helicase activity of the parental G2 protein. Lane 1, heated RNA substrate (hS); lane 2, untreated RNA substrate (S); lane 3, RNA helicase activity of 1 pmol of purified G2 protein; lane 4, as for lane 3 but omitting ATP and Mn^{2+}.

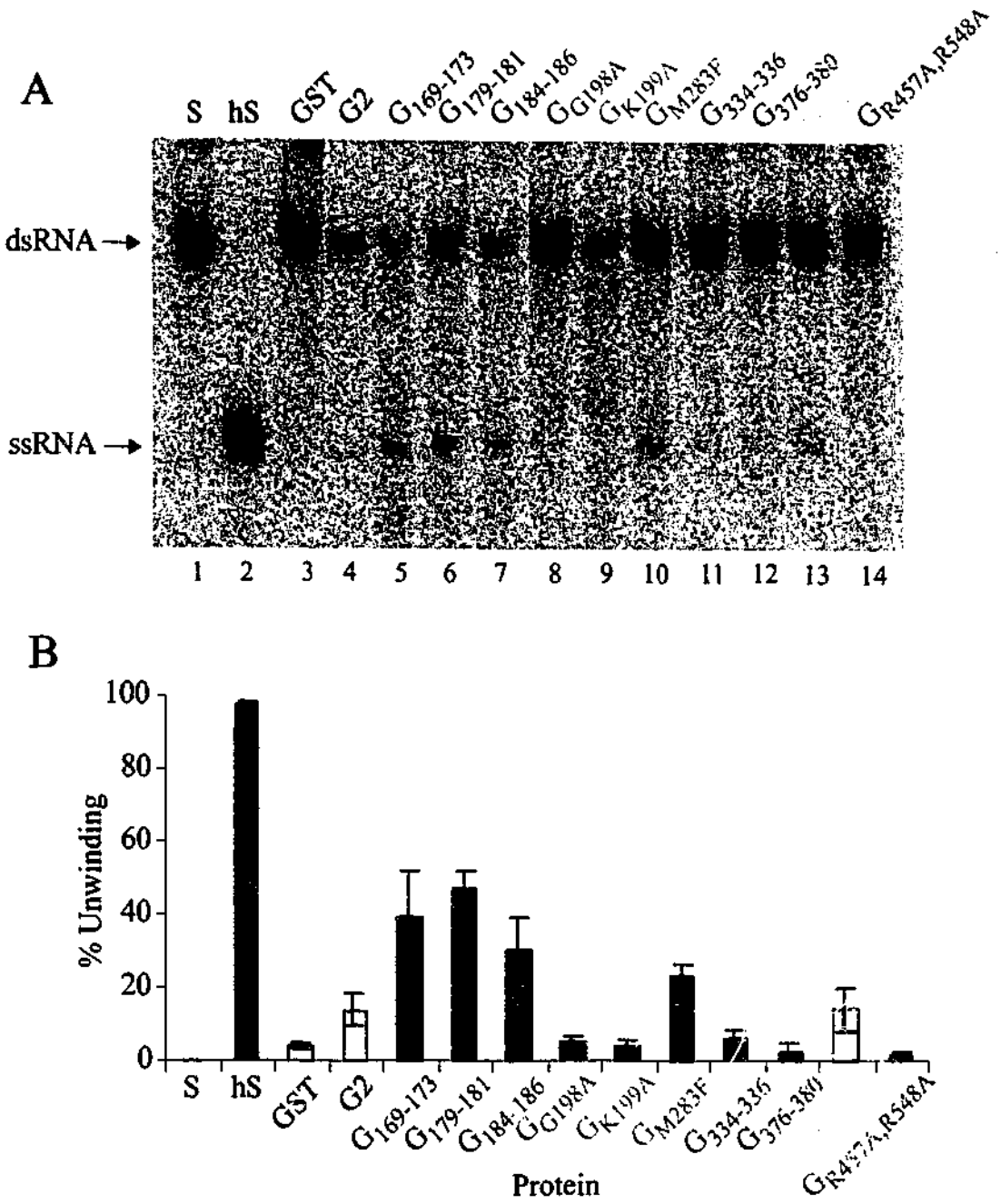

Fig. 4.19 RNA helicase assay of 74%NS3 fusion proteins. (A) RNA helicase activity of mutant fusion proteins. Lane 1, untreated RNA substrate (S); lane 2, heated RNA substrate (hS). (B) Percent unwinding of dsRNA to ssRNA. Means (columns) and range of values (single line bars) from three independent experiments are shown.

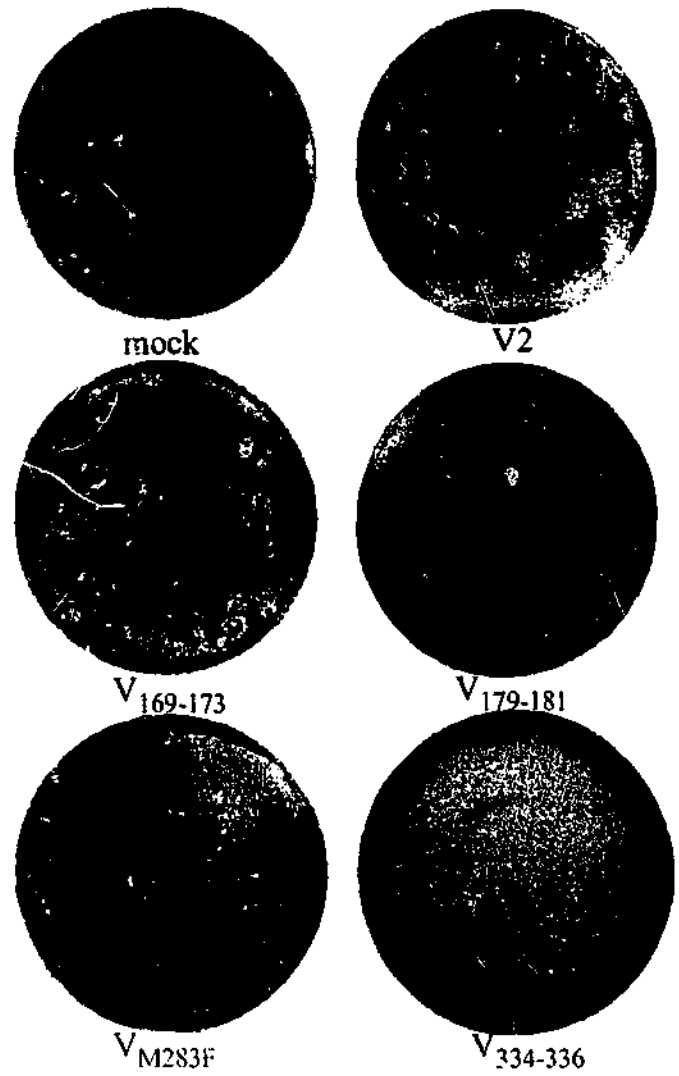

Fig. 4.20 Representative plaque sizes of mutant viruses in C6/36 cells at 28°C.

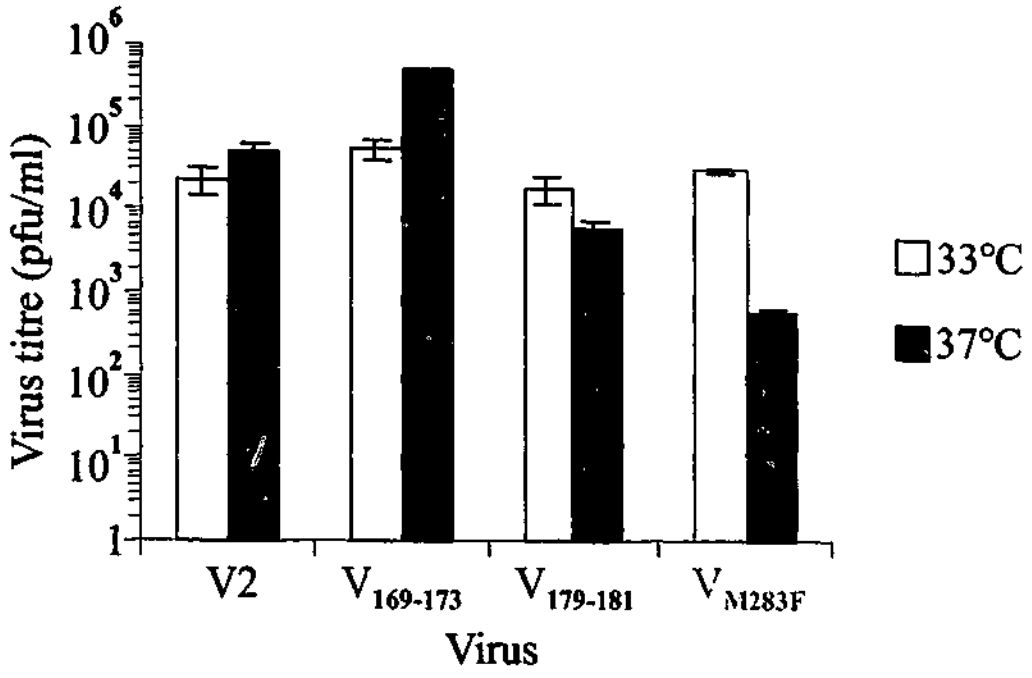

Fig. 4.21 Replication of selected mutant viruses in BHK-21 cells at 33°C and 37°C (MOI of 1.0). The cell culture medium was sampled at 72 hr p.i. and the virus titres were determined by plaque assay on C6/36 cells (28°C). Error bars show one standard deviation of the plaque titre.

A

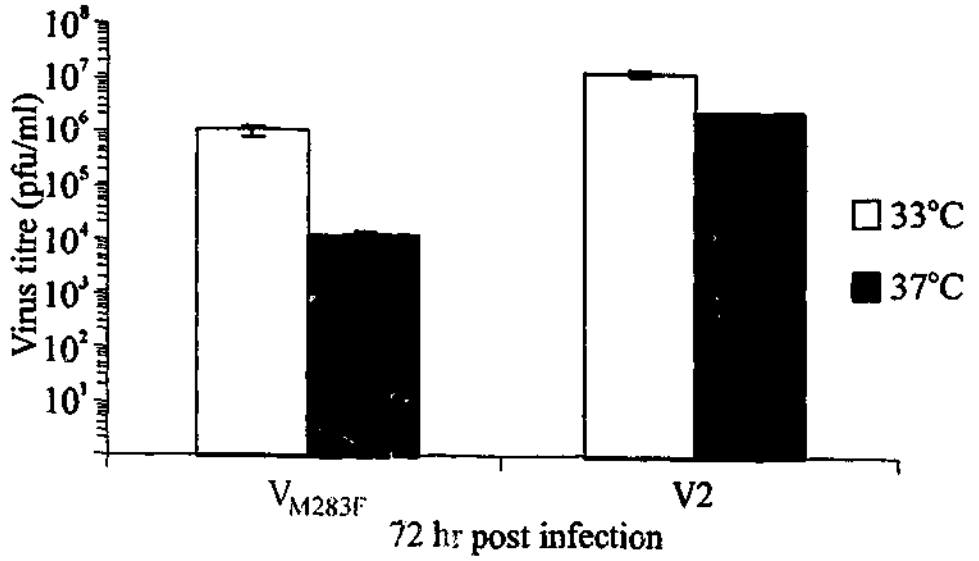

B

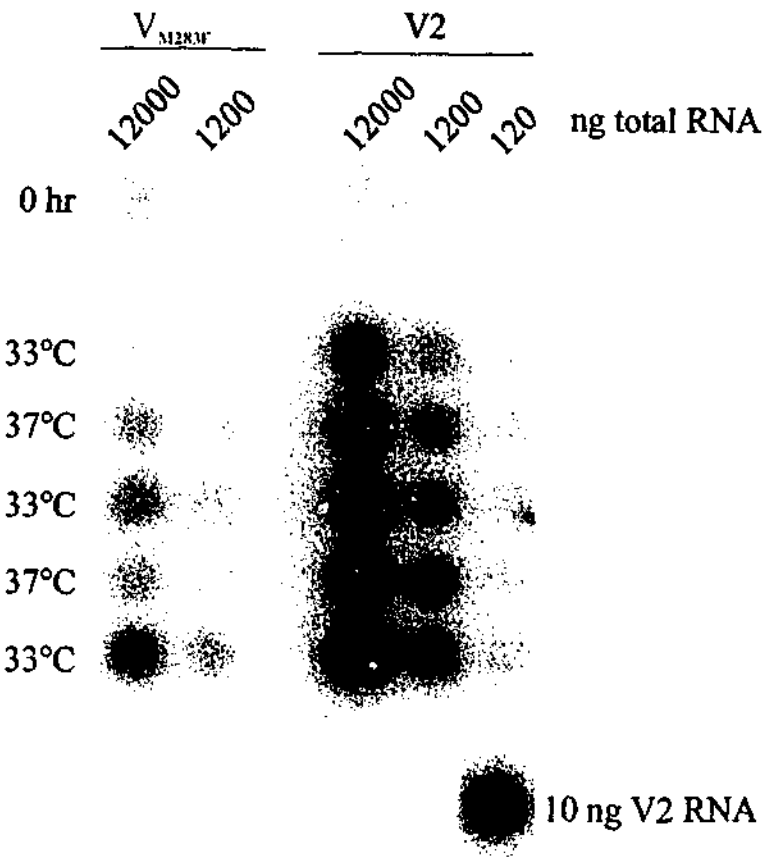

Fig. 4.22 Effect of temperature on virus replication and RNA synthesis of mutant virus V_{M283F}. (A) Replication of parental V2 and V_{M28F} viruses in BHK-21 cells shifted from 33°C to 37°C at 48 hr p.i.. Virus titres in culture fluid at 72 hr p.i. were determined by plaque assay on C6/36 cells (28°C). Error bars show one standard deviation of the plaque titre. (B) Dot blot hybridizations of total cell RNA using a ^{32}P-labeled dsDNA viral probe. Cells were harvested at 48, 64 and 72 hr p.i..

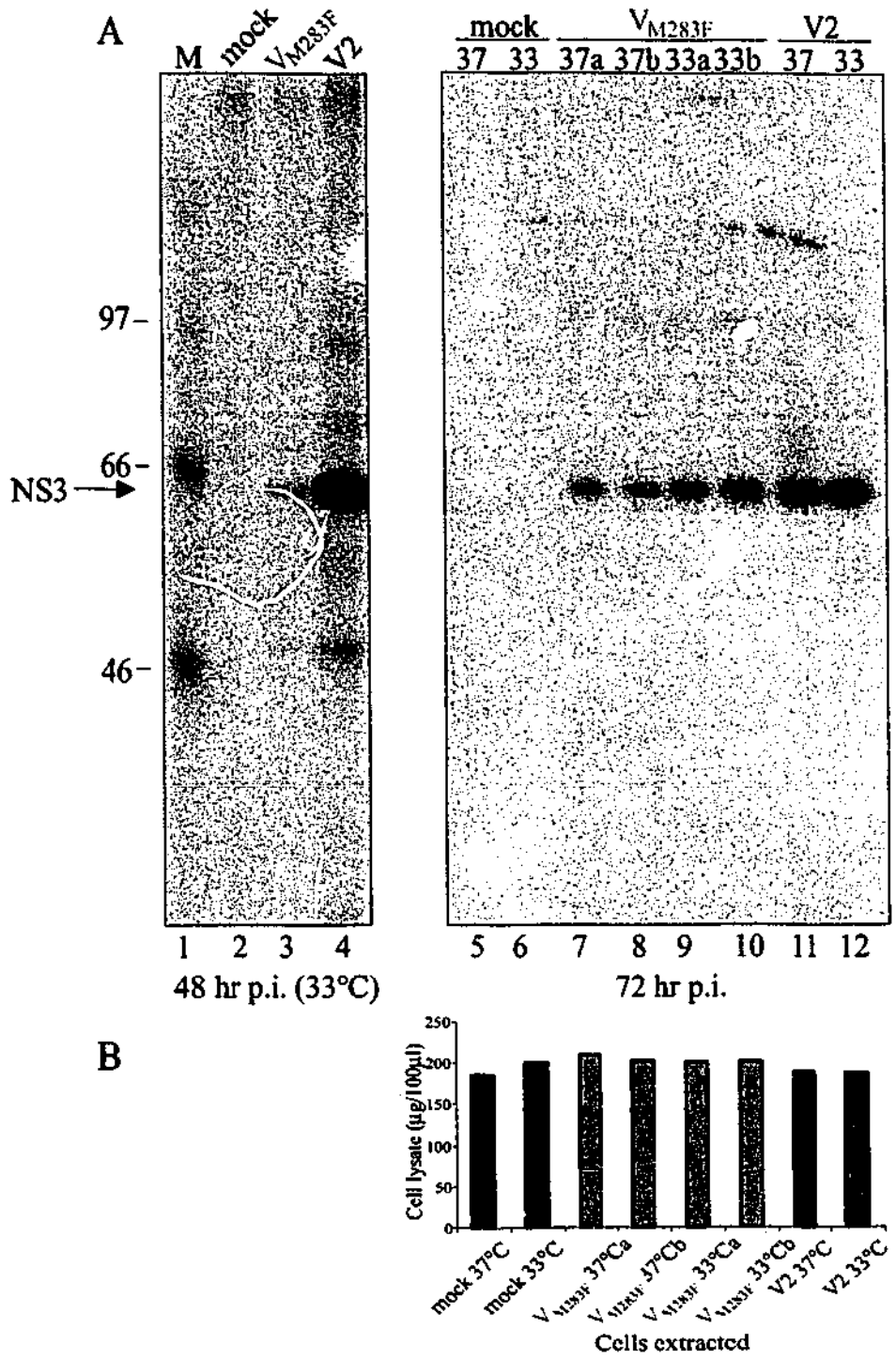

Fig. 4.23 Protein synthesis of parental V2 and V_{M283F} viruses in BHK-21 cells shifted from 33°C to 37°C at 48 hr p.i.. (A) Analysis by gel electrophoresis of ^{35}S-labelled protein immunoprecipitated by anti-NS3 antiserum (Teo & Wright, 1997). At 0 hr and 24 hr post shift (48 hr and 72 hr p.i.), cells for each virus at each temperature were starved of methionine for 2 hr and radiolabelled for a further 2 hr. Mock infected cells (lanes 2, 5, and 6) and size markers are shown (lane 1). (B) The bottom panel shows amounts (µg) of total cell protein in cell lysates before immunoprecipitation. The samples in lanes 7, 8 and 9, 10 are from independent duplicate experiments.

Table 4.1: Sequence of the primers used in OE-PCR.

Construct	Primer number	Primer designation[1]	Sequence[2] 5' to 3'	Primers used for sequencing of OE-PCR products
pGX74%NS3$_{169-173}$	2618[3]	a	ATCGAAGGTCGTGGGATCCCCCTATG^{5005}	2618, 2619
	4095	b	^{5020}CAGACTGcAgcAAGTATTGcAGACAATCCAGAGAT^{5055}	
	4096	c	^{5045}TTGTCTgCAATACTTgcTgCAGTGTGGGCTATAGCA^{5010}	
	2619	d	^{5568}CTCATGTCCAGAACTCCACGACG^{5545}	
pGX74%NS3$_{179-181}$	2618	a	ATCGAAGGTCGTGGGATCCCCCTATG^{5005}	2618, 2619
	7538	b	^{5050}GAGATCGcAGcTGcTATTTTTCGAAAGAG^{5078}	
	3640	c	^{5082}TTTTCTCTTTCGAAAAATGgCAgCTgCGATCTCTGGATTGTC^{5041}	
	2619	d	^{5568}CTCATGTCCAGAACTCCACGACG^{5545}	
pGX74%NS3$_{184-186}$	2618	a	ATCGAAGGTCGTGGGATCCCCCTATG^{5005}	2618, 2619
	4097	b	^{5065}TATTTTTgcAgcGgcAAAATTGACCATCATGGACC^{5099}	
	4098	c	^{5085}CAATTTTgcCgcTgcAAAAATATCATCTTCGATCTCTGG^{5047}	
	2619	d	^{5568}CTCATGTCCAGAACTCCACGACG^{5545}	
pGX74%NS3$_{G198A}$	2618	a	ATCGAAGGTCGTGGGATCCCCCTATG^{5005}	2618, 2619
	2620	b	^{5107}GGAGCGGctAAGACGAAGAGATACCTTCCG^{5136}	
	2621	c	^{5126}CTCTTCGTCTTagCCGCTCCTGGGTGGAGG^{5097}	
	2619	d	^{5568}CTCATGTCCAGAACTCCACGACG^{5545}	
pGX74%NS3$_{K199A}$	2618	a	ATCGAAGGTCGTGGGATCCCCCTATG^{5005}	2618, 2619
	2624	b	^{5107}GGAGCGGGAgcGACGAAGAGATACCTTCCG^{5136}	
	2625	c	^{5124}CTTCGTCgcTCCCGCTCCTGGGTGGAGGTC^{5095}	
	2619	d	^{5568}CTCATGTCCAGAACTCCACGACG^{5545}	

Construct	Primer number	Primer designation[1]	Sequence[2] 5' to 3'	Primers used for sequencing of OE-PCR products
pGX74%NS3$_{M283F}$	2618	a	ATCGAAGGTCGTGGGATCCCCCTATG^{5005}	2618, 2619
	2627	b	^{5364}CATCtTcGACGAAGCCCATTTCACAGACCC^{5393}	
	2626	c	^{5374}CGTCgAaGATGATCAGGTTGTAATTTGGC^{5346}	
	2619	d	^{5568}CTCATGTCCAGAACTCCACGACG^{5545}	
pGX74%NS3$_{334-336}$	3638	a	^{4792}GAAGAAGCCGCGGTCTTGGCATTGGAGCCTG^{4822}	2627
	4099	b	^{5516}TCATGGcTGcAGcAAGAGAAATCCCTGAACG^{5546}	
	4100	c	^{5533}CTCTTgCTgCAgCCATGATTGGTGCAT^{5507}	
	4318	d	^{6123}CACAAAGGTTTTCCTTGCTTCTCCTCTCAAGCGG^{6090}	
pGX74%NS3$_{376-380}$	3638	a	^{4792}GAAGAAGCCGCGGTCTTGGCATTGGAGCCTG^{4822}	2627
	4104	b	^{5641}TGCCTGgcAgcAAATGGAgcGAAAGTGATACAACTC^{5676}	
	4105	c	^{5666}ACTTTCgcTCCATTTgcTgcCAGGCAAGCTGCTATATC^{5629}	
	4318	d	^{6123}CACAAAGGTTTTCCTTGCTTCTCCTCTCAAGCGG^{6090}	
pGX74%NS3$_{436-439}$	3638	a	^{4792}GAAGAAGCCGCGGTCTTGGCATTGGAGCCTG^{4822}	2627
	4106	b	^{5821}CTAACAGcTGGTGcAGcGCGGGTGATCCTGGC^{5852}	
	4107	c	^{5843}ACCCGCgCTgCACCAgCTGTTAGTATAACTGG^{5812}	
	4318	d	^{6123}CACAAAGGTTTTCCTTGCTTCTCCTCTCAAGCGG^{6090}	

[1] a and d are flanking primers, b and c are mutagenic primers in OE-PCR (see Fig. 2.1).

[2] All sequences are listed 5′ to 3′, and the substituted nucleotides are written in lower case. Nucleotide numbering refers to the NGC DEN-2 sequence of Irie *et al.* (1989).

[3] The first 22 nt of primer 2318 is pGEX-3X sequence.

Table 4.2: Primers used to amplify and sequence RT-PCR products from C6/36 cells infected with second passage mutant virus.

Virus	RT primer	PCR primers	Location[1] of amplified DNA 33°C[2]	37°C[2]	Region sequenced[3]	Sequencing primer[4]
$V_{169\text{-}173}$[5]	Random hexamers	179, 3633, 3630, 2626, 2620, 4318, 4106, 1146	nt 4132-6375	nt 4609-5374	NS2B and NS3 nt 4132-6375	5998, 4056, 4105, 4099 1146, 4106, 2621,1396
$V_{179\text{-}181}$[5]	Random hexamers	179, 3633, 3630, 2626, 2620, 4318, 4106, 1146	nt 4132-6375	nt 4565-5374	NS2B and NS3 nt 4132-6375	5998, 4056, 4105, 4099 1146, 4106, 2621,1396
V_{M283F}	Random hexamers	179, 3633, 3630, 2626, 2620, 4318, 4106, 1146	nt 4132-6375	no product	NS2B and NS3 nt 4132-6375	5998, 4056, 4105, 4099 1146, 4106, 2621,1396
$V_{334\text{-}336}$	Random hexamers	179, 3633, 3630, 2626, 2620, 4318, 4106, 1146	nt 4132-6375	no product	NS2B and NS3 nt 4132-6375	5998, 4056, 4105, 4099 1146, 4106, 2621,1396

[1] Numbering follows the sequence of Irie *et al.* (1989).

[2] All sequenced products were from viral RNA obtained following electroporation of RNA into BHK-21 cells (maintained at 33°C or 37°C) and two passages of virus in C6/36 cells at 28°C.

[3] For products obtained from viruses obtained by maintaining BHK-21 cells initially at 37°C, only the region spanning the mutation was sequenced. For viruses $V_{169\text{-}173}$, $V_{179\text{-}181}$ V_{M283F} and $V_{334\text{-}336}$ obtained by maintaining BHK-21 cells initially at 33°C, RT-PCR products covering the entire NS2B and NS3 genes were sequenced (i.e. nt 4132-6375).

[4] For sequence of primers see Table 3.2.

[5] The data for these viruses was also presented in Table 3.3.

Table 4.3: Yields of mutant viruses following electroporation of RNA into BHK-21 cells and two passages of virus in C6/36 cells.

Site mutated	Virus		IF[1]	Virus titre[2] (pfu/ml)	Approximate Plaque size (mm)	RT-PCR[3]	ATPase activity[6]	Helicase activity[6]
	V2	33°C[4]	+++	$1.1 \pm 0.1 \times 10^6$	4	yes	+	+
		37°C	+++	$7.3 \pm 0.8 \times 10^6$	4	yes		
EKSIE	$V_{169\text{-}173}$	33°C[5]	+++	$2.7 \pm 0.2 \times 10^6$	3	yes	↑	↑
		37°C	+++	$2.2 \pm 0.5 \times 10^6$	3	yes		
EDD	$V_{179\text{-}181}$	33°C[5]	+++	$4.9 \pm 1.0 \times 10^5$	1	yes	↑	↑
		37°C	+++	$1.4 \pm 0.2 \times 10^6$	1	yes		
RKR	$V_{184\text{-}186}$	33°C	–	none detected		no	↑	↑
		37°C	–	none detected		no		
K199A	V_{K199A}	33°C	–	none detected		no	–	–
		37°C	–	none detected		no		
M283F	V_{M283F}	33°C	+++	$4.7 \pm 1.0 \times 10^5$	2	yes	↓	↑
		37°C	–	none detected		no		
DEE	$V_{334\text{-}336}$	33°C	+++	$7.3 \pm 1.1 \times 10^2$	1	yes	↓	↓
		37°C	–	none detected		no		
RKNGK	$V_{376\text{-}380}$	33°C	–	none detected		no	↓	–
		37°C	–	none detected		no		
DGEE	$V_{[illegible]}$	33°C	–	none detected		no	↑	↑
		37°C	–	none detected		no		
R457A,R458A	$V_{R457A,R458A}$	33°C	–	none detected		no	↓	–
		37°C	–	none detected		no		

[1] Immunofluorescence (IF) in BHK-21 cells at 5-6 days p.e. IF was scored (–) no positive cells, (+) 1-25% positive cells, (++) 25-50% positive cells, (+++) 50-75% positive cells, (++++) 75-100% positive cells.

[2] Plaque titres after passaging in C6/36 are expressed in pfu/ml ± one standard deviation. Each virus was derived at least twice from RNA transcripts, therefore the result shown for each virus is the average of two or more experiments.

[3] Detection of product after RT-PCR. All positive samples retained the required mutation and had no other changes in the NS2B/3 genes.

[4] Temperature at which BHK-21 cells were incubated immediately after electroporation i.e. 33°C or 37°C

[5] Data on these viruses also presented in Table 3.4.

[6] ATPase and RNA helicase activities. Activity was scored (-) no activity, (+) parental activity, (↑) activity increased compared with parental activity, (↓) activity reduced compared with parental activity.

Table 4.4: Serial passage of the low titre virus $V_{334\text{-}336}$.

Passage number	$V_{334\text{-}336}$	
	CPE[1]	Plaque titre[2]
2	–	$(2.2 \pm 0.3) \times 10^3$
3	–	$(4.7 \pm 1.2) \times 10^3$
4	–	n.t.[3]
5	–	$(2.6 \pm 0.3) \times 10^4$
6	–	n.t.
7	+ (day 5)	$(2.0 \pm 0.3) \times 10^5$
8	+ (day 3)	$(1.2 \pm 0.2) \times 10^5$
9	+ (day 2)[4]	$(1.6 \pm 0.1) \times 10^5$
10	+ (day 2)[4]	$(1.3 \pm 0.2) \times 10^7$
11	+ (day 2)[4]	$(1.4 \pm 0.3) \times 10^7$

[1] CPE of infected C6/36 cells was scored as (–) no CPE, (+) up to 20% of the cell monolayer showing CPE.

[2] Plaque titres are expressed in pfu/ml ± one standard deviation.

[3] n.t., not tested

[4] By day three of passage 9, 10 and 11, $V_{334\text{-}336}$ infected cells demonstrated extensive (>70%) cell monolayer destruction.

CHAPTER FIVE: GENERAL DISCUSSION AND CONCLUSIONS

One aim of this work was to identify changes in the DEN-2 NS3 gene that restrict virus replication. This involved the incorporation of mutations into a genomic length DEN-2 cDNA clone from which (infectious) RNA could be transcribed. The DEN-2 NS3 protein is multifunctional with a serine proteinase domain in the amino terminal one third, and a NTPase and helicase in the remaining carboxy terminal two thirds. Thirteen sites distributed throughout NS3 were mutagenized in this study. Five sites were in the amino terminal proteinase region external to conserved enzyme motifs (chapter three). Four of these were rich in charged amino acids and were considered possible sites of interaction with the hydrophilic 40 amino acid fragment of NS2B essential for proteinase activity, and with other viral proteins. Hence the approach of clustered charged-to-alanine mutagenesis was used in an attempt to isolate growth restricted proteinase mutants. In addition to the mutagenesis of the four charged sites, substitutions were made to the highly conserved hydrophobic region $G_{32}YSQI_{36}$ that also lies outside the conserved proteinase motifs.

Six charged sites were distributed through the helicase region and were considered possible sites of interaction with proteins of the replication complex. An additional four mutations located within helicase motifs I, II and VI were also generated to analyze the functions of the conserved motifs in NTPase and RNA helicase activities, and viral replication.

Previous experiments showed that mutations which abolished or strongly reduced NS2B/3 proteinase activity usually prevented or greatly reduced viral replication (Amberg & Rice, 1999; Chambers *et al.*, 1993; Nestorowicz *et al.*, 1994),

whereas mutations with less severe effects on cleavage generally allowed the recovery of infectious virus, albeit with reduced plaque titres and small plaque phenotypes (Amberg & Rice, 1999; Chambers *et al.*, 1995; Nestorowicz *et al.*, 1994). Two charged-to-alanine mutants and the conserved hydrophobic mutant were previously tested by Kelley (1996) and did not show severe inhibition of proteinase activity in COS cells (Matusan *et al.*, 2001). These mutants and a further two charged-to-alanine mutants (previously untested in COS cells) were incorporated into genomic length cDNA. All mutant viruses showed a range of reduced plaque phenotypes compared with parental V2 and replicated to variable yields. However, no proteinase mutant virus demonstrated a clear *ts* phenotype. It is possible that the very low yields of the potential *ts* mutants $V_{32\text{-}36}$ and $V_{91\text{-}94}$ would be improved by less severe mutagenesis i.e. substituting one or two residues rather than three. It would be of interest to investigate mutant NS3/NS2B interactions. Expression of recombinant NS2B and NS3 proteins in cell free systems or in transfected cells, and coprecipitation of an NS3/NS2B complex using anti-NS3 antiserum, as described by Arias *et al.* (1993), would allow investigation *in vitro*. Interaction may be monitored *in vivo* using anti-NS3 antiserum to immunoprecipitate NS3/NS2B protein complex from DEN-2 infected mosquito cells (Arias *et al.*, 1993), or by using immunofluoresence to look for colocalization (Westaway *et al.*, 1997*b*).

The availability of the NS3/2B model described in chapter three may also enable the selection of residues which are predicted to be important in NS2B/NS3 interactions, and which can be mutated and assayed for their effects on proteinase activity, protein-protein interactions and virus replication. Improved knowledge of proteinase and cofactor interactions is of broad relevance to flaviviruses and may (i)

aid in the development of antiviral agents such as proteinase inhibitors, and (ii) aid in the development of a recombinant vaccine.

Interestingly, the charged-to-alanine regions selected for mutagenesis spanning the helicase region of NS3 had a more detrimental effect on virus replication, with four out of the six mutant viruses ($V_{184\text{-}186}$, $V_{334\text{-}336}$, $V_{376\text{-}380}$, $V_{436\text{-}439}$) producing very low or undetectable yields of virus (chapter four). The two viruses which did replicate to parental levels were both located upstream of the first helicase motif, in the linker region between the helicase and proteinase domains of NS3, and were discussed in both chapters three and four. It appears that viral replication is more sensitive to mutation in the helicase than proteinase of DEN-2 NS3.

The charged-to-alanine mutations in the helicase proteins demonstrated variable effects on NTPase/RNA helicase enzymatic activities. It was evident that the absence of helicase activity *in vitro* corresponded with no virus recovery. However, this study also shows for the first time that mutations within NS3 which permit helicase activity *in vitro* may still prevent virus replication. This indicates that these charged residues may be on the surface of NS3 and involved in protein-protein (host or viral) or RNA-protein interactions within the replication complex (Chen *et al.*, 1997*a*; Kapoor *et al.*, 1995; Li *et al.*, 1999) that are required for virus replication. This type of mutational analysis of the helicase region of a positive strand RNA virus has not previously been described. It would be desirable to perform *in vitro* protein–protein (e.g. NS3 with NS5) (Kapoor *et al.*, 1995) and protein-RNA binding studies (Chen *et al.*, 1997*a*; Cui *et al.*, 1998) using these mutant proteins.

Several studies have used mutational analysis to characterize the role of the various helicase motifs in enzymatic activity (see chapter one). To date, only a single study on a positive strand virus (Gu *et al.*, 2000) has investigated the role of motif

mutants in virus replication using a genomic length cDNA. Gu *et al.* (2000) showed that mutation of conserved amino acids within motifs resulted in proteins having no helicase activity, and no virus was recovered. The researchers demonstrated that helicase activity was essential for viral minus strand RNA synthesis (Gu *et al.*, 2000). This present study agreed with the findings of Gu *et al.* (2000), in that mutation of conserved residues within helicase motifs abolished both helicase activity and virus replication. However, the precise helicase mechanism disrupted is unknown, and was not investigated.

Mutation of the lesser conserved Met_{283} residue within motif II resulted in the retention of helicase activity for the mutant protein G_{M283F}, and virus V_{M283F} which replicated less well than parental V2, displaying small plaques and temperature sensitivity. This is the first report of a *ts* flavivirus helicase mutant. The *ts* defect in virus production reflected reduced viral RNA and protein synthesis in infected cells following shift to a restrictive higher temperature (chapter four).

This study demonstrated that mutation of residues within motifs I, II and VI of DEN-2 NS3 can aid in the understanding of the roles of the motifs in NTPase/helicase activity and viral replication. Therefore a similar mutational analysis of the lesser investigated motifs Ia, IV and V (which to date have no clearly defined function) could shed further light on the role of these motifs in the mechanism of helicase activity and virus replication.

This work also identified two previously unknown regions ($R_{376}KNGK_{380}$ and $R_{457}R_{458}$) that are required for the coupling of ATPase and RNA helicase activities. These mutants demonstrated that helicase activity is essential for viral replication, as ATPase activity alone is not sufficient. Furthermore, this study identified a charged-to-alanine mutant protein, $G_{334\text{-}336}$, which had reduced enzymatic activity. This is the

first time that mutations of charged residues, external to helicase motifs, have altered helicase activity.

It would also be of interest to investigate the cumulative effects of both proteinase and helicase mutations investigated here, which retained or only minimally reduced virus replication. Such mutations inserted into the DEN-2 genomic length cDNA in various combinations may generate viruses with restricted replication.

A dengue vaccine should ideally protect against all four serotypes (Halstead, 1988; Sinniah & Igarashi, 1995). Genomic length cDNA offers the potential of producing a dengue vaccine that contains several mutations along the length of the genome which have been extensively studied and are known to attenuate the virus.

BIBLIOGRAPHY

Alber, T. (1989). Mutational effects on protein stability. *Annual Review of Biochemistry* **58**, 765-798.

Allison, S. L., Schalich, J., Stiasny, K., Mandl, C. W., Kunz, C. & Heinz, F. X. (1995). Oligomeric rearrangement of tick-borne encephalitis virus envelope proteins induced by an acidic pH. *Journal of Virology* **69**, 695-700.

Amberg, S. M., Nestorowicz, A., McCourt, D. W. & Rice, C. M. (1994). NS2B-3 proteinase-mediated processing in the yellow fever virus structural region: in vitro and in vivo studies. *Journal of Virology* **68**, 3794-3802.

Amberg, S. M. & Rice, C. M. (1999). Mutagenesis of the NS2B-NS3-mediated cleavage site in the flavivirus capsid protein demonstrates a requirement for coordinated processing. *Journal of Virology* **73**, 8083-8094.

Anderson, R., King, A. D. & Innis, B. L. (1992). Correlation of E protein binding with cell susceptibility to dengue 4 virus infection. *Journal of General Virology* **73**, 2155-2159.

Arias, C. F., Preugschat, F. & Strauss, J. H. (1993). Dengue 2 virus NS2B and NS3 form a stable complex that can cleave NS3 within the helicase domain. *Virology* **193**, 888-899.

Barrett, A. D., Mathews, J. H., Miller, B. R., Medlen, A. R., Ledger, T. N. & Roehrig, J. T. (1990). Identification of monoclonal antibodies that distinguish between 17D-204 and other strains of yellow fever virus. *Journal of General Virology* **71**, 13-18.

Bartenschlager, R., Ahlborn-Laake, L., Mous, J. & Jacobsen, H. (1993). Nonstructural protein 3 of the hepatitis C virus encodes a serine-type proteinase required for cleavage at the NS3/4 and NS4/5 junctions. *Journal of Virology* **67**, 3835-3844.

Bartenschlager, R., Lohmann, V., Wilkinson, T. & Koch, J. O. (1995). Complex formation between the NS3 serine-type proteinase of the hepatitis C virus and NS4A and its importance for polyprotein maturation. *Journal of Virology* **69**, 7519-7528.

Bass, S. H., Mulkerrin, M. G. & Wells, J. A. (1991). A systematic mutational analysis of hormone-binding determinants in the human growth hormone receptor. *Proceedings of the National Academy of Sciences of the United States of America* **88**, 4498-4502.

Bazan, J. F. & Fletterick, R. J. (1989). Detection of a trypsin-like serine protease domain in flaviviruses and pestiviruses. *Virology* **171**, 637-639.

Berman, H. M., Westbrook, J., Feng, Z., Gilliland, G., Bhat, T. N., Weissig, H., Shindyalov, I. N. & Bourne, P. E. (2000). The Protein Data Bank. *Nucleic Acids Research* **28**, 235-242.

Bernstein, F. C., Koetzle, T. F., Williams, G. J., Meyer, E. F., Jr., Brice, M. D., Rodgers, J. R., Kennard, O., Shimanouchi, T. & Tasumi, M. (1977). The Protein Data Bank. A computer-based archival file for macromolecular structures. *European Journal of Biochemistry* **80**, 319-324.

Bhamarapravati, N., Yoksan, S., Chayaniyayothin, T., Angsubphakorn, S. & Bunyaratvej, A. (1987). Immunization with a live attenuated dengue-2-virus candidate vaccine (16681-PDK 53): clinical, immunological and biological responses in adult volunteers. *Bulletin of the World Health Organization* **65**, 189-195.

Biedrzycka, A., Cauchi, M. R., Bartholomeusz, A., Gorman, J. J. & Wright, P. J. (1987). Characterization of protease cleavage sites involved in the formation of the envelope glycoprotein and three non-structural proteins of dengue virus type 2, New Guinea C strain. *Journal of General Virology* **68**, 1317-1326.

Black, M. E. & Hruby, D. E. (1992). Site-directed mutagenesis of a conserved domain in vaccinia virus thymidine kinase. Evidence for a potential role in magnesium binding. *Journal of Biological Chemistry* **267**, 6801-6806.

Blok, J., McWilliam, S. M., Butler, H. C., Gibbs, A. J., Weiller, G., Herring, B. L., Hemsley, A. C., Aaskov, J. G., Yoksan, S. & Bhamarapravati, N. (1992). Comparison of a dengue-2 virus and its candidate vaccine derivative: sequence relationships with the flaviviruses and other viruses. *Virology* **187**, 573-590.

Blok, J., Samuel, S., Gibbs, A. J. & Vitarana, U. T. (1989). Variation of the nucleotide and encoded amino acid sequences of the envelope gene from eight dengue-2 viruses. *Archives of Virology* **105**, 39-53.

Bonaldo, M. C., Caufour, P. S., Freire, M. S. & Galler, R. (2000). The yellow fever 17D vaccine virus as a vector for the expression of foreign proteins: development of new live flavivirus vaccines. *Memorias do Instituto Oswaldo Cruz* **95**, 215-223.

Borowski, P., Niebuhr, A., Mueller, O., Bretner, M., Felczak, K., Kulikowski, T. & Schmitz, H. (2001). Purification and characterization of West Nile virus nucleoside triphosphatase (NTPase)/helicase: evidence for dissociation of the NTPase and helicase activities of the enzyme. *Journal of Virology* **75**, 3220-3229.

Brinkworth, R. I., Fairlie, D. P., Leung, D. & Young, P. R. (1999). Homology model of the dengue 2 virus NS3 protease: putative interactions with both substrate and NS2B cofactor. *Journal of General Virology* **80**, 1167-1177.

Brinton, M. A. (1986). Replication of flaviviruses. In *The Togavividae and Flaviviridae.*, pp. 327-374. Edited by S. Schlesinger & M. J. Schlesinger. New York: Plenum Press.

Brinton, M. A. & Dispoto, J. H. (1988). Sequence and secondary structure analysis of the 5'-terminal region of flavivirus genome RNA. *Virology* **162**, 290-299.

Brinton, M. A., Fernandez, A. V. & Dispoto, J. H. (1986). The 3'-nucleotides of flavivirus genomic RNA form a conserved secondary structure. *Virology* **153**, 113-121.

Buckley, A., Gaidamovich, S., Turchinskaya, A. & Gould, E. A. (1992). Monoclonal antibodies identify the NS5 yellow fever virus non-structural protein in the nuclei of infected cells. *Journal of General Virology* **73**, 1125-1130.

Butkiewicz, N. J., Wendel, M., Zhang, R., Jubin, R., Pichardo, J., Smith, E. B., Hart, A. M., Ingram, R., Durkin, J., Mui, P. W., Murray, M. G., Ramanathan, L. & Dasmahapatra, B. (1996). Enhancement of hepatitis C virus NS3 proteinase activity by association with NS4A-specific synthetic

peptides: identification of sequence and critical residues of NS4A for the cofactor activity. *Virology* **225**, 328-338.

Butrapet, S., Huang, C. Y., Pierro, D. J., Bhamarapravati, N., Gubler, D. J. & Kinney, R. M. (2000). Attenuation markers of a candidate dengue type 2 vaccine virus, strain 16681 (PDK-53), are defined by mutations in the 5' noncoding region and nonstructural proteins 1 and 3. *Journal of Virology* **74**, 3011-3019.

Cahour, A., Falgout, B. & Lai, C. J. (1992). Cleavage of the dengue virus polyprotein at the NS3/NS4A and NS4B/NS5 junctions is mediated by viral protease NS2B-NS3, whereas NS4A/NS4B may be processed by a cellular protease. *Journal of Virology* **66**, 1535-1542.

Calisher, C. H., Karabatsos, N., Dalrymple, J. M., Shope, R. E., Porterfield, J. S., Westaway, E. G. & Brandt, W. E. (1989). Antigenic relationships between flaviviruses as determined by cross-neutralization tests with polyclonal antisera. *Journal of General Virology* **70**, 37-43.

Caruthers, J. M., Johnson, E. R. & McKay, D. B. (2000). Crystal structure of yeast initiation factor 4A, a DEAD-box RNA helicase. *Proceedings of the National Academy of Sciences of the United States of America* **97**, 13080-13085.

Castle, E., Nowak, T., Leidner, U. & Wengler, G. (1985). Sequence analysis of the viral core protein and the membrane-associated proteins V1 and NV2 of the flavivirus West Nile virus and of the genome sequence for these proteins. *Virology* **145**, 227-236.

Cauchi, M. R., Henchal, E. A. & Wright, P. J. (1991). The sensitivity of cell-associated dengue virus proteins to trypsin and the detection of trypsin-resistant fragments of the nonstructural glycoprotein NS1. *Virology* **180**, 659-667.

Chambers, T. J., Grakoui, A. & Rice, C. M. (1991). Processing of the yellow fever virus nonstructural polyprotein: a catalytically active NS3 proteinase domain and NS2B are required for cleavages at dibasic sites. *Journal of Virology* **65**, 6042-6050.

Chambers, T. J., Hahn, C. S., Galler, R. & Rice, C. M. (1990*a*). Flavivirus genome organization, expression and replication. *Annual Reviews of Microbiology* **44**, 649-688.

Chambers, T. J., Nestorowicz, A., Amberg, S. M. & Rice, C. M. (1993). Mutagenesis of the yellow fever virus NS2B protein: effects on proteolytic processing, NS2B-NS3 complex formation, and viral replication. *Journal of Virology* **67**, 6797-6807.

Chambers, T. J., Nestorowicz, A. & Rice, C. M. (1995). Mutagenesis of the yellow fever virus NS2B/3 cleavage site: determinants of cleavage site specificity and effects on polyprotein processing and viral replication. *Journal of Virology* **69**, 1600-1605.

Chambers, T. J., Tsai, T. F., Pervikov, Y. & Monath, T. P. (1997). Vaccine development against dengue and Japanese encephalitis: report of a World Health Organization meeting. *Vaccine* **15**, 1494-1502.

Chambers, T. J., Weir, R. C., Grakoui, A., McCourt, D. W., Bazan, J. F., Fletterick, R. J. & Rice, C. M. (1990*b*). Evidence that the N-terminal domain of nonstructural protein NS3 from yellow fever virus is a serine protease responsible for site-specific cleavages in the viral polyprotein. *Proceedings of the National Academy of Sciences of the United States of America* **87**, 8898-8902.

Chang, G.-J. (1997). Molecular biology of dengue viruses. In *Dengue and dengue hemorrhagic fever.*, pp. 175-198. Edited by D. J. Gubler & G. Kuno. Wallingford: CAB INTERNATIONAL.

Chang, S. C., Cheng, J. C., Kou, Y. H., Kao, C. H., Chiu, C. H., Wu, H. Y. & Chang, M. F. (2000). Roles of the AX(4)GKS and arginine-rich motifs of hepatitis C virus RNA helicase in ATP- and viral RNA-binding activity. *Journal of Virology* **74**, 9732-9737.

Chen, C. J., Kuo, M. D., Chien, L. J., Hsu, S. L., Wang, Y. M. & Lin, J. H. (1997*a*). RNA-protein interactions: involvement of NS3, NS5, and 3' noncoding regions of Japanese encephalitis virus genomic RNA. *Journal of Virology* **71**, 3466-3473.

Chen, Y., Maguire, T., Hileman, R. E., Fromm, J. R., Esko, J. D., Linhardt, R. J. & Marks, R. M. (1997*b*). Dengue virus infectivity depends

on envelope protein binding to target cell heparan sulfate. *Nature Medicine* **3**, 866-871.

Chen, Y. P., Maguire, T. & Marks, R. M. (1996). Demonstration of binding of dengue virus envelope protein to target cells. *Journal of Virology* **70**, 8765-8772.

Cho, H. S., Ha, N. C., Kang, L. W., Chung, K. M., Back, S. H., Jang, S. K. & Oh, B. H. (1998). Crystal structure of RNA helicase from genotype 1b hepatitis C virus. A feasible mechanism of unwinding duplex RNA. *Journal of Biological Chemistry* **273**, 15045-15052.

Chu, P. W. & Westaway, E. G. (1992). Molecular and ultrastructural analysis of heavy membrane fractions associated with the replication of Kunjin virus RNA. *Archives of Virology* **125**, 177-191.

Clertant, P. & Cuzin, F. (1982). Covalent affinity labeling by periodate-oxidized [alpha-^{32}P]ATP of the large-T proteins of polyoma and SV40 viruses. *Journal of Biological Chemistry* **257**, 6300-6305.

Clum, S., Ebner, K. E. & Padmanabhan, R. (1997). Cotranslational membrane insertion of the serine proteinase precursor NS2B-NS3(Pro) of dengue virus type 2 is required for efficient in vitro processing and is mediated through the hydrophobic regions of NS2B. *Journal of Biological Chemistry* **272**, 30715-30723.

Coia, G., Parker, M. D., Speight, G., Byrne, M. E. & Westaway, E. G. (1988). Nucleotide and complete amino acid sequences of Kunjin virus: definitive gene order and characteristics of the virus-specified proteins. *Journal of General Virology* **69**, 1-21.

Crawford, G. R. & Wright, P. J. (1987). Characterization of novel viral polyproteins detected in cells infected by the flavivirus Kunjin and radiolabelled in the presence of the leucine analogue hydroxyleucine. *Journal of General Virology* **68**, 365-376.

Cui, T., Sugrue, R. J., Xu, Q., Lee, A. K., Chan, Y. C. & Fu, J. (1998). Recombinant dengue virus type 1 NS3 protein exhibits specific viral RNA binding and NTPase activity regulated by the NS5 protein. *Virology* **246**, 409-417.

Cunningham, B. C. & Wells, J. A. (1989). High-resolution epitope mapping of hGH-receptor interactions by alanine-scanning mutagenesis. *Science* **244**, 1081-1085.

Dalgarno, L., Trent, D. W., Strauss, J. H. & Rice, C. M. (1986). Partial nucleotide sequence of the Murray Valley encephalitis virus genome. Comparison of the encoded polypeptides with yellow fever virus structural and non-structural proteins. *Journal of Molecular Biology* **187**, 309-323.

Della, P. A. & Westaway, E. G. (1972). Rapid preparation of hemagglutinins of togaviruses from infected cell culture fluids. *Applied Microbiology* **23**, 158-160.

Deubel, V., Kinney, R. M. & Trent, D. W. (1988). Nucleotide sequence and deduced amino acid sequence of the nonstructural proteins of dengue type 2 virus, Jamaica genotype: comparative analysis of the full-length genome. *Virology* **165**, 234-244.

Dharakul, T., Kurane, I., Bhamarapravati, N., Yoksan, S., Vaughn, D. W., Hoke, C. H. & Ennis, F. A. (1994). Dengue virus-specific memory T cell responses in human volunteers receiving a live attenuated dengue virus type 2 candidate vaccine. *Journal of Infectious Diseases* **170**, 27-33.

Diamond, S. E. & Kirkegaard, K. (1994). Clustered charged-to-alanine mutagenesis of poliovirus RNA-dependent RNA polymerase yields multiple temperature-sensitive mutants defective in RNA synthesis. *Journal of Virology* **68**, 863-876.

Droll, D. A., Krishna Murthy, H. M. & Chambers, T. J. (2000). Yellow fever virus NS2B-NS3 protease: charged-to-alanine mutagenesis and deletion analysis define regions important for protease complex fromation and function. *Virology* **275**, 335-347.

Eagles, R. M., Balmori-Melian, E., Beck, D. L., Gardner, R. C. & Forster, R. L. (1994). Characterization of NTPase, RNA-binding and RNA-helicase activities of the cytoplasmic inclusion protein of tamarillo mosaic potyvirus. *European Journal of Biochemistry* **224**, 677-684.

Eckart, M. R., Selby, M., Masiarz, F., Lee, C., Berger, K., Crawford, K., Kuo, C., Kuo, G., Houghton, M. & Choo, Q. L. (1993). The hepatitis C virus encodes a serine protease involved in processing of the putative

nonstructural proteins from the viral polyprotein precursor. *Biochemical and Biophysical research communication* **192**, 399-406.

Eckels, K. H., Scott, R. M., Bancroft, W. H., Brown, J., Dubois, D. R., Summers, P. L., Russell, P. K. & Halstead, S. B. (1984). Selection of attenuated dengue 4 viruses by serial passage in primary kidney cells. V. Human response to immunization with a candidate vaccine prepared in fetal rhesus lung cells. *American Journal of Tropical Medicine & Hygiene* **33**, 684-689.

Edelman, R., Tacket, C. O., Wasserman, S. S., Vaughn, D. W., Eckels, K. H., Dubois, D. R., Summers, P. L. & Hoke, C. H. (1994). A live attenuated dengue-1 vaccine candidate (45AZ5) passaged in primary dog kidney cell culture is attenuated and immunogenic for humans. *Journal of Infectious Diseases* **170**, 1448-1455.

Failla, C., Tomei, L. & De Francesco, R. (1994). Both NS3 and NS4A are required for proteolytic processing of hepatitis C virus nonstructural proteins. *Journal of Virology* **68**, 3753-3760.

Falgout, B., Chanock, R. & Lai, C. J. (1989). Proper processing of dengue virus nonstructural glycoprotein NS1 requires the N-terminal hydrophobic signal sequence and the downstream nonstructural protein NS2A. *Journal of Virology* **63**, 1852-1860.

Falgout, B. & Markoff, L. (1995). Evidence that flavivirus NS1-NS2A cleavage is mediated by a membrane-bound host protease in the endoplasmic reticulum. *Journal of Virology* **69**, 7232-7243.

Falgout, B., Miller, R. H. & Lai, C. J. (1993). Deletion analysis of dengue virus type 4 nonstructural protein NS2B: identification of a domain required for NS2B-NS3 protease activity. *Journal of Virology* **67**, 2034-2042.

Falgout, B., Pethel, M., Zhang, Y. M. & Lai, C. J. (1991). Both nonstructural proteins NS2B and NS3 are required for the proteolytic processing of dengue virus nonstructural proteins. *Journal of Virology* **65**, 2467-2475.

Forwood, J. K., Brooks, A., Briggs, L. J., Xiao, C. Y., Jans, D. A. & Vasudevan, S. G. (1999). The 37-amino-acid interdomain of dengue virus

NS5 protein contains a functional NLS and inhibitory CK2 site. *Biochemical & Biophysical Research Communications* **257**, 731-737.

Fu, J., Tan, B. H., Yap, E. H., Chan, Y. C. & Tan, Y. H. (1992). Full-length cDNA sequence of dengue type 1 virus (Singapore strain S275/90). *Virology* **188**, 953-958.

Fuller-Pace, F. V. (1994). RNA helicases: modulators of RNA structure. *Trends in cell biology* **4**, 271-274.

Gallinari, P., Brennan, D., Nardi, C., Brunetti, M., Tomei, L., Steinkuhler, C. & De Francesco, R. (1998). Multiple enzymatic activities associated with recombinant NS3 protein of hepatitis C virus. *Journal of Virology* **72**, 6758-6769.

Gavin, D. K., Young, S. M., Jr., Xiao, W., Temple, B., Abernathy, C. R., Pereira, D. J., Muzyczka, N. & Samulski, R. J. (1999). Charge-to-alanine mutagenesis of the adeno-associated virus type 2 Rep78/68 proteins yields temperature-sensitive and magnesium-dependent variants. *Journal of Virology* **73**, 9433-9445.

Gibbs, C. S. & Zoller, M. J. (1991). Rational scanning mutagenesis of a protein kinase identifies functional regions involved in catalysis and substrate interactions. *Journal of Biological Chemistry* **266**, 8923-8931.

Gorbalenya, A. E. & Koonin, E. V. (1989). Viral proteins containing the purine NTP-binding sequence pattern. *Nucleic Acids Research* **17**, 8413-8440.

Gould, E. A., Buckley, A., Higgs, S. & Gaidamovick, S. (1990). Antigenicity of flaviviruses. *Archives of Virology* **Suppl 1**, 137-152.

Grassmann, C. W., Isken, O. & Behrens, S. E. (1999). Assignment of the multifunctional NS3 protein of bovine viral diarrhea virus during RNA replication: an in vivo and in vitro study. *Journal of Virology* **73**, 9196-9205.

Greber, U. F., Singh, I. & Helenius, A. (1994). Mechanisms of virus uncoating. *Trends in Microbiology* **2**, 52-56.

Gritsun, T. S., Desai, A. & Gould, E. A. (2001). The degree of attenuation of tick-bourne encephalitis virus depends on the cumulative effects of point mutations. *Journal of General Virology* **82**, 1667-1675.

Gross, C. H. & Shuman, S. (1995). Mutational analysis of vaccinia virus nucleoside triphosphate phosphohydrolase II, a DExH box RNA helicase. *Journal of Virology* **69**, 4727-4736.

Gross, C. H. & Shuman, S. (1996*a*). The QRxGRxGRxxxG motif of the vaccinia virus DExH box RNA helicase NPH-II is required for ATP hydrolysis and RNA unwinding but not for RNA binding. *Journal of Virology* **70**, 1706-1713.

Gross, C. H. & Shuman, S. (1996*b*). Vaccinia virus RNA helicase: nucleic acid specificity in duplex unwinding. *Journal of Virology* **70**, 2615-2619.

Gruenberg, A. & Wright, P. J. (1992). Processing of dengue virus type 2 structural proteins containing deletions in hydrophobic domains. *Archives of Virology* **122**, 77-94.

Gu, B., Liu, C., Lin-Goerke, J., Maley, D. R., Gutshall, L. L., Feltenberger, C. A. & Del Vecchio, A. M. (2000). The RNA helicase and nucleotide triphosphatase activities of the bovine viral diarrhea virus NS3 protein are essential for viral replication. *Journal of Virology* **74**, 1794-1800.

Gualano, R. C., Pryor, M. J., Cauchi, M. R., Wright, P. J. & Davidson, A. D. (1998). Identification of a major determinant of mouse neurovirulence of dengue virus type 2 using stably cloned genomic-length cdna. *Journal of General Virology* **79**, 437-446.

Guirakhoo, F., Arroyo, J., Pugachev, K. V., Miller, C., Zhang, Z. X., Weltzin, R., Georgakopoulos, K., Catalan, J., Ocran, S., Soike, K., Ratterree, M. & Monath, T. P. (2001). Construction, safety, and immunogenicity in nonhuman primates of a chimeric yellow fever-dengue virus tetravalent vaccine. *Journal of Virology* **75**, 7290-7304.

Guirakhoo, F., Heinz, F. X. & Kunz, C. (1989). Epitope model of tick-borne encephalitis virus envelope glycoprotein E: analysis of structural properties, role of carbohydrate side chain, and conformational changes occurring at acidic pH. *Virology* **169**, 90-99.

Guirakhoo, F., Heinz, F. X., Mandl, C. W., Holzmann, H. & Kunz, C. (1991). Fusion activity of flaviviruses: comparison of mature and immature (prM-containing) tick-borne encephalitis virions. *Journal of General Virology* **72**, 1323-1329.

Guirakhoo, F., Weltzin, R., Chambers, T. J., Zhang, Z. X., Soike, K., Ratterree, M., Arroyo, J., Georgakopoulos, K., Catalan, J. & Monath, T. P. (2000). Recombinant chimeric yellow fever-dengue type 2 virus is immunogenic and protective in nonhuman primates. *Journal of Virology* **74**, 5477-5485.

Guyatt, K. (1999). Recombinant Kunjin virus NS5 protein exhibits RNA-dependent RNA polymerase activity *in vitro*., p. 120. In *XIth International congress of virology*. Sydney, Australia.

Gwack, Y., Kim, D. W., Han, J. H. & Choe, J. (1996). Characterization of RNA binding activity and RNA helicase activity of the hepatitis C virus NS3 protein. *Biochemical & Biophysical Research Communications* **225**, 654-659.

Gwack, Y., Kim, D. W., Han, J. H. & Choe, J. (1997). DNA helicase activity of the hepatitis C virus nonstructural protein 3. *European Journal of Biochemistry* **250**, 47-54.

Gwack, Y., Yoo, H., Song, I., Choe, J. & Han, J. H. (1999). RNA-Stimulated ATPase and RNA helicase activities and RNA binding domain of hepatitis G virus nonstructural protein 3. *Journal of Virology* **73**, 2909-2915.

Hahn, C. S., Dalrymple, J. M., Strauss, J. H. & Rice, C. M. (1987*a*). Comparison of the virulent Asibi strain of yellow fever virus with the 17D vaccine strain derived from it. *Proceedings of the National Academy of Sciences of the United States of America* **84**, 2019-2023.

Hahn, C. S., Hahn, Y. S., Rice, C. M., Lee, E., Dalgarno, L., Strauss, E. G. & Strauss, J. H. (1987*b*). Conserved elements in the 3' untranslated region of flavivirus RNAs and potential cyclization sequences. *Journal of Molecular Biology* **198**, 33-41.

Hahn, Y. S., Galler, R., Hunkapiller, T., Dalrymple, J. M., Strauss, J. H. & Strauss, E. G. (1988). Nucleotide sequence of dengue 2 RNA and comparison of the encoded proteins with those of other flaviviruses. *Virology* **162**, 167-180.

Halstead, S. B. (1988). Pathogenesis of dengue: challenges to molecular biology. *Science* **239**, 476-481.

Halstead, S. B. & O'Rourke, E. J. (1977*a*). Antibody-enhanced dengue virus infection in primate leukocytes. *Nature* **265**, 739-741.

Halstead, S. B. & O'Rourke, E. J. (1977*b*). Dengue viruses and mononuclear phagocytes. I. Infection enhancement by non-neutralizing antibody. *Journal of Experimental Medicine* **146**, 201-217.

Halstead, S. B., O'Rourke, E. J. & Allison, A. C. (1977). Dengue viruses and mononuclear phagocytes. II. Identity of blood and tissue leukocytes supporting in vitro infection. *Journal of Experimental Medicine* **146**, 218-229.

Hammon, W. M., Rudnick, A. & Sather, G. E. (1960). Viruses associated with epidemic hemorrhagic fevers in the Phillipines and Thailand. *Science* **131**, 1102-1103.

Hanahan, D. (1985). Techniques for transformation of *E. coli*. In *DNA Cloning: a pratical approach*, pp. 109-135. Edited by D. M. Glover. Oxford: IRL Press.

Hase, T., Summers, P. L. & Eckels, K. H. (1989). Flavivirus entry into cultured mosquito cells and human peripheral blood monocytes. *Archives of Virology* **104**, 129-143.

Heilek, G. M. & Peterson, M. G. (1997). A point mutation abolishes the helicase but not the nucleoside triphosphatase activity of hepatitis C virus NS3 protein. *Journal of Virology* **71**, 6264-6266.

Heinz, F. X., Stiasny, K., Puschner-Auer, G., Holzmann, H., Allison, S. L., Mandl, C. W. & Kunz, C. (1994). Structural changes and functional control of the tick-borne encephalitis virus glycoprotein E by the heterodimeric association with protein prM. *Virology* **198**, 109-117.

Ho, S. N., Hunt, H. D., Horton, R. M., Pullen, J. K. & Pease, L. R. (1989). Site-directed mutagenesis by overlap extension using the polymerase chain reaction. *Gene* **77**, 51-59.

Holbrook, M. R., Li, L., Suderman, M. T., Wang, H. & Barrett, A. D. T. (2000). The French neurotropic vaccine strain of yellow fever virus accumulates mutations slowly during passage in cell culture. *Virus Research* **69**, 31-39.

Hong, Z., Ferrari, E., Wright-Minogue, J., Chase, R., Risano, C., Seelig, G., Lee, C. G. & Kwong, A. D. (1996). Enzymatic characterization of hepatitis C virus NS3/4A complexes expressed in mammalian cells by using the herpes simplex virus amplicon system. *Journal of Virology* **70**, 4261-4268.

Hopp, T. P. & Woods, K. R. (1981). Prediction of protein antigenic determinants from amino acid sequences. *Proceedings of the National Academy of Sciences of the United States of America* **78**, 3824-3828.

Hori, H. & Lai, C. J. (1990). Cleavage of dengue virus NS1-NS2A requires an octapeptide sequence at the C terminus of NS1. *Journal of Virology* **64**, 4573-4577.

Huang, C. Y., Butrapet, S., Pierro, D. J., Chang, G. J., Hunt, A. R., Bhamarapravati, N., Gubler, D. J. & Kinney, R. M. (2000). Chimeric dengue type 2 (vaccine strain PDK-53)/dengue type 1 virus as a potential candidate dengue type 1 virus vaccine. *Journal of Virology* **74**, 3020-3028.

Huang, M., Zensen, R., Cho, M. & Martin, M. A. (1998). Construction and characterization of a temperature-sensitive human immunodeficiency virus type 1 reverse transcriptase mutant. *Journal of Virology* **72**, 2047-54.

Irie, K., Mohan, P. M., Sasaguri, Y., Putnak, R. & Padmanabhan, R. (1989). Sequence analysis of cloned dengue virus type 2 genome (New Guinea-C strain). *Gene* **75**, 197-211.

Jacobs, M. G., Robinson, P. J., Bletchly, C., Mackenzie, J. M. & Young, P. R. (2000). Dengue virus nonstructural protein 1 is expressed in a glycosyl-phosphatidylinositol-linked form that is capable of signal transduction. *FASEB Journal* **14**, 1603-1610.

Jan, L.-R., Yang, C.-S., Trent, D. W., Falgout, B. & Lai, C.-J. (1995). Processing of Japanese encephalitis virus nonstructural proteins: NS2B-NS3 complex and heterologous proteases. *Journal of General Virology* **76**, 573-580.

Jin, L. & Peterson, D. L. (1995). Expression, isolation, and characterization of the hepatitis C virus ATPase/RNA helicase. *Archives of Biochemistry & Biophysics* **323**, 47-53.

Kanai, A., Tanabe, K. & Kohara, M. (1995). Poly(U) binding activity of hepatitis C virus NS3 protein, a putative RNA helicase. *FEBS Letters* **376**, 221-224.

Kapoor, M., Zhang, L. W., Ramachandra, M., Kusukawa, J., Ebner, K. E. & Padmanabhan, R. (1995). Association between NS3 and NS5 proteins of dengue virus type 2 in the putative RNA replicase is linked to differential phosphorylation of NS5. *Journal of Biological Chemistry* **270**, 19100-19106.

Kaufman, B. M., Summers, P. L., Dubois, D. R., Cohen, W. H., Gentry, M. K., Timchak, R. L., Burke, D. S. & Eckels, K. H. (1989). Monoclonal antibodies for dengue virus prM glycoprotein protect mice against lethal dengue infection. *American Journal of Tropical Medicine & Hygiene* **41**, 576-580.

Kelley, P. G. (1996). Mutagenesis of hydrophillic and hydrophobic regions within the protease domain of dengue virus type 2 nonstructural protein NS3. Honours Thesis, *Department of Microbiology*. Clayton: Monash University.

Khromykh, A. A., Kenney, M. T. & Westaway, E. G. (1998). trans-Complementation of flavivirus RNA polymerase gene NS5 by using Kunjin virus replicon-expressing BHK cells. *Journal of Virology* **72**, 7270-7279.

Khromykh, A. A., Sedlak, P. L., Guyatt, K. J., Hall, R. A. & Westaway, E. G. (1999*a*). Efficient trans-complementation of the flavivirus kunjin NS5 protein but not of the NS1 protein requires its coexpression with other components of the viral replicase. *Journal of Virology* **73**, 10272-10280.

Khromykh, A. A., Sedlak, P. L. & Westaway, E. G. (1999*b*). trans-Complementation analysis of the flavivirus Kunjin NS5 gene reveals an essential role for translation of its N-terminal half in RNA replication. *Journal of Virology* **73**, 9247-9255.

Khromykh, A. A., Sedlak, P. L. & Westaway, E. G. (2000). cis- and trans-acting elements in flavivirus RNA replication. *Journal of Virology* **74**, 3253-3263.

Khu, Y.-L., Koh, E., Lim, S. P., Tan, Y. H., Brenner, S., Lim, S. G., Hong, W. J. & Goh, P. (2001). Mutations that affect dimer formation and helicase activity of the hepatitis C virus helicase. *Journal of Virology* **75**, 205-214.

Kim, D. W., Gwack, Y., Han, J. H. & Choe, J. (1995). C-terminal domain of the hepatitis C virus NS3 protein contains an RNA helicase activity. *Biochemical & Biophysical Research Communications* **215**, 160-166.

Kim, D. W., Gwack, Y., Han, J. H. & Choe, J. (1997*a*). Towards defining a minimal functional domain for NTPase and RNA helicase activities of the hepatitis C virus NS3 protein. *Virus Research* **49**, 17-25.

Kim, D. W., Kim, J., Gwack, Y., Han, J. H. & Choe, J. (1997*b*). Mutational analysis of the hepatitis C virus RNA helicase. *Journal of Virology* **71**, 9400-9409.

Kim, J. L., Morgenstern, K. A., Griffith, J. P., Dwyer, M. D., Thomson, J. A., Murcko, M. A., Lin, C. & Caron, P. R. (1998). Hepatitis C virus NS3 RNA helicase domain with a bound oligonucleotide: the crystal structure provides insights into the mode of unwinding. *Structure* **6**, 89-100.

Kim, J. L., Morgenstern, K. A., Lin, C., Fox, T., Dwyer, M. D., Landro, J. A., Chambers, S. P., Markland, W., Lepre, C. A., O'Malley, E. T., Harbeson, S. L., Rice, C. M., Murcko, M. A., Caron, P. R. & Thomson, J. A. (1996). Crystal structure of the hepatitis C virus NS3 protease domain complexed with a synthetic NS4A cofactor peptide. *Cell* **87**, 343-355.

Kimura, T. & Ohyama, A. (1988). Association between the pH-dependent conformational change of West Nile flavivirus E protein and virus-mediated membrane fusion. *Journal of General Virology* **69**, 1247-1254.

Kinney, R. M., Butrapet, S., Chang, G. J., Tsuchiya, K. R., Roehrig, J. T., Bhamarapravati, N. & Gubler, D. J. (1997). Construction of infectious cDNA clones for dengue 2 virus: strain 16681 and its attenuated vaccine derivative, strain PDK-53. *Virology* **230**, 300-308.

Koch, J. O., Lohmann, V., Herian, U. & Bartenschlager, R. (1996). In vitro studies on the activation of the hepatitis C virus NS3 proteinase by the NS4A cofactor. *Virology* **221**, 54-66.

Koonin, E. V. (1991). The phylogeny of RNA-dependent RNA polymerases of positive-strand RNA viruses. *Journal of General Virology* **72**, 2197-2206.

Koonin, E. V. & Dolja, V. V. (1993). Evolution and taxonomy of positive-strand RNA viruses: implications of comparative analysis of amino acid sequences. *Critical Reviews in Biochemistry & Molecular Biology* **28**, 375-430.

Korolev, S., Hsieh, J., Gauss, G. H., Lohman, T. M. & Waksman, G. (1997). Major domain swiveling revealed by the crystal structures of complexes of E. coli Rep helicase bound to single-stranded DNA and ADP. *Cell* **90**, 635-647.

Korolev, S., Yao, N., Lohman, T. M., Weber, P. C. & Waksman, G. (1998). Comparisons between the structures of HCV and Rep helicases reveal structural similarities between SF1 and SF2 super-families of helicases. *Protein Science* **7**, 605-610.

Kuno, G., Chang, G. J., Tsuchiya, K. R., Karabatsos, N. & Cropp, C. B. (1998). Phylogeny of the genus Flavivirus. *Journal of Virology* **72**, 73-83.

Kuo, M. D., Chin, C., Hsu, S. L., Shiao, J. Y., Wang, T. M. & Lin, J. H. (1996). Characterization of the NTPase activity of Japanese encephalitis virus NS3 protein. *Journal of General Virology* **77**, 2077-2084.

Kurane, I., Rothman, A. L., Livingston, P. G., Green, S., Gagnon, S. J., Janus, J., Innis, B. L., Nimmannitya, S., Nisalak, A. & Ennis, F. A. (1994). Immunopathologic mechanisms of dengue hemorrhagic fever and dengue shock syndrome. *Archives of Virology* **Suppl 9**, 59-64.

Kwong, A. D., Kim, J. L. & Lin, C. (2000). Structure and function of hepatitis C virus NS3 helicase. *Current Topics in Microbiology & Immunology* **242**, 171-196.

Kyte, J. & Doolittle, R. F. (1982). A simple method for displaying the hydropathic character of a protein. *Journal of Molecular Biology* **157**, 105-132.

Laemmli, U. K. (1970). Cleavage of structural proteins during assembly of the head of bacteriophage T4. *Nature* **227**, 680-685.

Lai, C. J., Zhao, B. T., Hori, H. & Bray, M. (1991). Infectious RNA transcribed from stably cloned full-length cDNA of dengue type 4 virus. *Proceedings of the National Academy of Sciences of the United States of America* **88**, 5139-5143.

Lain, S., Riechmann, J. L. & Garcia, J. A. (1990). RNA helicase: a novel activity associated with a protein encoded by a positive strand RNA virus. *Nucleic Acids Research* **18**, 7003-7006.

Lain, S., Riechmann, J. L., Martin, M. T. & Garcia, J. A. (1989). Homologous potyvirus and flavivirus proteins belonging to a superfamily of helicase-like proteins. *Gene* **82**, 357-362.

Laxton, C. D., Mcmillan, D., Sullivan, V. & Ackrill, A. M. (1998). Expression and characterization of the hepatitis G virus helicase. *Journal of Viral Hepatitis* **5**, 21-26.

Lee, E., Stocks, C. E., Amberg, S. M., Rice, C. M. & Lobigs, M. (2000). Mutagenesis of the signal sequence of yellow fever virus prM protein: enhancement of signalase cleavage In vitro is lethal for virus production. *Journal of Virology* **74**, 24-32.

Leitmeyer, K. C., Vaughn, D. W., Watts, D. M., Salas, R., Villalobos, I., de, C., Ramos, C. & Rico-Hesse, R. (1999). Dengue virus structural differences that correlate with pathogenesis. *Journal of Virology* **73**, 4738-4747.

Levin, M. K. & Patel, S. S. (1999). The helicase from hepatitis C virus is active as an oligomer. *Journal of Biological Chemistry* **274**, 31839-31846.

Lewis, J. G., Chang, G. J., Lanciotti, R. S. & Trent, D. W. (1992). Direct sequencing of large flavivirus PCR products for analysis of genome variation and molecular epidemiological investigations. *Journal of Virological Methods* **38**, 11-23.

Li, H. T., Clum, S., You, S. H., Ebner, K. E. & Padmanabhan, R. (1999). The serine protease and RNA-stimulated nucleoside triphosphatase and RNA helicase functional domains of dengue virus type 2 NS3 converge within a region of 20 amino acids. *Journal of Virology* **73**, 3108-3116.

Lim, H. Y. & Ng, M. L. (1999). A different mode of entry by dengue-2 neutralisation escape mutant virus. *Archives of Virology* **144**, 989-995.

Lin, C., Amberg, S. M., Chambers, T. J. & Rice, C. M. (1993*a*). Cleavage at a novel site in the NS4A region by the yellow fever virus NS2B-3 proteinase is a prerequisite for processing at the downstream 4A/4B signalase site. *Journal of Virology* **67**, 2327-2335.

Lin, C., Chambers, T. J. & Rice, C. M. (1993*b*). Mutagenesis of conserved residues at the yellow fever virus 3/4A and 4B/5 dibasic cleavage sites: effects on cleavage efficiency and polyprotein processing. *Virology* **192**, 596-604.

Lin, C. & Kim, J. L. (1999). Structure-based mutagenesis study of hepatitis C virus NS3 helicase. *Journal of Virology* **73**, 8798-8807.

Lin, C., Thomson, J. A. & Rice, C. M. (1995). A central region in the hepatitis C virus NS4A protein allows formation of an active NS3-NS4A serine proteinase complex in vivo and in vitro. *Journal of Virology* **69**, 4373-4380.

Lindenbach, B. D. & Rice, C. M. (1997). trans-Complementation of yellow fever virus NS1 reveals a role in early RNA replication. *Journal of Virology* **71**, 9608-9617.

Lindenbach, B. D. & Rice, C. M. (1999). Genetic interaction of flavivirus nonstructural proteins NS1 and NS4A as a determinant of replicase function. *Journal of Virology* **73**, 4611-4621.

Lobigs, M. (1992). Proteolytic processing of a Murray Valley encephalitis virus non-structural polyprotein segment containing the viral proteinase: accumulation of a NS3-4A precursor which requires mature NS3 for efficient processing. *Journal of General Virology* **73**, 2305-2312.

Lobigs, M. (1993). Flavivirus premembrane protein cleavage and spike heterodimer secretion require the function of the viral proteinase NS3. *Proceedings of the National Academy of Sciences of the United States of America* **90**, 6218-6222.

Love, R. A., Parge, H. E., Wickersham, J. A., Hostomsky, Z., Habuka, N., Moomaw, E. W., Adachi, T. & Hostomska, Z. (1996). The crystal structure

of hepatitis C virus NS3 proteinase reveals a trypsin-like fold and a structural zinc binding site. *Cell* **87**, 331-342.

Luking, A., Stahl, U. & Schmidt, U. (1998). The protein family of RNA helicases. *Critical Reviews in Biochemistry & Molecular Biology* **33**, 259-296.

Lum, L. C., Lam, S. K., Choy, Y. S., George, R. & Harun, F. (1996). Dengue encephalitis: a true entity? *American Journal of Tropical Medicine and Hygiene* **54**, 256-259.

Machius, M., Henry, L., Palnitkar, M. & Deisenhofer, J. (1999). Crystal structure of the DNA nucleotide excision repair enzyme UvrB from Thermus thermophilus. *Proceedings of the National Academy of Sciences of the United States of America* **96**, 11717-11722.

Mackenzie, J. M., Jones, M. K. & Westaway, E. G. (1999). Markers for trans-Golgi membranes and the intermediate compartment localize to induced membranes with distinct replication functions in flavivirus-infected cells. *Journal of Virology* **73**, 9555-9567.

Mackenzie, J. M., Jones, M. K. & Young, P. R. (1996). Immunolocalization of the dengue virus nonstructural glycoprotein NS1 suggests a role in viral RNA replication. *Virology* **220**, 232-240.

Mackenzie, J. M., Khromykh, A. A., Jones, M. K. & Westaway, E. G. (1998). Subcellular localization and some biochemical properties of the flavivirus Kunjin nonstructural proteins NS2A and NS4A. *Virology* **245**, 203-215.

Mackow, E., Makino, Y., Zhao, B. T., Zhang, Y. M., Markoff, L., Buckler, W. A., Guiler, M., Chanock, R. & Lai, C. J. (1987). The nucleotide sequence of dengue type 4 virus: analysis of genes coding for nonstructural proteins. *Virology* **159**, 217-228.

Mandl, C. W., Guirakhoo, F., Holzmann, H., Heinz, F. X. & Kunz, C. (1989*a*). Antigenic structure of the flavivirus envelope protein E at the molecular level, using tick-borne encephalitis virus as a model. *Journal of Virology* **63**, 564-571.

Monath, T. P. (1994). Dengue: the risk to developed and developing countries. *Proceedings of the National Academy of Sciences of the United States of America* **91**, 2395-2400.

Monath, T. P. & Heinz, F. X. (1996). Flaviviruses. In *Fields Virology*. Edited by B. N. Fields, D. M. Knipe, P. M. Howley, R. M. Chanock, J. L. Melnick, T. P. Monath, B. Roizman & S. E. Straus. Philadelphia, Pa.: Lippincott-Raven.

Murphy, F. A. (1980). Togavirus morphology and morphogenesis. In *The Togaviruses: Biology, Structure, Replication.*, pp. 241-316. Edited by R. W. Schlesinger. New York: Academic Press.

Murray, J. M., Aaskov, J. G. & Wright, P. J. (1993). Processing of the dengue virus type 2 proteins prM and C-prM. *Journal of General Virology* **74**, 175-182.

Murthy, H., Clum, S. & Padmanabhan, R. (1999). Dengue virus NS3 serine protease - Crystal structure and insights into interaction of the active site with substrates by molecular modeling and structural analysis of mutational effects. *Journal of Biological Chemistry* **274**, 5573-5580.

Muylaert, I. R., Galler, R. & Rice, C. M. (1997). Genetic analysis of the yellow fever virus NS1 protein - identification of a temperature-sensitive mutation which blocks RNA accumulation. *Journal of Virology* **71**, 291-298.

Nestorowicz, A., Chambers, T. J. & Rice, C. M. (1994). Mutagenesis of the yellow fever virus NS2A/2B cleavage site: effects on proteolytic processing, viral replication, and evidence for alternative processing of the NS2A protein. *Virology* **199**, 114-123.

Ni, H., Burns, N. J., Chang, G. J., Z' ang, M. J., Wills, M. R., Trent, D. W., Sanders, P. G. & Barrett, A. D. (.٩٩4). Comparison of nucleotide and deduced amino acid sequence of the 5' non-coding region and structural protein genes of the wild-type Japanese encephalitis virus strain SA14 and its attenuated vaccine derivatives. *Journal of General Virology* **75**, 1505-1510.

Nimmannitya, S. (1987). Clinical spectrum and management of dengue haemorrhagic fever. *Southeast Asian Journal of Tropical Medicine & Public Health* **18**, 392-397.

Nowak, T., Farber, P. M., Wengler, G. & Wengler, G. (1989). Analyses of the terminal sequences of West Nile virus structural proteins and of the in vitro translation of these proteins allow the proposal of a complete scheme of the proteolytic cleavages involved in their synthesis. *Virology* **169**, 365-376.

Nowak, T. & Wengler, G. (1987). Analysis of disulfides present in the membrane proteins of the West Nile flavivirus. *Virology* **156**, 127-137.

O'Reilly, E. K. & Kao, C. C. (1998). Analysis of RNA-dependent RNA polymerase structure and function as guided by known polymerase structures and computer predicitons of secondary structure. *Virology* **252**, 287-303.

Osatomi, K. & Sumiyoshi, H. (1990). Complete nucleotide sequence of dengue type 3 virus genome RNA. *Virology* **176**, 643-647.

Pai, E. F., Krengel, U., Petsko, G. A., Goody, R. S., Kabsch, W. & Wittinghofer, A. (1990). Refined crystal structure of the triphosphate conformation of H-ras p21 at 1.35 Å resolution: implications for the mechanism of GTP hydrolysis. *EMBO Journal* **9**, 2351-2359.

Paolini, C., De Francesco, R. & Gallinari, P. (2000*a*). Enzymatic properties of hepatitis C virus NS3-associated helicase. *Journal of General Virology* **81**, 1335-1345.

Paolini, C., Lahm, A., De Francesco, R. & Gallinari, P. (2000*b*). Mutational analysis of hepatitis C virus NS3-associated helicase. *Journal of General Virology* **81**, 1649-1658.

Parkin, N. T., Chiu, P. & Coelingh, K. L. (1996). Temperature sensitive mutants of influenza A virus generated by reverse genetics and clustered charged to alanine mutagenesis. *Virus Research* **46**, 31-44.

Pause, A., Methot, N. & Sonenberg, N. (1993). The HRIGRXXR region of the DEAD box RNA helicase eukaryotic translation initiation factor 4A is required for RNA binding and ATP hydrolysis. *Molecular & Cellular Biology* **13**, 6789-6798.

Pethel, M., Falgout, B. & Lai, C. J. (1992). Mutational analysis of the octapeptide sequence motif at the NS1-NS2A cleavage junction of dengue type 4 virus. *Journal of Virology* **66**, 7225-7231.

Pletnev, A. G., Yamshchikov, V. F. & Blinov, V. M. (1990). Nucleotide sequence of the genome and complete amino acid sequence of the polyprotein of tick-borne encephalitis virus. *Virology* **174**, 250-263.

Porter, D. J., Short, S. A., Hanlon, M. H., Preugschat, F., Wilson, J. E., Willard, D. H., Jr. & Consler, T. G. (1998). Product release is the major contributor to k_{cat} for the hepatitis C virus helicase-catalyzed strand separation of short duplex DNA. *Journal of Biological Chemistry* **273**, 18906-18914.

Porterfield, J. S. (1985). Antibody enhanced viral growth in macrophages. *Immunology Letters* **11**, 213-217.

Preugschat, F., Averett, D. R., Clarke, B. E. & Porter, D. J. T. (1996). A steady-state and pre-steady-state kinetic analysis of the NTPase activity associated with the hepatitis C virus NS3 helicase domain. *Journal of Biological Chemistry* **271**, 24449-24457.

Preugschat, F. & Strauss, J. H. (1991). Processing of nonstructural proteins NS4A and NS4B of dengue 2 virus in vitro and in vivo. *Virology* **185**, 689-697.

Preugschat, F., Yao, C. W. & Strauss, J. H. (1990). In vitro processing of dengue virus type 2 nonstructural proteins NS2A, NS2B, and NS3. *Journal of Virology* **64**, 4364-4374.

Pryor, M. J., Carr, J. M., Hocking, H., Davidson, A. D. & Wright, P. J. (2001). Replication of dengue virus type 2 in human monocyte-derived macrophages: comparisons of isolates and recombinant viruses with substitutions at amino acid 390 in the envelope glycoprotein. *American Journal of Tropical Medicine & Hygiene*, in press.

Pryor, M. J. & Wright, P. J. (1993). The effects of site-directed mutagenesis on the dimerization and secretion of the NS1 protein specified by dengue virus. *Virology* **194**, 769-780.

Pugachev, K. V., Nomokonova, N. Y., Dobrikova, E. & Wolf, Y. I. (1993). Site-directed mutagenesis of the tick-borne encephalitis virus NS3 gene reveals the putative serine protease domain of the NS3 protein. *Febs Letters* **328**, 115-8.

Pugachev, K. V., Nomokonova, N., Morozova, O. V. & Pletnev, A. G. (1992). A short form of the tick-borne encephalitis virus NS3 protein. *Febs Letters* **297**, 67-69.

Puri, B., Nelson, W. M., Henchal, E. A., Hoke, C. H., Eckels, K. H., Dubois, D. R., Porter, K. R. & Hayes, C. G. (1997). Molecular analysis of dengue virus attenuation after serial passage in primary dog kidney cells. *Journal of General Virology* **78**, 2287-2291.

Randolph, V. B., Winkler, G. & Stollar, V. (1990). Acidotropic amines inhibit proteolytic processing of flavivirus prM protein. *Virology* **174**, 450-458.

Rey, F. A., Heinz, F. X., Mandl, C., Kunz, C. & Harrison, S. C. (1995). The envelope glycoprotein from tick-borne encephalitis virus at 2 Å resolution. *Nature* **375**, 291-298.

Rice, C. M. (1996). *Flaviviridae:* The viruses and their replication. In *Fields Virology*, 3rd edn, pp. 931-959. Edited by B. N. Fields, D. M. Knipe, P. M. Howley, R. M. Chanock, J. L. Melnick, T. P. Monath, B. Roizman & S. E. Straus. Philadelphia, Pa.: Lippincott-Raven.

Rice, C. M., Aebersold, R., Teplow, D. B., Pata, J., Bell, J. R., Vorndam, A. V., Trent, D. W., Brandriss, M. W., Schlesinger, J. J. & Strauss, J. H. (1986). Partial N-terminal amino acid sequences of three nonstructural proteins of two flaviviruses. *Virology* **151**, 1-9.

Rice, C. M., Lenches, E. M., Eddy, S. R., Shin, S. J., Sheets, R. L. & Strauss, J. H. (1985). Nucleotide sequence of yellow fever virus: implications for flavivirus gene expression and evolution. *Science* **229**, 726-733.

Rice, C. M. & Strauss, J. H. (1990). Production of flavivirus polypeptides by proteolytic processing. *Seminars in Virology* **1**, 357-367.

Ruiz, L. A., Cahour, A., Despres, P., Girard, M. & Bouloy, M. (1989). Processing of yellow fever virus polyprotein: role of cellular proteases in maturation of the structural proteins. *Journal of Virology* **63**, 4199-4209.

Rush, B. (1789). An account of the bilious remitting fever, as it appeared in Philadelphia in the summer and autumn of the year 1780. In *Medical Inquiries and Observations*, pp. 104. Philadelphia: Pritchard and Hall.

Ryan, C., Ivanova, L. & Schlesinger, M. J. (1998). Mutations in the Sindbis virus capsid gene can partially suppress mutations in the cytoplasmic domain of the virus E2 glycoprotein spike. *Virology* **243**, 380-387.

Sabin, A. B. & Schlesinger, R. W. (1945). Production of immunity to dengue with virus modified by propagation in mice. *Science* **101**, 640-642.

Salas-Benito, J. S. & del Angel, R. M. (1997). Identification of two surface proteins from C6/36 cells that bind dengue type 4 virus. *Journal of Virology* **71**, 7246-7252.

Sambrook, J., Fritsch, E. F. & Maniatis, T. (1989). Molecular cloning: A laboratory manual., 2nd edn. New York: Cold Spring Habor Laboratory Press.

Saraste, M., Sibbald, P. R. & Wittinghofer, A. (1990). The P-loop - a common motif in ATP- and GTP-binding proteins. *Trends in Biochemical Sciences* **15**, 430-434.

Schechter, I. & Berger, A. (1967). On the size of the active site in proteases. I. Papain. *Biochemical and Biophysical Research Communications* **27**, 157-162.

Schmid, S. R. & Linder, P. (1992). D-E-A-D protein family of putative RNA helicases. *Molecular Microbiology* **6**, 283-291.

Se-Theo, S. Y., Ling, A. E. & Ng, M. M. L. (2000). Alteration of virus entry mode: a neutralisation mechanism for dengue-2 virus. *Journal of Medical Virology* **62**, 364-376.

Shapiro, D., Brandt, W. E., Cardiff, R. D. & Russell, P. K. (1971). The proteins of Japanese encephalitis virus. *Virology* **44**, 108-124.

Shurtleff, A. C., Beasley, D. W. C., Chen, J. J. Y., Ni, H. L., Suderman, M. T., Wang, H. M., Xu, R. L., Wang, E., Weaver, S. C., Watts, D. M.,

Russell, K. L. & Barrett, A. D. T. (2001). Genetic variation in the 3' noncoding region of dengue viruses. *Virology* **281**, 75-87.

Sinniah, M. & Igarashi, A. (1995). Dengue haemorrhagic fever. *Reviews in Medical Virology* **5**, 193-203.

Speight, G., Coia, G., Parker, M. D. & Westaway, E. G. (1988). Gene mapping and positive identification of the non-structural proteins NS2A, NS2B, NS3, NS4B and NS5 of the flavivirus Kunjin and their cleavage sites. *Journal of General Virology* **69**, 23-34.

Stadler, K., Allison, S. L., Schalich, J. & Heinz, F. X. (1997). Proteolytic activation of tick-borne encephalitis virus by furin. *Journal of Virology* **71**, 8475-8481.

Stocks, C. E. & Lobigs, M. (1995). Posttranslational signal peptidase cleavage at the flavivirus C-prM junction in vitro. *Journal of Virology* **69**, 8123-8126.

Stocks, C. E. & Lobigs, M. (1998). Signal peptidase cleavage at the flavivirus C-prM junction: dependence on the viral NS2B-3 protease for efficient processing requires determinants in C, the signal peptide, and prM. *Journal of Virology* **72**, 2141-2149.

Stollar, V., Schlesinger, R. W. & Stevens, T. M. (1967). Studies on the nature of dengue viruses. III. RNA synthesis in celss infected with type 2 dengue virus. *Virology* **33**, 650-658.

Subramanya, H. S., Bird, L. E., Brannigan, J. A. & Wigley, D. B. (1996). Crystal structure of a DExx box DNA helicase. *Nature* **384**, 379-383.

Summers, P. L., Cohen, W. H., Ruiz, M. M., Hase, T. & Eckels, K. H. (1989). Flaviviruses can mediate fusion from without in Aedes albopictus mosquito cell cultures. *Virus Research* **12**, 383-392.

Suzich, J. A., Tamura, J. K., Palmer-Hill, F., Warrener, P., Grakoui, A., Rice, C. M., Feinstone, S. M. & Collett, M. S. (1993). Hepatitis C virus NS3 protein polynucleotide-stimulated nucleoside triphosphatase and comparison with the related pestivirus and flavivirus enzymes. *Journal of Virology* **67**, 6152-6158.

Tai, C. L., Chi, W. K., Chen, D. S. & Hwang, L. H. (1996). The helicase activity associated with hepatitis C virus nonstructural protein 3 (NS3). *Journal of Virology* **70**, 8477-8484.

Takegami, T., Miyamoto, H., Nakamura, H. & Yasui, K. (1982). Biological activities of the structural proteins of Japanese encephalitis virus. *Acta Virologica* **26**, 312-320.

Takegami, T., Sakamuro, D. & Furukawa, T. (1994). Japanese encephalitis nonstructural protein NS3 has RNA binding and ATPase activities. *Virus Genes* **9**, 105-112.

Tamura, J. K., Warrener, P. & Collett, M. S. (1993). RNA-stimulated NTPase activity associated with the p80 protein of the pestivirus bovine viral diarrhea virus. *Virology* **193**, 1-10.

Tan, B. H., Fu, J., Sugrue, R. J., Yap, E. H., Chan, Y. C. & Tan, Y. H. (1996). Recombinant dengue type 1 virus NS5 protein expressed in Escherichia coli exhibits RNA-dependent RNA polymerase activity. *Virology* **216**, 317-325.

Teo, K. F. & Wright, P. J. (1997). Internal proteolysis of the ns3 protein specified by dengue virus 2. *Journal of General Virology* **78**, 337-341.

Theiler, M. & Smith, H. H. (1937). The effect of prolonged cultivation in vitro upon the pathogenicity of yellow fever virus. *Journal of Experimental Medicine* **65**, 767-786.

Theis, K., Chen, P. J., Skorvaga, M., Van Houten, B. & Kisker, C. (1999). Crystal structure of UvrB, a DNA helicase adapted for nucleotide excision repair. *EMBO Journal* **18**, 6899-6907.

Tolou, H. J., Couissinier-Paris, P., Durand, J. P., Mercier, V., de Pina, J. J., de Micco, P., Billoir, F., Charrel, R. N. & de Lamballerie, X. (2001). Evidence for recombination in natural populations of dengue virus type 1 based on the analysis of complete genome sequences. *Journal of General Virology* **82**, 1283-1290.

Tomei, L., Failla, C., Vitale, R. L., Bianchi, E. & De Francesco, R. (1996). A central hydrophobic domain of the hepatitis C virus NS4A protein is

necessary and sufficient for the activation of the NS3 protease. *Journal of General Virology* **77**, 1065-1070.

Trent, D. W., Kinney, R. M. & Huang, C. Y.-H. (1997). Recombinant dengue virus vaccines. In *Dengue and dengue hemorrhagic fever.*, pp. 379-403. Edited by D. J. Gubler & G. Kuno. Wallingford: CAB INTERNATIONAL.

Utama, A., Shimizu, H., Hasebe, F., Morita, K., Igarashi, A., Shoji, I., Matsuura, Y., Hatsu, M., Takamizawa, K., Hagiwara, A. & Miyamura, T. (2000*a*). Role of the DExH motif of the Japanese encephalitis virus and hepatitis C virus NS3 proteins in the ATPase and RNA helicase activities. *Virology* **273**, 316-324.

Utama, A., Shimizu, H., Morikawa, S., Hasebe, F., Morita, K., Igarashi, A., Hatsu, M., Takamizawa, K. & Miyamura, T. (2000*b*). Identification and characterization of the RNA helicase activity of Japanese encephalitis virus NS3 protein. *FEBS Letters* **465**, 74-78.

Valle, R. & Falgout, B. (1998). Mutagenesis of the NS3 protease of dengue virus type 2. *Journal of Virology* **72**, 624-632.

van Regenmortel, M. H. V., Fauqet, C. M., Bishop, D. H. L., CArstens, E. B., Estes, M. K., Lemon, S. M., Maniloff, J., Mayo, M. A., McGeoch, D. J., Pringle, C. R., Wickner, R. B. (2000). Virus Taxonomy. In *Eighth report of the International Committee on Taxonomy of Viruses.* San Diego: Academic Press.

Vaughn, D. W., Hoke, C. H., Jr., Yoksan, S., LaChance, R., Innis, B. L., Rice, R. M. & Bhamarapravati, N. (1996). Testing of a dengue 2 live-attenuated vaccine (strain 16681 PDK 53) in ten American volunteers. *Vaccine* **14**, 329-336.

Walker, J. E., Saraste, M., Runswick, M. J. & Gay, N. J. (1982). Distantly related sequences in the alpha- and beta-subunits of ATP synthase, myosin, kinases and other ATP-requiring enzymes and a common nucleotide binding fold. *EMBO Journal* **1**, 945-951.

Wallner, G., Mandl, C. W., Kunz, C. & Heinz, F. X. (1995). The flavivirus 3'-noncoding region: extensive size heterogeneity independent of evolutionary

relationships among strains of tick-borne encephalitis virus. *Virology* **213**, 169-178.

Wardell, A. D., Errington, W., Ciaramella, G., Merson, J. & McGarvey, M. J. (1999). Characterization and mutational analysis of the helicase and NTPase activities of hepatitis C virus full-length NS3 protein. *Journal of General Virology* **80**, 701-709.

Warrener, P. & Collett, M. S. (1995). Pestivirus NS3 (p80) protein possesses RNA helicase activity. *Journal of Virology* **69**, 1720-1726.

Warrener, P., Tamura, J. K. & Collett, M. S. (1993). RNA-stimulated NTPase activity associated with yellow fever virus NS3 protein expressed in bacteria. *Journal of Virology* **67**, 989-996.

Wengler, G. & Wengler, G. (1989). Cell-associated West Nile flavivirus is covered with E+pre-M protein heterodimers which are destroyed and reorganized by proteolytic cleavage during virus release. *Journal of Virology* **63**, 2521-2526.

Wengler, G. & Wengler, G. (1991). The carboxy-terminal part of the NS3 protein of the West Nile flavivirus can be isolated as a soluble protein after proteolytic cleavage and represents an RNA-stimulated NTPase. *Virology* **184**, 707-715.

Wengler, G. & Wengler, G. (1993). The NS 3 nonstructural protein of flaviviruses contains an RNA triphosphatase activity. *Virology* **197**, 265-273.

Wertman, K. F., Drubin, D. G. & Botstein, D. (1992). Systematic mutational analysis of the yeast ACT1 gene. *Genetics* **132**, 337-350.

Westaway, E. G. (1987). Flavivirus replication strategy. *Advances in Virus Research* **33**, 45-90.

Westaway, E. G. & Blok, J. (1997). Taxonomy and evolutionary relationships of flaviviruses. In *Dengue and dengue hemorrhagic fever.*, pp. 147-173. Edited by D. J. Gubler & G. Kuno. Wallingford: CAB INTERNATIONAL.

Westaway, E. G., Khromykh, A. A., Kenney, M. T., Mackenzie, J. M. & Jones, M. K. (1997*a*). Proteins C and NS4B of the flavivirus Kunjin translocate independently into the nucleus. *Virology* **234**, 31-41.

Westaway, E. G., Khromykh, A. A. & Mackenzie, J. M. (1999). Nascent flavivirus RNA colocalized in situ with double-stranded RNA in stable replication complexes. *Virology* **258**, 108-117.

Westaway, E. G., Mackenzie, J. M., Kenney, M. T., Jones, M. K. & Khromykh, A. A. (1997*b*). Ultrastructure of Kunjin virus-infected cells: colocalization of NS1 and NS3 with double-stranded RNA, and of NS2B with NS3, in virus-induced membrane structures. *Journal of Virology* **71**, 6650-6661.

Winkler, G., Maxwell, S. E., Ruemmler, C. & Stollar, V. (1989). Newly synthesized dengue-2 virus nonstructural protein NS1 is a soluble protein but becomes partially hydrophobic and membrane-associated after dimerization. *Virology* **171**, 302-305.

Winkler, G., Randolph, V. B., Cleaves, G. R., Ryan, T. E. & Stollar, V. (1988). Evidence that the mature form of the flavivirus nonstructural protein NS1 is a dimer. *Virology* **162**, 187-196.

Wiskerchen, M. & Muesing, M. A. (1995). Identification and characterization of a temperature-sensitive mutant of human immunodeficiency virus type 1 by alanine scanning mutagenesis of the integrase gene. *Journal of Virology* **69**, 597-601.

Worobey, M., Rambaut, A. & Holmes, E. C. (1999). Widespread intra-serotype recombination in natural populations of dengue virus. *Proceedings of the National Academy of Sciences of the United States of America* **96**, 7352-7357.

Wright, P. J., Cauchi, M. R. & Ng, M. L. (1989). Definition of the carboxy termini of the three glycoproteins specified by dengue virus type 2. *Virology* **171**, 61-67.

Xie, H., Cass, A. R. & Barrett, A. D. T. (1998). Yellow fever 17D vaccine virus isolated from healthy vaccinees accumulates very few mutations. *Virus Research* **55**, 93-99.

Yamshchikov, V. F. & Compans, R. W. (1993). Regulation of the late events in flavivirus protein processing and maturation. *Virology* **192**, 38-51.

Yamshchikov, V. F. & Compans, R. W. (1994). Processing of the intracellular form of the west nile virus capsid protein by the viral NS2B-NS3 protease - an in vitro study. *Journal of Virology* **68**, 5765-5771.

Yamshchikov, V. F. & Compans, R. W. (1995). Formation of the flavivirus envelope: role of the viral NS2B-NS3 protease. *Journal of Virology* **69**, 1995-2003.

Yamshchikov, V. F., Trent, D. W. & Compans, R. W. (1997). Upregulation of signalase processing and induction of prM-E secretion by the flavivirus NS2B-NS3 protease: roles of protease components. *Journal of Virology* **71**, 4364-4371.

Yan, H. G. & Tsai, M. D. (1991). Mechanism of adenylate kinase. Demonstration of a functional relationship between aspartate 93 and Mg^{2+} by site-directed mutagenesis and proton, phosphorus-31, and magnesium-25 NMR. *Biochemistry* **30**, 5539-5546.

Yan, Y., Li, Y., Munshi, S., Sardana, V., Cole, J. L., Sardana, M., Steinkuehler, C., Tomei, L., De Francesco, R., Kuo, L. C. & Chen, Z. (1998). Complex of NS3 protease and NS4A peptide of BK strain hepatitis C virus: a 2.2 Å resolution structure in a hexagonal crystal form. *Protein Science* **7**, 837-847.

Yao, N., Hesson, T., Cable, M., Hong, Z., Kwong, A. D., Le, H. V. & Weber, P. C. (1997). Structure of the hepatitis C virus RNA helicase domain. *Nature Structural Biology* **4**, 463-467.

Yoksan, S., Bhamarapravati, N. & Halstead, S. B. (1986). Arbovirus Research in Australia. Proceedings of the Fourth Symposium. Edited by T. D. St. George, B. H. Kay & J. Blok. CSIRO/QMIR, Brisbane, Australia.

Zanotto, P. M., Gould, E. A., Gao, G. F., Harvey, P. H. & Holmes, E. C. (1996). Population dynamics of flaviviruses revealed by molecular phylogenies. *Proceedings of the National Academy of Sciences of the United States of America* **93**, 548-553.

Zhang, L. & Padmanabhan, R. (1993). Role of protein conformation in the processing of dengue virus type 2 nonstructural polyprotein precursor. *Gene* **129**, 197-205.

Journal of General Virology (2001), 82, 1647–1656. Printed in Great Britain

Mutagenesis of the dengue virus type 2 NS3 proteinase and the production of growth-restricted virus

Anita E. Matusan,[1] Peter G. Kelley,[1] Melinda J. Pryor,[1] James C. Whisstock,[2] Andrew D. Davidson[1] and Peter J. Wright[1]

Department of Microbiology[1] and Department of Biochemistry and Molecular Biology[2], Monash University, PO Box 53, Victoria 3800, Australia

The N-terminal one-third of the NS3 protein of *Dengue virus type 2* (DEN-2) complexes with co-factor NS2B to form an active serine proteinase which cleaves the viral polyprotein. To identify sites within NS3 that may interact with NS2B, seven regions within the NS3 proteinase outside the conserved flavivirus enzyme motifs were mutated by alanine replacement. Five sites contained clusters of charged residues and were hydrophilic. Two sites were hydrophobic and highly conserved among flaviviruses. The effects of five mutations on NS2B/3 processing were examined using a COS cell expression system. Four retained significant proteinase activity. Three of these mutations and two more were introduced into genomic-length cDNA and tested for their effects on virus replication. The five mutant viruses showed reduced plaque size and two of the five showed significantly reduced titres. All seven mutations were mapped on the X-ray crystal structure of the DEN-2 NS3 proteinase: three were located at the N terminus and two at the C terminus of the NS2B-binding cleft. Two mutations were at the C terminus of the proteinase domain and one was solvent-exposed. The study demonstrated that charged-to-alanine mutagenesis in the viral proteinase can be used to produce growth-restricted flaviviruses that may be useful in the production of attenuated vaccine strains.

Introduction

There are four serotypes of dengue virus that are transmitted by the *Aedes* mosquito in tropical and subtropical regions (Halstead, 1988; van Regenmortel *et al.*, 2000). The viruses are classified in the genus *Flavivirus* of the family *Flaviviridae* and are responsible for dengue fever, haemorrhagic fever and shock syndrome (Monath, 1994). No commercial dengue virus vaccine is currently available and mosquito control programs are difficult to implement and maintain, making the development of new antiviral drugs and a safe vaccine imperative.

The flavivirus genome is a positive-sense RNA molecule of approximately 11000 nucleotides encoding the proteins C–prM–E–NS1–NS2A–NS2B–NS3–NS4A–NS4B–NS5 in a single long open reading frame. Co- and post-translational polyprotein processing by host and viral proteinases generate three structural proteins, namely C (capsid), M (membrane) and E (envelope), and seven nonstructural (NS) proteins, namely NS1 through to NS5 (reviewed by Rice, 1996).

Author for correspondence: Peter Wright.
[redacted]

The focus of this paper is the viral NS2B/3 proteinase of *Dengue virus type 2* (DEN-2). NS2B/3 cleaves at the NS2A/NS2B, NS2B/NS3, NS3/NS4A and NS4B/NS5 junctions. It also cleaves within C, NS2A, NS4A and NS3, in the latter case producing NS3′ and NS3″ (Arias *et al.*, 1993; Teo & Wright, 1997). Proteolysis occurs following a pair of basic amino acids or Gln–Arg and preceding either Gly, Ser or Ala (Rice, 1996). The motifs and catalytic triad typical of a trypsin-like serine proteinase are located in the N-terminal one-third of NS3 (Bazan & Fletterick, 1989); the X-ray crystal structure for this part of NS3 was described recently (Murthy *et al.*, 1999). The active form of the viral proteinase is a complex between NS3 and NS2B (Preugschat *et al.*, 1990; Falgout *et al.*, 1991). A hydrophilic region of 40 amino acids in NS2B containing a short central hydrophobic segment is required for the association of NS2B with NS3 and for enzyme activity (Falgout *et al.*, 1993; Chambers *et al.*, 1993; Yusoff *et al.*, 2000). Similarly, an NS3-containing complex is an active proteinase of *Hepatitis C virus* (HCV), which also belongs to the family

0001-7598

Flaviviridae, but to the genus *Hepacivirus*. In this case the complex is formed between NS3 and NS4A (Failla *et al.*, 1995; Lin *et al.*, 1995).

Initial studies on the cleavage of the flavivirus polyprotein targeted either the four regions of homology shared between serine proteinases and the flavivirus NS3 protein, or the cleavage sites in the polyprotein (Chambers *et al.*, 1990; Valle & Falgout, 1998). However, in this study, seven locations in NS3 outside these regions and sites were chosen for mutagenesis. By avoiding motifs containing the catalytic triad and residues known to be involved in substrate binding, it was reasoned that sites involved in NS2B–NS3 interaction may be mutated and that suitable modification at such sites had the potential to reduce, without abolishing, proteinase activity and virus replication. Virus mutants of this type are candidates for incorporation into live vaccine strains of DEN-2 and other flaviviruses. Mutations were tested for their effects on NS2B/3 proteinase activity by transient expression of the NS2B/3 genes in COS cells, virus replication by the incorporation into genomic-length DEN-2 cDNA or both. Results are interpreted below with reference to the location of the mutations mapped on the X-ray crystal structure of the DEN-2 NS3 proteinase (Murthy *et al.*, 1999) and a model of the NS2B/3 complex.

Methods

■ **Cells, virus and antisera.** Growth of BHK-21, *A. albopictus* C6/36 and COS cells, the preparation of stocks of DEN-2 viruses and plaque assays in C6/36 cells at 28 °C have all been described previously (Gualano *et al.*, 1998; Pryor *et al.*, 1998). For plaque assays, virus inoculum was removed from the monolayers and cells were overlaid with medium containing 1% SeaPlaque agarose (FMC BioProducts). At 5 days after infection, cells were overlaid with the same mixture containing 0·018% neutral red. Plaques were then counted 7 days after infection. Concentrated stocks of some viruses were produced by precipitation with polyethylene glycol (PEG) (Della-Porta & Westaway, 1972). The preparation of rabbit polyclonal antiserum directed against DEN-2 NS3 (residues 355–593) has been described previously (Teo & Wright, 1997).

■ **Transient expression of DEN-2 genes in COS cells.** The vector pSV.SPORT 1 (Gibco BRL) was used to express DEN-2 cDNA (strain New Guinea C) encoding NS2B/NS3. The construction of plasmid pSV.NS2B/3 (S2, the parental NS2B/NS3 construct) (Fig. 1) was described previously (Teo & Wright, 1997). The nucleotide numbering used to describe the mutants below follows that of Irie *et al.* (1989). Four mutant constructs derived from pSV.NS2B/3 (S2) were prepared by replacing the *Eco*RV^{4331}–*Bst*BI^{5070} fragment (Fig. 1) with a mutated fragment prepared by overlap extension PCR (Ho *et al.*, 1989), i.e. constructs pSV.NS2B/3_{17-20} (S_{17-20}), pSV.NS2B/3_{32-36} (S_{32-36}), pSV.NS2B/3_{63-65} (S_{63-66}) and pSV.NS2B/3_{95-96} (S_{95-96}); the plasmid pSV.NS2B/$3_{179-181}$ ($S_{179-181}$) was prepared by conventional PCR using a mutagenic primer overlapping the *Bst*BI^{5070} site. The PCR-derived regions of all clones were sequenced. The plasmid pSV.NS2B/3_{32-36} was initially designed to encode only the substitutions $G_{32}A$ and $Y_{33}A$. However, an additional $I_{36}V$ change was introduced during PCR.

Constructs were electroporated into COS cells as described by Teo & Wright (1997). Cells were maintained at 31 °C or 37 °C for 48 h and then starved of methionine for 2 h prior to radiolabelling with [^{35}S]methionine for either 3 h at 31 °C or 1 h at 37 °C (Pryor & Wright, 1993). Cell lysates were analysed by radioimmunoprecipitation, gel electrophoresis and fluorography (Pryor & Wright, 1993; Teo & Wright, 1997).

■ **Insertion of mutations into genomic-length DEN-2 cDNA.** The plasmid pDVWS501 containing genomic-length New Guinea C strain DEN-2 cDNA has been described in detail (Gualano *et al.*, 1998). For these experiments, transient expression was used to examine the effects of five mutations in the NS3 proteinase on proteolytic activity. Three mutations were selected and then inserted into genomic-length DEN-2 cDNA to study their effects on virus replication. Two additional charged-to-alanine mutations that were external to proteinase motifs were also inserted into the genomic-length DEN-2 cDNA (Fig. 1).

The plasmid pDVWS501NS3_{32-36} was prepared by replacing the *Nhe*I^{2544}–*Nsi*I^{4700} fragment of pDVWS501 with a mutated fragment prepared by overlap extension PCR (Fig. 1). The other four mutations were initially constructed in the subclone pDVSO8298 prior to ligation into pDVWS501. This strategy was devised following consideration of the available restriction enzyme sites. Plasmid pDVSO8298 contained DEN-2 cDNA corresponding to nucleotides 4494 (upstream of *Nsi*I^{4700}) to 8744 (downstream of *Stu*I^{7874}) cloned into *Xba*I/*Kpn*I-digested pSPORT 1 (Gibco BRL). cDNA encoding mutations KRIE (63–66) (underlined residues changed to alanine) or EDD (179–181) in the NS3 hydrophilic regions was cloned into pDVSO8298 by removing the mutated *Nsi*I^{4700}–*Ppu*MI^{5854} fragment from the corresponding pSV.NS2B/3 plasmid and ligating this into *Nsi*I^{4700}/*Ppu*MI^{5854}-digested pDVSO8298. The two remaining charged-to-alanine mutations, EGEE (91–94) and EKSIE (169–173), were introduced into *Nsi*I^{4700}/*Ppu*MI^{5854}-digested pDVSO8298 as overlap extension PCR fragments. All four mutants (*Nsi*I^{4700}–*Stu*I^{7874}-mutated fragments) were then removed from the appropriate pDVSO8298 plasmid and ligated into *Nsi*I^{4700}/*Stu*I^{7874}-digested pDVWS501. PCR-derived regions were sequenced.

■ **Production of virus from genomic-length cDNA.** Procedures for transcription of RNA, electroporation and immunofluorescence of BHK-21 cells and passaging of virus in C6/36 cells have been described previously (Gualano *et al.*, 1998). Briefly, capped transcripts were produced from plasmids containing genomic-length DEN-2 cDNA using the Promega RiboMAX kit. Approximately 7–10 μg of transcript RNA and 50 μg of carrier tRNA were electroporated into BHK-21 cells, which were then incubated at 33 °C or 37 °C. Cells were examined for immunofluorescence 4 to 6 days later using anti-E monoclonal antibodies (Gruenberg & Wright, 1992). After 7 days, the culture medium was used to infect C6/36 cells. The culture medium from these infected C6/36 cells was then used 4 to 5 days later to initiate a second passage. When approximately 50% of the cells exhibited cytopathic effects, or 5 days later if no cytopathic effects were visible, these second passage virus stocks were titred by plaque assay on C6/36 cells.

Each virus was derived at least twice from its parental construct. To confirm that each mutation was present after electroporation and passaging, total RNA was extracted from infected C6/36 cells or supernatant and RT–PCR of viral RNA was performed (Gualano *et al.*, 1998; Pryor *et al.*, 1998). The complete NS2B and NS3 genes were sequenced to confirm the presence of the introduced mutation and the absence of any other changes that may have been introduced during virus passaging.

■ **Co-ordinates and calculations.** The crystal structures of the DEN-2 NS3 serine proteinase (protein database identifier 1BEF; Murthy *et al.*, 1999) and the HCV NS3/NS4A proteinase–co-factor complex (protein database identifier 1NS3; Yan *et al.*, 1998) were obtained from the protein database (Bernstein *et al.*, 1977; Berman *et al.*, 2000).

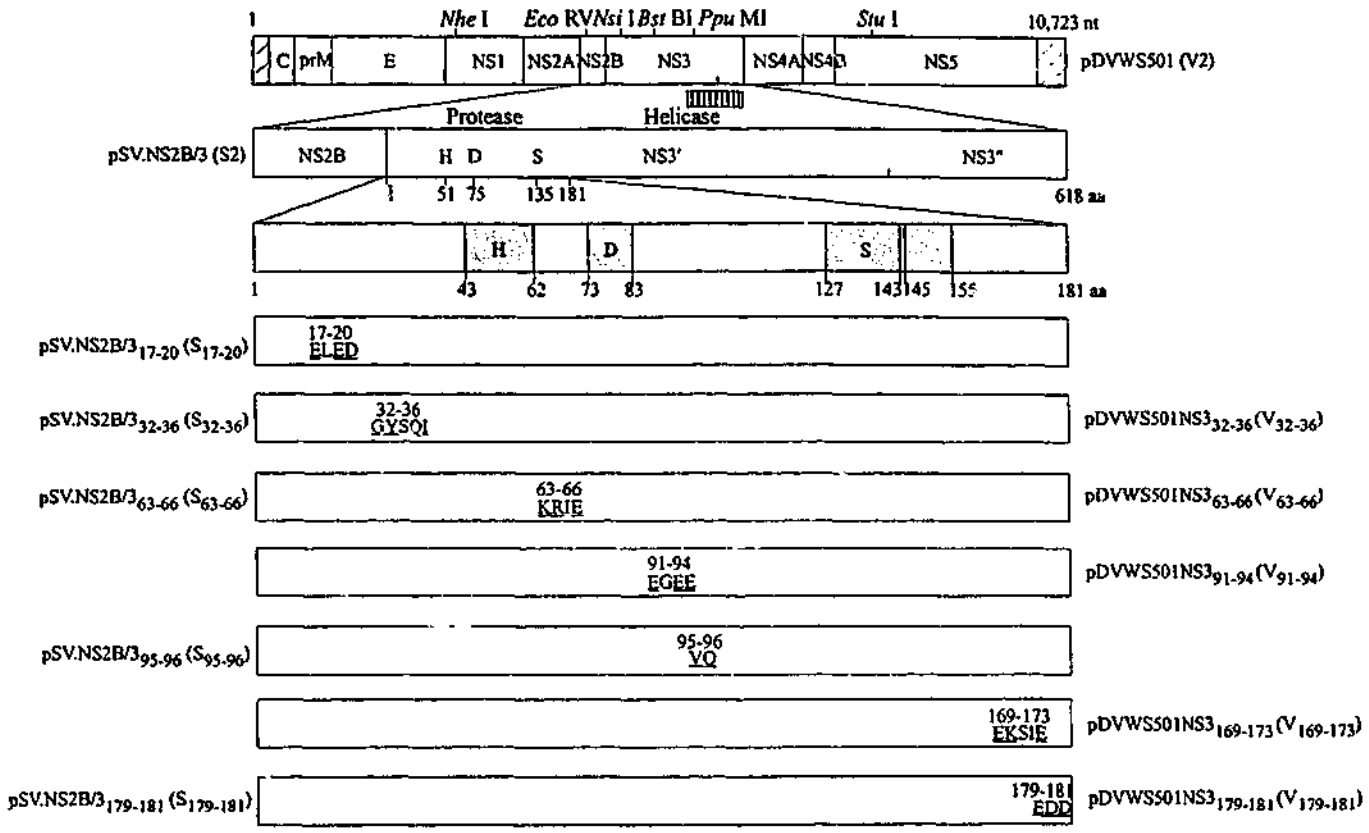

Fig. 1. Genomic map of DEN-2 and NS3 proteins encoded by mutant constructs. The catalytic residues H, D and S and the serine proteinase motifs (shaded) are shown (Bazan & Fletterick, 1989); residue numbers within NS3 are given. The full (pSV) and abbreviated (S) designations of the gene constructs encoding NS2B/3 in pSV.SPORT 1 are shown on the left. S designations are also used for the corresponding encoded mutant proteins where appropriate. The names of the plasmids containing genomic-length cDNA (pDVWS) and derived viruses (V) are shown on the right. Antiserum against a bacterial fusion protein raised in rabbits (Teo & Wright, 1997) was directed against a segment of NS3 (vertical stripes). Underlined residues were mutated to alanine (with the exception of $I_{36}V$).

The model between the DEN-2 NS3 proteinase and a portion of the NS2B co-factor was generated using the Quanta/CHARMm software (MSI). The peptide sequence G_{69}SSPILSITISE$_{80}$ within NS2B corresponds to the portion of the NS4A co-factor seen in the structure of the HCV proteinase (Brinkworth *et al.*, 1999). The DEN-2 and HCV proteinases were superimposed and the NS4A peptide within the HCV proteinase structure was used as a template to model the NS2B sequence (GSSPILSITISE) into the DEN-2 NS3 proteinase. The model was then subjected to rounds of CHARMm minimization, initially with constraints that were applied to the proteinase; the co-factor was allowed to move freely. Later rounds were performed to convergence with no constraints. Dihedral constraints were applied to four residues in non-allowed conformations. A Ramachandran plot of the final model indicated that all residues were in allowed conformations.

We examined the positions of the mutations described in Fig. 1 with respect to the interactions seen in the crystal structure of the DEN-2 NS3 proteinase. In addition, the model between the NS3 proteinase and the NS2B co-factor was used to analyse three groups of mutations that mapped to the NS2B-binding cleft.

Results

Mutagenesis of the N-terminal 181 amino acids of NS3

Hydrophilic regions were targeted using clustered charged-to-alanine mutagenesis (Diamond & Kirkegaard, 1994). Charged amino acids probably occupy exposed positions in the tertiary structure and therefore interact with other proteins. Previous experiments with DEN-4 identified a 40 amino acid segment of NS2B that was, overall, hydrophilic and essential for protease activity (Falgout *et al.*, 1993). This segment also contained a short, central hydrophobic sequence of approximately 12 amino acids. It was possible that changes to the hydrophilicity of NS3 might modify the interaction of NS3 with NS2B and the proteinase activity of the NS2B/3 complex.

The first 181 amino acids of NS3 were scanned for clusters of five residues that contained at least three charged amino acids. Five such clusters outside proteinase motifs were chosen for mutagenesis and the charged residues were changed to alanine (Fig. 1) (Bass *et al.*, 1991). The changes made in DEN-2 NS3 were as follows: $E_{17}A$, $E_{19}A$ and $D_{20}A$; $K_{63}A$, $R_{64}A$ and $E_{66}A$; $E_{91}A$, $E_{93}A$ and $E_{94}A$; $E_{169}A$, $K_{170}A$ and $E_{173}A$; and lastly $E_{179}A$, $D_{180}A$ and $D_{181}A$. Alanine was chosen as the replacement amino acid since it removes the side chain beyond the β-carbon and also minimizes any steric effects within the polypeptide caused by the replacement (Cunningham & Wells, 1989). In addition, two hydrophobic regions were chosen (Fig. 1) on the basis of hydropathy plot data (Hahn *et al.*, 1988) and conservation of sequence across the flaviviruses (Westaway & Blok, 1997; Chang, 1997). They were $G_{32}A$ and $Y_{33}A$, and $V_{95}A$ and $Q_{96}A$. Thus a total of seven sites were mutated.

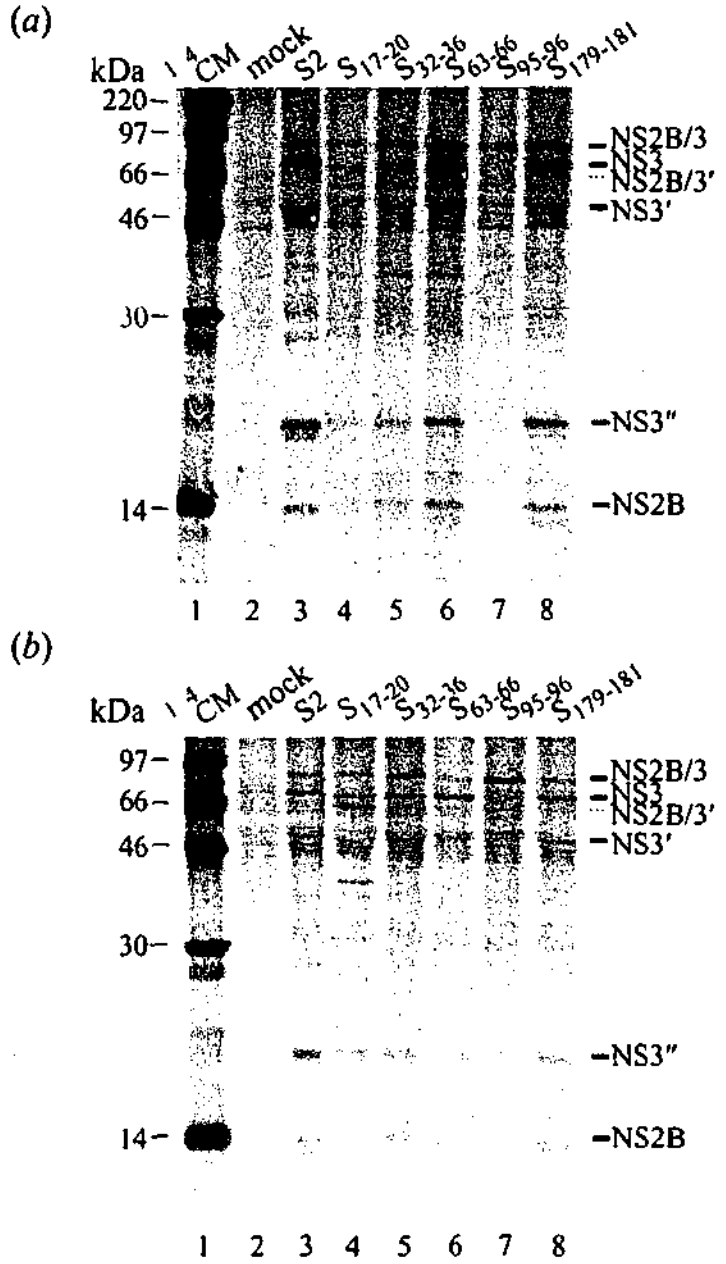

Fig. 2. Analysis of NS2B/3 proteinase activity in transfected COS cells. Cells were transfected with parental S2 (lane 3) or mutant S_{17-20} to $S_{179-181}$ (lanes 4–8) constructs and labelled for (*a*) 1 h at 37 °C or (*b*) 3 h at 31 °C. Proteins were immunoprecipitated with antiserum directed against NS3 and separated by 14% SDS–PAGE. Size markers are shown on the left.

Transient expression and proteolysis of NS2B/3

The first experiments were designed to test for proteinase activity of mutant NS2B/3 proteins using transient expression of the pSV constructs in COS cells. We did not wish to investigate virus replication with mutations that abolished proteinase activity. Five constructs were tested. COS cells were transfected with the pSV plasmids listed in Fig. 1, radiolabelled and analysed by radioimmunoprecipitation and electrophoresis (Fig. 2). As reported previously (Teo & Wright, 1997), in cells transfected with the parental construct S2 and radiolabelled for 1 h at 37 °C, several polypeptides indicative of proteinase activity were detected using anti-NS3 antiserum (Fig. 2*a*, lane 3). They were uncleaved NS2B/3 (83 kDa) and the cleavage products NS3 (69 kDa), NS2B/3′ (64 kDa), NS3′ (50 kDa) and NS3″ (19 kDa). The bands corresponding to NS2B/3′ and NS3′ were faint and not well-resolved from host proteins; however, bands of NS2B/3, NS3 and NS3″ were clear and sufficient for the assessment of proteolysis. NS2B (14 kDa) was detected by co-precipitation using anti-NS3 antiserum, as described for dengue virus and other flaviviruses (Arias *et al.*, 1993; Chambers *et al.*, 1993; Jan *et al.*, 1995; Teo & Wright, 1997). The number and sizes of the observed proteins demonstrated that cleavage was occurring at the NS2B/NS3 and NS3′/NS3″ sites. Proteinase activity was also detected in cells transfected by S_{17-20}, S_{32-36}, S_{63-66} or $S_{179-181}$ and maintained at 37 °C (Fig. 2*a*, lanes 4–6, 8). However, little or no cleavage occurred in cells transfected with the construct S_{95-96}; only NS2B/3 was readily detected (Fig. 2*a*, lane 7).

To assess the effects of lower temperature on proteolysis, transfected cells were radiolabelled at 31 °C for 3 h. The results obtained at 31 °C (Fig. 2*b*) were similar to those observed at 37 °C (Fig. 2*a*). The presence of NS3, NS3′, NS3″ and NS2B indicated that cleavage occurred at the NS2B/NS3 and NS3′/NS3″ sites for the parental construct (Fig. 2*b*, lane 3) and mutants S_{17-20}, S_{32-36}, S_{63-66} and $S_{179-181}$ (Fig. 2*b*, lanes 4–6, 8). Again no significant proteolysis was detected for the mutant construct S_{95-96} (Fig. 2*b*, lane 7).

For all mutants shown in Fig. 2, with the exception of S_{95-96}, NS2B was co-precipitated with NS3 by anti-NS3 antiserum. The band corresponding to this protein was faint for S_{17-20} (Fig. 2, lanes 4), but was readily seen on longer exposure. Thus for these mutants, interaction between NS2B and NS3 was retained, consistent with the retention of proteinase activity.

Analysis of virus replication

Previous experiments showed that mutations that abolished or strongly reduced NS2B/3 proteinase activity usually prevented or greatly reduced virus replication (Nestorowicz *et al.*, 1994; Chambers *et al.*, 1993; Amberg & Rice, 1999), whereas mutations that retained activity generally allowed the recovery of infectious virus, albeit with reduced plaque titres and small plaque phenotypes (Nestorowicz *et al.*, 1994; Chambers *et al.*, 1995; Amberg & Rice, 1999). Hence five mutations were chosen for incorporation into genomic-length cDNA and examination of their effects on virus replication. All three of the charged-to-alanine mutants tested (S_{17-20}, S_{63-66} and $S_{179-181}$) did not show severe inhibition of proteinase activity in COS cells. We selected the mutations in two of these (S_{63-66} and $S_{179-181}$) for incorporation into genomic-length cDNA and added a further two of the charged-to-alanine-type mutations (Fig. 1) without prior testing in COS cells. For the mutations within hydrophobic regions (S_{32-36} and S_{95-96}), only the changes of S_{32-36} (cleavage of NS2B/3 detected) were incorporated into genomic-length cDNA.

Virus was produced from genomic-length cDNA by established procedures (Gualano *et al.*, 1998). RNA was

Table 1. Yields of mutant viruses

RNA was transcribed from genomic-length cDNA and electroporated into BHK-21 cells maintained at 33 °C or 37 °C. Virus produced at each temperature was passaged twice in C6/36 cells at 28 °C. Immunofluorescence in BHK-21 cells at 5–6 days post-electroporation was scored as 0 (−), 1–25% (+), 26–50% (+ +), 51–75% (+ + +) or 76–100% (+ + + +) positive cells. Plaque titres after passaging in C6/36 cells are expressed in p.f.u./ml ± SD. Each virus was derived at least twice from RNA transcripts; therefore, the result shown for each virus is the average of two or more experiments. All samples testing positive by RT–PCR retained the required mutation and had no other changes in the NS2B/3 genes.

Mutation site	Virus*	Immunofluoresence	Virus titre (p.f.u./ml)	Approximate plaque size (mm)	RT–PCR
Parental	V2 33 °C	+ + + +	$(1{\cdot}1 \pm 0{\cdot}1) \times 10^6$	4	Yes
	37 °C	+ + + +	$(7{\cdot}3 \pm 0{\cdot}8) \times 10^6$	4	Yes
GYSQI	V_{32-36} 33 °C	+	$(3{\cdot}0 \pm 0{\cdot}9) \times 10^1$	1	Not
	37 °C	−	ND	−	Not
KRIE	V_{63-66} 33 °C	+ + + +	$(4{\cdot}6 \pm 0{\cdot}9) \times 10^5$	1	Yes
	37 °C	+ + +	$(7{\cdot}0 \pm 1{\cdot}5) \times 10^5$	1	Yes
EGEE	V_{91-94} 33 °C	+	$(2{\cdot}4 \pm 0{\cdot}3) \times 10^3$	1	Yes
	37 °C	−	ND	−	Not
EKSIE	$V_{169-173}$ 33 °C	+ + + +	$(2{\cdot}7 \pm 0{\cdot}2) \times 10^6$	3	Yes
	37 °C	+ + + +	$(2{\cdot}2 \pm 0{\cdot}5) \times 10^6$	3	Yes
EDD	$V_{179-181}$ 33 °C	+ + +	$(4{\cdot}9 \pm 1{\cdot}0) \times 10^5$	1	Yes
	37 °C	+ + +	$(1{\cdot}4 \pm 0{\cdot}2) \times 10^6$	1	Yes

* BHK-21 cells were incubated at either 33 °C or 37 °C immediately after electroporation
† RT–PCR product was not obtained due to low titre.
ND, Not detected.

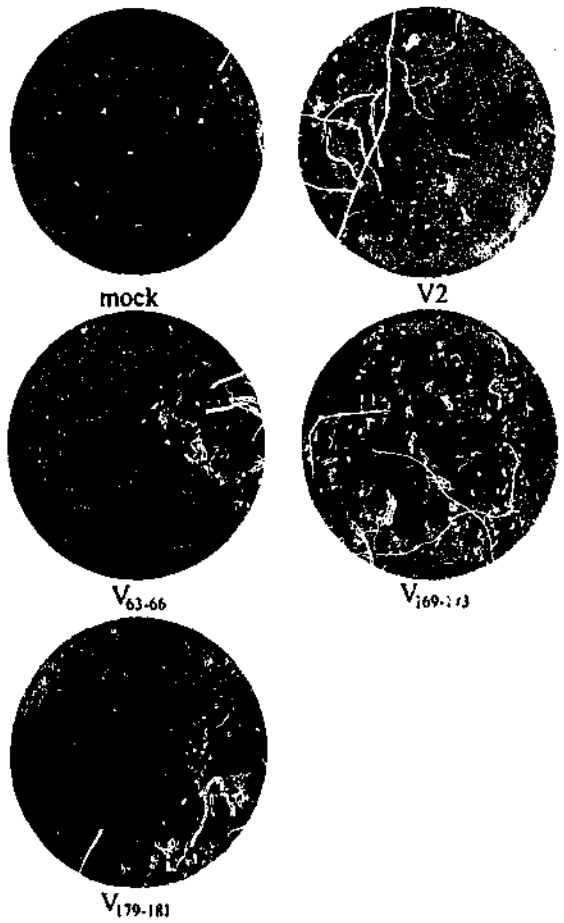

Fig. 3. Plaques of mutant viruses in C6/36 cells at 28 °C. The plaque morphologies of three mutant viruses compared with the parental virus V2 are shown.

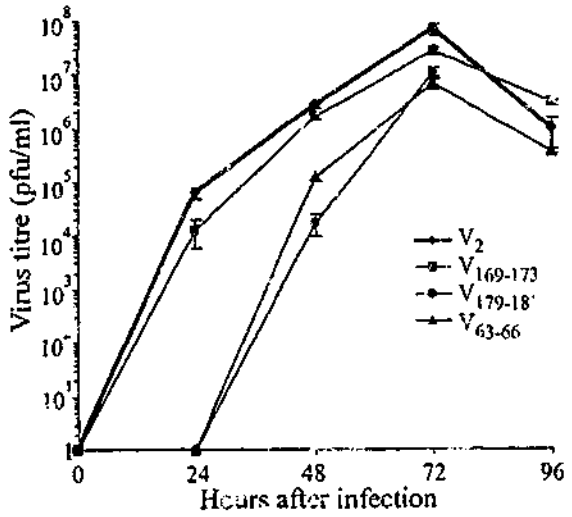

Fig. 4. Replication of mutant viruses in C6/36 cells at 28 °C. Cells were infected at an m.o.i. of 1 and the culture medium was sampled at the times indicated; virus titres were determined by plaque assay in C6/36 cells. The presence of the original mutations in the recovered viruses was confirmed by RT–PCR and sequencing.

transcribed and electroporated into BHK-21 cells and the cells were incubated at 33 °C or 37 °C. BHK-21 cells were tested for immunofluorescence with anti-E antibodies. Medium from the transfected BHK-21 cells was passaged twice in C6/36 cells at 28 °C and virus titre was determined after the second passage by plaque assay in C6/36 cells. Viral RNA was then amplified by RT–PCR and the complete NS2B and NS3 genes were sequenced to check that the mutation was retained during

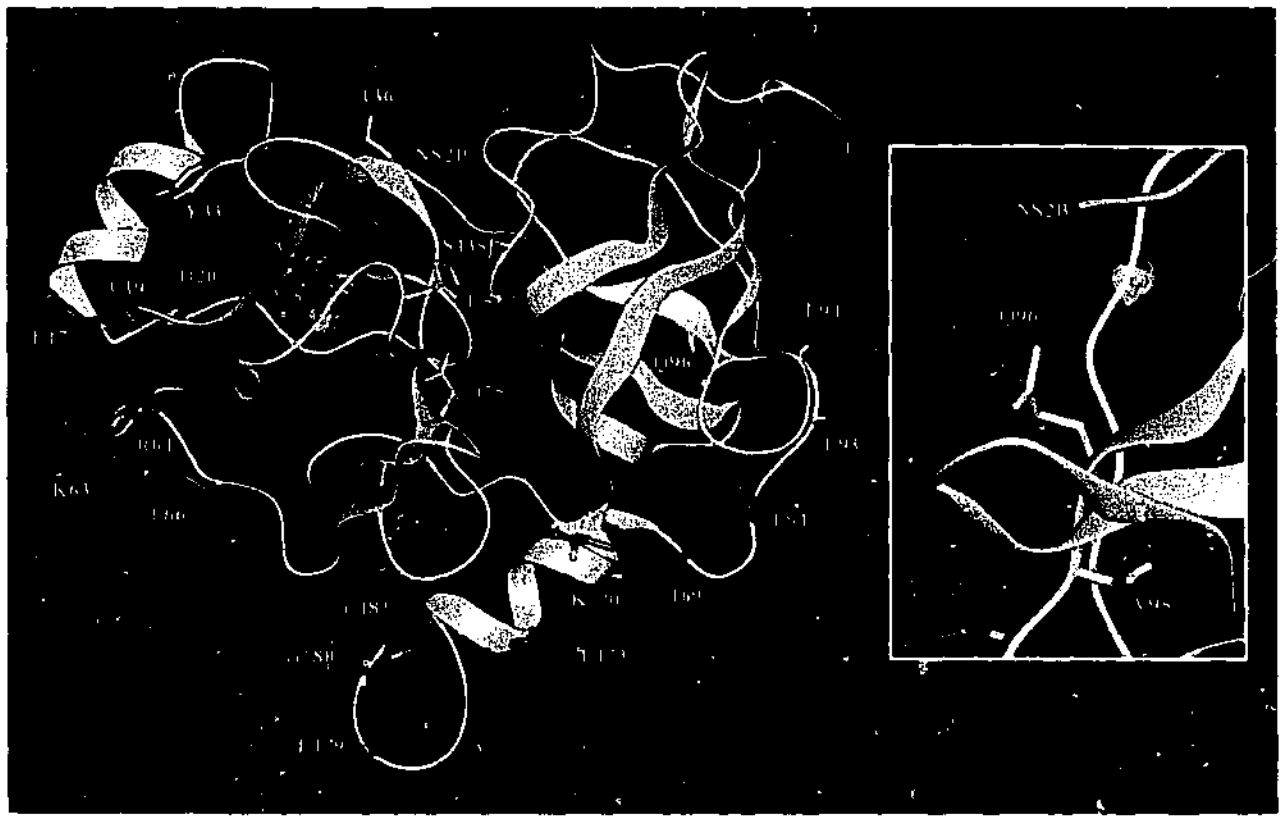

Fig. 5. X-ray crystal structure of the DEN-2 NS3 proteinase (aquamarine) with the NS2B peptide (pink) modelled into the binding cleft. The active site triad, H_{51}, D_{75} and S_{135}, is shown in green stick. Charged regions that were mutated to alanine are labelled and in red. The two conserved hydrophobic regions that were mutated are shown in yellow. The inset shows the proximity of Q_{96} to the C-terminal end of the NS2B peptide.

passaging and that no other base substitutions were introduced. Virus was derived at least twice for each construct and the results are summarized in Table 1. Virus titres were determined for each experiment and the mean ± SD corresponding to each construct is shown. Similar results were obtained consistently for a given construct.

The parental (V2) and mutant (V_{63-66}, $V_{169-173}$ and $V_{179-181}$) viruses grew to comparable titres of 10^5 to 10^6 p.f.u./ml following initial electroporation at 33 °C or 37 °C (Table 1). All three mutant viruses showed a reduced plaque size, particularly V_{63-66} and $V_{179-181}$ (Table 1, Fig. 3). For viruses V_{32-36} and V_{91-94}, detectable virus was recovered only following electroporation at 33 °C and at low titres (3×10^1 and $2{\cdot}4 \times 10^3$ p.f.u./ml respectively). These results suggested that V_{32-36} and V_{91-94} were severely restricted in replication and were possibly heat-sensitive.

To examine the properties of these viruses further, more concentrated stocks were prepared by PEG precipitation. We wished to obtain sufficiently high titres to enable infection of cells at an m.o.i. of 1. This proved possible only for viruses V2, V_{63-66}, $V_{169-173}$ and $V_{179-181}$.

Growth of viruses V2, V_{63-66}, $V_{169-173}$ and $V_{179-181}$ in C6/36 and BHK-21 cells

C6/36 cells were infected with viruses V2, V_{63-66}, $V_{169-173}$ or $V_{179-181}$ at an m.o.i. of 1, maintained at 28 °C and the medium was sampled at 24 h intervals up to 96 h post-infection. Virus titres were determined by plaque assay in C6/36 cells. The resulting curves of released virus are shown in Fig. 4. The two viruses with the smallest plaque size (V_{63-66} and $V_{179-181}$, Table 1) initially lagged in virus release, although by 48 h after infection, their titres had reached from 1 to 8×10^4 p.f.u./ml, and by 72 h after infection, the yields of all four viruses were comparable (Fig. 4). The observed delay in virus release for V_{63-66} and $V_{179-181}$ was consistent with their very small plaque size. The presence of the respective mutations in the recovered viruses was confirmed by RT–PCR and sequencing.

To analyse the effect of temperature on the replication of V2, V_{63-66}, $V_{169-173}$ and $V_{179-181}$ in a more rigorous manner than in the experiments summarized in Table 1, BHK-21 cells were infected at an m.o.i. of 1 and cells were incubated at 33 °C or 37 °C. The culture medium was sampled at 72 h after infection and virus titres were determined by plaque assay in C6/36 cells. All four viruses showed no significant temperature sensitivity, as defined by a 100-fold or greater difference in titre between temperatures (data not shown). The integrity of each mutation in recovered virus was reconfirmed by RT–PCR and sequencing.

Modelling the interaction of NS3 and NS2B

The 40 amino acid segment of NS2B required for the activity of the NS2B/3 proteinase is, overall, hydrophilic (L_{53}–E_{92}) and shares no significant similarity with a protein of

known structure. It contains a central hydrophobic region G_{69}SSPILSITISE$_{80}$ (Falgout *et al.*, 1993; Brinkworth *et al.*, 1999), which was identified as the probable homologue to the HCV NS4A peptide in the HCV NS3/4A proteinase and was used to construct an homology model of the DEN-2 NS3/2B proteinase (Brinkworth *et al.*, 1999). The homology model was based on the structure of the HCV complex of NS3 (N-terminal 179 amino acids) and NS4A (peptide G_{21}–R_{34}) (Yan *et al.*, 1998). However, an improved model for DEN-2 NS3/2B is now possible (Fig. 5) using the coordinates for the crystal structure of the N-terminal 185 amino acids of DEN-2 NS3 (Murthy *et al.*, 1999). This model is useful for analysing the interactions between the NS2B peptide G_{69}–E_{80} and NS3, but further predictions on the effect of NS2B binding to the substrate-binding cleft or any direct interactions between NS2B and substrate would be overspeculative until the X-ray crystal structure of the NS2B/3 complex is determined.

Discussion

Seven sites distributed through the N-terminal proteinase region of DEN-2 NS3 and outside conserved enzyme motifs were mutated in these experiments. Five sites were rich in charged amino acids (Fig. 1) and were considered to be possible sites of interaction with the hydrophilic 40 amino acid fragment of NS2B that is essential for activity (Falgout *et al.*, 1993). The approach of charged-to-alanine mutagenesis was first used successfully with *Poliovirus* to isolate growth-restricted polymerase mutants (Diamond & Kirkegaard, 1994). Ten temperature-sensitive mutants were obtained following mutagenesis of 27 sites and the recovery of 12 viruses. Fewer mutants have been reported for other viruses following charged-to-alanine mutagenesis. Single temperature-sensitive mutants have been described for *Human immunodeficiency virus* with mutations located in the reverse transcriptase and integrase genes (Wiskerchen & Muesing, 1995; Huang *et al.*, 1998), and *Adeno-associated virus type* 2 following mutagenesis of the Rep78/68 helicase genes (Gavin *et al.*, 1999). Mutagenesis of the polymerase subunit PB2 of *Influenza A virus* generated three temperature-sensitive mutants after mutagenesis of ten sites (Parkin *et al.*, 1996). The only reported growth-restricted mutant of a flavivirus obtained following charged-to-alanine mutagenesis was a temperature-sensitive *Yellow fever virus* (YFV) mutated in the NS1 protein (Muylaert *et al.*, 1997).

Of the five charged sites mutated to alanine in DEN-2 NS3, three were examined by transient expression in COS cells, four were tested for their effects on virus replication and three were tested by both methods. For no mutant tested was proteinase activity or virus production abolished. Mutations related, but not identical, to those at $E_{17}LED_{20}$, $K_{63}RIE_{66}$, $E_{91}GEE_{94}$ and $E_{169}KSIE_{173}$ were tested for their effect on the activity of YFV NS2B/3 proteinase (Droll *et al.*, 2000). No mutation reduced enzyme activity significantly except for those at $E_{21}D_{22}$ (YFV numbering). However, for the DEN-2 mutants, the yield of virus V_{91-94}, and to a lesser extent V_{63-66} (Table 1), were reduced compared with $V_{169-173}$ and $V_{179-181}$ and the parental virus V2. All mutant viruses showed reduced plaque size (Table 1, Fig. 3). The locations of the five charged sites were then mapped into a model of NS2B/3 (Fig. 5). The model is based on the crystal structure of DEN-2 NS3 proteinase (Murthy *et al.*, 1999) and a fragment of NS2B corresponding to the fragment of NS4A seen in the structure of HCV proteinase (Brinkworth *et al.*, 1999).

The X-ray crystal structure of DEN-2 NS3 reveals that region $E_{91}GEE_{94}$, mutated in the low-yielding virus V_{91-94}, does not form part of the active-site cleft, nor does it interact with the fragment of NS2B in the model. E_{91} and E_{93} form salt bridges to R_{107}. The loss of two salt bridges in the $A_{91}GAA_{94}$ mutation would be predicted to have a deleterious effect upon proteinase stability and possibly virus yield. However, the Q_{96} residue (see below) does form part of the predicted NS2B-binding cleft and we cannot exclude the possibility that $E_{91}GEE_{94}$ interacts with full-length NS2B. In HCV, the loops equivalent to residues 90–94 and 140–145 in DEN-2 NS3 are linked by interactions with a zinc ion. Interestingly, in the DEN-2 NS3 structure, the primary interaction between these loops is a hydrogen bond between the carbonyl oxygen of E_{94} and the side chain of K_{142}. These data conflict with the prediction of Brinkworth *et al.* (1999) that E_{93} forms a salt bridge with K_{145}. However, this prediction was based on an homology model developed from the HCV NS3 protein X-ray crystal structure before the availability of the DEN-2 NS3 proteinase structure.

The residues $K_{63}RIE_{66}$ (virus V_{63-66}) and $E_{17}LED_{20}$ (mutation not tested in virus) are both located at the N-terminal end of the NS2B-binding cleft. K_{63}, R_{64} and E_{66} are solvent-exposed residues located at one end of the NS2B-binding cleft. The model of the NS3–NS2B complex predicts that R_{64} makes a hydrogen bond to the carbonyl oxygen of the first residue in the NS2B peptide. We predict that more extensive interactions between R_{64} and E_{66} may be made with the full-length NS2B protein. The disruption of any one of these interactions, either alone or in combination, may explain the observed reduction in yield of virus V_{63-66}. The residues $E_{17}LED_{20}$ line the N-terminal end of the NS2B-binding cleft. We predict that E_{17} directly interacts with the carbonyl oxygen of G_1 in the NS2B peptide.

The residues $E_{169}KSIE_{173}$ and $E_{179}DD_{181}$ lie at the C terminus of the proteinase at its junction with the helicase domain of NS3. Both sites are excluded from the minimal proteinase domain, defined as the N-terminal 167 amino acids of NS3 (Li *et al.*, 1999) using *in vitro* transcription and translation. Residues $E_{169}KSIE_{173}$ form an α-helix (Fig. 5) and the individual residues form hydrogen bonds with solvent molecules, apart from K_{170}, which forms a hydrogen bond to the carbonyl oxygen of E_{167}. These residues are located at the end of the substrate-binding cleft (on the P side; Schechter & Berger, 1967) and thus may be important for determining

substrate specificity. For $E_{179}DD_{181}$, the structure of NS3 reveals that D_{180} forms a hydrogen bond to the side chain of W_{69}. The interaction with W_{69} is of particular interest, as this residue is located six residues N-terminal to the catalytic D_{75}. Disruption of this hydrogen bond by the introduction of an alanine at position 180 may affect the conformation of the β-strand containing the catalytic aspartic acid and thus may impair proteinase activity.

In addition to the mutagenesis of the five charged sites, substitutions were made in two hydrophobic regions, $G_{32}YSQI_{36}$ and $V_{95}Q_{96}$. The residues G_{32} and $V_{95}Q_{96}$ lie outside the enzyme motifs but are highly conserved in members of the genus *Flavivirus* (Chang, 1997). The protein S_{32-36} had autocatalytic activity (Fig. 2, lanes 4), but the yield of V_{32-36} was the lowest noted. G_{32} and Y_{33} line the N-terminal end of the NS2B-binding cleft. Interestingly, the crystal structure of NS3 reveals that Y_{33} bridges across the cleft, forming a hydrogen bond to the carbonyl oxygen of P_{10}. We would expect a mutation at this position to affect NS2B binding. G_{32} forms part of a pocket that contains S_3 from the NS2B peptide. We predict that mutation of this residue will affect the size of this pocket.

The mutations at $V_{95}Q_{96}$ are of particular interest as they are located at the C terminus of the NS2B-binding cleft. Substitution of these residues by alanine severely reduced self-cleavage of the S_{95-96} protein (Fig. 2, lanes 7). Examination of the structure of NS3 reveals that V_{95} is buried in the hydrophobic core of the proteinase and that Q_{96} is solvent-exposed. In our model of NS3 complexed with the NS2B peptide, Q_{96} is directly beneath the C terminus of the NS2B peptide (Fig. 5) and forms part of the binding cleft. The inability of the S_{95-96} protein to self cleave suggests that mutation of these residues may affect the pre-cleavage interaction between NS3 and the NS2B co-factor and prevent proper processing at the NS2B/NS3 cleavage site.

Overall, the seven mutated sites were distributed evenly over the primary sequence of the NS3 proteinase and represented distinct regions in the model of NS3 complexed with the NS2B co-factor peptide. Of the mutations located, three ($E_{17}LED_{20}$, $K_{63}RIE_{66}$ and $G_{32}YSQI_{36}$) were at the N terminus of the NS2B-binding cleft, one ($V_{95}Q_{96}$) was at the C terminus of the cleft, two ($E_{169}KSIE_{173}$ and $E_{179}DD_{181}$) were at the C terminus of the proteinase domain and one ($E_{91}GEE_{94}$) was solvent-exposed. Thus, two of the charged regions ($E_{17}LED_{20}$ and $K_{63}RIE_{66}$) were adjacent to the NS2B-binding cleft. At present, it is unknown whether any of the other three charged regions interact with full-length NS2B. It is also possible that the basis for their effect on virus replication is unrelated to proteinase activity and may lie, for example, in the interaction of NS3 with other viral proteins such as NS5 (Kapoor *et al.*, 1995; Chen *et al.*, 1997). Substitutions to alanine in conserved hydrophobic regions were more disruptive to self-cleavage (protein S_{95-96}) and virus production (virus V_{32-36}) than to changes in charged regions. A total of five viruses with reduced plaque size on C6/36 cells was obtained; two of these, V_{32-36} and V_{91-94}, were possibly temperature-sensitive but did not grow sufficiently well for adequate testing (Table 1). The remaining three viruses grew to reach good titres (Fig. 4) and displayed small plaques but did not show the temperature-sensitive phenotype that has been observed for some viruses with charged-to-alanine mutations in non-structural genes (Diamond & Kirkegaard, 1994; Parkin *et al.*, 1996; Muylaert *et al.*, 1997; Huang *et al.*, 1998; Gavin *et al.*, 1999). Virus V_{32-36} replicated too poorly to be of further use and therefore the viruses of most interest with respect to growth restriction were V_{63-66} and V_{91-94}. Both viruses contained mutations in charged amino acids, showed small plaque phenotypes and replicated less well than parental virus (V_{63-66} only marginally less). The mutations contained in these viruses may be suitable for incorporation into growth-restricted vaccine strains. It may be possible to enhance the yield of V_{91-94} by reducing the number of charged residues changed to alanine in the sequence $E_{91}GEE_{94}$ while retaining some growth restriction and a small plaque phenotype.

The results demonstrate that charged-to-alanine mutagenesis may be useful for obtaining growth-restricted viruses of other flavivirus species, either with mutations in the proteinase region or perhaps in other non-structural proteins. In our studies with DEN-2 NS3, we recovered infectious virus for all four of the charged-to-alanine mutants tested and the viruses displayed a useful range of growth restriction. Comparisons of the deduced amino acid sequences of flaviviruses show high conservation of hydrophilicity across the viral polyprotein, regardless of the considerable variation in primary sequence (Westaway & Blok, 1997) and thus it may be possible to extend these results to the other dengue virus serotypes and encephalitic flaviviruses. The mutations that were introduced here required multiple nucleotide and codon changes. In theory, multiple changes reduce the risk of reversion to parental phenotype when introduced into a potential vaccine strain. However, it would be necessary initially to assess each amino acid mutated in a cluster for its contribution to the mutant phenotype. The preferred situation is for each amino acid to make some contribution, rather than for one to be dominant.

The model of the NS3 complexed with an NS2B peptide co-factor enabled the definition of some individual residues important in the interaction between the two proteins. We predict that substitutions of these residues by amino acids other than alanine, both individually and in clusters, will confirm these interactions and expand our understanding of the flavivirus proteinase.

This work was supported by grants from the National Healt and Medical Research Council of Australia and the World Health Organization Global Programme for Vaccines and Immunization. J. C. Whisstock is a Peter Doherty Research Fellow of the National Health and Medical Research Council of Australia.

References

Amberg, S. M. & Rice, C. M. (1999). Mutagenesis of the NS2B–NS3-mediated cleavage site in the flavivirus capsid protein demonstrates a requirement for coordinated processing. *Journal of Virology* **73**, 8083–8094.

Arias, C. F., Preugschat, F. & Strauss, J. H. (1993). Dengue 2 virus NS2B and NS3 form a stable complex that can cleave NS3 within the helicase domain. *Virology* **193**, 888–899.

Bass, S. H., Mulkerrin, M. G. & Wells, J. A. (1991). A systematic mutational analysis of hormone-binding determinants in the human growth hormone receptor. *Proceedings of the National Academy of Sciences, USA* **88**, 4498–4502.

Bazan, J. F. & Fletterick, R. J. (1989). Detection of a trypsin-like serine protease domain in flaviviruses and pestiviruses. *Virology* **171**, 637–639.

Berman, H. M., Westbrook, J., Feng, Z., Gilliland, G., Bhat, T. N., Weissig, H., Shindyalov, I. N. & Bourne, P. E. (2000). The Protein Data Bank. *Nucleic Acids Research* **28**, 235–242.

Bernstein, F. C., Koetzle, T. F., Williams, G. J., Meyer, E. F., Jr, Brice, M. D., Rodgers, J. R., Kennard, O., Shimanouchi, T. & Tasumi, M. (1977). The Protein Data Bank. A computer-based archival file for macromolecular structures. *European Journal of Biochemistry* **80**, 319–324.

Brinkworth, R. I., Fairlie, D. P., Leung, D. & Young, P. R. (1999). Homology model of the dengue 2 virus NS3 protease: putative interactions with both substrate and NS2B cofactor. *Journal of General Virology* **80**, 1167–1177.

Chambers, T. J., Weir, R. C., Grakoui, A., McCourt, D. W., Bazan, J. F., Fletterick, R. J. & Rice, C. M. (1990). Evidence that the N-terminal domain of nonstructural protein NS3 from yellow fever virus is a serine protease responsible for site-specific cleavages in the viral polyprotein. *Proceedings of the National Academy of Sciences, USA* **87**, 8898–8902.

Chambers, T. J., Nestorowicz, A., Amberg, S. M. & Rice, C. M. (1993). Mutagenesis of the yellow fever virus NS2B protein: effects on proteolytic processing, NS2B–NS3 complex formation, and viral replication. *Journal of Virology* **67**, 6797–6807.

Chambers, T. J., Nestorowicz, A. & Rice, C. M. (1995). Mutagenesis of the yellow fever virus NS2B/3 cleavage site: determinants of cleavage site specificity and effects on polyprotein processing and viral replication. *Journal of Virology* **69**, 1600–1605.

Chang, G.-J. (1997). Molecular biology of dengue viruses. In *Dengue and Dengue Hemorrhagic Fever*, pp. 175–198. Edited by D. J. Gubler & G. Kuno. Wallingford: CAB International.

Chen, C. J., Kuo, M. D., Chien, L. J., Hsu, S. L., Wang, Y. M. & Lin, J. H. (1997). RNA–protein interactions: involvement of NS3, NS5, and 3′ noncoding regions of Japanese encephalitis virus genomic RNA. *Journal of Virology* **71**, 3466–3473.

Cunningham, B. C. & Wells, J. A. (1989). High-resolution epitope mapping of hGH-receptor interactions by alanine-scanning mutagenesis. *Science* **244**, 1081–1085.

Della-Porta, A. J. & Westaway, E. G. (1972). Rapid preparation of hemagglutinins of togaviruses from infected cell culture fluids. *Applied Microbiology* **23**, 158–160.

Diamond, S. E. & Kirkegaard, K. (1994). Clustered charged-to-alanine mutagenesis of poliovirus RNA-dependent RNA polymerase yields multiple temperature-sensitive mutants defective in RNA synthesis. *Journal of Virology* **68**, 863–876.

Droll, D. A., Murthy, H. M. K. & Chambers, T. J. (2000). Yellow fever virus NS2B–NS3 protease: charged-to-alanine mutagenesis and deletion analysis define regions important for protease complex formation and function. *Virology* **275**, 335–347.

Failla, C., Tomei, L. & Defrancesco, R. (1995). An amino-terminal domain of the hepatitis C virus NS3 protease is essential for interaction with NS4A. *Journal of Virology* **69**, 1769–1777.

Falgout, B., Pethel, M., Zhang, Y. M. & Lai, C. J. (1991). Both nonstructural proteins NS2B and NS3 are required for the proteolytic processing of dengue virus nonstructural proteins. *Journal of Virology* **65**, 2467–2475.

Falgout, B., Miller, R. H. & Lai, C. J. (1993). Deletion analysis of dengue virus type 4 nonstructural protein NS2B: identification of a domain required for NS2B–NS3 protease activity. *Journal of Virology* **67**, 2034–2042.

Gavin, D. K., Young, S. M., Jr, Xiao, W., Temple, B., Abernathy, C. R., Pereira, D. J., Muzyczka, N. & Samulski, R. J. (1999). Charge-to-alanine mutagenesis of the adeno-associated virus type 2 Rep78/68 proteins yields temperature-sensitive and magnesium-dependent variants. *Journal of Virology* **73**, 9433–9445.

Gruenberg, A. & Wright, P. J. (1992). Processing of dengue virus type 2 structural proteins containing deletions in hydrophobic domains. *Archives of Virology* **122**, 77–94.

Gualano, R. C., Pryor, M. J., Cauchi, M. R., Wright, P. J. & Davidson, A. D. (1998). Identification of a major determinant of mouse neurovirulence of dengue virus type 2 using stably cloned genomic-length cDNA. *Journal of General Virology* **79**, 437–446.

Hahn, Y. S., Galler, R., Hunkapiller, T., Dalrymple, J. M., Strauss, J. H. & Strauss, E. G. (1988). Nucleotide sequence of dengue 2 RNA and comparison of the encoded proteins with those of other flaviviruses. *Virology* **162**, 167–180.

Halstead, S. B. (1988). Pathogenesis of dengue: challenges to molecular biology. *Science* **239**, 476–481.

Ho, S. N., Hunt, H. D., Horton, R. M., Pullen, J. K. & Pease, L. R. (1989). Site-directed mutagenesis by overlap extension using the polymerase chain reaction. *Gene* **77**, 51–59.

Huang, M., Zensen, R., Cho, M. & Martin, M. A. (1998). Construction and characterization of a temperature-sensitive human immunodeficiency virus type 1 reverse transcriptase mutant. *Journal of Virology* **72**, 2047–2054.

Irie, K., Mohan, P. M., Sasaguri, Y., Putnak, R. & Padmanabhan, R. (1989). Sequence analysis of cloned dengue virus type 2 genome (New Guinea-C strain). *Gene* **75**, 197–211.

Jan, L.-R., Yang, C.-S., Trent, D. W., Falgout, B. & Lai, C.-J. (1995). Processing of Japanese encephalitis virus non-structural proteins: NS2B–NS3 complex and heterologous proteases. *Journal of General Virology* **76**, 573–580.

Kapoor, M., Zhang, L. W., Ramachandra, M., Kusukawa, J., Ebner, K. E. & Padmanabhan, R. (1995). Association between NS3 and NS5 proteins of dengue virus type 2 in the putative RNA replicase is linked to differential phosphorylation of NS5. *Journal of Biological Chemistry* **270**, 19100–19106.

Li, H. T., Clum, S., You, S. H., Ebner, K. E. & Padmanabhan, R. (1999). The serine protease and RNA-stimulated nucleoside triphosphatase and RNA helicase functional domains of dengue virus type 2 NS3 converge within a region of 20 amino acids. *Journal of Virology* **73**, 3108–3116.

Lin, C., Thomson, J. A. & Rice, C. M. (1995). A central region in the hepatitis C virus NS4A protein allows formation of an active NS3–NS4A serine proteinase complex *in vivo* and *in vitro*. *Journal of Virology* **69**, 4373–4380.

Monath, T. P. (1994). Dengue: the risk to developed and developing countries. *Proceedings of the National Academy of Sciences, USA* **91**, 2395–2400.

Murthy, H., Clum, S. & Padmanabhan, R. (1999). Dengue virus NS3 serine protease: crystal structure and insights into interaction of the active site with substrates by molecular modeling and structural analysis of mutational effects. *Journal of Biological Chemistry* **274**, 5573–5580.

Muylaert, I. R., Galler, R. & Rice, C. M. (1997). Genetic analysis of the yellow fever virus NS1 protein: identification of a temperature-sensitive mutation which blocks RNA accumulation. *Journal of Virology* **71**, 291–298.

Nestorowicz, A., Chambers, T. J. & Rice, C. M. (1994). Mutagenesis of the yellow fever virus NS2A/2B cleavage site: effects on proteolytic processing, viral replication, and evidence for alternative processing of the NS2A protein. *Virology* **199**, 114–123.

Parkin, N. T., Chiu, P. & Coelingh, K. L. (1996). Temperature-sensitive mutants of influenza A virus generated by reverse genetics and clustered charged to alanine mutagenesis. *Virus Research* **46**, 31–44.

Preugschat, F., Yao, C. W. & Strauss, J. H. (1990). *In vitro* processing of dengue virus type 2 nonstructural proteins NS2A, NS2B, and NS3. *Journal of Virology* **64**, 4364–4374.

Pryor, M. J. & Wright, P. J. (1993). The effects of site-directed mutagenesis on the dimerization and secretion of the NS1 protein specified by dengue virus. *Virology* **194**, 769–780.

Pryor, M. J., Gualano, R. C., Lin, B., Davidson, A. D. & Wright, P. J. (1998). Growth restriction of dengue virus type 2 by site-specific mutagenesis of virus-encoded glycoproteins. *Journal of General Virology* **79**, 2631–2639.

Rice, C. M. (1996). *Flaviviridae*: The viruses and their replication. In *Fields Virology*, 3rd edn, pp. 931–959. Edited by B. N. Fields, D. M. Knipe & P. M. Howley. Philadelphia: Lippincott–Raven.

Schechter, I. & Berger, A. (1967). On the size of the active site in proteases. I. Papain. *Biochemical and Biophysical Research Communications* **27**, 157–162.

Teo, K. F. & Wright, P. J. (1997). Internal proteolysis of the NS3 protein specified by dengue virus 2. *Journal of General Virology* **78**, 337–341.

Valle, R. & Falgout, B. (1998). Mutagenesis of the NS1 protease of dengue virus type 2. *Journal of Virology* **72**, 624–632.

van Regenmortel, M. H. V., Fauquet, C. M., Bishop, D. H. L., Carstens, E. B., Estes, M. K., Lemon, S. M., Maniloff, J., Mayo, M. A., McGeoch, D. J., Pringle, C. R. & Wickner, R. B. (2000). *Virus Taxonomy. Seventh Report of the International Committee on Taxonomy of Viruses*. San Diego: Academic Press.

Westaway, E. G. & Blok, J. (1997). Taxonomy and evolutionary relationships of flaviviruses. In *Dengue and Dengue Hemorrhagic Fever*, pp. 147–173. Edited by D. J. Gubler & G. Kuno. Wallingford: CAB International.

Wiskerchen, M. & Muesing, M. A. (1995). Identification and characterization of a temperature-sensitive mutant of human immunodeficiency virus type 1 by alanine scanning mutagenesis of the integrase gene. *Journal of Virology* **69**, 597–601.

Yan, Y. W., Li, Y., Munshi, S., Sardana, V., Cole, J. L., Sardana, M., Steinkuehler, C., Tomei, L., Defrancesco, R., Kuo, L. C. & Chen, Z. G. (1998). Complex of NS3 protease and NS4A peptide of BK strain hepatitis C virus: a 2·2 Å resolution structure in a hexagonal crystal form. *Protein Science* **7**, 837–847.

Yusoff, R., Clum, S., Wetzel, M., Murthy, H. M. K. & Padmanabhan, R. (2000). Purified NS2B/NS3 serine proteinase of dengue virus type 2 exhibits cofactor NS2B dependence for cleavage of substrates with dibasic amino acids *in vitro*. *Journal of Biological Chemistry* **275**, 9963–9969.

Received 14 December 2000; Accepted 14 March 2001

JOURNAL OF VIROLOGY, Oct. 2001, p. 9633–9643
0022-538X/01/$04.00+0 DOI: 10.1128/JVI.75.20.9633–9643.2001

Vol. 75, No. 20

Mutagenesis of the *Dengue Virus Type 2* NS3 Protein within and outside Helicase Motifs: Effects on Enzyme Activity and Virus Replication

ANITA E. MATUSAN, MELINDA J. PRYOR, ANDREW D. DAVIDSON, AND PETER J. WRIGHT*

Department of Microbiology, Monash University, Clayton, Victoria 3168, Australia

Received 27 March 2001/Accepted 12 July 2001

The protein NS3 of *Dengue virus type 2* (DEN-2) is the second largest nonstructural protein specified by the virus and is known to possess multiple enzymatic activities, including a serine proteinase located in the N-terminal region and an NTPase-helicase in the remaining 70% of the protein. The latter region has seven conserved helicase motifs found in all members of the family *Flaviviridae*. DEN-2 NS3 lacking the proteinase region was synthesized as a fusion protein with glutathione *S*-transferase in *Escherichia coli*. The effects of 10 mutations on ATPase and RNA helicase activity were examined. Residues at four sites within enzyme motifs I, II, and VI were substituted, and six sites outside motifs were altered by clustered charged-to-alanine mutagenesis. The mutations were also tested for their effects on virus replication by incorporation into genomic-length cDNA. Two mutations, both in motif I (G198A and K199A) abolished both ATPase and helicase activity. Two further mutations, one in motif VI (R457A,R458A) and the other a clustered charged-to-alanine substitution at $R_{376}KNGK_{380}$, abolished helicase activity only. No virus was detected for any mutation which prevented helicase activity, demonstrating the requirement of this enzyme for virus replication. The remaining six mutations resulted in various levels of enzyme activities, and four permitted virus replication. For the two non-replicating viruses encoding clustered changes at $R_{184}KR_{186}$ and $D_{436}GEE_{439}$, we propose that the substituted residues are surface located and that the viruses are defective through altered interaction of NS3 with other components of the viral replication complex. Two of the replicating viruses displayed a temperature-sensitive phenotype. One contained a clustered mutation at $D_{334}EE_{336}$ and grew too poorly for further characterization. However, virus with an M283F substitution in motif II was examined in a temperature shift experiment (33 to 37°C) and showed reduced RNA synthesis at the higher temperature.

The four serotypes of *Dengue virus* (types 1 to 4) belong to the family *Flaviviridae*, which consists of the genera *Flavivirus*, *Pestivirus*, and *Hepacivirus* (52). The dengue virus genome is positive-sense RNA of 11 kb and encodes the proteins C-prM-E-NS1-NS2A-NS2B-NS3-NS4A-NS4B-NS5 in a single open reading frame. Co- and posttranslational polyprotein processing by host and viral proteinases generates three structural proteins, namely, C (capsid), M (membrane associated) and E (envelope), and seven nonstructural (NS) proteins, NS1 through NS5 (reviewed in reference 45). Biochemical functions have been demonstrated for some nonstructural proteins. NS5 possesses RNA-dependent RNA polymerase activity (49). A complex of NS2B and NS3 acts as a chymotrypsin-like serine proteinase; the N-terminal 30% of NS3 is sufficient for this activity (15, 42). The C-terminal 70% of NS3 has seven motifs characteristic of RNA helicases of the DExH subfamily. Recombinant proteins containing the C-terminal helicase region of dengue virus NS3 possess nucleoside triphosphatase (NTPase) (10, 33) and RNA helicase activities (33).

RNA helicases catalyze the unidirectional unwinding of duplex RNAs (containing a single-stranded RNA region of at least 3 nucleotides [nt]) in the presence of a divalent cation and require the hydrolysis of the β-γ bond of a suitable deoxynucleoside triphosphate or nucleoside triphosphate (NTP) (usually ATP) as an energy source (32, 40). Known and putative RNA helicases of viral origin possess conserved amino acid sequence motifs enabling their classification into three distinct superfamilies. Superfamilies 1 and 2 have seven conserved motifs, while superfamily 3 has only three (30). The helicase of the flavivirus *Dengue virus type 2* (DEN-2) is a member of superfamily 2, which includes the helicases of the pestivirus *Bovine viral diarrhea virus* (BVDV) and the hepacivirus *Hepatitis C virus* (HCV). Helicases can be further classified into DEAD, DExH, and DExx subfamilies based on the sequence of motif II (35, 46). The multifunctional flavivirus NS3 helicase protein is believed to be a component of the viral RNA replication complex with the RNA-dependent RNA polymerase NS5 protein (26). There is evidence that NS3 interacts with both NS5 and stem-loop structures in the genomic 3′ untranslated region, possibly playing an important role in the initiation of negative-strand RNA synthesis (8, 26).

Several X-ray crystal structures of the HCV NS3 helicase domain have been determined (9, 29, 58) and together with site-directed mutagenesis have helped to define the function of some helicase motifs. The first reported mutagenesis studies of HCV and other positive-strand viruses targeted the helicase motifs I, II, III, and VI. Motif I (GxGKT), conserved in all three superfamilies, is involved in binding the β and γ phosphate groups of NTPs. Motif II (DExH), also present in all

* Corresponding author. Mailing address: Department of Microbiology, P.O. Box 53, Monash University, Victoria 3800, Australia. Phone: 61 3 9905 4828. Fax: 61 3 9905 4811. E-mail: Peter.Wright@med.monash.edu.au.

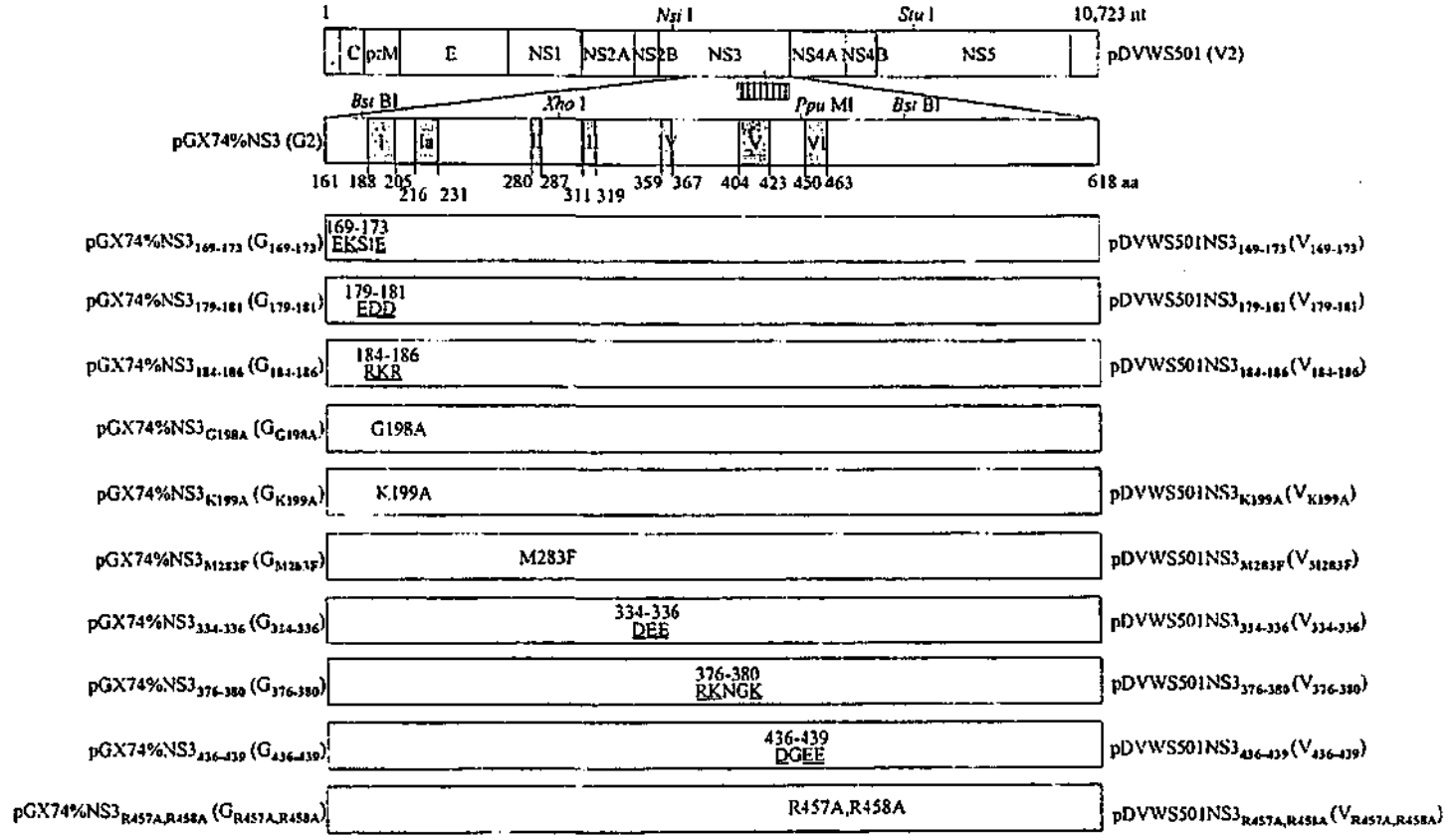

FIG. 1. Constructs used to synthesize NS3 fusion proteins and prepare mutant viruses. The seven helicase motifs are shaded (29); residue numbers within NS3 are given. On the left are the full (pGX) and abbreviated (G) designations of the truncated NS3 gene constructs in pGEX-3X. The G designations are also used for the corresponding encoded mutant fusion proteins where appropriate. On the right are the names of the plasmids containing genomic-length cDNA (pDVWS) and derived virus (V). Antiserum raised in rabbits against a bacterial fusion protein (50) was directed against a segment of NS3 (vertical stripes). For clustered charged-to-alanine mutants, the underlined residues were mutated to alanine.

three superfamilies, is predicted to bind Mg^{2+}, making a complex with the terminal phosphates of the NTP. Several residues and motifs have been implicated in the coupling of NTP hydrolysis with RNA unwinding; they are the histidine residue of motif II, motif III (TAT box), and the glutamine and arginine residues of motif VI ([Q/x]RxGRxxR) (16, 18, 21, 28, 41, 51, 53, 58). More recently, the roles of residues outside motifs were examined using site-directed mutagenesis and a crystal structure of the HCV NS3 helicase-$(dU)_8$ complex (29, 34, 41). Several conserved HCV helicase residues which contact the oligonucleotide were shown to be involved in RNA binding, duplex unwinding, and polynucleotide-stimulated ATPase activity.

This study investigated the importance of selected residues in the DEN-2 NS3 helicase region for enzyme activity and viral replication. Two types of mutations were introduced. The first type was the substitution of residues within motifs, I, II, and VI, and the second type was the replacement with alanine of amino acids in clusters of charged amino acids outside motifs. Mutant proteins were synthesized as N-terminally truncated fusion proteins in *Escherichia coli*, purified, and assayed for ATPase and RNA helicase activities. Mutations were also incorporated into genomic-length DEN-2 cDNA to investigate the effects of changes on viral yield. This work is the first report of extensive mutagenesis of a flavivirus helicase, examining both enzyme activity and viral replication.

MATERIALS AND METHODS

Cell lines, virus, and antiserum. BHK-21 and *Aedes albopictus* C6/36 cells were grown and maintained as described previously (43). Stocks of DEN-2 viruses were prepared, and titers were determined by plaque assay in C6/36 cells at 28°C (22). Concentrated stocks of some viruses were produced by precipitation with polyethylene glycol (12). The preparation of rabbit polyclonal antiserum directed against DEN-2 NS3 (residues 355 to 593) has been described (50).

Constructs encoding NS3 fusion proteins. For the following cloning strategies, the locations of restriction enzyme sites cleaving in DEN-2 cDNA (25) are shown in superscript, and sites present in plasmid vectors are not numbered. To obtain a plasmid encoding the C-terminal region of the DEN-2 NS3 protein, an $NdeI^{5002}$-$SpeI$ cDNA fragment (containing nt 5002 to 6375 of the DEN-2 New Guinea C [NGC] genome) was excised from the vector pSV.NS3, which encodes full-length NS3 and contains a stop codon at the 3′ end of the NS3 gene (50), and cloned into the *Sma*I site of pGEX-3X (Pharmacia Biotech). The resulting plasmid pGX74%NS3 encodes the glutathione *S*-transferase (GST) fused to residues 161 to 618 of DEN-2 NS3 (Fig. 1). The plasmid pGX74%NS3 was used as a template for mutagenesis by overlap extension PCR (OE-PCR) (24). Sequences of oligonucleotides used in mutagenesis are shown in Table 1. Six mutant constructs (Fig. 1) derived from pGX74%NS3 were prepared by replacing the $BamHI$-$XhoI^{5426}$ fragment (*Bam*HI is located in the pGEX-3X multiple cloning site immediately upstream of *Sma*I) with a mutagenized fragment prepared by OE-PCR; the constructs were pGX74%$NS3_{169-173}$, pGX74%$NS3_{179-181}$, pGX74%$NS3_{184-186}$, pGX74%$NS3_{G198A}$, pGX74%$NS3_{K199A}$ and pGX74%$NS3_{M283F}$. The plasmid pGX74%$NS3_{R457A,R458A}$ was constructed by removing the mutagenized $XhoI^{5426}$-*Sna*BI fragment from the plasmid pSV.NS2B/$3_{457,458}$ (50) and ligating this into $XhoI^{5426}$-*Bsa*AI-digested pGX74%NS3. The remaining three mutant constructs were derived from pGX74%NS3 by replacing the $XhoI^{5426}$-*Ppu* MI^{5852} fragment with mutagenized fragments prepared by OE-PCR; they were pGX74%$NS3_{334-336}$, pGX74%$NS3_{376-380}$, pGX74%$NS3_{436-439}$. The PCR-derived regions of all clones were sequenced.

TABLE 1. Oligonucleotides used in OE-PCR

Mutant	Primer no.	Primer designation[a]	Sequence[b] (5′ to 3′)
$E_{169}KSIE_{173}$[c]	2618	a	4980ATCGAAGGTCGTGGGATCCCCCTATG5005
	4095	b	5020CAGACTGcAgcAAGTATTGcAGACAATCCAGAGAT5055
	4096	c	5045TTGTCTgCAATACTTgcTgCAGTGTGGGCTATAGCA5010
	2619	d	5568CTCATGTCCAGAACTCCACGACG5545
$E_{179}DD_{181}$	2618	a	4980ATCGAAGGTCGTGGGATCCCCCTATG5005
	7538	b	5050GAGATCGcAGcTGcTATTTTTCGAAAGAG5078
	3640	c	5082TTTTCTCTTTCGAAAAATGgCAgCTgCGATCTCTGGATTGTC5041
	2619	d	5568CTCATGTCCAGAACTCCACGACG5545
$R_{184}KR_{186}$	2618	a	4980ATCGAAGGTCGTGGGATCCCCCTATG5005
	4097	b	5065TATTTTTgcAgcGgcAAAATTGACCATCATGGACC5099
	4098	c	5085CAATTTTgcCgcTgcAAAAATATCATCTTCGATCTCTGG5047
	2619	d	5568CTCATGTCCAGAACTCCACGACG5545
G198A	2618	a	4980ATCGAAGGTCGTGGGATCCCCCTATG5005
	2620	b	5107GGAGCGGctAAGACGAAGACATACCTTCCG5136
	2621	c	5126CTCTTCGTCTTagCCGCTCCTGGGTGGAGG5097
	2619	d	5126CTCTTCGTCTTagCCGCTCCTGGGTGGAGG5097
K199A	2618	a	5126ATCGAAGGTCGTGGGATCCCCCTATG5005
	2624	b	5107GGAGCGGGAgcGACGAAGAGATACCTTCCG5136
	2625	c	5124CTTCGTCgcTCCCGCTCCTGGGTGGAGGTC5095
	2619	d	5568CTCATGTCCAGAACTCCACGACG5545
M283F	2618	a	4980ATCGAAGGTCGTGGGATCCCCCTATG5005
	2627	b	5361CATCtTcGACGAAGCCCATTTCACAGACCC5393
	2626	c	5374CGTCgAaGATGATCAGGTTGTAATTTGGC5346
	2619	d	5568CTCATGTCCAGAACTCCACGACG5545
$D_{334}EE_{336}$	3638	a	4792GAAGAAGCCGCGGTCTTGGCATTGGAGCCTG4822
	4099	b	5517CATGGcTGcAGcAAGAGAAATCCCTGAACG5546
	4100	c	5533CTCTTgCTgCAgCCATGATTGGTGCAT5507
	4318	d	6123CACAAAGGTTTTCCTTGCTTCTCCTCTCAAGCGG6090
$R_{376}KNGK_{380}$	3638	a	4792GAAGAAGCCGCGGTCTTGGCATTGGAGCCTG4822
	4104	b	5641TGCCTGgcAgcAAATGGAgcGAAAGTGATACAACTC5676
	4105	c	5667CACTTTCgcTCCATTTgcTgcCAGGCAAGCTGCTATATC5629
	4318	d	6123CACAAAGGTTTTCCTTGCTTCTCCTCTCAAGCGG6090
$D_{436}GEE_{439}$	3638	a	4792GAAGAAGCCGCGGTCTTGGCATTGGAGCCTG4822
	4106	b	5821CTAACAGcTGGTGcAGcGCGGGTGATCCTGGCA5853
	4107	c	5842CCCGCgCTgCACCAgCTGTTAGTATAACTGG5812
	4318	d	6123CACAAAGGTTTTCCTTGCTTCTCCTCTCAAGCGG6090

[a] Primers designated a and d are flanking primers; primers designated c and b are mutagenic primers.
[b] All sequences are listed 5′ to 3′, and the substituted nucleotides are in lowercase type. Nucleotide numbering refers to the NGC DEN-2 sequence of Irie et al. (25).
[c] For clustered charged-to-alanine mutants, the underlined residues were mutated to alanine. Amino acid numbering refers to the position of the residue in NS3.

Synthesis and purification of NS3 proteins. The recombinant proteins containing an N-terminal GST tag were expressed in *E. coli* DH5α cells grown at 37°C in Luria-Bertani medium containing ampicillin (100 μg/ml). Synthesis of the recombinant proteins was induced by the addition of 0.1 mM isopropyl-β-D-thiogalactopyranoside. Two hours later, the cells were collected by centrifugation, resuspended in ice-cold phosphate-buffered saline containing lysozyme (33 μg/ml), and held on ice for 10 min. Triton X-100, at a final concentration of 0.1%, was added to the cells prior to their sonication on ice for 2 min. The cell lysate was clarified by centrifugation at 12,000 × *g* for 10 min. The soluble fraction was mixed with glutathione-Sepharose 4B beads (Pharmacia Biotech) and gently mixed at 4°C for 30 min. The beads were washed three times with phosphate-buffered saline, and bound protein was eluted twice in elution buffer (10 mM glutathione and 50 mM Tris-HCl [pH 8.0]) at 25°C for 15 min. All protein preparations were adjusted to 10% glycerol and stored at −70°C. Protein concentrations were estimated by densitometer scanning of Coomassie blue-stained acrylamide gels and Bradford assay (Bio-Rad).

ATPase assay. The ATPase assay was a modified procedure of Warrener et al. (54). Briefly, the final volume of the standard assay used to test mutated proteins was 10 μl, containing 50 mM Tris-HCl (pH 8.0), 10 mM NaCl, 2.5 mM $MgCl_2$, 1 μCi of [α-^{32}P]ATP (800 Ci/mmol; DuPont) and 0.4 pmol of protein sample. Reaction mixes were incubated for 1 h at 24°C, and the reactions were terminated by the addition of EDTA to a final concentration of 20 mM. A 0.5-μl sample of the reaction mixture was spotted onto plastic-backed polyethyleneimine-cellulose sheets, and ^{32}P-labeled ATP and ADP were separated by ascending chromatography in 0.375 M potassium phosphate (pH 3.5). The sheets were dried and exposed to X-ray film. The percentage of conversion of ATP to ADP was estimated by measuring the radioactivity in separated nucleotides by liquid scintillation counting.

The values of K_m and k_{cat} were calculated from a Lineweaver-Burk plot of ATP hydrolysis activity over a range of ATP concentrations from 1 to 5 mM. The concentration of poly(A), if present, was 0.17 μg/μl (0.5 mM measured as mononucleotide equivalents).

Helicase assay. A partial double-stranded RNA (dsRNA) substrate was prepared using a modified pGEM-4Z (Promega) plasmid. A 24-bp region of the polylinker was removed by digestion with *Eco*RI and *Hin*dIII, filling in of recessed ends with Klenow DNA polymerase, and blunt-end ligation to generate the plasmid pGEM-4ZΔ24.

*Nde*I-digested plasmid pGEM-4ZΔ24 was transcribed with T7 RNA polymerase to produce a 259-nt strand. *Ban*I-digested plasmid pGEM-4ZΔ24 was transcribed with SP6 RNA polymerase in the presence of [α-^{32}P]ATP to produce a radiolabeled 144-nt strand. Reaction mixes were treated with RQI RNase-Free DNase (Promega) and extracted with phenol-chloroform, and the RNA was precipitated with ethanol. Transcripts were combined in annealing buffer containing 10 mM Tris-HCl (pH 7.5), 0.1 mM EDTA, and 200 mM NaCl. The mixture was heated for 5 min at 95°C and 1 h at 65°C and then was allowed to cool to room temperature over 3 h. RNA sample buffer (5×; 25 mM EDTA, 0.25% bromophenol blue, 50% glycerol, 0.5% sodium dodecyl sulfate [SDS]) was added to the hybridization mixture, which was then electrophoresed through a 6% polyacrylamide gel (acrylamide-bisacrylamide [30:0.8], 0.5× TBE [90 mM Tris borate, pH 7.5; 2 mM EDTA], 0.1% SDS). The region of the gel containing the RNA duplex was localized by autoradiography, excised from the gel, and pulverized, and RNA was eluted overnight at 37°C with a solution containing 500 mM ammonium acetate, 10 mM magnesium acetate, 1 mM EDTA, and 0.1% SDS. The eluted RNA was precipitated with ethanol and resuspended in water.

The RNA helicase assay was carried out in a total volume of 20 μl containing radiolabeled substrate, 25 mM MOPS (morpholinepropanesulfonic acid)-KOH

(pH 6.5), 5 mM ATP, 3 mM $MnCl_2$, 2 mM dithiothreitol, 100 μg/ml bovine serum albumin, 5 U of RNasin (Promega), and 1 pmol of protein. Reaction mixtures were incubated for 30 min at 37°C and terminated by the addition of 5× RNA sample buffer. The reaction mixture was analyzed by electrophoresis through a 6% polyacrylamide gel. Gels were dried and exposed to the storage phosphor screen (Molecular Dynamics). The phosphor screen was analyzed using a STORM PhosphorImager system, and ImageQuant image analysis software (Molecular Dynamics) was used to estimate the percentage of ^{32}P-labeled fragment unwound.

Insertion of mutations into genomic-length DEN-2 cDNA. The plasmid pDVWS501, which contains genomic-length DEN-2 cDNA, was described in detail (22). For these experiments, the mutated NS3 helicase fusion proteins were examined for ATPase and RNA helicase activity, and then the mutations were inserted into genomic-length DEN-2 cDNA to study their effects on virus replication (except the G198A mutant) (Fig. 1).

The plasmids pDVWS501NS3$_{334-336}$, pDVWS501NS3$_{376-380}$, and pDVWS501NS3$_{436-439}$ were prepared by replacing the *Bst*BI^{5069}-*Bst*BI^{6036} fragment of pDVWS501 with a mutagenized fragment prepared by OE-PCR. Sequences of oligonucleotides used in mutagenesis are shown in Table 1. The plasmids pDVWS501NS3$_{K199A}$, pDVWS501NS3$_{M283F}$, and pDVWS501NS3$_{R457A,R458A}$ were prepared by removing the mutagenized *Bst*BI^{5069}-*Bst*BI^{6046} fragments from the corresponding pGX74%NS3 plasmid and ligation into *Bst*BI-digested pDVWS501 (Fig. 1).

The other three mutations were initially constructed in the plasmid pDVSO8298 (pSPORT 1 containing nt 4494 to 8744 of DEN-2 NGC) prior to ligation into pDVWS501. A cDNA fragment encoding the mutation EDD (residues 179 to 181) (underlined residues changed to alanine) was cloned into pDVSO8298 by removing the mutagenized *Nsi*I^{4760}-*Ppu* MI^{5854} fragment from the corresponding pSV.NS2B/3 plasmid and ligation into *Nsi*I-*Ppu*MI-digested pDVSO8298. The two remaining charged-to-alanine mutations, EKSIE (169–173) and RKR (184–186), were introduced into *Nsi*I-*Ppu*MI-digested pDVSO8298 as OE-PCR fragments. For all three mutants, *Nsi*I^{4760}-*Stu*I^{7874} mutagenized fragments were then removed from the appropriate pDVSO8298 plasmid and ligated into *Nsi*I-*Stu*I-digested pDVWS501. PCR-derived regions were sequenced.

Production of virus from genomic-length cDNA. Procedures for transcription of RNA, electroporation, and immunofluorescence of BHK-21 cells and passaging of virus in C6/36 cells have been described (22). Briefly, capped transcripts were produced from plasmids containing genomic-length DEN-2 cDNA using the Promega RiboMAX kit. Approximately 7 to 10 μg of transcript RNA and 50 μg of carrier tRNA were electroporated into BHK-21 cells, which were then incubated at 33 or 37°C. The cells were examined for immunofluorescence 4 to 6 days later using anti-E monoclonal antibodies (20). At 7 days the culture medium was used to infect C6/36 cells. Four to five days later, the culture medium from the C6/36 cells was used to initiate a second passage in C6/36 cells. When approximately 50% of the cells exhibited cytopathic effects, or 4 days later if no cytopathic effects were visible, these second passage virus stocks were collected, and titers were determined by plaque assay in C6/36 cells.

To confirm that each mutation was present after electroporation and passaging, total RNA was extracted from infected C6/36 cells or supernatant, and reverse transcription (RT)-PCR of viral RNA was performed (22, 43). The complete NS2B and NS3 genes were sequenced to confirm the presence of the introduced mutation and the absence of any other changes that may have been introduced during virus passaging.

Temperature shift experiments. RNA extracts of infected cells were prepared using RNeasy columns (Qiagen) for analysis of viral RNA content by dot blot hybridization. A ^{32}P-labeled DNA probe spanning nt 5364 to 6123 of the DEN-2 genome was produced by random primed labeling using [α-^{32}P]dATP (3,000 Ci/mmol), labeling mix-dCTP and pd(N)$_n$ (Pharmacia Biotech). RNA samples were diluted in RNA dilution buffer (diethyl pyrocarbonate-treated H_2O-20× SSC [1× SSC is 0.15 M NaCl plus 0.015 M sodium citrate]-formaldehyde [5:3:2]) and held at 65°C for 15 min to remove RNA secondary structure. The samples were applied to a Hybond-N+ nylon membrane (Amersham), presoaked in 10× SSC, using an SRC 96 D Minifold I dot blotter (Schleicher and Schuell). The membrane was allowed to dry at room temperature, cross-linked with UV light, and prehybridized at 68°C for 2 h in hybridization solution (5× SSC, 1% SDS, 1% bovine serum albumin). Labeled DNA probe at 10^7 cpm/ml was heated at 95°C and added to fresh hybridization solution, and the membrane was incubated for a further 16 h in the presence of the probe. The membrane was then washed twice at room temperature in 2× SSC and 0.1% SDS, and this was followed by two washes at 68°C in 0.1× SSC and 0.1% SDS. Bound radioactivity was detected using the STORM PhosphorImager system (Molecular Dynamics).

To assess the effect of temperature shift on viral protein synthesis, infected BHK-21 cells were radiolabeled with *trans*-[^{35}S]methionine (1,150 Ci/mmol) for 2 h. The methods for labeling procedures, cell lysis, radioimmunoprecipitation (RIP), gel electrophoresis, and fluorography have been described (44, 50).

RESULTS

Mutagenesis of the helicase region of NS3. In order to test the importance of residues in the helicase region of DEN-2 NS3 for enzyme activity and virus replication, two types of mutations were introduced. First, changes were made in motifs I, II, and VI. These were single alanine substitutions G198A and K199A (motif I) and a double change at R457A,R458A (motif VI). In motif II, the substitution was M283F; phenylalanine is the second most common residue (after methionine) at this position in positive-strand viruses (30). Based on previous mutational studies and X-ray crystallography data of related viral RNA helicases (16, 19, 21, 28, 41, 51, 53), these motifs are known to be involved in the binding and hydrolysis of ATP and/or the coupling of helicase and ATPase activities. Thus, we hypothesized that the first three mutations would reduce enzyme activity and virus replication, although there were no previous studies on the replication of flaviviruses carrying these types of mutations. The possible effect of the substitution M283F was unknown.

The second type of mutation was the replacement with alanine of three amino acids in clusters of charged amino acids. Charged amino acids are likely to occupy exposed positions in the tertiary structure and therefore interact with other proteins (1, 13). Several studies have demonstrated an association between the flavivirus NS3 protein and other viral nonstructural proteins, including NS2B and NS5, both in vitro and during viral replication (5, 6, 8, 14, 15, 26, 57). The central region of NS3, spanning amino acids 161 through 463, was scanned for clusters of five residues which contained at least three charged amino acids (...., 55). Six such clusters outside helicase motifs (30) were chosen for mutagenesis, and the charged residues were changed to alanine (Fig. 1). These were as follows: E169A, K170A, and E173A; E179A, D180A, and D181A; R184A, K185A, and R186A; D334A, E335A, and E336A; R376A, K377A, and K380A; and lastly, D436A, E438A, and E439A. Alanine was chosen as the replacement amino acid since it removes the side chain beyond the beta carbon and also minimizes any steric effects within the polypeptide caused by the replacement (11). It was of interest to determine whether these changes in hydrophilicity outside helicase motifs modified the enzyme activity of NS3 in the absence of any other viral protein or whether any effects of the changes could be detected only by examining virus replication, when not only helicase activity but also interactions between NS3 and other viral or host proteins may be required.

Synthesis of truncated parental and mutant NS3 in *E. coli*. To provide a source of flavivirus NS3 protein for biochemical studies, truncated (amino acids 161 to 618) parental and mutant polypeptides were synthesized as GST fusion proteins in *E. coli* DH5α cells. Proteins were purified from the cell lysate by affinity chromatography, and purified parental GST:74% NS3 fusion protein (G2) with a molecular mass of 78 kDa was detected following SDS-polyacrylamide gel electrophoresis (Fig. 2A, lane 2). In addition to the G2 protein, several proteins of lower molecular mass were also detected. These were possibly generated by either proteolytic degradation or prema-

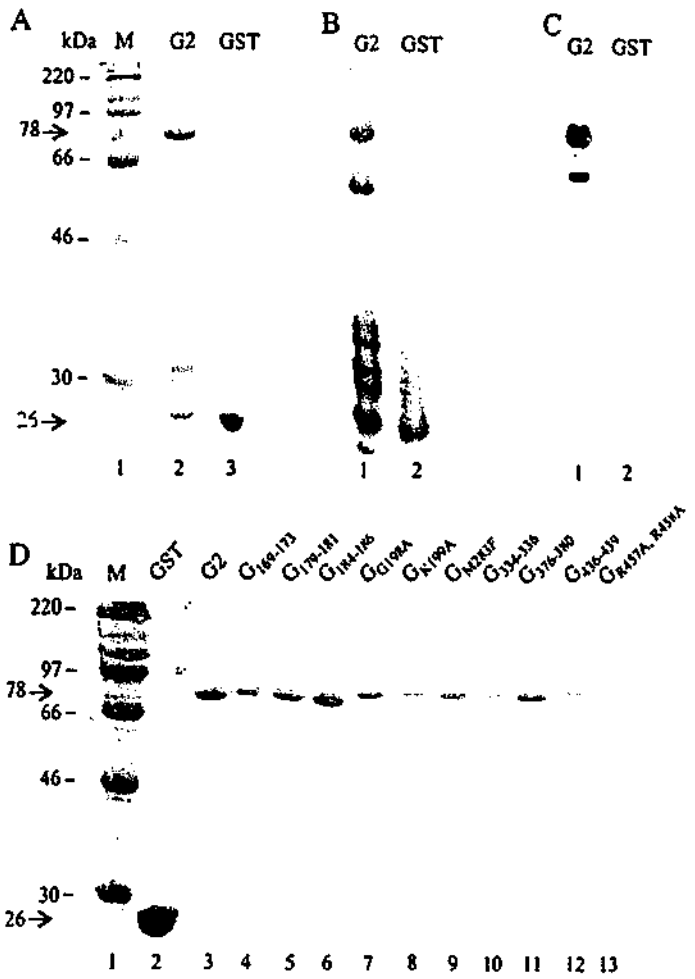

FIG. 2. Analysis on 10% polyacrylamide gels of partially purified parental and mutant GST:74%NS3 fusion proteins. (A) Coomassie blue staining. (B) Immunoblot using anti-GST antibodies (Pharmacia). (C) Immunoblot using anti-NS3 antiserum. (D) Coomassie blue staining of the GST:74%NS3 mutant fusion proteins used for enzyme assays. Size markers are shown on the left.

ture translational termination, as they were recognized by anti-GST and anti-NS3 antibodies (Fig. 2B and C, lanes 1). GST (26 kDa) was also synthesized in *E. coli* to use as a negative control for the in vitro enzyme assays (Fig. 2A, lane 3; Fig. 2B, lane 2). Preparations of all mutant fusion proteins used for enzyme assays are shown in Fig. 2D.

NS3-mediated ATPase activity. The ATPase activity of increasing amounts of the parental NS3 fusion protein G2 was first measured over 45 min in the presence of 5 mM ATP (Fig. 3A). The rate of hydrolysis was directly proportional to the amount of enzyme. Using 1 pmol of enzyme and 5 mM ATP, the rate of hydrolysis was linear from 15 to 90 min (not shown). To determine the K_m of G2, the ATPase activity of 1 pmol of G2 was measured at ATP concentrations from 1 to 5 mM for 60 min in the presence or absence of poly(A). The Lineweaver-Burk plots were linear in this range (Fig. 3B). The K_m values for the parental protein were 3.0 or 2.6 mM in the absence or presence of poly(A), respectively. Corresponding k_{cat} values were 1.2 and 1.5 s^{-1}. The measure of catalytic efficiency, k_{cat}/K_m, increased from 4.0×10^2 (mol/liter)$^{-1}s^{-1}$ in the absence of poly(A) to 5.8×10^2 (mol/liter)$^{-1}s^{-1}$ in the presence of poly(A). Thus, the stimulation of ATPase activity (1.45-fold) by poly(A) was low.

The results of testing the ATPase activity of the mutant NS3 fusion proteins are shown in Fig. 4. The chromatographic analyses of a typical experiment are displayed in Fig. 4A, the means of three experiments are shown in Fig. 4B, and an overall summary is presented in Table 2. As expected, mutation of the highly conserved G198 and K199 residues within ATP binding motif I abolished ATPase activity (Fig. 4A, lanes 7 and 8). Mutation of the less-conserved residues in motifs II and VI also reduced ATPase activity (Fig. 4A, lanes 9 and 13), although to a lesser extent than the motif I mutants. The clustered charged-to-alanine mutants located outside helicase motifs demonstrated a range of ATPase activities, from levels lower (Fig. 4A, lanes 10 and 11) to levels higher (Fig. 4A, lanes 4, 5, 6, and 12) than that of the parental protein. It is interesting that mutated clusters located within the linker region (residues 161 to 188) between the final proteinase box 4 (residues 145 to 155) (3) and upstream of the first helicase motif I (residues 188 to 205) stimulated ATPase activity.

RNA helicase activity of NS3 mutants. Helicase activity was tested by using an RNA substrate which consisted of a 259-nt RNA strand hybridized to a 144-nt radiolabeled RNA strand to produce a partially duplex RNA substrate containing 3′ single-stranded regions with a 24-bp duplex region (Fig. 5A). The G2 protein had RNA helicase activity in the presence of Mn^{2+} and ATP as shown by the release of the radiolabeled

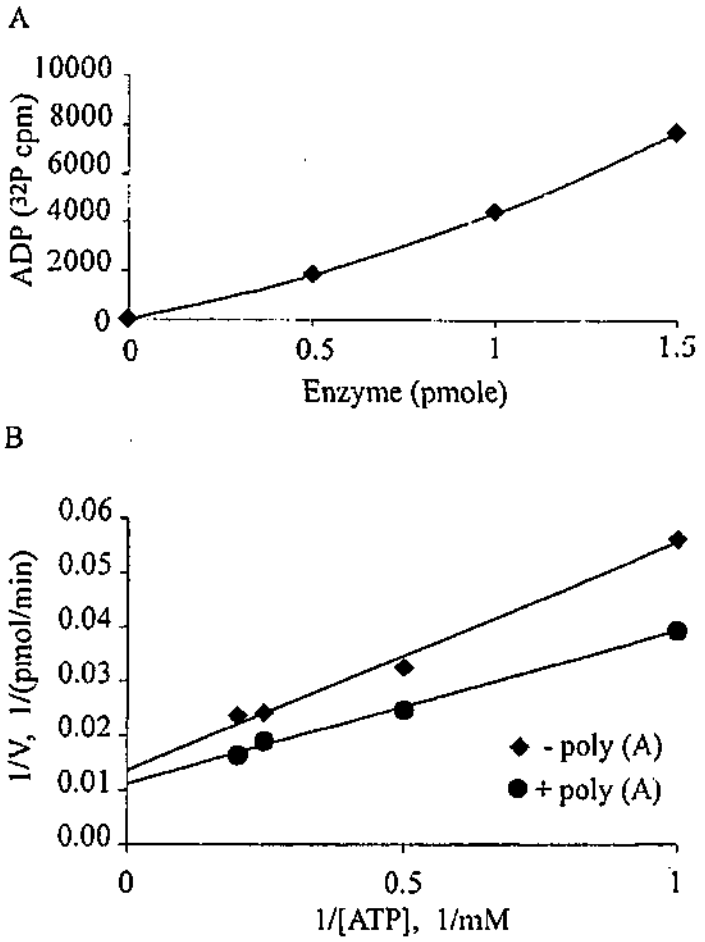

FIG. 3. (A) ATPase activity of increasing amounts of parental GST:74%NS3 fusion protein measured by the production of [α^{32}P] ADP. (B) Lineweaver-Burk plots of ATPase activity in the presence or absence of 0.5 mM poly(A). A reaction volume of 10 μl contained 1 pmol of enzyme.

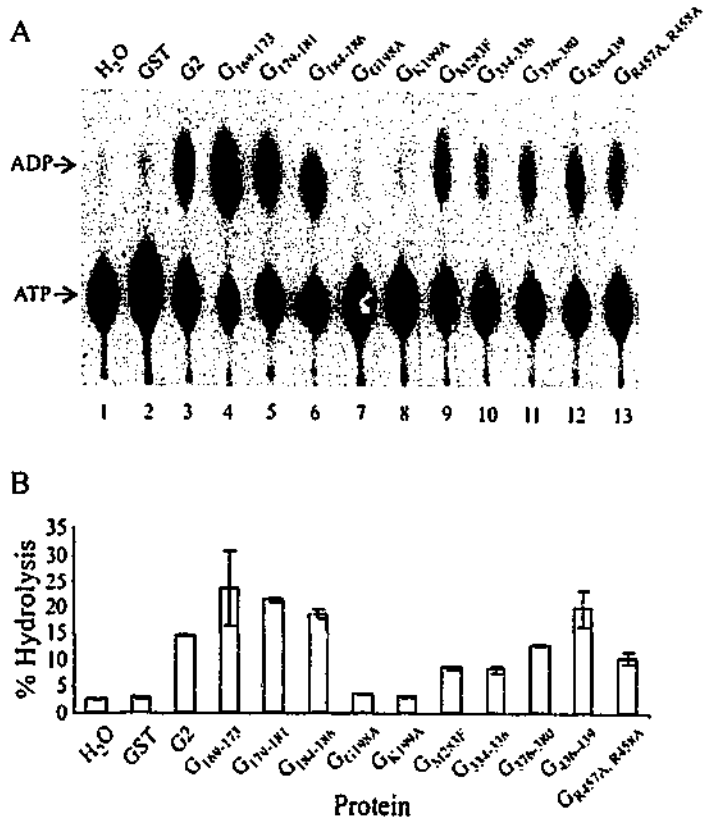

FIG. 4. (A) ATPase activities of parental and mutant 74%NS3 fusion proteins. Radioactive ADP and ATP were separated by thin-layer chromatography. (B) Percent hydrolysis of ATP to ADP. Means (columns) and range of values (error bars) from three independent experiments are shown.

strand (Fig. 5B, lane 3). In the absence of the G2 protein (lane 2), or Mn^{2+} and ATP (lane 4), no activity was detected.

Next, the mutant NS3 proteins were examined in the RNA helicase assay (Fig. 5C) (summary shown in Table 2). As expected, mutation of the ATP binding motif I abolished RNA helicase activity (lanes 8 and 9); the extent of unwinding was the same as for GST only (lane 3), confirming that no RNA helicase activity was detected in the absence of ATPase activity. Interestingly, mutation M283F in motif II demonstrated reduced ATPase activity (Fig. 4A, lane 9) and increased helicase activity (Fig. 5C, lane 10) compared to the parental G2 protein (Fig. 4A, lane 3, and Fig. 5C, lane 4). Also, the protein with changes R457A and R458A in motif VI which retained ATPase activity (Fig 4A, lane 13) showed no detectable RNA unwinding (Fig. 5C, lane 14). These results demonstrate that the NTPase and RNA helicase activities of the DEN-2 NS3 protein can be functionally uncoupled by mutations within motifs.

Mutation of the clustered charged regions external to the helicase motifs had variable effects on RNA unwinding. The three mutants $G_{169-173}$, $G_{179-181}$, and $G_{184-186}$, upstream of motif I, demonstrated a large increase in RNA unwinding (Fig. 5C, lanes 5 to 7) compared with parental NS3, which corresponded to their increased ATPase activity (Fig. 4). However, the $G_{436-439}$ mutant, which also exhibited enhanced ATP hydrolysis, showed only a slight increase in helicase activity over parental G2 (Fig. 5C, lane 13). The remaining two mutants, $G_{334-336}$ and $G_{376-380}$, each demonstrated ATPase activity but only low or no RNA unwinding (Fig. 5C, lanes 11 and 12). These results show uncoupling of ATPase and helicase activity by mutagenesis outside enzyme motifs.

Analysis of virus replication. To test the effects of the mutations described above on virus replication, all mutants except G198A were incorporated into genomic-length cDNA. We considered it unnecessary to test both the motif I mutants, G198A and K199A.

Virus was produced from genomic-length cDNA by established procedures (22). RNA was transcribed and electroporated into BHK-21 cells, and the cells were incubated at 33 or 37°C. BHK-21 cells were tested for immunofluorescence with anti-E antibodies. Medium from the transfected BHK-21 cells was passaged twice in C6/36 cells at 28°C, and the virus titer was determined after the second passage by plaque assay in C6/36 cells. Viral RNA was then amplified by RT-PCR, and the entire NS2B and NS3 genes were sequenced to check that the mutation was retained during the passaging and that no other changes were present within this region. These procedures were completed at least twice for each construct, and the results are summarized in Table 2.

The parental virus V2 and mutant viruses $V_{169-173}$ and $V_{179-181}$ grew to comparable titers of 10^5 to 10^6 PFU/ml following initial electroporation at 33 or 37°C (Table 2), although both mutant viruses showed a small-plaque phenotype. The corresponding NS3 fusion proteins G2 and mutants $G_{169-173}$ and $G_{179-181}$ all possessed in vitro ATPase and RNA helicase activities. For viruses V_{M283F} and $V_{334-336}$, virus was detected following electroporation at 33°C only, at reduced titers (4.7×10^5 and 7.3×10^2 PFU/ml, respectively), and with a small-plaque phenotype (Table 2). These results suggested that V_{M283F} and $V_{334-336}$ were restricted in replication and possibly heat sensitive. The G_{M283F} and $G_{334-336}$ fusion proteins both had reduced ATPase activity in vitro (Fig. 4B) and helicase activity that was either increased or reduced, respectively (Fig. 5D).

No virus was detected for five constructs. The lack of virus from the three constructs containing mutation K199A (motif I) or R457A,R458A (motif VI) or clustered charged-to-alanine changes $R_{376}KNGK_{380}$ corresponded to the lack of helicase activity detected for the corresponding fusion proteins. However, clustered changes at $R_{184}KR_{186}$ and $D_{436}GEE_{439}$ did not reduce helicase activity of the fusion proteins, and yet no virus was recovered. We hypothesize that these residues are required for other NS3 functions, such as the interaction with proteins in the viral replication complex.

Growth of viruses V2, $V_{169-173}$, $V_{179-181}$, and V_{M283F} in BHK cells. To examine further the properties of the viruses, more concentrated stocks were prepared by polyethylene glycol precipitation of all viruses except $V_{334-336}$. Virus $V_{334-336}$ did not replicate adequately to obtain sufficient titers for further experiments.

BHK-21 cells were infected at a multiplicity of infection (MOI) of 1, and cells were incubated at 33 or 37°C. Experiments maintaining the BHK-21 cells at 39°C were unsuccessful because of poor cell survival. The culture medium was sampled at 72 h after infection, and virus titers were determined by plaque assay in C6/36 cells (Fig. 6). Of the four viruses, only V_{M283F} showed significant temperature sensitivity. At 72 h after infection, supernatant from cells infected with virus V_{M283F} and maintained at 33°C contained $(3.0 \pm 0.4) \times$

TABLE 2. Yields of mutant viruses following electroporation of RNA into BHK-21 cells and two passages of virus in C6/36 cells

Site(s) mutated	Virus		IF[a]	Virus titer[b] (PFU/ml)	Approx plaque size (mm)	RT-PCR[c]	ATPase activity[f]	Helicase activity[f]
	Mutant	Temp (°C)[d]						
	V2	33	++++	$(1.1 \pm 0.1) \times 10^6$	4	Yes	+	+
	V2	37	++++	$(7.3 \pm 0.8) \times 10^6$	4	Yes		
$E_{169}KSIE_{173}$	$V_{169-173}$	33[e]	++++	$(2.7 \pm 0.2) \times 10^6$	3	Yes	↑	↑
	$V_{169-173}$	37	++++	$(2.2 \pm 0.5) \times 10^6$	3	Yes		
$E_{179}DD_{181}$	$V_{179-181}$	33[e]	+++	$(4.9 \pm 1.0) \times 10^5$	1	Yes	↑	↑
	$V_{179-181}$	37	+++	$(1.4 \pm 0.2) \times 10^6$	1	Yes		
$R_{184}KR_{186}$	$V_{184-186}$	33	−	None detected		No	↑	↑
	$V_{184-186}$	37	−	None detected		No		
K199A	V_{K199A}	33	−	None detected		No	−	−
	V_{K199A}	37	−	None detected		No		
M283F	V_{M283F}	33	+	$(4.7 \pm 1.0) \times 10^5$	2	Yes	↓	↑
	V_{M283F}	37	−	None detected		No		
$D_{334}EE_{336}$	$V_{334-336}$	33	++++	$(7.3 \pm 1.1) \times 10^2$	1	Yes	↓	↓
	$V_{334-336}$	37	−	None detected		No		
$R_{376}KNGK_{380}$	$V_{376-380}$	33	−	None detected		No	↓	−
	$V_{376-380}$	37	−	None detected		No		
$D_{436}GEE_{439}$	$V_{436-439}$	33	−	None detected		No	↑	↑
	$V_{436-439}$	37	−	None detected		No		
R457A,R458A	$V_{R457A,R458A}$	33	−	None detected		No	↓	−
	$V_{R457A,R458A}$	37	−	None detected		No		

[a] Immunofluorescence (IF) in BHK-21 cells at 5 to 6 days postelectroporation. IF was scored as follows: −, no positive cells; +, 1 to 25% positive cells; ++, 25 to 50% positive cells; +++, 50 to 75% positive cells; ++++, 75 to 100% positive cells.

[b] Plaque titers after passaging in C6/36 are expressed as means ± one standard deviation. Each virus was derived at least twice from RNA transcripts; therefore, the result shown for each virus is the average of two or more experiments.

[c] Detection of product after RT-PCR. All positive samples retained the required mutation and had no other changes in the NS2B/3 genes.

[d] Temperature at which BHK-21 cells were incubated immediately after electroporation.

[e] Data for this virus are published in reference 37.

[f] ATPase and RNA helicase activities at 25°C. Activity was scored as no activity (−), parental activity (+), activity increased compared with parental activity (↑), or activity reduced compared with parental activity (↓) (Fig. 4B and Fig. 5D).

10^4 PFU/ml, whereas cells maintained at 37°C contained $(5.7 \pm 0.4) \times 10^2$ PFU/ml. The presence of each mutation in recovered virus was reconfirmed by RT-PCR and sequencing.

Temperature shift experiments with virus V_{M283F}. To assess the effect of temperature shift on viral RNA synthesis and replication of V_{M283F}, duplicate BHK-21 cell monolayers were infected with the parental V2 or mutant V_{M283F} viruses at an MOI of 10 and incubated for 48 h at 33°C. At this time monolayers were maintained at 33°C or shifted to 37°C.

At 24 h after the shift (72 h after infection) the cell culture medium was assayed for virus yield (Fig. 7A). The titers for the mutant and parental viruses were both higher at 33°C than at 37°C. However, the shift to 37°C clearly had a greater effect on mutant V_{M283F} than on V2. The reductions in titer ($\log_{10}$) were 0.7 and 1.9, respectively. At 0, 16, and 24 h after the shift (48, 64, and 72 h after infection) RNA extracts of infected cells were prepared for analysis of accumulated viral RNA content by dot blot hybridization. Overall, the V2-infected cells contained more viral RNA than those infected with the mutant V_{M283F} (Fig. 7B), consistent with the higher yield of virus from the former (Fig. 7A). Following the shift, V2-infected cells showed similar viral RNA content at the two temperatures at 64 and 72 h, whereas for the mutant V_{M283F}, the cells maintained at 33°C clearly had more viral RNA than at 37°C. Both positive- and negative-strand viral RNA were detected by the dsDNA probe.

To assess the effect of the temperature shift on viral protein synthesis, the accumulations of labeled proteins at the permissive (33°C) and nonpermissive (37°C) temperatures were compared. The timing of the experiment was similar to that described above for the dot blot assay. BHK-21 cell monolayers were infected with the V2 or mutant V_{M283F} viruses at an MOI of 10 and incubated for 48 h at 33°C. At 48 h after infection monolayers were maintained at 33°C or shifted to 37°C. At 0 and 24 h postshift, media were replaced with fresh medium lacking methionine for 2 h. Proteins were then radiolabeled with [^{35}S]methionine for a further 2 h. As a measure of overall viral protein synthesis, the amount of NS3 protein was assessed by RIP of cell lysates (Fig. 7C). As for viral RNA, less NS3 was detected in the cells infected by the mutant virus V_{M283F} than by V2. In addition, cells infected by the mutant contained less NS3 at the higher temperature (Fig. 7C, lanes 7 and 8 compared with lanes 9 and 10), whereas V2-infected cells (Fig. 7C, lanes 11 and 12) were more similar in NS3 content.

The bottom panel of Fig. 7C shows that the amount of protein in cell lysates before immunoprecipitation varied little.

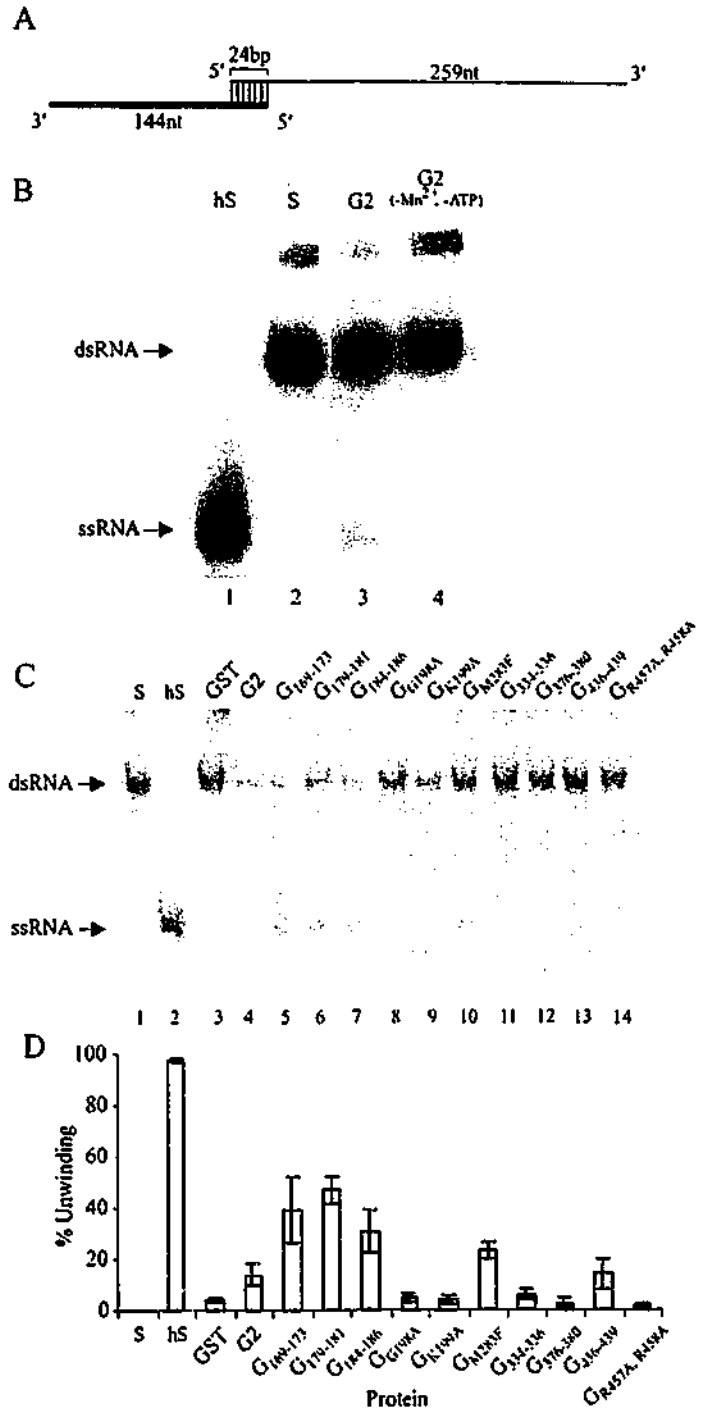

FIG. 5. RNA helicase assay of 74%NS3 fusion proteins. (A) Structure of the 3′-tailed dsRNA substrate; the lower strand of RNA was labeled with [α-^{32}P]ATP. (B) RNA helicase activity of the parental G2 protein. Lane 1, heated RNA substrate (hS); lane 2, untreated RNA substrate (S); lane 3, RNA helicase activity of 1 pmol of purified G2 protein; lane 4, same as lane 3 but omitting ATP and Mn^{2+}. (C) RNA helicase activity of mutant fusion proteins. (D) Percent unwinding of dsRNA to single-stranded RNA (ssRNA). Means (columns) and range of values (error bars) from three independent experiments are shown.

This demonstrated that the differences in levels of NS3 seen following RIP were probably due to the availability of template viral RNA for protein synthesis and not to variation in the number of cells in the monolayer or efficiency of lysis. RIPs were also performed with anti-E monoclonal antibodies, and identical results were obtained with respect to the relative amounts of viral proteins (data not shown). Therefore, the mutant virus V_{M283F} was temperature (heat) sensitive in RNA synthesis, protein synthesis, and virus yield.

DISCUSSION

Ten sites distributed through the helicase region of DEN-2 NS3 were mutagenized in these experiments. Four were located in enzyme motifs, and a further six that were rich in charged amino acids were altered by charged-to-alanine mutagenesis of three residues (Fig. 1).

Ten mutant proteins were synthesized in *E. coli* and tested in vitro for their effects on ATPase and RNA helicase activities. The ATPase activity of the parental protein G2 was stimulated only modestly by poly(A) in these experiments. The increase in the k_{cat}/K_m ratio was 1.45-fold, corresponding to an increase in V_{max} of 1.25-fold. This was in contrast to the results obtained by Li et al. (33) who showed a 9.7-fold increase in V_{max} for a DEN-2 NS3 in the presence of poly(A), using a protein with a similar N-terminal truncation but containing a C-terminal His tag rather than the much larger N-terminal GST tag of our experiments. Other significant differences in NTPase activities among NS3 proteins in the presence of polynucleotides have also been described (4, 31, 47, 48, 54). The reasons for the differences have not been identified, but they probably reflect variation in the types, sizes, and locations of fused peptides; the degree of truncation of the enzymes; the methods of expression (e.g., in bacteria, insect, or mammalian cells); the purification procedures; and the assay conditions.

Patterns of activity. In our experiments we examined both ATPase and helicase activity in vitro. Five patterns of activity were observed, and they are discussed in turn below: (i) no ATPase and no helicase, (ii) enhanced ATPase and enhanced helicase, (iii) reduced ATPase and no helicase, (iv) reduced ATPase and reduced helicase, and (v) reduced ATPase and enhanced helicase.

(i) No ATPase and no helicase. Only two of the ten mutant fusion proteins assayed for enzymatic activity in this study lacked both in vitro ATPase and RNA helicase activities. They contained a substitution of the invariant G_{198} or K_{199} residues in NTP-binding motif I. Substitution of the residue cor-

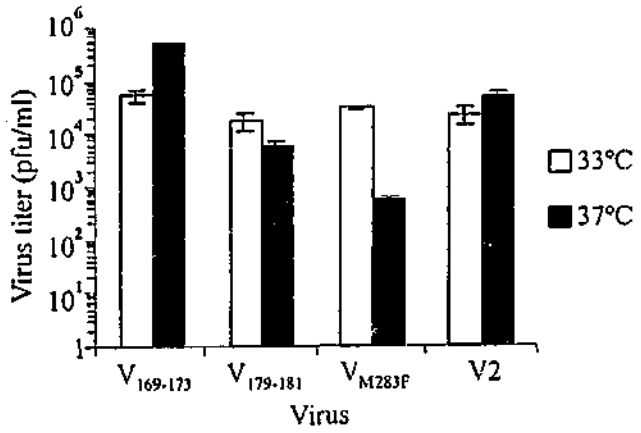

FIG. 6. Replication of selected mutant viruses in BHK-21 cells at 33 and 37°C (MOI of 1.0). The cell culture medium was sampled at 72 h postinfection, and the virus titers were determined by plaque assay on C6/36 cells (28°C). Error bars show one standard deviation of the plaque titer.

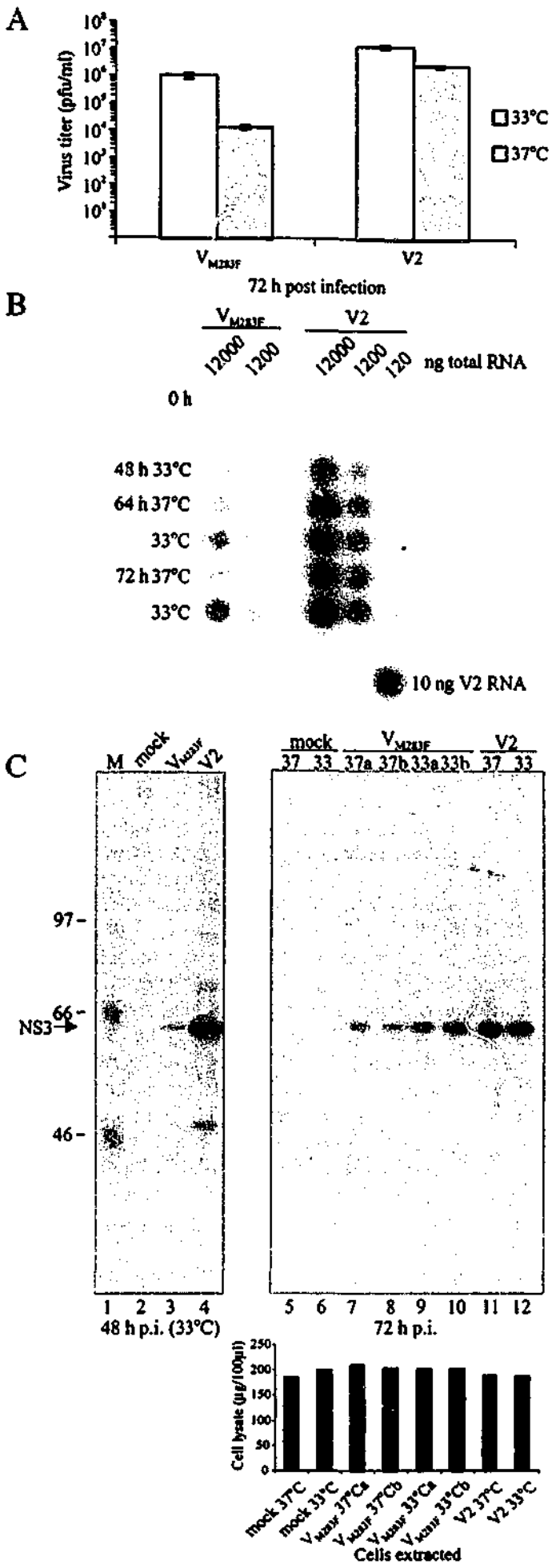

FIG. 7. (A) Replication of parental V2 and V_{M283F} viruses in BHK-21 cells shifted from 33 to 37°C at 48 h postinfection (h p.i.). Virus titers in cell culture fluid at 72 h p.i. were determined by plaque assay on C6/36 cells (28°C). Error bars show one standard deviation of the plaque titer. (B) Dot blot hybridizations of total infected cell RNA using a ^{32}P-labeled dsDNA viral probe. Cells were harvested at 48, 64, and 72 h p.i. (C) Analysis by gel electrophoresis of ^{35}S-labeled protein immunoprecipitated by anti-NS3 antiserum (50). Mock-infected cells (lanes 2, 5, and 6) and size markers (lane 1) are shown. The bottom panel shows amounts of total cell protein in cell lysates before immunoprecipitation. RIPs were prepared using anti-NS3 antiserum. The samples in lanes 7, 8, 9, and 10 are from independent duplicate experiments.

responding to K_{199} in EVDV and HCV was previously shown to greatly reduce ATPase and RNA helicase activities (21, 23, 28, 38, 53).

(ii) Enhanced ATPase and enhanced helicase. All six proteins with charged-to-alanine mutations had ATPase activity. Of these, four proteins—$G_{169-173}$, $G_{179-181}$, $G_{184-186}$, and $G_{436-439}$—were more active than parental G2 (Fig. 4). Increased ATPase corresponded to increased helicase activity (Fig. 5; Table 2). Previous studies have also shown enhanced NTPase activity for some flavivirus and poxvirus enzyme mutants. Li et al. (33) generated a DEN-2 NS3 mutant $Q_{184}NGN_{187}$, comparable to our $R_{184}KRK_{187}$, and demonstrated that it had a twofold increase in ATPase activity in the absence of poly(A). Substitution of the conserved histidine residue of motif II with alanine in NS3 of HCV and *Japanese encephalitis virus*, and in the NTP phosphohydrolase II (NPH-II) of *Vaccinia virus* also caused an increase in NTPase activity in the absence of poly(A) compared with parental protein (17, 23, 51).

(iii) Reduced ATPase and no helicase. In this study, the motif VI mutant $G_{R457A,R458A}$ and the charged-to-alanine mutant $G_{376-380}$ had reduced ATPase activity and no helicase activity, identifying two regions required for coupling of the two activities. The role of the arginine residues in motif VI has been examined in *Vaccinia virus* NPH-II and HCV NS3 helicases. Mutation of the first arginine (corresponding to R_{457} in DEN-2) in NPH-II and of the second arginine (corresponding to R_{458} in DEN-2) in HCV decreased RNA binding (7, 18, 28). Thus, by comparison with these viruses, the lack of detectable helicase activity of the DEN-2 $G_{R457A,R458A}$ double mutant protein was possibly due to inhibition of RNA binding. In contrast to $G_{R457A,R458A}$, mutagenesis of the region corresponding to $G_{376-380}$ has not been reported, and analysis of the HCV structure at this location provides no understanding of the role of these residues in enzyme activity. However, the substitution of basic residues by alanine may also have an adverse effect on RNA binding. Recent structure-based mutagenesis of HCV NS3 helicase demonstrated that substitution with alanine of several residues (external to helicase motifs) proposed to interact with RNA also uncoupled the two enzyme activities (34).

(iv) Reduced ATPase and reduced helicase. The remaining charged-to-alanine mutant $G_{334-336}$ showed reduced levels of both ATPase and RNA helicase activities.

(v) Reduced ATPase and enhanced helicase. The only protein which demonstrated reduced ATPase activity and in-

creased helicase activity with respect to parental G2 was the motif II mutant G_{M283F}. The mutation in this protein was of particular interest because the residue at this position (methionine in DEN-2 motif II L_{280}IIMDEAH$_{287}$) (30) has not been previously mutagenized for any virus. Phenylalanine commonly occurs at this position in positive-strand viruses (30). Analysis of the HCV NS3 crystal structure indicates that the adjoining aspartic and glutamic acid residues potentially interact with the bound ATP γ-phosphate and amino acid residues in motif I via Mg^{2+} binding (29), and both residues are required for NTPase and helicase activities (51, 53). However, the reason for the increase in helicase activity observed in this study is unknown. Analysis of the HCV helicase structure demonstrates that the residue equivalent to DEN-2 M_{283} is buried within the secondary structure, suggesting that it is not directly involved in ATPase or helicase activity (J. C. Whisstock, personal communication).

With the availability of genomic-length cDNA, we were able to test the effect on virus replication of nine mutations modifying ATPase and helicase activity in vitro. As described above, the mutations produced five patterns of enzyme activity in vitro, and their effects on replication were of considerable interest. The introduction of helicase mutations into viral genomes has been reported for only one positive-strand RNA virus, BVDV (21). For BVDV, three mutations, two point mutations in motifs I and II and a deletion mutant in motif VI, abolished helicase activity and virus replication (21). Likewise for DEN-2, the mutations in motif I (K199A) and motif VI (R457A, R458A) that abolished helicase activity also prevented virus replication. In addition, the charged-to-alanine mutation at R_{376}KNGK$_{380}$ in DEN-2 NS3 also stopped helicase activity and virus replication. Thus, for both these members of the family *Flaviviridae*, lack of helicase in vitro correlated directly with no detectable virus replication.

On the other hand, mutations permitting helicase activity in vitro did not necessarily permit virus replication. There were four mutations that allowed replication, i.e., E_{169}KSIE$_{173}$, E_{179}DD$_{181}$, M283F, and D_{334}EE$_{336}$ (although with smaller plaque phenotype and in two instances temperature sensitivity), and two that did not, i.e., R_{184}KR$_{186}$ and D_{436}GEE$_{439}$. With the exception of M283F (motif II mutant), these mutations were all of the charged-to-alanine type and therefore likely to be located on the surface of NS3 and involved in protein-protein or RNA-protein interactions (1, 13). NS3 has been identified in NS3-NS5 complexes (8, 26) and associated with the nonstructural proteins NS1, NS2A, NS4A, and NS5 in replication complexes (27, 36, 57). It is therefore likely that subtle or substantial changes in these interactions led to the observed range of phenotypes. In particular, the charged residues at R_{184}KR$_{186}$, D_{334}EE$_{336}$, and D_{436}GEE$_{439}$ are worthy of further investigation. Less severe mutagenesis of these sites would establish the relative contribution of individual residues to enzyme activity and virus replication. Additional experiments which may assist in determining the roles of residues are binding assays in vitro for analysis of protein-protein and RNA-protein interactions (10). Since the hydrophilicity profiles of proteins specified by viruses within the genus *Flavivirus* are highly conserved (56), the results obtained using DEN-2 would be potentially applicable across the genus.

We had limited success in producing temperature-sensitive mutants by charged-to-alanine mutagenesis. Here, one potential mutant ($V_{334-336}$) was obtained after mutagenesis of six different sites. Only one temperature-sensitive mutant produced by this technique has been reported for the flaviviruses, in NS1 of *Yellow fever virus* (39). However, we were successful in generating a temperature-sensitive mutant, V_{M283F}, with the M283F substitution in motif II. As noted above for the hydrophilicity profiles, the conservation of the sequence MDEAH in motif II suggests the results with V_{M283F} may hold for other flaviviruses. The data shown in Fig. 7B demonstrated that cells infected with this virus were defective in RNA synthesis at the nonpermissive temperature. Further experiments are in progress to determine the basis of this defect.

In summary, we have identified residues in the NS3 helicase region of DEN-2 within and outside motifs that modify enzyme activities in vitro and alter virus phenotype. Mutations that abolished helicase but not ATPase activity were identified. In some instances enhancement of enzyme activities was observed. Absence of helicase activity in vitro correlated directly with lack of virus replication. Our results are likely to be applicable to other flaviviruses and are of importance in the development of antiviral strategies directed at the inhibition of NTP and RNA binding, the coupling of NTPase and RNA helicase activities, and protein-protein interactions within the replication complex.

ACKNOWLEDGMENTS

This work was supported by grants from the National Health and Medical Research Council of Australia and the World Health Organization Global Program for Vaccines and Immunization.

REFERENCES

1. **Alber, T.** 1989. Mutational effects on protein stability. Annu. Rev. Biochem. 58:765–798.
2. **Buss, S. H., M. G. Mulkerrin, and J. A. Wells.** 1991. A systematic mutational analysis of hormone-binding determinants in the human growth hormone receptor. Proc. Natl. Acad. Sci. USA 88:4498–4502.
3. **Bazan, J. F., and R. J. Fletterick.** 1989. Detection of a trypsin-like serine protease domain in flaviviruses and pestiviruses. Virology 171:637–639.
4. **Bartowski, P., A. Niebuhr, O. Mueller, M. Bretner, K. Felczak, T. Kulikowski, and H. Schmitz.** 2001. Purification and characterization of West Nile virus nucleoside triphosphatase (NTPase)/helicase: evidence for dissociation of the NTPase and helicase activities of the enzyme. J. Virol. 75:3220–3229.
5. **Chambers, T. J., A. Grakoui, and C. M. Rice.** 1991. Processing of the yellow fever virus nonstructural polyprotein: a catalytically active NS3 proteinase domain and NS2B are required for cleavages at dibasic sites. J. Virol. 65: 6042–6050.
6. **Chambers, T. J., A. Nestorowicz, S. M. Amberg, and C. M. Rice.** 1993. Mutagenesis of the yellow fever virus NS2B protein: effects on proteolytic processing, NS2B-NS3 complex formation, and viral replication. J. Virol. 67: 6797–6807.
7. **Chang, S. C., J. C. Cheng, Y. H. Kou, C. H. Kao, C. H. Chiu, H. Y. Wu, and M. F. Chang.** 2000. Roles of the AX_4GKS and arginine-rich motifs of hepatitis C virus RNA helicase in ATP- and viral RNA-binding activity. J. Virol. 74:9732–9737.
8. **Chen, C. J., M. D. Kuo, L. J. Chien, S. L. Hsu, Y. M. Wang, and J. H. Lin.** 1997. RNA-protein interactions: involvement of NS3, NS5, and 3′ noncoding regions of Japanese encephalitis virus genomic RNA. J. Virol. 71:3466–3473.
9. **Cho, H. S., N. C. Ha, L. W. Kang, K. M. Chung, S. H. Back, S. K. Jang, and B. H. Oh.** 1998. Crystal structure of RNA helicase from genotype 1b hepatitis C virus. A feasible mechanism of unwinding duplex RNA. J. Biol. Chem. 273: 15045–15052.
10. **Cui, T., R. J. Sugrue, Q. Xu, A. K. Lee, Y. C. Chan, and J. Fu.** 1998. Recombinant dengue virus type 1 NS3 protein exhibits specific viral RNA binding and NTPase activity regulated by the NS5 protein. Virology 246: 409–417.
11. **Cunningham, B. C., and J. A. Wells.** 1989. High-resolution epitope mapping of hGH-receptor interactions by alanine-scanning mutagenesis. Science 244: 1081–1085.
12. **Della, P. A., and E. G. Westaway.** 1972. Rapid preparation of hemagglutinins of togaviruses from infected cell culture fluids. Appl. Microbiol. 23:158–160.
13. **Diamond, S. E., and K. Kirkegaard.** 1994. Clustered charged-to-alanine

mutagenesis of poliovirus RNA-dependent RNA polymerase yields multiple temperature-sensitive mutants defective in RNA synthesis. J. Virol. 68:863–876.
14. **Falgout, B., R. H. Miller, and C. J. Lai.** 1993. Deletion analysis of dengue virus type 4 nonstructural protein NS2B: identification of a domain required for NS2B-NS3 protease activity. J. Virol. 67:2034–2042.
15. **Falgout, B., M. Pethel, Y. M. Zhang, and C. J. Lai.** 1991. Both nonstructural proteins NS2B and NS3 are required for the proteolytic processing of dengue virus nonstructural proteins. J. Virol. 65:2467–2475.
16. **Grassmann, C. W., O. Isken, and S. E. Behrens.** 1999. Assignment of the multifunctional NS3 protein of bovine viral diarrhea virus during RNA replication: an in vivo and in vitro study. J. Virol. 73:9196–9205.
17. **Gross, C. H., and S. Shuman.** 1995. Mutational analysis of vaccinia virus nucleoside triphosphate phosphohydrolase II, a DExH box RNA helicase. J. Virol. 69:4727–4736.
18. **Gross, C. H., and S. Shuman.** 1996. The QRxGRxGRxxxG motif of the vaccinia virus DExH box RNA helicase NPH-II is required for ATP hydrolysis and RNA unwinding but not for RNA binding. J. Virol. 70:1706–1713.
19. **Gross, C. H., and S. Shuman.** 1996. Vaccinia virus RNA helicase: nucleic acid specificity in duplex unwinding. J. Virol. 70:2615–2619.
20. **Gruenberg, A., and P. J. Wright.** 1992. Processing of dengue virus type 2 structural proteins containing deletions in hydrophobic domains. Arch. Virol. 122:77–94.
21. **Gu, B., C. Liu, J. Lin-Goerke, D. R. Maley, L. L. Gutshall, C. A. Feltenberger, and A. M. Del Vecchio.** 2000. The RNA helicase and nucleotide triphosphatase activities of the bovine viral diarrhea virus NS3 protein are essential for viral replication. J. Virol. 74:1794–1800.
22. **Gualano, R. C., M. J. Pryor, M. R. Cauchi, P. J. Wright, and A. D. Davidson.** 1998. Identification of a major determinant of mouse neurovirulence of dengue virus type 2 using stably cloned genomic-length cDNA. J. Gen. Virol. 79:437–446.
23. **Heilek, G. M., and M. G. Peterson.** 1997. A point mutation abolishes the helicase but not the nucleoside triphosphatase activity of hepatitis C virus NS3 protein. J. Virol. 71:6264–6266.
24. **Ho, S. N., H. D. Hunt, R. M. Horton, J. K. Pullen, and L. R. Pease.** 1989. Site-directed mutagenesis by overlap extension using the polymerase chain reaction. Gene 77:51–59.
25. **Irie, K., P. M. Mohan, Y. Sasaguri, R. Putnak, and R. Padmanabhan.** 1989. Sequence analysis of cloned dengue virus type 2 genome (New Guinea-C strain). Gene 75:197–211.
26. **Kapoor, M., L. W. Zhang, M. Ramachandra, J. Kusukawa, K. E. Ebner, and R. Padmanabhan.** 1995. Association between NS3 and NS5 proteins of dengue virus type 2 in the putative RNA replicase is linked to differential phosphorylation of NS5. J. Biol. Chem. 270:19100–19106.
27. **Khromykh, A. A., P. L. Sedlak, and E. G. Westaway.** 1999. *trans*-complementation analysis of the flavivirus Kunjin NS5 gene reveals an essential role for translation of its N-terminal half in RNA replication. J. Virol. 73:9247–9255.
28. **Kim, D. W., J. Kim, Y. Gwack, J. H. Han, and J. Choe.** 1997. Mutational analysis of the hepatitis C virus RNA helicase. J. Virol. 71:9400–9409.
29. **Kim, J. L., K. A. Morgenstern, J. P. Griffith, M. D. Dwyer, J. A. Thomson, M. A. Murcko, C. Lin, and P. R. Caron.** 1998. Hepatitis C virus NS3 RNA helicase domain with a bound oligonucleotide: the crystal structure provides insights into the mode of unwinding. Structure 6:89–100.
30. **Koonin, E. V., and V. V. Dolja.** 1993. Evolution and taxonomy of positive-strand RNA viruses: implications of comparative analysis of amino acid sequences. Crit. Rev. Biochem. Mol. Biol. 28:375–430.
31. **Kuo, M. D., C. Chin, S. L. Hsu, J. Y. Shiao, T. M. Wang, and J. H. Lin.** 1996. Characterization of the NTPase activity of Japanese encephalitis virus NS3 protein. J. Gen. Virol. 77:2077–2084.
32. **Lain, S., J. L. Riechmann, and J. A. Garcia.** 1990. RNA helicase: a novel activity associated with a protein encoded by a positive strand RNA virus. Nucleic Acids Res. 18:7003–7006.
33. **Li, H. T., S. Chun, S. H. You, K. E. Ebner, and R. Padmanabhan.** 1999. The serine protease and RNA-stimulated nucleoside triphosphatase and RNA helicase functional domains of dengue virus type 2 NS3 converge within a region of 20 amino acids. J. Virol. 73:3108–3116.
34. **Lin, C., and J. L. Kim.** 1999. Structure-based mutagenesis study of hepatitis C virus NS3 helicase. J. Virol. 73:8798–8807.
35. **Luking, A., U. Stahl, and U. Schmidt.** 1998. The protein family of RNA helicases. Crit. Rev. Biochem. Mol. Biol. 33:259–296.
36. **Mackenzie, J. M., A. A. Khromykh, M. K. Jones, and E. G. Westaway.** 1998. Subcellular localization and some biochemical properties of the flavivirus Kunjin nonstructural proteins NS2A and NS4A. Virology 245:203–215.
37. **Matusan, A. E., P. G. Kelley, M. J. Pryor, J. C. Whisstock, A. D. Davidson, and P. J. Wright.** 2001. Mutagenesis of the dengue virus type 2 NS3 proteinase and the production of growth-restricted virus. J. Gen. Virol. 82:1647–1656.
38. **Min, K. H., Y. C. Sung, S. Y. Choi, and B. Y. Ahn.** 1999. Functional interactions between conserved motifs of the hepatitis C virus RNA helicase protein NS3. Virus Genes 19:33–43.
39. **Muylaert, I. R., R. Galler, and C. M. Rice.** 1997. Genetic analysis of the yellow fever virus NS1 protein: identification of a temperature-sensitive mutation which blocks RNA accumulation. J. Virol. 71:291–298.
40. **Paolini, C., R. De Francesco, and P. Gallinari.** 2000. Enzymatic properties of hepatitis C virus NS3-associated helicase. J. Gen. Virol. 81:1335–1345.
41. **Paolini, C., A. Lahm, R. De Francesco, and P. Gallinari.** 2000. Mutational analysis of hepatitis C virus NS3-associated helicase. J. Gen. Virol. 81:1649–1658.
42. **Preugschat, F., C. W. Yao, and J. H. Strauss.** 1990. In vitro processing of dengue virus type 2 nonstructural proteins NS2A, NS2B, and NS3. J. Virol. 64:4364–4374.
43. **Pryor, M. J., R. C. Gualano, B. Lin, A. D. Davidson, and P. J. Wright.** 1998. Growth restriction of dengue virus type 2 by site-specific mutagenesis of virus-encoded glycoproteins. J. Gen. Virol. 79:2631–2639.
44. **Pryor, M. J., and P. J. Wright.** 1993. The effects of site-directed mutagenesis on the dimerization and secretion of the NS1 protein specified by dengue virus. Virology 194:769–780.
45. **Rice, C. M.** 1996. *Flaviviridae*: the viruses and their replication, p. 931–959. *In* B. N. Fields, D. M. Knipe, P. M. Howley, R. M. Chanock, J. L. Melnick, T. P. Monath, B. Roizman, and S. E. Straus (ed.), Fields virology, 3rd ed. Lippincott-Raven, Philadelphia, Pa.
46. **Schmid, S. R., and P. Linder.** 1992. D-E-A-D protein family of putative RNA helicases. Mol. Microbiol. 6:283–291.
47. **Suzich, J. A., J. K. Tamura, F. Palmer-Hill, P. Warrener, A. Grakoui, C. M. Rice, S. M. Feinstone, and M. S. Collett.** 1993. Hepatitis C virus NS3 protein polynucleotide-stimulated nucleoside triphosphatase and comparison with the related pestivirus and flavivirus enzymes. J. Virol. 67:6152–6158.
48. **Tamura, J. K., P. Warrener, and M. S. Collett.** 1993. RNA-stimulated NTPase activity associated with the p80 protein of the pestivirus bovine viral diarrhea virus. Virology 193:1–10.
49. **Tan, B. H., J. Fu, R. J. Sugrue, E. H. Yap, Y. C. Chan, and Y. H. Tan.** 1996. Recombinant dengue type 1 virus NS5 protein expressed in Escherichia coli exhibits RNA-dependent RNA polymerase activity. Virology 216:317–325.
50. **Teo, K. F., and P. J. Wright.** 1997. Internal proteolysis of the NS3 protein specified by dengue virus 2. J. Gen. Virol. 78:337–341.
51. **Utama, A., H. Shimizu, F. Hasebe, K. Morita, A. Igarashi, I. Shoji, Y. Matsuura, M. Hatsu, K. Takamizawa, A. Hagiwara, and T. Miyamura.** 2000. Role of the DExH motif of the Japanese encephalitis virus and hepatitis C virus NS3 proteins in the ATPase and RNA helicase activities. Virology 273:316–324.
52. **van Regenmortel, M. H. V., C. M. Fauquet, D. H. L. Bishop, C. E. B. Arstens, M. K. Estes, S. M. Lemon, J. Maniloff, M. A. Mayo, D. J. McGeoch, C. R. Pringle, R. B. Wickner.** 2000. Virus taxonomy. Academic Press, San Diego, Calif.
53. **Wardell, A. D., W. Errington, G. Ciaramella, J. Merson, and M. J. McGarvey.** 1999. Characterization and mutational analysis of the helicase and NTPase activities of hepatitis C virus full-length NS3 protein. J. Gen. Virol. 80:701–709.
54. **Warrener, P., J. K. Tamura, and M. S. Collett.** 1993. RNA-stimulated NTPase activity associated with yellow fever virus NS3 protein expressed in bacteria. J. Virol. 67:989–996.
55. **Wertman, K. F., D. G. Drubin, and D. Botstein.** 1992. Systematic mutational analysis of the yeast ACT1 gene. Genetics 132:337–350.
56. **Westaway, E. G., and J. Blok.** 1997. Taxonomy and evolutionary relationships of flaviviruses, p. 147–173. *In* D. J. Gubler and G. Kuno (ed.), Dengue and dengue hemorrhagic fever. CAB International, Wallingford, Conn.
57. **Westaway, E. G., J. M. Mackenzie, M. T. Kenney, M. K. Jones, and A. A. Khromykh.** 1997. Ultrastructure of Kunjin virus-infected cells: colocalization of NS1 and NS3 with double-stranded RNA, and of NS2B with NS3, in virus-induced membrane structures. J. Virol. 71:6650–6661.
58. **Yao, N., T. Hesson, M. Cable, Z. Hong, A. D. Kwong, H. V. Le, and P. C. Weber.** 1997. Structure of the hepatitis C virus RNA helicase domain. Nat. Struct. Biol. 4:463–467.

Fig. 3.4 Genomic map of DEN-2 and NS3 mutations incorporated into genomic length cDNA.

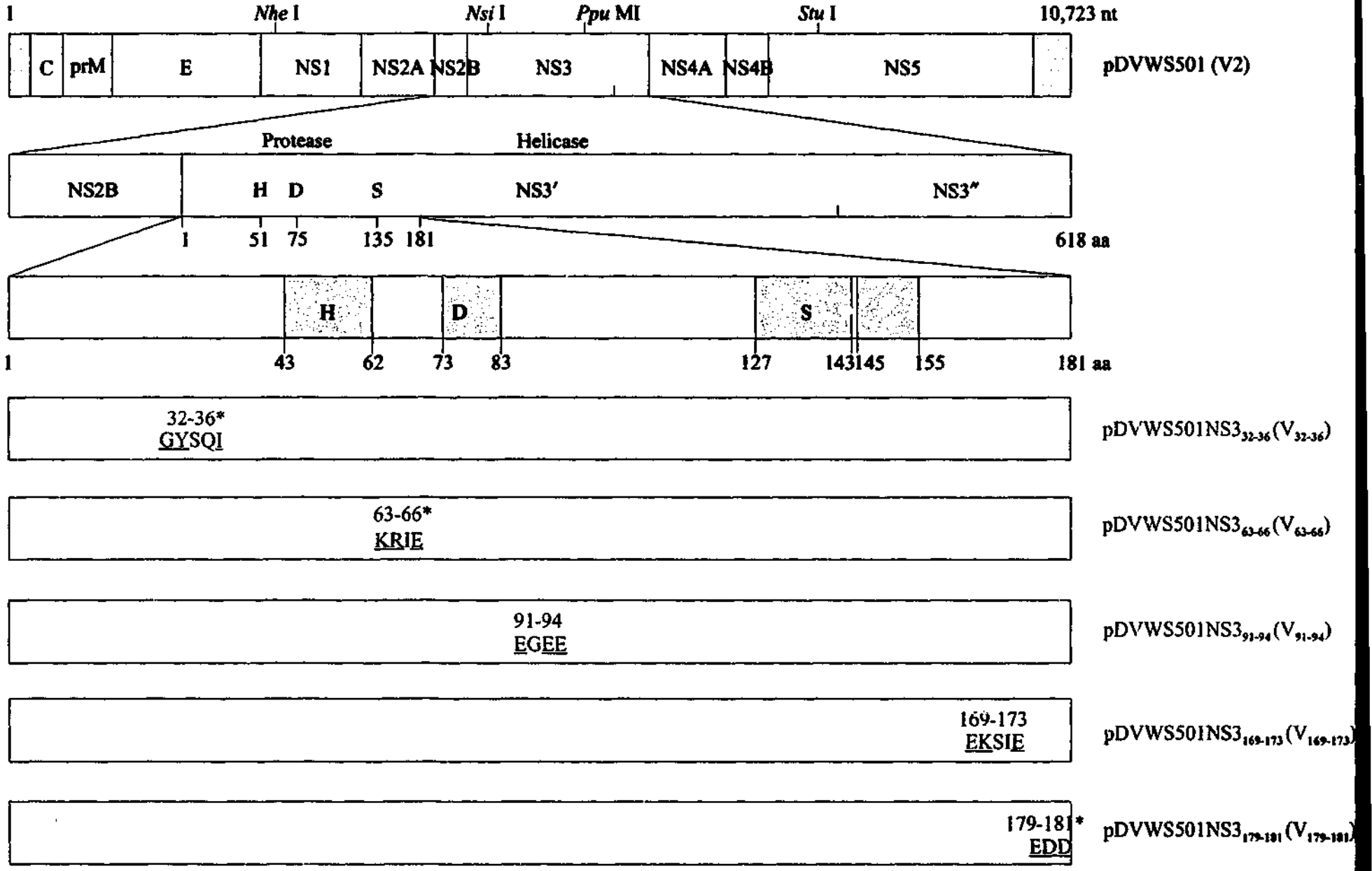

Fig. 4.3 Constructs used to synthesize NS3 fusion proteins and prepare mutated viruses.